Characterisation of Reversed Phase Chromatography Peptide Separation Systems

Strathclyde Institute of Pharmacy and Biomedical Sciences

Jennifer Kathryn Field

(PhD, Year of Submission 2019)

201670008

Under the Supervision of Prof. Mel Euerby (University of Strathclyde & Shimadzu UK Ltd) and Assoc. Prof. Patrik Petersson (Uppsala University & Novo Nordisk).

Declaration

'This thesis is the result of the author's original research. It has been composed by the author and has not been previously submitted for examination which has led to the award of a degree.

Signed:  Date: 1st October 2019

Acknowledgments

Firstly, I would like to thank my supervisors, Prof. Mel Euerby and Assoc. Prof. Patrik Petersson. You have both provided me with amazing support, knowledge and have helped me grow as a chromatographer. It's been a privilege to work with you both and I look forward to our future collaborations.

I'd also like to thank Novo Nordisk and the Novo Nordisk R&D STAR programme for giving me the opportunity to complete this PhD in such an exciting and novel subject area, and specifically Jesper Lau, Henning Thøgersen, Kim Haselmann, Marie Østergaard Pedersen, Natasja Weismann Andersen and Lene Villadsen for their helpful discussions and assistance with experiments. Also, the University of Strathclyde for allowing me to attend a world renown institution.

Thank you to Shimadzu Ltd for providing me with cutting edge technology. It's a pleasure to work every day with such kind and supportive people at Shimadzu UK, and I'd like to thank you for welcoming me.

This project would be impossible without the contributions provided by the column manufacturers; Agilent, Phenomenex, Supelco and Waters. It is with your generosity that this project can proceed and for that I thank you.

And, finally, I'd like to thank my family. To my husband, Andy; I would never have started this journey without your support and drive. And to my parents and sisters; you have always encouraged me to achieve my full potential. For that, and more, thank you.

Contents

i. Abstract

With the advancement of the biopharmaceutical industry, it is imperative to have a firm understanding of the peptide separation system. The chromatographic profile can be extremely complex for peptides with various impurities or degradation products, thus it is essential to be able to maximise selectivity differences to identify each species. This thesis endeavoured to understand the influencing factors to enable rational decisions to be made during method development strategies.

A peptide-based characterisation protocol was developed and applied to commercialised stationary phases, known as the Peptide RPC Column Characterisation Protocol. A design of experiment robustness study was executed to ensure the validity of the protocol was maintained. Chemometric analysis was performed which identified three classifications of columns from which stationary phases can be selected with either similar or different selectivity. The approach was validated using two tryptic digested peptides, with promising results. Although there are small molecule characterisation protocols already defined in the literature, it was confirmed that the peptide-based protocol is needed due to a lack of correlation between the small molecule and peptide-based protocols.

A comprehensive mobile phase study on a typical C18 phase also identified vast selectivity differences over a range of pH values, which was achieved using different ammonium-based salts, with interesting additives and ion pairs. The study ascertained the greatest differences were achieved under low pH conditions, thus the main focus for method development should be in that region. An initial study which observed the effect of temperature and organic modifiers identified the importance of evaluating these parameters during method development. Finally, the applicability of the results on other columns was determined.

The conclusions can provide a firm platform to develop a comprehensive method development strategy, which should provide a more rational approach for screening relevant stationary phases and mobile phases to truly maximise selectivity differences.

ii. List of Tables

iii. List of Figures

iv. Abbreviations

AA	Acetic acid
ACD/Labs	Advanced Chemistry Developments, inc.
API	Active pharmaceutical ingredient
BEH	Ethylene bridged hybrid
Bno	5-Butyl-5-nonyl
Boc	*t*-Butyloxycarbonyl
$BuSO_3$	Sodium butane-1-sulfonic acid
Bzl	Benzyl
Cbz	Carbobenzoxy
CD	Circular dichroism
CI	Confidence interval
CMC	Chemistry, manufacturing and controls
CSH	Charged surface hybrid
DFA	Difluoroacetic acid
Die	1,1-Diisopropylethyl
DMSO	Dimethylsulfoxide
DoE	Design of experiment
DVB	Divinylbenzene
EIC	Extracted ion chromatogram
EP	European Pharmacopoeia
FA	Formic acid
Fmoc	9-Fluoroenylmethoxycarbonyl
GLP-2	Glucagon-like peptide 2
H_2O	Water
H_3PO_4	Phosphoric acid
HCl	Hydrochloric acid
HF	Hydrofluoric acid
HFBA	Heptafluorobutyric acid
HILIC	Hydrophilic interaction liquid chromatography

HSM	Hydrophobic Subtraction Model
HSS	High strength silica
I.D.	Internal diameter
IEC	Ion exchange chromatography
KH_2PO_4	Potassium phosphate monobasic
logP	Partition coefficient
logD	Distribution coefficient
MeCN	Acetonitrile
MeOH	Methanol
MLR	Multiple linear regression
MS	Mass spectrometry
MSA	Methane sulfonic acid
MW	Molecular weight
m/z	Mass to charge ratio
Na_2SO_4	Sodium sulfate
NaCl	Sodium chloride
$NaClO_4$	Sodium perchlorate
$(NH_4)_2HPO_4$	Ammonium monohydrogen phosphate
$(NH_4)_2SO_4$	Ammonium sulfate
NH_4AA	Ammonium acetate
NH_4FA	Ammonium formate
$NH_4H_2PO_4$	Ammonium dihydrogen phosphate
NH_4HCO_3	Ammonium bicarbonate
NH_4OH	Ammonium hydroxide
NMR	Nuclear magnetic resonance
OFAT	One factor at a time
PCA	Principal component analysis
pI	Isoelectric point
pK_a	Acid dissociation constant
PQRI	Product Quality Research Institute

2-PrOH	Isopropanol
PSA	Polar surface area
PTM	Post translational modifications
R^2	Regression coefficient
Q2	Estimate of the predictive ability of the model
RPC	Reversed phase chromatography
%RSD	% Relative standard deviation
SD	Standard deviation
SIM	Selected ion monitoring
SPPS	Solid phase peptide synthesis
SST	System suitability test
TEA	Triethylamine
TFA	Trifluoroacetic acid
TFE	Trifluoroethanol
TIC	Total ion chromatogram
USP	United States Pharmacopoeia
ZDV	Zero dead volume union

v. Symbols

a_i	Retention model parameter
B	Gradient slope (%/mL)
b	Gradient steepness $b = V_m m B = V_m m(s/F)$
C	Concentration of salt counter ion in IEC (mM)
C^*	Concentration of salt counter ion in IEC as the analyte passes the mid-point of the column (mM)
C_0	Initial gradient concentration of salt counter ion in IEC (mM)
F	Flow rate (mL/min)
d_c	Column internal diameter (mm)
d_p	Particle size (µm)
k	Retention factor

k_0	k at initial gradient conditions
k_f	k as the analyte leaves the column in gradient elution
k^*	Gradient retention factor. Instantaneous k as the analyte passes the mid-point of the column
L	Column length (mm)
m	Retention model parameter in RPC $\log k = a_1 + m\phi$ (1/%)
P_c	Peak capacity
s	Gradient rate (%/min)
$t_{0.5}$	time at half the absorbance (min)
t_d	Dwell time (min)
t_{eq}	Re-equilibration time, gradient elution (min)
t_g	Retention time, gradient elution (min)
t^*_g	Normalised retention time, gradient elution (min)
t_G	Gradient time for a single segment linear gradient (min)
t_m	Dead time (min)
t_R	Isocratic retention time (min)
T	Column temperature (°C)
u	Velocity (mm/sec)
V_d	Dwell volume (mL)
V_m	Dead volume (mL)
w	Peak width at base defined as 4σ (min)
w_h	Peak width at half height defined as 2.35σ (min)
z	Effective charge of an analyte in IEC
α	Selectivity factor
α^*	Selectivity factor, gradient elution
σ	Standard deviation of a Gaussian curve
ϕ	Fraction of organic modifier.
ϕ^*	Fraction of organic modifier as the analyte passes the mid-point of the column (%)
ϕ_0	Initial fraction of organic modifier (%)

1. Introduction

1.1 Biopharmaceuticals and Background

The global biopharmaceutical market has increased substantially in recent years, with pharmaceutical companies recognising the importance of this type of medication. Indeed, seven of the top ten selling drugs between 2015-2017 and six in 2018 were biologically based [1-5]. Considerable resources are being utilised to develop expertise in not only developing these sophisticated structures but also in the successful manufacture of them [6].

The products on the market are typically proteins which differ significantly from small molecular drugs, as further discussed in *Section 1.3*. However, to be able to understand the protein separation system, it is important to build up knowledge. Thus, it was considered that a greater understanding in peptide analyses would lay a firmer foundation for the future analyses of protein molecules. The contents of this thesis shall therefore focus on the analysis of peptides.

The complexity of these compounds can make analysis of these active pharmaceutical ingredients (API) and their impurities / degradation products particularly challenging. These degradation products and impurities typically possess similar physico-chemical properties, making it difficult to achieve separation using reversed-phase (RP) HPLC. Isomers in particular are difficult to separate from the API and to identify by mass spectrometry (MS) due to being isobaric in nature. Attempts have been made to assist chromatographers with these separations by predicting retention times based on factors such as amino acid sequence and secondary structure. These approaches include look-up, index-based, modelling-based and machine learning methods [7-12]. The task is not simple, with various limitations to all approaches (i.e. a large number of test peptides are required to build a model using the index-based approach which is then only accurate for those particular chromatographic conditions), as highlighted in the peptide retention prediction review by Moruz [7]. The reviewer suggested the machine learning method was the most adaptable and flexible to predict outside of the chromatographic conditions tested and has the ability to adapt to the inclusion

of new information to the dataset. However, it had lower accuracy in comparison to some other methods described. Conformation and thus second order structure is likely to be affected by both the organic modifier as well as the stationary phase, which would make predicting peptide retention in RPC extremely difficult or unlikely to be successful. The difficulty of predicting retention times does highlight the need to develop a robust method development platform which maximises the chromatographic selectivity differences which are of critical importance for screening these biological products.

There is currently little research conducted into the best approach for maximising selectivity differences when analysing peptides. Screening and optimisation are often performed based on past experience and stationary phase selection based on small molecule characterisation protocols. There are various protocols described to probe reversed phase stationary phases using small molecules (Tanaka, Euerby *et al.* and Snyder *et al.* [13-19]), however, there is limited research conducted into the relevance of small molecule column characterisation techniques when working with peptides [20, 21]. A small study which looked at a range of artificial peptides without nearest neighbour effects on six stationary phases from one column manufacturer compared the results against a small molecule column characterisation database [20, 21]. The data suggested there was little correlation between the two approaches which highlights the necessity for analysing column performance with relevant probes (i.e. small molecule probes for small molecular work and peptides for peptide separations). Selectivity of peptides is also highly dependent on mobile phase, in particular pH, additives and type of organic modifier, however, there are no significant studies which combine all these factors to aid the chromatographic method development process.

1.2 Formation of Peptides

Amino acids contain a carboxylic acid and amine group backbone with a side chain (denoted R) which is specific to each amino acid. The side chain plays a crucial role in the properties of the compound, such as altering the pK_a or hydrophobicity. The

21 proteinogenic amino acids are shown below (*Figure 1*) and can be divided into different groups based on the side chain; aliphatic, hydroxyl / sulfur / selenium containing, cyclic, aromatic, basic and acidic / amide derivatives.

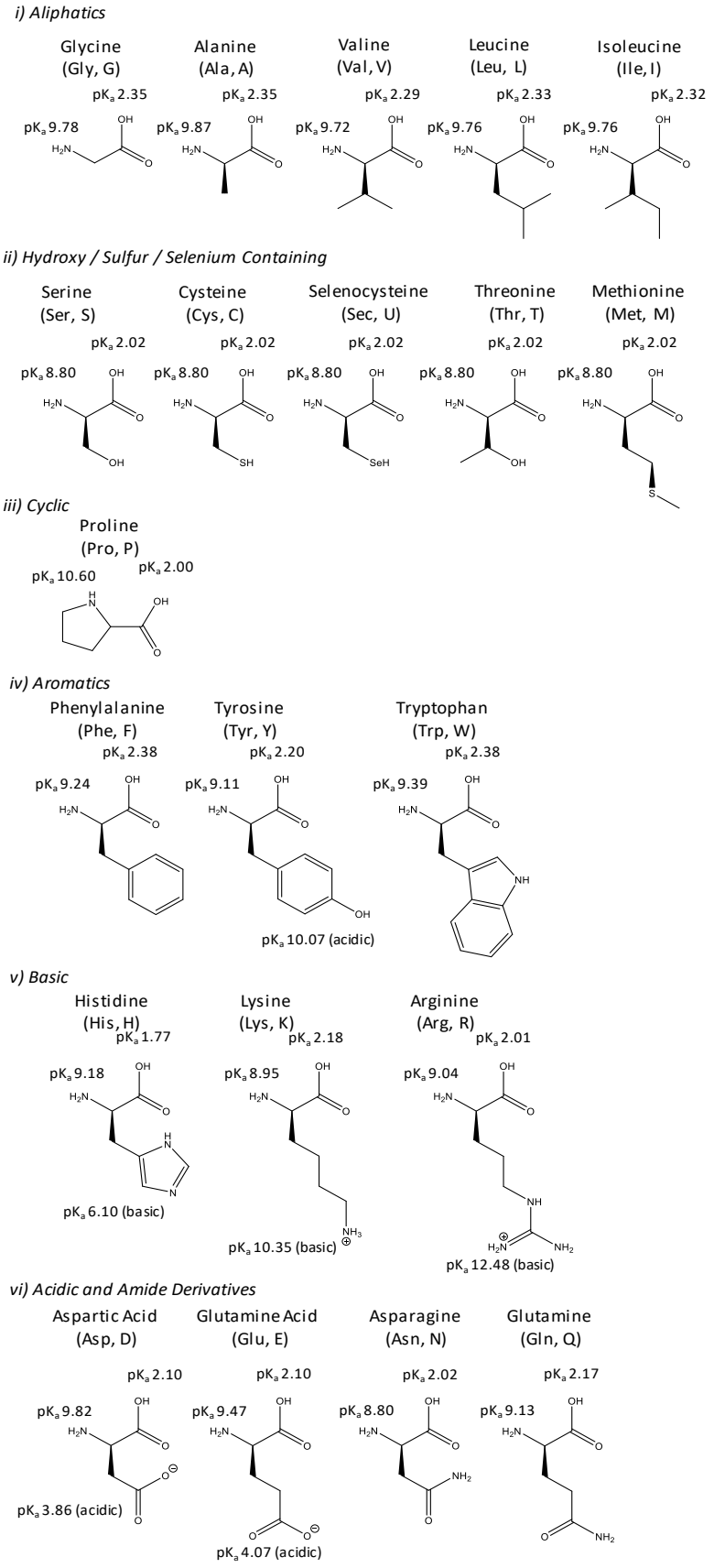

Figure 1 Structures of proteinogenic amino acids. [22]

The synthetic process for peptides has developed significantly over the last century, from solution-phase methods through to solid-phase peptide synthesis (SPPS), first conceived by Merrifield in 1963 [23]. It is an iterative process, demonstrated in *Figure 2*, where an amino acid is temporarily protected at the side chain and the alpha amino group to prevent polymerisation, and is covalently bonded to a resin. All by-products and excess reagents are removed by filtration, before removal of the amino protection group and further washing protocols. The next N-protected amino acid in the sequence is then coupled via the unprotected amine group of the amino acid on the solid phase, where the process continues until the desired peptide is complete. The side chains are then deprotected and resin washed, before the peptide is cleaved, typically with hydrofluoric acid (HF), from the resin.

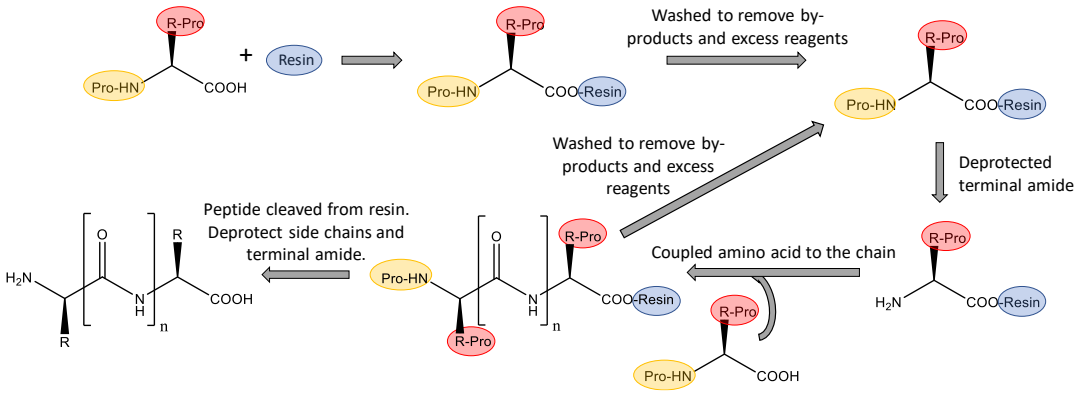

Figure 2 Schematic of the solid phase peptide synthesis pathway.

There have been some advances in the technique with new resins and protecting groups, but the fundamental approach is still the same [24, 25]. Solution-phase synthesis is still operational in a number of laboratories where large scale manufacturing is necessary, however, the golden standard is SPPS, with its automation, improved yields and comparatively short production cycles making it more advantageous in certain laboratories. Liquid phase synthesis is also limited in the number of amino acids in the sequence (~2-10 amino acids), whilst SPPS typically can produce 30-50 amino acid sequences on average. However, this is not to say SPPS does not have disadvantages. The cost of materials can be relatively higher than other methodologies and the chemistry must be extremely controlled in

order to avoid by-product formation and racemisation products, which can lead to complex impurity profiles. Another common problem is deletion peptides where an amino acid is missing because of a step failure.

To successfully synthesise a peptide with the correct sequence, amino acids require protecting groups. This should minimise side reactions which form undesirable products. The side chain must remain protected despite repetitive deprotection of the N^{α}-protecting group for further amino acid coupling. Therefore, the protecting group used on the side chains should utilise different deprotection conditions to the alpha amino group [26]. Desirable traits for the protecting groups include ease and efficiency of attaching and removing the group and the stability under reaction conditions. Merrifield first utilised carbobenzoxy (Cbz) as the N^{α}-protecting group which was created by Bergmann and Zervas (cited in [24]), before utilising *t*-butyloxycarbonyl (Boc) in 1967 [27]. The side chains, such as hydroxy and thiol moieties, were typically protected by benzyl based protecting groups (Bzl). Both Boc / Bzl protection groups require acidic conditions for deprotection, however, the benzyl-based group requires much stronger conditions, such as TFA, HF or hydrogenation [28-31]. The protecting group 9-fluorenylmethoxycarbonyl (Fmoc) was first suggested in 1970 by Carpino and Han as a base labile N^{α}-protection group, which provided orthogonal deprotecting conditions to the side chain protection group [32-35].

Specialised protecting groups are sometimes required for specific amino acids which are known to be problematic. For example, aspartic acid can undergo aspartimide formation if exposed to a strong base which then has the ability to form by-products under certain conditions. The formation is exacerbated if small, less bulky protecting groups are used, such as 1,1-diisopropylethyl (Die) [24, 26]. Recent developments in protecting groups suggest larger groups such as 5-butyl-5-nonyl (Bno) reduces the risk of the aspartimide formation but cannot eliminate the formation entirely [24]. Another example is histidine which is notorious for racemisation from the L- to the D- form. It is caused by the imidazole ring promoting the enolization of histidine active esters, therefore the imidazole ring

must be protected. A number of solutions have been suggested, however, they can have their own drawbacks such as expense and side reactions [26].

The selection of resin can also be crucial for the synthesis of peptides, with an abundance of options available [36, 37]. The most common resin is polystyrene with 1-2% divinylbenzene (DVB) as a crosslinking agent, which improves the stability of the support to most common solvents. Alternative supports of note include Merrifield resin (a chloromethylated polystyrene), Wang resin (mostly used for acidic substrates with a 4-hydroxybenzyl alcohol linker) and Rink resin (a TFA labile resin typically used with Fmoc peptides) [24].

An alternative to synthetic pathways for the production of peptides is to use recombinant methodologies using bacterial or mammalian cell cultures [38-40]. This approach is quite frequently required for peptides which have greater than 25-50 amino acids, to prepare acceptable purity and yields. Bacterial cell cultures, such as the commonly used *Escherichia coli*, are often advantageous for their rapid production and ease of use whilst mammalian cells allow for the expression of peptides and proteins with post translational modifications (PTM) similar to those found in humans. The main difference between these two types of cultures are the cellular anatomy, where bacterial cells don't possess the same organelles as mammalian cells (i.e. nucleus or Golgi apparatus) which influence its ability to perform PTM. Selection of the culture is often based on the aim of the synthesis (i.e. sufficient yield, speed, or PTM).

1.3 Challenges in Analysing Peptides

Peptides present a different analytical challenge to small molecules, due to their size and physico-chemical properties, which can influence the degree of interaction in the separation. This is in addition to the peptide kinetics which can reduce the mass transfer of peptides, as further explained below.

A change in functional group on a small molecule (e.g. by a change in pH that deprotonates a carboxylic acid side chain) will display large differences in

chromatographic properties since the change constitutes a large change of the structure of the molecule. For a peptide, such a change of one functional group may result in a relatively small change in retention since this modification only takes place for a relatively small part of a large molecule, particularly if there is a higher order structure which can hinder access to functional groups. This limitation on the selectivity of the peptide increases the difficulty of the separation.

Mobile phase additives can be critical to selectivity, however, proteins often contain ions which form insoluble salts with phosphate buffers at high and mid pH. An example of such is calmodulin which contains Ca^{2+} and zinc finger which contains Zn^{2+} ions [41, 42]. This can limit the additives required for maximum selectivity differences. Proteins are also affected by extreme conditions, i.e. low / high pH, high % MeCN or high temperature, where the structure of the protein can either change (i.e. denature) or fall apart [43, 44]. A change to the higher order structure of the protein can lead to aggregation and even precipitation.

Large peptides have low chromatographic efficiency and diffuse slowly, thus a large mass transfer term in the expanded van Deemter (Equation 1), which results in broad peaks. A van Deemter plot allows column performance to be evaluated and compared whilst also determining the optimum linear velocity [45].

$$H = 2\lambda d_p + 2\frac{\gamma D_m}{v} + \frac{\omega d_p^2}{D_m} v \qquad \textit{Equation 1}$$

where H is the plate height, λ is particle shape, d_p is particle size, γ and ω are constants, D_m is the diffusion coefficient of the mobile phase, and v is the linear velocity in mm/sec, determined by dividing the length of the column by the retention of an unretained species (t_m). The first term correlates to the eddy diffusion and mobile phase mass transfer effects, the second term relates to the longitudinal molecular diffusion, and the third term connects to the mass transfer resistance which describes the interaction of the compounds with the stationary phase. Plate height (H) is a measure of column efficiency per unit length of column, which can be converted to reduced plate height by dividing H by the particle size

(d_p). Eddy diffusion is a contributing factor to band broadening which describes the multiple flow paths available through the column for the mobile phase or analyte. It is highly dependent on the particle size distribution and the uniformity of the packed column bed. A poorly packed bed generates different flow paths which can cause the band to spread by molecules lagging or accelerating through faster streams. An efficiently packed bed, however, has a uniform flow path which keeps the band packed closer together, thus reducing band broadening and increase chromatographic performance. Longitudinal diffusion is time dependent, where the longer the analyte band is in the system (i.e. low linear velocities or long / wide tubing is used), the more the band is dispersed, which reduces the chromatographic efficiency. The final term in the van Deemter, mass transfer, is a measure of the molecular diffusion into the pores of the stationary phase. Molecules will penetrate into the pores to differing degrees which then cause the band to broaden. This effect is reduced at lower linear velocities and exacerbated at high linear velocities. The use of smaller particle sizes can also reduce the mass transfer term, where smaller particles have a shorter diffusion pathway thus allowing faster diffusion of the molecule into the pores of the particle. The speed of the process of entering the pores and returning to the bulk solvent is increased which reduces band spreading, thus chromatographic performance increases.

The curve of three compounds with different molecular weights was simulated, to highlight the differences in each of the van Deemter terms (*Figure 3*). The larger molecular weight compounds have a sharp increase in the mass transfer term, and a narrow range for the optimum linear velocity, which limits the potential efficiency window. The optimal velocity for most peptides and certainly for proteins also becomes very low and results in extremely long retention times, which is not realistic to use for practical separations. The smaller solute, however, has a flatter mass transfer term, which provides a larger range for linear velocity, therefore wider window for maximum performance. Simulated data was based on calculated diffusion coefficients. It is possible to generate experimental data, however, large proteins respond strongly to small changes in organic and also display poor peak

shape, which makes generation of data more difficult to compile than for small molecules.

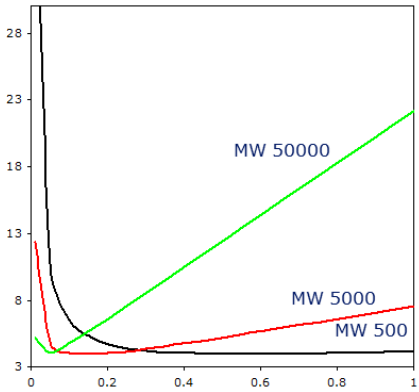

Figure 3 Simulated van Deemter data for molecules of differing molecular weight on a 1.7 µm packing material (Data produced by Novo Nordisk).

The strong response to small changes in organic can be rationalised based on the relationship described in Reference [46], and visualised in *Figure 4*. Snyder explained the relationship of *Equation 2,* where *k** is the average retention factor during gradient elution, *ø** is the corresponding value of *ø*, and k_w and *S* are constants for a given compound. As the molecular weight increases, the constant, *S*, increases. The increased value of *S* can have dramatic changes in k with only small changes in the organic, as demonstrated in *Figure 4*, where the 100 kDa compound has a much steeper decline in retention factor with a small increase in organic compared to the 100 Da molecule.

$$log\, k^* = log\, k_w - S\emptyset^* \qquad \textit{Equation 2}$$

$$S \approx 0.25(MW)^{0.5} \qquad \textit{Equation 3}$$

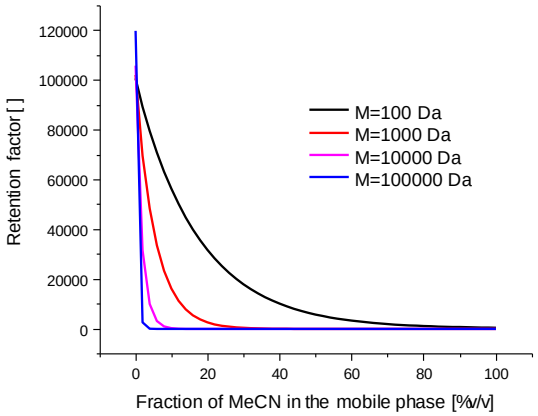

Figure 4 Isocratic retention factor versus amount of organic modifier for molecules of different size. All assumed to have strong retention in totally aqueous conditions (that is, logK_0 is assumed to be 5).

1.4 Aims and Objectives

This study will focus on gaining a greater understanding of peptides. It is a possibility that the understanding gained from this study could be used as stepping stone to a better insight into protein separations, however, due to size and folding / tertiary structure, peptides and proteins are likely to behave differently.

Peptides are complex compounds which cannot be analysed as small molecules. Despite a range of models appearing which aim to predict retention of peptides, there is very little literature which specifically aims to help provide a guide to method development for peptides in regard to column and mobile phase selection. As such, this research aims to design relevant peptides to probe reversed phase stationary phases. This includes observing general mechanisms but also more specifically looking at separations involving degradation and isomeric species. By producing suitable chromatographic conditions, a peptide characterisation protocol can be devised, known as the Peptide RPC Column Characterisation Protocol, which can be compared against protocols defined for small molecules. Evaluation of stationary phases using the peptide-based protocol can provide significant information regarding maximum selectivity differences for method development. Also, in aid of method development, a column database can be created from the Peptide RPC Column Characterisation Protocol to determine suitable column

selection for screening and help identify backup columns which is critical for the chemistry, manufacturing and controls (CMC) life cycle management. The database will be validated by using the information to select chromatographically similar stationary phases to act as “back-up” columns to produce comparable chromatographic profiles of peptides. It can also be validated by selected chromatographically dissimilar stationary phases which can produce different peptide profiles, ideal for method development strategies. The results from the peptide-based column characterisation protocol will be critically evaluated against two small molecule column characterisation protocols to determine if there is any correlation between the probes. A lack of correlation is desirable to highlight the necessity of a peptide-based approach.

The second stage of this research shall focus on the effect of mobile phases on selectivity for peptide separations. The specifically designed probes employed to interrogate the stationary phases shall also be applied to the mobile phases to assess chromatographic performance (i.e. peak capacity and peak symmetry) and evaluate selectivity differences. This comprehensive study will observe the effects of organic, ion pairing reagents, pH, buffers and salts. Acetonitrile is quite typically selected as the organic component of the mobile phase for peptide methods partially due to its volatility, low viscosity and strong eluting strength. However, methanol or isopropanol / acetonitrile mixtures could offer viable alternatives which are seldom explored for maximising selectivity, as demonstrated by Hodges’ *et al*. who observed differences in peptide elution profiles when substituting acetonitrile for methanol [21]. Some of the most commonly applied additives include phosphate salt-based systems and ion pairs, such as TFA [47, 48]. They typically offer advantages such as improved peak shape provided by their higher ionic strength. The exploration of additional ion pairs, such as triethylamine (TEA) and heptafluorobutyric acid (HFBA), or kosmotropic / chaotropic salts, such as ammonium sulfate and sodium perchlorate respectively, is essential for providing a rational pathway for method development and understanding how to gain substantial selectivity differences for complex samples such as peptides. The most diverse range of mobile phases will then be applied to a selection of stationary

phases which were deemed to be chromatographically diverse by the peptide-based column characterisation database. The effect of temperature on the select few mobile phases and columns will also be observed, which can aid a greater understanding of the contribution of temperature in relation to mobile phase.

2. Materials and Methods

2.1 Chromatographic Instrumentation

Unless otherwise specified, analyses were performed on a Shimadzu Nexera X2 equipped with binary pumps (LC-30AD, S/N L20555472999 and L20555473004), degassers (DGU-20A$_{5R,}$ S/N L20705466800 and L20705466811), Prominence column oven with column switch (CTO-20AC, S/N L20215477201 and FCV-14AH, S/N L20215465470, respectively), autosampler (SIL-30AC, S/N L20565471427), diode array detector (SPD-M30A, S/N L20775470238) and communication bus module (CBM-20A, S/N L20235478166) (Shimadzu UK Limited, Milton Keynes, UK). A Shimadzu Mass Spectrometer single quadrupole (LCMS 2020, S/N O10155470152) was used as a secondary detector. The software used to control the LC system was LabSolutions (Version 5.86). System dispersion and dwell volume can be seen in *Table 20*.

2.2 Balances

An Avery Weigh-Tronix Reflex HP-220DC (hence forth known as the 4 decimal place (d.p.) balance) or an Avery Weigh-Tronix Reflex HP4200C (hence forth known as the 2 d.p. balance, Avery Weigh-Tronik, Smethwick, UK) was used to measure all masses. Both balances operate full-automatic calibration daily, however, additional calibration was performed periodically using weights of known quantity between 1 mg to 100 g to ensure the integrity of the automatic calibration.

2.3 pH Meter

pH measurements were determined using a Jenway 3310 pH meter (Cole-Parmer, Stone, UK), which was calibrated between pH 7 and 2 (Certipur ®, VWR International LLC, Darmstadt, Germany). Care was taken to prevent contamination using the pH probe by flushing the probe with deionised water.

2.4 Pipetman P1000L

The Pipetman P1000L (Gilson Scientific Ltd, Dunstable, UK) was calibrated before every use to ensure an accurate volume was dispensed. It is specified by the

manufacturer to be accurate between 100 to 1000 µL to ±1.00% and ±0.6%, respectively. The Pipetman dispensed 1000 µL of water at ambient temperature which was weighed using the 4 d.p. balance to confirm 1.000 g (±0.0011 g based on six repeat measures) was delivered.

2.5 Solvents and Reagents used for Samples and Mobile Phases

Table 1 Sample chemicals

Chemical / Reagent	Manufacturer	Batch / Lot Number
Acetone, >99.8%	Honeywell (Seelze, Germany)	SZBG200AH
Acquity UPLC Absorb Start-up Solution	Waters	186006683
Phenol, 99%	Sigma Aldrich (Poole, UK)	131773612507040
Benzyl alcohol, 99%	ACROS Organics (Geel, Belgium)	A0402997
Uracil, >99%	Sigma Aldrich (Poole, UK)	SLBD1250V
Toluene, >99.5%	Sigma Aldrich (Poole, UK)	SHBH1932V
Benzene sulfonic acid, 98%	Sigma Aldrich (Poole, UK)	BCBR6772V
Pentylbenzene, 96%	Alfa Aesar (Heysham, UK)	10215513
Butylbenzene, >99%	Sigma Aldrich (Poole, UK)	00941853V
o-Terphenyl, 99%	Sigma Aldrich (Poole, UK)	-
Triphenylene, 98%	ACROS Organics (Geel, Belgium)	A0398951
Benzylamine hydrochloride, 99%	Sigma Aldrich (Poole, UK)	BCBV5878
Caffeine, 99%	Sigma Aldrich (Poole, UK)	1317736
Nitrobenzene, analytical standard	Sigma Aldrich (Poole, UK)	-
1,2-Dinitrobenzene, >99%	Sigma Aldrich (Poole, UK)	SZBF139XV
1,3-Dinitrobenzene, analytical standard	Sigma Aldrich (Poole, UK)	SZBD071XV
1,4-Dinitrobenzene, 98%	Sigma Aldrich (Poole, UK)	SZBD221XV
1,3,5-Trinitrobenzene, certified reference	Supelco (Bellefonte, USA)	LC08343V
Bovine GLP-2 (1-15)*	Apigenex (Prague, Czech Republic)	-
[D-His1]-Bovine GLP-2 (1-15)*	Apigenex (Prague, Czech Republic)	-
[L-Asp3]-Bovine GLP-2 (1-15)*	Apigenex (Prague, Czech Republic)	-
[L-isoAsp3]-Bovine GLP-2 (1-15)*	Apigenex (Prague, Czech Republic)	-
[D-isoAsp3]-Bovine GLP-2 (1-15)*	Apigenex (Prague, Czech Republic)	-
[D-Ser5]-Bovine GLP-2 (1-15)*	Apigenex (Prague, Czech Republic)	-
[D-Ser7]-Bovine GLP-2 (1-15)*	Apigenex (Prague, Czech Republic)	-
[Met(O)10]-Bovine GLP-2 (1-15)*	Apigenex (Prague, Czech Republic)	-
[L-Asp11]-Bovine GLP-2 (1-15)*	Apigenex (Prague, Czech Republic)	-
[D-Asp11]-Bovine GLP-2 (1-15)*	Apigenex (Prague, Czech Republic)	-
[L-isoAsp11]-Bovine GLP-2 (1-15)*	Apigenex (Prague, Czech Republic)	-
[D-isoAsp11]-Bovine GLP-2 (1-15)*	Apigenex (Prague, Czech Republic)	-
Bovine GLP-2 (16-33)*	Apigenex (Prague, Czech Republic)	-

[D-Ser16]-Bovine GLP-2 (16-33)*	Apigenex (Prague, Czech Republic)	-
[Ile26,Leu27]-Bovine GLP-2 (16-33)*	Apigenex (Prague, Czech Republic)	-
[Gly22]-Bovine GLP-2 (16-33)*	Apigenex (Prague, Czech Republic)	-
[D-Asp21,Gly22]-Bovine GLP-2 (16-33)*	Apigenex (Prague, Czech Republic)	-
[L-isoAsp21,Gly22]-Bovine GLP-2 (16-33)*	Apigenex (Prague, Czech Republic)	-
[D-isoAsp21,Gly22]-Bovine GLP-2 (16-33)*	Apigenex (Prague, Czech Republic)	-
[Val26]-Bovine GLP-2 (16-33)*	Apigenex (Prague, Czech Republic)	-
[Ile26]-Bovine GLP-2 (16-33)*	Apigenex (Prague, Czech Republic)	-
[Phe26]-Bovine GLP-2 (16-33)*	Apigenex (Prague, Czech Republic)	-
[Trp26]-Bovine GLP-2 (16-33)*	Apigenex (Prague, Czech Republic)	-
[Tyr26]-Bovine GLP-2 (16-33)*	Apigenex (Prague, Czech Republic)	-
[Lys20]-Bovine GLP-2 (16-33)*	Apigenex (Prague, Czech Republic)	-
[Lys26]-Bovine GLP-2 (16-33)*	Apigenex (Prague, Czech Republic)	-
Trypsin, USP from bovine pancreas	Sigma Aldrich (Poole, UK)	SLBR5744V
Carbonic anhydrase, bovine	Sigma Aldrich (Poole, UK)	SLBR4228V
Insulin from bovine pancreas	Sigma Aldrich (Poole, UK)	SLBW1822

* Peptides supplied as freeze-dried material in the TFA salt form.

Table 2 Mobile phase reagents and solvents

Chemical / Reagent	Manufacturer	Batch / Lot Number
Water, MilliQ	Millipore (Molshiem, France)	F3SA79023A
Water, LC-MS grade	Honeywell (Seelze, Germany)	H1530
Isopropanol, LC-MS grade	Honeywell, (Seelze, Germany)	K49039481
Methanol, LC-MS grade	Honeywell (Seelze, Germany)	SZBG291BH
Acetonitrile, LC-MS grade	Honeywell (Seelze, Germany)	SZBG230S
Acetic acid, HPLC grade	Sigma Aldrich (Poole, UK)	I046BIL
Ammonia (25% w/w), LC-MS grade	Sigma Aldrich (Poole, UK)	Z0442730 719
Ammonium acetate, LC-MS grade	Sigma Aldrich (Poole, UK)	BCBZ6101
Ammonium carbonate. LC-MS grade	Sigma Aldrich (Poole, UK)	SLBV1392
Ammonium formate, LC-MS grade	Sigma Aldrich (Poole, UK)	BCBT8380
Ammonium phosphate monobasic, HPLC grade	Sigma Aldrich (Poole, UK)	BCBW0622
Ammonium phosphate dibasic, HPLC grade	Sigma Aldrich (Poole, UK)	BCBW9374
Ammonium sulfate, ACS grade	Sigma Aldrich (Poole, UK)	BCBX0577
Buffer solution pH 2.0	VWR (Darmstadt, Germany)	HC73532112
Buffer solution pH 7.0	VWR (Darmstadt, Germany)	HC74406602
Difluoroacetic acid, LC-MS grade	Waters	-
Dimethyl sulfoxide (anhydrous), HPLC grade	Alfa Aesar (Haverhill, USA)	W23B668
Formic acid, LC-MS grade	Sigma Aldrich (Poole, UK)	H1630
Heptafluorobutyric acid, >99.5%	Sigma Aldrich (Poole, UK)	BCBV8424
Hydrochloric acid (37% w/w), ACS reagent	Sigma Aldrich (Poole, UK)	1350615
Methane sulfonic acid, >99%	Sigma Aldrich (Poole, UK)	STBH6537
Potassium phosphate monobasic, HPLC grade	Sigma Aldrich (Poole, UK)	SLBR5465V
Phosphoric acid (85% w/w), FG grade	Sigma Aldrich (Poole, UK)	STBC3341V
Potassium hydroxide, analysis grade	Alfa Aesar (Haverhill, USA)	A18854
Triethylamine, Puriss grade	Sigma Aldrich (Poole, UK)	STBH8268
Trifluoroacetic acid, LC-MS grade	ThermoFisher	I3230
TRIS buffer, primary standard	Sigma Aldrich (Poole, UK)	SLBW7403
TRIS HCl, reagent grade	Sigma Aldrich (Poole, UK)	SLBW1307
Sodium butane-1-sulfonic acid	Sigma Aldrich (Poole, UK)	BCBW1477
Sodium chloride, Puriss grade	Sigma Aldrich (Poole, UK)	STBH7768 804
Sodium sulfate, ACS reagent	Merck (Darmstadt, Germany)	A0134649 026
Sodium perchlorate, ACS reagent	Merck (Darmstadt, Germany)	A1190564
Uracil, >99.0%	Sigma Aldrich (Poole, UK)	SLBD1250V

2.6 LC Characterisation

2.6.1 Dwell Volume Determination Operating Conditions

Mobile Phase: Line A: Water

Line B: Uracil (5 mg/L) in Water.

Gradient:

Time (mins)	%B
0.0	10
5.0	10
15.0	20
20.0	20
20.5	10
25.0	10

Flow Rate: 0.3 mL/min

Oven Temperature: 22 °C

Sample: Water

Injection Volume: 1 µL

Wavelength: 265 nm (8) Ref 360, 100.

Column: ZDV union plus 2 m red peek tubing (0.125 mm I.D.) for added back pressure.

Three repeat injections were performed after the system was fully stabilised.

2.6.2 Dispersion Operating Conditions

Mobile Phase: Water / Methanol (51:49 v/v)

Flow Rate: 0.1 mL/min

Oven Temperature: 40 °C

Sample: 0.1% v/v acetone in water

Injection Volume: 0.5 µL

Wavelength: 254 nm (8) Ref 360, 100.

Column: ZDV union

Six repeat injections were performed after the system was fully stabilised.

2.6.3 Autosampler Accuracy Operating Conditions

Mobile Phase: A: Water

B: Acetonitrile

Gradient:

Time (mins)	%B
0.0	10
5.0	90
6.0	90
7.0	10
10.0	10

Flow Rate: 1 mL/min

Oven Temperature: 60 °C

Sample: Acquity UPLC Absorb Start-Up Solution

Injection Volume: 10 µL

Wavelength: 254 nm (8) Ref 360, 100.

Column: Agilent Zorbax SB-C18, 5 µm, SN USFA002732

50 x 4.6 mm

Six repeat injections were performed after the system was fully stabilised.

2.7 Extended Tanaka Characterisation Protocol for 150 x 2.1 mm Column Formats

2.7.1 Mobile Phase Preparation

2.7.1.1 Potassium Phosphate pH 2.5 Stock Buffer Preparation

A 50 mM potassium phosphate monobasic stock solution was prepared by weighing 6.27 g on the 2 d.p. balance, which was dissolved in approximately 800 mL MilliQ water using a magnetic stirrer. Phosphoric acid (85% w/w) was added dropwise to lower the pH to 2.5, where pH was determined using a Jenway 3310 pH meter (*Section 2.3*). The solution was made to 1 L volume using MilliQ water.

2.7.1.2 Potassium Phosphate pH 2.7 Stock Buffer Preparation

A 200 mM potassium phosphate monobasic stock solution was prepared by weighing 27.22 g on the 2 d.p. balance, which was dissolved in approximately 800 mL MilliQ water using a magnetic stirrer. Phosphoric acid (85% w/w) was added dropwise to lower the pH to 2.7, where pH was determined using a Jenway 3310 pH meter (*Section 2.3*). The solution was made to 1 L volume using MilliQ water.

2.7.1.3 Potassium Phosphate pH 7.6 Stock Buffer Preparation

A 200 mM potassium phosphate monobasic stock solution was prepared by weighing 27.22 g on the 2 d.p. balance, which was dissolved in approximately 800 mL MilliQ water using a magnetic stirrer. Potassium hydroxide solution was added dropwise to change the pH to 7.6, where pH was determined using a Jenway 3310 pH meter (*Section 2.3*). The solution was made to 1 L volume using MilliQ water.

2.7.1.4 Premixed Mobile Phase: Potassium Phosphate Monobasic in Methanol / Water Mixtures

The ensuing premixed mobile phases were produced by measuring the HPLC grade solvents in the following ratios using Grade A measuring cylinders. The solutions were shaken to ensure thorough mixing.

Table 3 Buffered mobile phase preparation for the Extended Tanaka protocols

Mobile Phase	HPLC Grade Water (mL)	HPLC Grade Methanol (mL)	Buffer (mL)
5 mM Potassium Phosphate Monobasic pH 2.5 in Methanol / Water (65:35 v/v)	250	650	100 (*Section 2.7.1.1*)
20 mM Potassium Phosphate Monobasic pH 2.7 in Methanol / Water (30:70 v/v)	600	300	100 (*Section 2.7.1.2*)
20 mM Potassium Phosphate Monobasic pH 7.6 in Methanol / Water (30:70 v/v)	600	300	100 (*Section 2.7.1.3*)

2.7.1.5 Premixed Mobile Phase: Organic / Water Mixtures

The ensuing premixed mobile phases were produced by measuring the HPLC grade solvents in the following ratios using Grade A measuring cylinders. The solutions were shaken to ensure thorough mixing.

Table 4 Premixed organic / water preparation

Mobile Phase	HPLC Grade Water (mL)	HPLC Grade Organic (mL)
Methanol / Water (80:20 v/v)	200	800
Methanol / Water (50:50 v/v)	500	500
Methanol / Water (40:60 v/v)	600	400
Methanol / Water (30:70 v/v)	700	300
Acetonitrile / Water (50:50 v/v)*	500	500

*Used for a column flush at the end of each sequence.

2.7.2 Operating Conditions and Sample Preparation

All methods utilised a flow rate of 0.21 mL/min, a column temperature of 40 °C, injection volume of 1 µL and wavelength detection at 210 and 254 nm (8) ref 360, 100. The specific mobile phase and samples used per test are shown below [17-19, 49, 50]:

Hydrophobicity and Shape Selectivity

Mobile Phase: Methanol / Water (80:20 v/v)

Sample:

Test Mix	Compound	Concentration	Quantity in Test Mix
A	Pentylbenzene	0.6 µL/mL MeOH	500 µL
	Butylbenzene	0.4 µL/mL MeOH	500 µL
B	o-Terphenyl	0.5 mg/mL MeOH	500 µL
	Triphenylene	0.5 mg/mL MeOH	500 µL

Hydrogen Bonding

Mobile Phase: Methanol / Water (30:70 v/v)

Sample:

Test Mix	Compound	Concentration	Quantity in Test Mix
C	Caffeine	0.5 mg/mL MeOH/H_2O (30:70 v/v)	500 µL
	Phenol	1.0 mg/mL MeOH/H_2O (30:70 v/v)	500 µL

Cation Exchange Capacity

Mobile Phase: 20 mM KH_2PO_4 pH 2.7 or 7.6 in Methanol / Water (30:70 v/v)

Sample:

Test Mix	Compound	Concentration	Quantity in Test Mix
D	Phenol	0.5 mg/mL MeOH/H_2O (30:70 v/v)	200 µL
	Benzylamine hydrochloride	0.5 mg/mL MeOH/H_2O (30:70 v/v)	200 µL
	Benzyl alcohol	0.3 µL/mL MeOH/H_2O (30:70 v/v)	500 µL

Nitro-Aromatic

Mobile Phase: Methanol / Water (50:50 v/v)

Sample:

Test Mix	Compound	Concentration	Quantity in Test Mix
E	Toluene	0.6 µL/mL MeOH	300 µL each plus 300 µL MeOH
	Nitrobenzene	0.3 µL/mL MeOH	
	1,3-Nitrobenzene	0.3 mg/mL MeOH	
	1,3,5-Trinitrobenzene	0.25 mg/mL MeOH	

Dinitro-Aromatics

Mobile Phase: Methanol / Water (40:60 v/v)

Sample:

Test Mix	Compound	Concentration	Quantity in Test Mix
F	Toluene	0.6 µL/mL MeOH	150 µL each plus 600 µL MeOH
	1,2-Dinitrobenzene	0.2 mg/mL MeOH	
	1,3-Dinitrobenzene	0.3 mg/mL MeOH	
	1,4-Dinitrobenzene	0.5 mg/mL MeOH	

Acidic Character

Mobile Phase: 5 mM KH_2PO_4 pH 2.5 in Methanol / Water (65:35 v/v)

Sample:

Test Mix	Compound	Concentration	Quantity in Test Mix
G	Phenol	0.3 mg/mL MeOH / H_2O (1:1 v/v)	200 µL
	Benzyl alcohol	0.3 µL/mL MeOH / H_2O (8:2 v/v)	200 µL
	Toluene	0.3 µL/mL MeOH / H_2O (1:1 v/v)	200 µL
	Benzene sulfonic acid	0.3 mg/mL H_2O	200 µL

2.8 System Suitability Test (SST) Conditions for a 150 x 2.1 mm Column Format

2.8.1 Mobile Phase Preparation

2.8.1.1 Premixed Mobile Phase: Formic Acid Gradient

The mobile phase used online A was 0.1% formic acid v/v in water which was produced as follows:

1000 µL LC-MS grade formic acid was accurately dispensed using a Pipetman P1000L into LC-MS grade water and made to 1000 mL volume with LC-MS grade water using a grade A measuring cylinder.

The mobile phase online B was 0.1% formic acid v/v in acetonitrile which was produced as follows:

1000 µL LC-MS grade formic acid was accurately dispensed using a Pipetman P1000L into LC-MS grade acetonitrile and made to 1000 mL volume with LC-MS grade acetonitrile using a Grade A measuring cylinder.

2.8.2 LC Retention Modelling of SST Conditions

2.8.2.1 Instrumentation

The SST conditions were optimised on a Waters H-Class binary system at Novo Nordisk in Denmark, with a 250 µL TFA mixer, and a dwell of 0.53 mL.

2.8.2.2 Method Development Operating Conditions

Mobile Phase: As described in *Section 2.8.1.1*

Gradient:

Input Time 1 (mins)	Input Time 2 (mins)	Validation Time (mins)	%B
0.0	0.0	0.0	5
10.0	30.0	20.0	95
12.0	32.0	22.0	95
12.1	32.1	22.1	5
24.1	54.1	44.1	5

Flow Rate: 0.3 mL/min

Oven Temperature: 40 °C

Sample: See *Section 2.8.3*

Injection Volume: 1 µL

Wavelength: 215 nm (8) Ref 360, 100.

Autosampler Cooler: 10 °C (used to reduce evaporation of volatile analytes).

Stationary Phases:

Stationary Phase	Serial Number
[1]Acquity HSS C18, 1.8 µm	01443619715737
[1]Acquity HSS C18-SB, 1.8 µm	01223609816614
[1]Acquity BEH C4, 1.7 µm	01273618718211
[1]Acquity CSH Fluorophenyl, 1.7 µm	01123618118013
[2]Polaris Amide C18, 3 µm	461575

[1] 150 x 2.1 mm, [2] 150 x 2.0 mm

2.8.2.3 Developed Method Operating Conditions

The SST utilised the following chromatographic conditions:

Mobile Phase: As described in *Section 2.8.1.1*

Gradient:

Time (mins)	%B
0.0	5
20.0	100
22.0	100
22.1	5
24.1	5

Flow Rate: 0.3 mL/min

Oven Temperature: 40 °C

Sample: See *Section 2.8.3*

Injection Volume: 1 µL

Wavelength: 215 nm (8) Ref 360, 100.

Autosampler Cooler: 10 °C (used to reduce evaporation of volatile analytes).

2.8.3 Sample Preparation

Table 5 Sample preparation for the System Suitable Test mix.

Compound	Concentration	Quantity in Test Mix (µL)
Uracil	0.3 mg/mL MeOH / H_2O (1:1 v/v)	200
Benzene sulfonic acid	0.3 mg/mL H_2O	200
Benzyl alcohol	0.3 µL/mL MeOH / H_2O (8:2 v/v)	200
Benzylamine hydrochloride	0.5 mg/mL MeOH / H_2O (30:70 v/v)	200
Butylbenzene	0.4 µL/mL MeOH	500
Caffeine	0.5 mg/mL MeOH / H_2O (30:70 v/v)	500
Pentylbenzene	0.6 µL/mL MeOH	500
Phenol	0.3 mg/mL MeOH / H_2O (1:1 v/v)	200
Toluene	0.3 µL/mL MeOH / H_2O (1:1 v/v)	200

2.9 Development of the Peptide RPC Column Characterisation Protocol

2.9.1 LC Retention Modelling Mobile Phase Preparation

2.9.1.1 Ammonium Formate Native pH Stock Solution

A 200 mM ammonium formate stock solution was prepared by weighing 12.61 g on the 2 d.p. balance, which was dissolved in approximately 800 mL LC-MS grade water using a magnetic stirrer. The solution was made to 1 L volume using LC-MS grade water, gravimetrically. pH of the native solution was recorded using a Jenway 3310 pH meter (*Section 2.3*).

2.9.1.2 Premixed Mobile Phase: Ammonium Formate Gradient

The mobile phase used online A for the development of the Peptide RPC Column Characterisation Protocol was 20 mM ammonium formate in water which was produced as follows:

900.00 g of LC-MS grade water (density 1 g/cm^3) was accurately weighed on the 2 d.p. balance and combined with 100.00 g of the ammonium formate buffer described in *Section 2.9.1.1*.

The mobile phase used online B was 20 mM ammonium formate in acetonitrile / water (90:10 w/w) was produced as follows:

707.40 g of LC-MS grade acetonitrile (density 0.786 g/cm^3) was accurately weighed on the 2 d.p. balance and combined with 100.00 g of the ammonium formate buffer described in *Section 2.9.1.1*.

2.9.1.3 Premixed Mobile Phase: Formic Acid Gradient

The mobile phase used online A was 0.1% formic acid v/v in water which was produced as follows:

1000 µL LC-MS grade formic acid was accurately dispensed using a Pipetman P1000L, which was checked using a balance each day to minimise variation, into 999.00 g of LC-MS grade water.

The mobile phase online B was 0.1% formic acid v/v in acetonitrile which was produced as follows:

1000 µL LC-MS grade formic acid was accurately dispensed using a Pipetman P1000L, which was checked using a balance each day to minimise variation, into 785.21 g of LC-MS grade acetonitrile.

2.9.2 LC Retention Modelling Conditions for the Peptide RPC Column Characterisation Protocol

2.9.2.1 Instrumentation

The LC conditions for the Peptide RPC Column Characterisation Protocol were optimised on a Waters H-Class binary system at Novo Nordisk in Denmark, with a 250 µL TFA mixer, and a dwell of 0.53 mL. The MS conditions were optimised using the instrument described in *Section 2.1*.

2.9.2.2 LC Retention Modelling using Ammonium Formate and Formic Acid

Mobile Phase: As described in *Section 2.9.1.2* for ammonium formate

As described in *Section 2.9.1.3* for formic acid.

Gradient:

Input Time 1 (mins)	Input Time 2 (mins)	Validation Time (mins)	%B
0.0	0.0	0.0	10
10.0	30.0	20.0	50
12.0	32.0	22.0	50
12.1	32.1	22.1	10
24.1	54.1	44.1	10

Flow Rate: 0.3 mL/min

Oven Temperature: 40 °C

Sample:

Peptide	Concentration	Volume
Bovine GLP-2 (1-15 Bovine GLP-2 (16-33) [Trp26]-Bovine GLP-2 (16-33) [Lys26]-Bovine GLP-2 (16-33)	0.25 mg/mL in DMSO/H_2O (80:20 v/v)	1:1:1:1 v/v/v/v

Injection Volume: 1 µL

Wavelength: 215 nm (8) Ref 360, 100.

Autosampler Cooler: 10 °C (to ensure maximum stability of the peptides).

Stationary Phases:

Stationary Phase	Serial Number
[1]Acquity HSS C18, 1.8 µm	01443619715737
[1]Acquity HSS C18-SB, 1.8 µm	01223609816614
[1]Acquity BEH C4, 1.7 µm	01273618718211
[1]Acquity CSH Fluorophenyl, 1.7 µm	01123618118013
[2]Polaris Amide C18, 3 µm	461575

[1] 150 x 2.1 mm, [2] 150 x 2.0 mm

2.9.2.3 MS Operating Parameters Design of Experiment

See *Section 2.9.3* for the LC operating conditions.

Stationary Phases: [1]Acquity HSS C18, 1.8 µm, S/N 01443619715737

[2]Polaris Amide C18, 3 µm, S/N 461575

[1]150 x 2.1 mm, [2]150 x 2.0 mm

MS Mode: Selected ion monitoring (SIM), Positive mode

Sample:

Peptide	*m/z*	Concentration	Volume
Bovine GLP-2 (1-15	$[M+2H]^+$ 820	0.25 mg/mL in DMSO/H_2O (80:20 v/v)	1:1:1:1 v/v/v/v
Bovine GLP-2 (16-33)	$[M+2H]^+$ 1068		
[Trp26]-Bovine GLP-2 (16-33)	$[M+2H]^+$ 1105		
[Lys26]-Bovine GLP-2 (16-33)	$[M+2H]^+$ 1076		

Design of Experiments:

Table 6 Design of Experiment conditions for investigating the important factors for the mass spectrometer.

Exp No	Exp Name	Run Order	Drying Gas (L/min)	Heat Block (°C)	DL Temp (°C)	Nebulizing Gas (L/min)
1	N1	3	5	100	100	0.5
2	N2	10	15	100	100	1.5
3	N3	6	5	300	100	1.5
4	N4	7	15	300	100	0.5
5	N5	11	5	100	300	1.5
6	N6	5	15	100	300	0.5
7	N7	2	5	300	300	0.5
8	N8	4	15	300	300	1.5
9	N9	9	10	200	200	1
10	N10	8	10	200	200	1
11	N11	1	10	200	200	1

2.9.3 Developed Method for the Peptide RPC Column Characterisation Protocol Operating Conditions

The development of the Peptide RPC Column Characterisation Protocol utilised the following operating conditions:

Mobile Phase 1: A: 20 mM ammonium formate in H_2O

B: 20 mM ammonium formate in MeCN / H_2O (80:20 w/w)

Gradient 1:

Time (mins)	%B
0.0	5
40.0	55
42.0	55
42.1	5
54.1	5

Mobile Phase 2: A: 0.1% v/v formic acid in H_2O

B: 0.1% v/v formic acid in MeCN

Gradient 2:

Time (mins)	%B
0.0	10
40.0	50
42.0	50
42.1	10
54.1	10

Flow Rate: 0.3 mL/min

Oven Temperature: 40 °C

Injection Volume: 2 µL

Wavelength: 215 nm (8) Ref 360, 100.

MS Conditions: SIM, Positive mode

DL Temperature: 300 °C

Heat Block: 300 °C

Drying Gas: 5 L/min

Nebulising Gas: 0.5 L/min

Autosampler Cooler: 10 °C (used to ensure maximum stability of the peptides).

Columns:

Stationary Phase	Serial Number
Polaris Amide C18, 3 µm	461575
Acquity BEH C4, 1.7 µm	01273618712811
Acquity BEH C8, 1.7 µm	01433621818202
Acquity BEH C18, 1.7 µm	02833615515713
Acquity BEH Shield RP18, 1.7 µm	01663618216648
Acquity CSH C18, 1.7 µm	01373616715707
Acquity CSH Fluoro Phenyl, 1.7 µm	01123618118013
Acquity CSH Phenyl Hexyl, 1.7 µm	01123616215121
Acquity HSS C18, 1.8 µm	01443619715737
Acquity HSS C18-SB, 1.8 µm	01223609816614
Acquity HSS T3, 1.8 µm	01853622915102
Ascentis Express Biphenyl, 2.6 µm	USLPF001256
Fortis Diphenyl, 1.7 µm	B03172807-1
Acclaim Mixed Mode WCX, 3 µm	001269

2.9.4 Sample Preparation

All peptides (as seen in *Table 1*) were provided by Apigenex (Prague, Czech Republic) in 1 mg vials, which were dissolved to 0.25 mg/mL using DMSO/H_2O (80:20 v/v). Solutions were stored at -20 °C prior to analysis and stored at 10 °C in the LC autosampler while awaiting analysis.

Cocktails were produced using an injector programme with the following combination of peptides (see *Appendix vii* for a typical injector programme).

Table 7 Cocktail mixtures produced via injector programme for the development of the Peptide RPC Column Characterisation Protocol.

Peptide	*m/z*	Volume (µL)	Peptide	*m/z*	Volume (µL)
	TM1			**TM5**	
[Met(O)10]-	$[M+2H]^+$ 828	2.0	[Met(O)10]-	$[M+2H]^+$ 828	2.0
Bovine GLP-2 (1-15)	$[M+2H]^+$ 820	2.0	[L-Asp3]-	$[M+2H]^+$ 820	2.0
Bovine GLP-2 (16-33)	$[M+2H]^+$ 1068	2.0	[Lys20]-	$[M+2H]^+$ 1055	2.0
[D-isoAsp,Gly22]-	$[M+2H]^+$ 1024	2.0	[Lys26]-	$[M+2H]^+$ 1076	2.0
[Trp26]-	$[M+2H]^+$ 1105	2.0	[Trp26]-	$[M+2H]^+$ 1105	2.0
	TM2			**TM6**	
[Met(O)10]-	$[M+2H]^+$ 828	2.0	[Met(O)10]-	$[M+2H]^+$ 828	2.0
[L-Asp11]-	$[M+2H]^+$ 820	2.0	[D-Ser5]-	$[M+2H]^+$ 820	3.0
[Val26]-	$[M+2H]^+$ 1062	2.0	[D-Ser16]-	$[M+2H]^+$ 1069	2.0
[Ile26]-	$[M+2H]^+$ 1069	2.0	[D-Ser7]-	$[M+2H]^+$ 820	1.0
[Trp26]-	$[M+2H]^+$ 1105	2.0	[Trp26]-	$[M+2H]^+$ 1105	2.0
	TM3			**TM7**	
[Met(O)10]-	$[M+2H]^+$ 828	2.0	[Met(O)10]-	$[M+2H]^+$ 828	2.0
[D-Asp11]-	$[M+2H]^+$ 820	0.5	[L-isoAsp3]	$[M+2H]^+$ 820	3.0
[L-isoAsp11]-	$[M+2H]^+$ 820	3.5	[D-isoAsp3]	$[M+2H]^+$ 820	1.0
[D-isoAsp11]-	$[M+2H]^+$ 820	2.0	[Ile26,Leu27]-	$[M+2H]^+$ 1069	2.0
[Trp26]-	$[M+2H]^+$ 1105	2.0	[L-Asp,Gly22]-	$[M+2H]^+$ 1024	2.0
			[Trp26]-	$[M+2H]^+$ 1105	2.0
	TM4			**TM8**	
[Met(O)10]-	$[M+2H]^+$ 828	2.0	[Met(O)10]-	$[M+2H]^+$ 828	2.0
[D-His1]-	$[M+2H]^+$ 820	2.0	[D-Asp,Gly22]-	$[M+2H]^+$ 1024	2.0
[Phe26]-	$[M+2H]^+$ 1086	2.0	[L-isoAsp,Gly22]-	$[M+2H]^+$ 1024	1.0
[Tyr26]-	$[M+2H]^+$ 1094	2.0	[Trp26]-	$[M+2H]^+$ 1105	2.0
[Trp26]-	$[M+2H]^+$ 1105	2.0			

2.10 Optimisation of the Peptide RPC Column Characterisation Protocol

2.10.1 Mobile Phase Preparation

2.10.1.1 Ammonium Formate pH 6.1 Stock Solution

A 200 mM ammonium formate stock solution was prepared by weighing 12.61 g on the 2 d.p. balance, which was dissolved in approximately 800 mL LC-MS grade water using a magnetic stirrer. Formic acid was added dropwise to lower the pH to 6.1, where pH was determined using a Jenway 3310 pH meter (*Section 2.3*). The solution was made to 1000.00 g using LC-MS water.

2.10.1.2 Ammonium Formate pH 6.35 Stock Solution

A 200 mM ammonium formate stock solution was prepared by weighing 12.61 g on the 2 d.p. balance, which was dissolved in approximately 800 mL LC-MS grade water using a magnetic stirrer. Formic acid was added dropwise to lower the pH to 6.35, where pH was determined using a Jenway 3310 pH meter (*Section 2.3*). The solution was made to 1000.00 g using LC-MS water.

2.10.1.3 Ammonium Formate pH 6.6 Stock Solution

A 200 mM ammonium formate stock solution was prepared by weighing 12.61 g on the 2 d.p. balance, which was dissolved in approximately 800 mL LC-MS grade water using a magnetic stirrer. Ammonia solution (25% w/w) was added dropwise to increase the pH to 6.6, where pH was determined using a Jenway 3310 pH meter (*Section 2.3*). The solution was made to 1000.00 g using LC-MS water.

2.10.1.4 Premixed Mobile Phase: Ammonium Formate Gradient

The mobile phases used on Pump A and B are described in *Table 8* and *Table* 9, respectively, which were accurately weighed on a 2 d.p. balance:

Table 8 Buffered mobile phase A preparation for ammonium formate at pH 6.1, pH 6.35 and 6.6, prepared by weight. The density of water and acetonitrile are 1 g/cm^3 and 0.786 g/cm^3 respectively

Mobile Phase A	LCMS Grade Water (g)	LCMS Grade Acetonitrile (g)	Buffer (g)
20 mM Ammonium formate pH 6.1 in water	900	0	100 (*Section 2.10.1.1*)
20 mM Ammonium formate pH 6.35 in water	900	0	100 (*Section 2.10.1.2*)
20 mM Ammonium formate pH 6.6 in water	900	0	100 (*Section 2.10.1.3*)

Table 9 Buffered mobile phase B preparation for ammonium formate at pH 6.1, pH 6.35 and pH 6.6, prepared by weight. The density of water and acetonitrile are 1 g/cm^3 and 0.786 g/cm^3 respectively. Solutions corresponded to 20 mM ammonium formate in MeCN / H_2O (80:20 v/v).

Mobile Phase B	LCMS Grade Water (g)	LCMS Grade Acetonitrile (g)	Buffer (g)
20 mM Ammonium formate pH 6.1 in water / acetonitrile	100	628.80	100 (*Section 2.10.1.1*)
20 mM Ammonium formate pH 6.35 in water / acetonitrile	100	628.80	100 (*Section 2.10.1.2*)
20 mM Ammonium formate pH 6.6 in water / acetonitrile	100	628.80	100 (*Section 2.10.1.3*)

2.10.1.5 Premixed Mobile Phase: Formic Acid Gradients

The mobile phases used on Pump A and B are described in *Table 10* and *Table* 11, respectively. The formic acid was accurately dispensed using a Pipetman P1000L which was checked using a balance each day to minimise variation, whilst the solvent was weighed using a 2 d.p. balance.

Table 10 Buffered mobile phase A preparation for formic acid at different volumes, with solvent prepared by weight. The density of water and acetonitrile are 1 g/cm^3 and 0.786 g/cm^3 respectively

Mobile Phase B	LCMS Grade Water (g)	Formic acid (µL)

0.095% formic acid v/v in water	999.05	950
0.100% formic acid v/v in water	999.00	1000
0.105% formic acid v/v in water	998.05	1050

Table 11 Buffered mobile phase B preparation for formic acid at different volumes, with solvent prepared by weight. The density of water and acetonitrile are 1 g/cm^3 and 0.786 g/cm^3 respectively.

Mobile Phase B	LCMS Grade Acetonitrile (g)	Formic acid (µL)
0.095% formic acid v/v in acetonitrile	785.25	950
0.100% formic acid v/v in acetonitrile	785.21	1000
0.105% formic acid v/v in acetonitrile	784.47	1050

2.10.2 Nominal Peptide RPC Column Characterisation Protocol Conditions

The base method for the Peptide RPC Column Characterisation Protocol utilised the following operating conditions:

Mobile Phase: As described in *Section 2.10.1.4* for ammonium formate pH 6.45

As described in *Section 2.10.1.5* for 0.1% formic acid.

Gradient:

Time (mins)	%B Ammonium Formate	%B Formic Acid
0.0	5	5
40.0	55	45
42.0	55	45
42.1	5	5
54.1	5	5

Flow Rate: 0.3 mL/min

Oven Temperature: 40 °C

Injection Volume: 1 µL

Wavelength: 215 nm (8) Ref 360, 100.

Autosampler Cooler: 10 °C (to ensure maximum stability of the peptides).

2.10.3 Sample Preparation

All peptides (*Table 1*) were provided by Apigenex (Prague, Czech Republic) in 1 mg vials, which were dissolved to 0.25 mg/mL using DMSO / H_2O (80:20 v/v). Solutions were stored at -20 °C prior to analysis and stored at 10 °C in the LC autosampler while awaiting analysis.

Cocktails were prepared as shown in *Table 12* (see *Appendix vii* for a typical injector programme).

Table 12 Cocktail mixtures produced via injector programme for the Peptide RPC Column Characterisation Protocol.

Peptide	Peptide Number	*m/z*	Volume (µL)
	TM1		
[Met(O)10]-Bovine GLP-2 (1-15)	8	$[M+2H]^+$ 828	1.0
Bovine GLP-2 (1-15)	1	$[M+2H]^+$ 820	1.0
[L-Asp11]-Bovine GLP-2 (1-15)	9	$[M+2H]^+$ 820	0.5
[Gly22]-Bovine GLP-2 (16-33)	16	$[M+2H]^+$ 1024	0.5
[Tyr26]-Bovine GLP-2 (16-33)	24	$[M+2H]^+$ 1094	0.5
Bovine GLP-2 (16-33)	13	$[M+2H]^+$ 1069	1.0
[Ile26,Leu27]-Bovine GLP-2 (16-33)	15	$[M+2H]^+$ 1069	0.3
	TM2		
[Met(O)10]-Bovine GLP-2 (1-15)	8	$[M+2H]^+$ 828	1.0
[L-Asp11]-Bovine GLP-2 (1-15)	9	$[M+2H]^+$ 820	1.0
[D-Asp11]-Bovine GLP-2 (1-15)	10	$[M+2H]^+$ 820	0.5
[Lys26]-Bovine GLP-2 (16-33)	26	$[M+2H]^+$ 1076	1.0
Bovine GLP-2 (16-33)	13	$[M+2H]^+$ 1069	1.0
[Ile26,Leu27]-Bovine GLP-2 (16-33)	15	$[M+2H]^+$ 1069	0.3
	TM3		
[Met(O)10]-Bovine GLP-2 (1-15)	8	$[M+2H]^+$ 828	1.0
Bovine GLP-2 (1-15)	1	$[M+2H]^+$ 820	1.0
[L-Asp3]-Bovine GLP-2 (1-15)	3	$[M+2H]^+$ 820	0.5
Bovine GLP-2 (16-33)	13	$[M+2H]^+$ 1069	1.0
[D-Ser16]-Bovine GLP-2 (16-33)	14	$[M+2H]^+$ 1069	0.5
[Ile26,Leu27]-Bovine GLP-2 (16-33)	15	$[M+2H]^+$ 1069	0.3

2.10.4 Design of Experiment (DoE)

Table 13 Design of Experiment conditions for investigating the important factors for the ammonium formate gradient.

Experiment Name	Run Order	Temp (°C)	Gradient Accuracy (%B)	Flow (mL/min)	pH of Stock Solution	MeCN (w/w) Composition in the B Line	Dwell Volume (µL)
N1	3	38	-0.4	0.295	6.51	80.1	500
N2	8	42	-0.4	0.295	6.39	79.9	500
N3	4	38	+0.4	0.295	6.39	80.1	100
N4	9	42	+0.4	0.295	6.51	79.9	100
N5	11	38	-0.4	0.305	6.51	79.9	100
N6	1	42	-0.4	0.305	6.39	80.1	100
N7	10	38	+0.4	0.305	6.39	79.9	500
N8	7	42	+0.4	0.305	6.51	80.1	500
N9	5	40	0.0	0.300	6.45	80.0	300
N10	6	40	0.0	0.300	6.45	80.0	300
N11	2	40	0.0	0.300	6.45	80.0	300

Table 14 Design of Experiment conditions for investigating the important factors for the formic acid gradient.

Experiment Name	Run Order	Temp (°C)	Gradient Accuracy (%B)	Flow (mL/min)	%FA in A Solvent (%)	%FA in B Solvent (%)	Dwell Volume (µL)
N1	3	38	-0.4	0.295	0.105	0.105	500
N2	8	42	-0.4	0.295	0.095	0.095	500
N3	4	38	+0.4	0.295	0.095	0.105	100
N4	9	42	+0.4	0.295	0.105	0.095	100
N5	11	38	-0.4	0.305	0.105	0.095	100
N6	1	42	-0.4	0.305	0.095	0.105	100
N7	10	38	+0.4	0.305	0.095	0.095	500
N8	7	42	+0.4	0.305	0.105	0.105	500
N9	5	40	0.0	0.300	0.100	0.100	300
N10	6	40	0.0	0.300	0.100	0.100	300
N11	2	40	0.0	0.300	0.100	0.100	300

2.10.5 Finalised Peptide RPC Column Characterisation Protocol

Mobile Phase: A1: 0.1% (±0.005%) v/v formic acid in water

B1: 0.1% (±0.005%) v/v formic acid in acetonitrile

A2: 20 mM ammonium formate in water

B2: MeCN

Gradient:

Time (mins)	%B
0.0	4.5
40.0	50.0
42.0	50.0
42.1	4.5
54.1	4.5

Flow Rate: 0.3 mL/min (±0.005 mL/min)

Oven Temperature: 40 °C (±2 °C)

Injection Volume: See *Table 15*

Wavelength: 215 nm (8) Ref 360, 100.

MS: Selected Ion Monitoring (z=2)

Autosampler Cooler: 10 °C (to ensure maximum stability of the peptides).

2.10.6 Sample Preparation

All peptides (*Table 1*) were provided by Apigenex (Prague, Czech Republic) in 1 mg vials, which were dissolved to 0.25 mg/mL using DMSO / H_2O (80:20 v/v). Solutions were stored at -20 °C prior to analysis and stored at 10 °C in the LC autosampler while awaiting to be analysed.

Cocktails were prepared as shown in *Table 15* (see *Appendix vii* for a typical injector programme).

Table 15 Cocktail mixtures produced via injector programme for the Peptide RPC Column Characterisation Protocol.

Peptide	Peptide Number	*m/z*	Volume (µL)
	TM1		
[Met(O)10]-Bovine GLP-2 (1-15)	8	$[M+2H]^+$ 828	1.0
Bovine GLP-2 (1-15)	1	$[M+2H]^+$ 820	1.0
[L-Asp11]-Bovine GLP-2 (1-15)	9	$[M+2H]^+$ 820	0.5
Bovine GLP-2 (16-33)	13	$[M+2H]^+$ 1069	1.0
[Ile26,Leu27]-Bovine GLP-2 (16-33)	15	$[M+2H]^+$ 1069	0.3
	TM2		
[Met(O)10]-Bovine GLP-2 (1-15)	8	$[M+2H]^+$ 828	1.0
[Tyr26]-Bovine GLP-2 (16-33)	24	$[M+2H]^+$ 1094	0.5
[Lys26]-Bovine GLP-2 (16-33)	26	$[M+2H]^+$ 1076	1.0
Bovine GLP-2 (16-33)	13	$[M+2H]^+$ 1069	1.0
[Ile26,Leu27]-Bovine GLP-2 (16-33)	15	$[M+2H]^+$ 1069	0.3
	TM3		
[Met(O)10]-Bovine GLP-2 (1-15)	8	$[M+2H]^+$ 828	1.0
[Gly22]-Bovine GLP-2 (16-33)	16	$[M+2H]^+$ 1024	0.5
Bovine GLP-2 (16-33)	13	$[M+2H]^+$ 1069	1.0
[D-Ser16]-Bovine GLP-2 (16-33)	14	$[M+2H]^+$ 1069	0.5
[Ile26,Leu27]-Bovine GLP-2 (16-33)	15	$[M+2H]^+$ 1069	0.3

2.11 Protein Digests

2.11.1 Operating Conditions for the Tryptic Digest of Proteins

Mobile Phase: As described in *Section 2.10.1.4* for ammonium formate pH 6.45

As described in *Section 2.10.1.5* for 0.1% formic acid

Gradient: As described in *Section 2.10.5*

Flow Rate: 0.3 mL/min

Oven Temperature: 40 °C

Injection Volume: 1 µL

Wavelength: 215 nm (8) Ref 360, 100.

Autosampler Cooler: 10 °C (to ensure maximum stability of the peptides).

Stationary Phases:

Stationary Phase	Serial Number
Acquity CSH C18, 1.7 µm	01513820518406
Luna Omega PS C18, 1.6 µm	H18-016921
Ascentis Express C18, 2.7 µm	USWM003484
Poroshell HPH C18, 2.7 µm	USGYN01217
Ascentis Express Biphenyl, 2.7 µm	USLPF001258
Kinetex Biphenyl, 2.6 µm	H18-086495
Polaris Amide C18, 3 µm	550014
Zorbax 300 C18 SB, 1.8 µm	USEDN01037
Acquity BEH C8, 1.7 µm	01513823418330

2.11.2 Sample Preparation

Trypsin was added to either carbonic anhydrase or bovine insulin (all 0.4 mg/mL) in a ratio of 1:20 respectively, and dissolved in 50 mM TRIS buffer pH 7.5 (7.4 mM TRIS base and 42.6 mM TRIS HCl). The solutions were stored at 37 °C for 24 hours. The digestion was stopped by the addition of 37% w/w HCl to reduce the pH to 2.5.

2.12 Mobile Phase Study

2.12.1 Mobile Phase Preparation

2.12.1.1 Stock Buffer Preparation

100 mM of each buffer (unless otherwise stated) was prepared by weighing the prescribed weight from *Table 16* on the 2 d.p. balance and dissolved in approximately 400 g LC-MS water using a magnetic stirrer. The solution was made to 500 g using LC-MS water. The solutions were shaken to ensure thorough mixing.

Table 16 Mass of each buffer required for 100 mM stock solutions (unless otherwise stated). Key: H_3PO_4 = phosphoric acid, $NH_4H_2PO_4$ = ammonium dihydrogen phosphate, FA = formic acid, NH_4FA = ammonium formate, AA = acetic acid, NH_4AA = ammonium acetate, $(NH_4)_2HPO_4$ = ammonium monohydrogen phosphate, NaCl = sodium chloride, Na_2SO_4 = sodium sulfate, $(NH_4)_2SO_4$ = ammonium sulfate, $NaClO_4$ = sodium perchlorate, TEA = triethylamine, TFA = trifluoroacetic acid, HFBA = heptafluorobutyric acid, $BuSO_3$ = sodium butane-1-sulfonate, DFA = difluoroacetic acid, MSA = methanesulfonic acid, NH_4OH = ammonium hydroxide, NH_4HCO_3 = ammonium bicarbonate

Buffer	Mass (g)	Buffer	Mass (g)
H_3PO_4	4.90	NaCl (1 M)	29.22
$NH_4H_2PO_4$	5.75	$(NH_4)_2SO_4$ (1 M)	66.07
$NH_4H_2PO_4$ (1 M)	57.52	$NaClO_4$ (1M)	61.22
FA	2.30	TEA	5.06
NH_4FA	3.15	TFA	5.70
AA	3.00	HFBA	10.7
NH_4AA	3.85	$BuSO_3$	8.01
$(NH_4)_2HPO_4$	6.60	NH_4OH	1.75
$(NH_4)_2HPO_4$ (1 M)	66.03	NH_4HCO_3	3.95

2.12.1.2 0.1% v/v Modifiers Preparation

The ensuing mobile phases were produced be weighing the LC-MS grade solvent and pipetting the necessary volume of additive. The solutions were shaken to ensure thorough mixing.

Table 17 Preparation of 0.1% v/v solutions for the Mobile Phase Study

Mobile Phase	Additive (µL)	LC-MS Grade Water (g)
0.1% v/v H_3PO_4	500	499.50
0.1% v/v TFA	500	499.50
0.1% v/v DFA	500	499.50
0.1% v/v FA	500	499.50
0.05%/0.05% v/v TFA/FA	250 per additive	499.50
0.1% v/v MSA	500	499.50
0.1% v/v NH_4OH	500	499.50

2.12.1.3 20 mM and 100 mM Total Ionic Strength Buffer Preparation

The following mobile phases were prepared using the stock solutions in *Section 2.12.1.1*. The buffering capacity for each of the mobile phases described in *Table 18* can be located in *Table 64*. Each solution was shaken to ensure thorough mixing. The pH was measured to confirm expected values.

Table 18 Preparation of buffers used in the mobile phase study. For the abbreviation key, see Table 16.

Mobile Phase	Mobile Phase Number	pH	Total Ionic Strength (mM)	Additive Concentration (mM)	Reagent 1 (g)	Reagent 2 (g)	Reagent 3 (g)	Water (g)
$H_3PO_4/NH_4H_2PO_4$	4	2.3	20	-	98.05	85.25	-	316.70
FA/NH_4FA	22	3.6	20	-	122.75	99.25	-	278.00
AA/NH_4AA	28	5.1	20	-	38.75	100.00	-	361.25
$(NH_4)_2HPO_4/NH_4H_2PO_4$	43	7.5	20	-	31.15	8.65	-	460.20
H_3PO_4*/$NH_4H_2PO_4$*	6	2.3	100	-	29.12	48.22	-	422.66
H_3PO_4*/$(NH_4)_2HPO_4$*	24	3.1	100	-	29.35	24.85	-	445.80
$(NH_4)_2HPO_4$*/$NH_4H_2PO_4$*	39	7.5	100	-	15.99	2.91	-	481.11
NaCl*/$H_3PO_4/NH_4H_2PO_4$	10	2.3	100	20	37.70	95.55	87.75	279.00
NaCl*/FA/NH_4FA	23	3.6	100	20	38.90	112.75	109.25	239.10
NaCl*/AA/NH_4AA	34	5.1	100	20	38.30	37.05	117.00	307.65
NaCl*/$(NH_4)_2HPO_4/NH_4H_2PO_4$	38	7.5	100	20	39.48	33.65	6.15	420.72
Na_2SO_4*/$H_3PO_4/NH_4H_2PO_4$	9	2.3	100	20	3.14	95.55	87.75	313.56
$(NH_4)_2SO_4$*/$H_3PO_4/NH_4H_2PO_4$	8	2.3	100	20	3.16	95.55	87.75	313.54
$(NH_4)_2SO_4$*/FA/NH_4FA	18	3.6	100	20	3.24	112.45	109.45	242.94
$(NH_4)_2SO_4$*/AA/NH_4AA	29	5.1	100	20	3.29	33.75	105.0	357.96
$(NH_4)_2SO_4$*/$(NH_4)_2HPO_4/NH_4H_2PO_4$	42	7.5	100	20	3.29	33.65	6.15	456.91
$NaHClO_4$*/$H_3PO_4/NH_4H_2PO_4$	16	2.3	100	20	37.70	95.55	112.75	254.00
$NaHClO_4$*/FA/NH_4FA	26	3.6	100	20	38.90	112.75	109.25	239.10
$NaHClO_4$*/AA/NH_4AA	33	5.1	100	20	39.50	33.75	105.00	321.75
$NaHClO_4$*/$(NH_4)_2HPO_4/NH_4H_2PO_4$	46	7.5	100	20	39.41	33.65	6.15	420.79
$TEA/FA/NH_4FA$	20	3.6	20	5	25.00	147.75	74.25	253
$TEA/AA/NH_4AA$	27	5.1	20	5	25.00	63.75	75.00	336.25
$TEA/(NH_4)_2HPO_4/NH_4H_2PO_4$	37	7.5	20	5	25.00	0.58	3.40	471.02
$TEA/FA/NH_4HCO_3$	36	7.9	20	5	25.00	23.50	77.00	374.50
$TFA/H_3PO_4/NH_4H_2PO_4$	5	2.3	20	5	25.00	49.40	70.60	355.00
$TFA/FA/NH_4FA$	21	3.6	20	5	25.00	68.55	100.30	306.15
$TFA/AA/NH_4AA$	30	5.1	20	5	25.00	4.50	100.20	370.30
$TFA/(NH_4)_2HPO_4/NH_4H_2PO_4$	40	7.5	20	5	25.00	37.50	0.00	437.50

HFBA	14	1.8	20	20	100.00	-	-	400.00
HFBA/H_3PO_4/$NH_4H_2PO_4$	13	2.3	20	5	25.00	49.40	70.60	355.00
HFBA/FA/NH_4FA	25	3.6	20	5	25.00	68.55	100.30	306.15
HFBA/AA/NH_4AA	32	5.1	20	5	25.00	4.50	100.20	370.30
HFBA/$(NH_4)_2HPO_4$/$NH_4H_2PO_4$	49	7.5	20	5	25.00	37.50	0.00	437.50
$BuSO_3$/H_3PO_4/$NH_4H_2PO_4$	2	2.3	20	5	25.00	77.40	50.45	347.15
$BuSO_3$/FA/NH_4FA	19	3.6	20	5	25.00	74.85	94.00	306.15
$BuSO_3$/AA/NH_4AA	31	5.1	20	5	25.00	29.50	75.20	370.30
$BuSO_3$/$(NH_4)_2HPO_4$/$NH_4H_2PO_4$	44	7.5	20	5	25.00	23.50	6.60	444.90
TFA	12	1.8	20	-	100.00	-	-	400.00
NH_4AA	41	7.0	20	-	100.00	-	-	400.00
NH_4FA	35	6.5	20	-	100.00	-	-	400.00
NH_4HCO_3	45	7.9	20	-	100.00	-	-	400.00

* Prepared using 1 M stock solutions

2.12.2 Operating Conditions for the Mobile Phase Study

Mobile Phase: A: See *Table 17* and *Table 18*

B: Acetonitrile / Water (80:20 v/v)

Gradient:

Time (mins)	%B
0.0	5.6
40.0	62.5
42.0	62.5
42.1	5.6
54.1	5.6

Gradient corresponds to 100% acetonitrile conditions used in the Peptide RPC Column Characterisation Protocol

Flow Rate: 0.3 mL/min

Oven Temperature: 40 °C

Injection Volume: See *Table 15 for the test mixtures and injection volume*

Wavelength: 215 nm (8) Ref 360, 100.

Autosampler Cooler: 10 °C (to ensure maximum stability of the peptides).

Stationary Phases:

Stationary Phase	Serial Number
Ascentis Express C18	USWM003516
Ascentis Express C18	USWM003517
Ascentis Express C18	USWM003518
Ascentis Express C18	USWM003519
Ascentis Express C18	USWM003520
Ascentis Express C18	USWM003521

150 x 2.1 mm. batch S19022

2.12.3 Operating Conditions for the Extended Mobile Phase Study – Effect of Temperature

Mobile Phase: A1: pH 1.9 0.1% v/v TFA

A2: pH 2.3 100 mM H_3PO_4 / $NH_4H_2PO_4$ / $(NH_4)_2SO_4$

A3: pH 2.7 0.1% v/v FA

A4: pH 5.1 20 mM $BuSO_3$ / AA / NH_4AA

A5: pH 6.5 20 mM NH_4FA

A6: pH 7.5 20 mM $(NH_4)_2HPO_4$ / $NH_4H_2PO_4$

See *Table 17* and *Table 18* for mobile phase preparation

B: Acetonitrile / Water (80:20 v/v)

Gradient:

Time (mins)	%B
0.0	5.6
40.0	62.5
42.0	62.5
42.1	5.6
54.1	5.6

Gradient corresponds to 100% acetonitrile conditions used in the Peptide RPC Column Characterisation Protocol

Flow Rate: 0.3 mL/min

Oven Temperature: 20, 40 and 60 °C

Injection Volume: See *Table 15 for the test mixtures and injection volume*

Wavelength: 215 nm (8) Ref 360, 100.

Autosampler Cooler: 10 °C (to ensure maximum stability of the peptides).

Stationary Phases:

Stationary Phase	Serial Number
Ascentis Express C18	USWM003516
Ascentis Express C18	USWM003517
Ascentis Express C18	USWM003518
Ascentis Express C18	USWM003519
Ascentis Express C18	USWM003520
Ascentis Express C18	USWM003521

150 x 2.1 mm. batch S19022

2.12.4 Operating Conditions for the Extended Mobile Phase Study – Effect of Stationary Phase

Mobile Phase: A1: pH 1.9 0.1% v/v TFA

A2: pH 2.3 100 mM H_3PO_4 / $NH_4H_2PO_4$ / $(NH_4)_2SO_4$

A3: pH 2.7 0.1% v/v FA

A4: pH 5.1 20 mM $BuSO_3$ / AA / NH_4AA

A5: pH 6.5 20 mM NH4FA

A6: pH 7.5 20 mM $(NH_4)_2HPO_4$ / $NH_4H_2PO_4$

See *Table 17* and *Table 18* for mobile phase preparation

B1: Acetonitrile / Isopropanol / Water (60:20:20 v/v/v)

B2: Acetonitrile / Isopropanol / Water (65:15:20 v/v/v)

B3: Acetonitrile / Isopropanol / Water (70:10:20 v/v/v)

B4: Acetonitrile / Isopropanol / Water (75:5:20 v/v/v)

B5: Methanol / Water (80:20 v/v)

Gradient:

Time (mins)	%B
0.0	5.6
40.0	62.5
42.0	62.5
42.1	5.6
54.1	5.6

Gradient corresponds to 100% acetonitrile conditions used in the Peptide RPC Column Characterisation Protocol

Flow Rate: 0.3 mL/min

Oven Temperature: 40 °C

Injection Volume: See *Table 15 for the test mixtures and injection volume*

Wavelength: 215 nm (8) Ref 360, 100.

Autosampler Cooler: 10 °C (to ensure maximum stability of the peptides).

Stationary Phases:

Stationary Phase	Serial Number
Ascentis Express Biphenyl	USLPF001275
Ascentis Express Biphenyl	USLPF001276
Ascentis Express Biphenyl	USLPF001277
Polaris Amide C18	572862
Polaris Amide C18	572535
Polaris Amide C18	572858
Acquity CSH Fluoro Phenyl	01133717716610
Acquity CSH Fluoro Phenyl	01133717716613
Acquity CSH Fluoro Phenyl	01143823516701

150 x 2.1 mm.

2.13 Additional Software

Principal component analysis (PCA) was performed using Simca whilst factorial design was implemented using Modde (Version 14.1 and 11 respectively, Umetrics, Umeå, Sweden). Method translations, retention modelling and logD / logP descriptors were performed using ACD/Labs (Version 2016.1.1. Advanced Chemistry Development Inc., Toronto, Canada) and amino acid structures drawn using Chem3D Pro (Version 16.0.0.82. CambridgeSoft, Cambridge, USA). Dwell volumes (via integration under the curve) were calculated using OriginPro 2016 (Version 2016, OriginLab Corporation, Northampton, USA). The net charges and isoelectric point of the peptide probes were calculated using General Protein/Mass Analysis for Windows (GPMAW) software (Version 9.51, Lighthouse Data, Odense, Denmark). Mobile phase combinations, buffering capacity and ionic strength were calculated using BufferMaker (Version 1.1.0.0, ChemBuddy, BPP Marcin Borkowski, Poland).

3. Results and Discussion

3.1 Rationale for LC Characterisation

The contribution of each component in the HPLC system should be considered and defined in order to optimise column performance. This includes valves, columns, tubes and detectors which can all impact on extra column band broadening and on the overall volume of the system.

3.1.1 Dwell Volume

Dwell volume (V_d) is an extremely influential parameter of selectivity [51]. The dwell volume is defined as the point of mixing up to the head of the column. This volume will vary from instrument to instrument based on their system configuration (i.e. size of mixer, type of pump, high *versus* low pressure mixing, tube internal diameter and length). Dwell volume determination is critical when working with gradient chromatography as the ratio between dwell volume and column volume (V_d/V_m) will affect the selectivity of the separation [51].

The EP [52] states dwell volume should be determined using a linear gradient with 0.1% acetone v/v tracer in Line B from 0-100% over 10 minutes at 2 mL/min with the UV response recorded. V_d is then determined by measuring the maximum absorbance which is halved ($A_{0.5}$) to correspond to a particular time ($t_{0.5}$) as demonstrated in *Figure 5*. The dwell time (t_d) is determined *using Equation 4,* which can then be used to calculate dwell volume (V_d, *Equation 5*).

$$t_d = t_{0.5} - \left(\frac{t_G}{2}\right) \qquad \textit{Equation 4}$$

$$V_d = t_d \times F \qquad \textit{Equation 5}$$

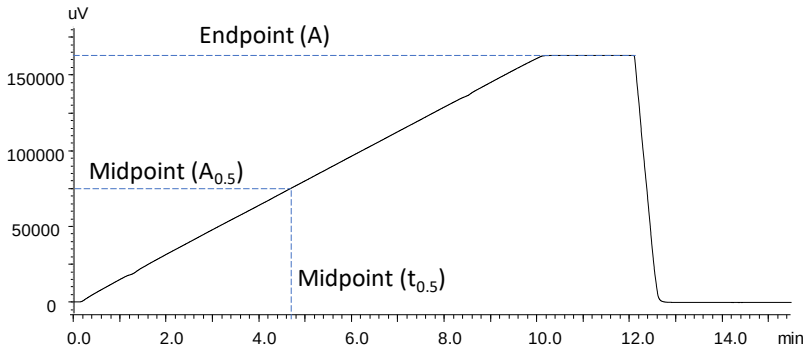

Figure 5 Typical chromatogram produced for determination of dwell volume. Performed on the Shimadzu Nexera X2 LC instrument. Mobile phase A: 0.1% v/v acetone in water, mobile phase B: water, column: zero dwell volume union, gradient: 0-100%B over 10 mins, flow rate: 2 mL/min, column oven: 40 °C, UV detection: 264 nm.

Agilent and Waters suggest an alternative means of measuring V_d by using a step gradient [53].

Both methodologies pose advantages and disadvantages. The linear methodology takes into account the mixing profile which can highlight any issues regarding the efficiency of the mixer. This is important information as highlighted in *Figure 6*, where two mixers were compared. Mixer A provided a linear response suggesting consistent mixing, however, Mixer B had a non-linear response as the mobile phase composition changed. Due to the small change in %B used in the step methodology, this non-linear response might be missed.

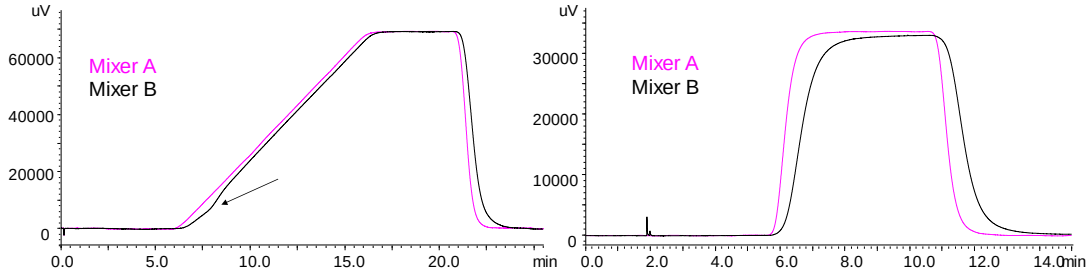

Figure 6 Comparison of linear (10-20%B, 10 min t_G) versus step (50-55%B, 0.1 min t_G) gradient dwell volume determination using two different types of mixers on the Shimadzu Nexera X2.

However, the acetone used by the EP method is volatile and therefore has the potential to create issues in the degasser, such as changes in composition, through evaporating. Also, to be relevant for a given separation, both techniques should use the same flow rate and a %/min change in accordance to the final separation, yet the EP utilises generic conditions which can generates volumes which are too high or too low. The step gradient suggests uracil as the tracer which removes the issues regarding volatile solvents, however, initial results suggest the profile of the gradient is highly dependent on the style and size of mixer. For example, the microfabricated "maze" type mixers tested to date present a more asymmetrical profile in comparison to the bead mixers, and the phenomenon is exacerbated with increased mixer volume size (data not included). In itself, the asymmetric profile is not an issue, however, estimations of dwell volume cannot be measured at 50% of the step as it underestimates the true volume. Therefore, specialist software is required to determine the area under the curve. This can dissuade end-users from measuring this essential parameter.

Thus, an alternative approach was suggested: a linear gradient at the flow rate and a %/min change in accordance to the final separation which can be analysed using the $t_{0.5}$ methodology. The different methodologies were compared on the same instrument (*Table 19*), with the dwell volume determined using either integration or 50% of the slope. A 2-m peek capillary (0.125 mm I.D.) was used to provide adequate pressure to the system, which contributed 25 µL additional volume to the dwell (0.127 µL/cm). The results in *Table 19* were corrected for the additional volume. The dwell volumes recorded using the linear methodology were extremely similar using either $t_{0.5}$ or integrated approach suggesting either method is suitable (highlighted green in *Table 19*), but $t_{0.5}$ is practically more applicable. The dwell volume for the step 10-90% gradient using both integration and $t_{0.5}$ are at least 10% lower than at the reduced flow / smaller %B range. Therefore, the new approach is the most appropriate for determination of dwell volume. The corrected dwell volume determined using this alternative approach was compared between the Nexera X2 and a Waters H-Class (*Table 20*).

Table 19 Dwell volume comparison using both linear and step gradients and integrated or 50% of the slope. Performed on the Shimadzu Nexera X2 LC instrument.

Methodology	Flow (mL/min)	%B Range	Tracer	Method for Determining Dwell Volume	Dwell Volume (µL)
Step	1	10-90	Uracil	Integrated	306
Step	1	10-90	Uracil	$t_{0.5}$	293
Linear	0.3	10-20	Uracil	Integrated	341
Linear	0.3	10-20	Uracil	$t_{0.5}$	340

3.1.2 Instrument Bandwidth and System Retention Volume

Band broadening is both an intra- and extra-column effect. Intra-column band broadening is a result of the column packing, which is beyond the control of the analyst. The system volume is the delay between the injector and detector, excluding the column contribution, whilst instrument band width (or extra-column band broadening) is a measure of the dispersion of the peak between the injector and detector but excludes the column contribution. With the advancement in column technology (i.e. smaller, more efficient particles, improved packing techniques and narrower columns) the effect of dispersion contributions outside of the column have become more pronounced and can prove detrimental to the separation. The contributing factors associated with instrument bandwidth (i.e. connecting unions, tubing, instrument components) need to be minimised in order to achieve optimised chromatographic performance. The total peak variance is described in *Equation 6*, illustrating the components in the flow path. Ideally the instrument bandwidth should be minimised, particularly when using small I.D. columns, which are typical for analyses of peptides. The instrument bandwidth for the Waters H-class equipped with a column manager and 250 µL mixer and Shimadzu Nexera X2 can also be seen in *Table 20,* using *Equation 7-9.*

$$\sigma^2_{Total} = \sigma^2_{Column} + \sigma^2_{Injection\ volume} + \sigma^2_{Injector} + \sigma^2_{Tubing} + \sigma^2_{Detector} + etc$$ *Equation 6*

$$System\ Contribution\ to\ retention\ volume = t_R F$$ *Equation 7*

$$Instrument\ bandwidth = 4\sigma$$ *Equation 8*

$$\sigma = \left(\frac{R_t F}{\sqrt{N_{0.5}}}\right)$$ *Equation 9*

Where t_R is the retention of an unretained species (acetone) in minutes and flow in µL/min.

Table 20 Dwell volume and system retention volume and instrument band width for the Waters H-class and Shimadzu Nexera X2.

	Corrected Dwell Volume (mL)	System Retention Volume (µL)	Instrument Bandwidth (µL)
Waters H-Class, 250 µL mixer	0.553	27	12
Shimadzu Nexera X2, 100 µL mixer	0.342	14	9

3.1.3 Repeatability

The Waters Acquity UPLC Systems, Absorbance Start-Up Solution (Rev A) was injected onto an Agilent Zorbax SB-C18 column six times after sufficient equilibration (20 column volumes) and analysed using gradient chromatography. The solution contained 2-acetylfuran, acetanilide, acetophenone, propiophenone, butylparaben, benzophenone and valerophenone, each at a concentration of 4.0 µg/mL in H_2O / MeCN (90:10 v/v). The retention times and peak areas were recorded for each peak to ascertain the accuracy of the injector and LC system as a whole. Repeatable and accurate retention times and peak areas indicate the pumps are consistently dispensing the gradient mobile phase and the autosampler is constantly delivering the same volume of sample. Ideally for a UHPLC system, the relative standard deviation (%RSD) should be below 0.5% for the retention time and 1% for the peak area based on instrument specifications. As shown in *Table 21*, the %RSD for retention times are all below 0.15% and the peak areas below 0.2%, suggesting the system is suitable for any future study. In addition, the results can be

used as a baseline for the system performance, thus can indicate any potential problems with the instrument should it deviate substantially from the current results.

Table 21 Retention time and peak area repeatability (n=6) of a neutral seven compound test mixture using gradient chromatography on the Nexera X2 instrument.

	2-Acetylfuran		***Acetanilide***		***Acetophenone***		***Propiophenone***		***Butylparaben***		***Benzophenone***		***Valerophenone***	
Injection	t_g	***PA***	t_g	***PA***	t_g	***PA***	t_g	***PA***	t_g	***PA***	t_g	***PA***	t_g	***PA***
1	1.660	109999	1.854	116206	2.686	131863	3.290	92467	3.484	178185	3.924	202939	4.181	71429
2	1.656	109903	1.849	116073	2.680	131680	3.285	92376	3.478	178300	3.919	202879	4.175	71336
3	1.657	109956	1.850	116083	2.681	131692	3.285	92350	3.478	178192	3.919	202804	4.175	71297
4	1.661	110019	1.854	116120	2.686	131690	3.290	92386	3.483	178253	3.924	203064	4.180	71417
5	1.659	110009	1.852	116076	2.683	131649	3.287	92397	3.480	178286	3.921	203297	4.177	71601
6	1.662	109944	1.854	116089	2.685	131654	3.289	92074	3.482	177974	3.923	202875	4.179	71221
Mean	1.659	109972	1.852	116108	2.684	131705	3.288	92342	3.481	178198	3.922	202976	4.178	71384
%RSD	0.14%	0.04%	0.12%	0.04%	0.10%	0.06%	0.07%	0.15%	0.07%	0.07%	0.06%	0.09%	0.06%	0.18%

3.2 Rationale for Column System Suitability Test (SST)

The efficacy of the data can depend on the integrity of the stationary phase. The stationary phase will degrade over the course of its lifespan but can be further accelerated under certain conditions (i.e. intermediate/high pH, high temperature, poor column storage). Thus, a system suitability test (SST) was devised using probes to determine if there was any loss of ligand, change in hydrogen bonding capacity or increase in positive character. A loss of ligand can occur by hydrolysis which would change the degree of hydrophobicity on the phase, as well as possibly increase residual silanols capable of undergoing hydrogen bonding. This could express itself as retention loss and peak tailing for susceptible compounds.

The probes used in the SST all possess various physico-chemical properties; thus, a gradient must be used to elute all peaks within a reasonable time frame. A gradient methodology can also provide information regarding the function of the LC instrumentation. Additionally, the peptide characterisation protocol utilises gradient chromatography, therefore the SST should also represent this technique.

The SST utilised the same mobile phase as the low pH peptide screen gradient of 0.1% formic acid v/v in H_2O in Line A and 0.1% formic acid v/v in MeCN in Line B. The probes in the test are uracil and water (t_0 markers), benzene sulfonic acid (a probe which investigates positive character, where the negatively charged acid will increase in retention with increase in positive character on the stationary phase, or decrease in retention with an increase in negative charge i.e. increase in silanophilic activity), benzylamine hydrochloride (silanophilic activity probe), caffeine (hydrogen bonding probe), phenol (phenolic marker), benzyl alcohol, toluene (neutral marker), butylbenzene and pentylbenzene (hydrophobic markers which will decrease in retention with any loss of stationary phase). By monitoring the peak capacity (P_C), peak symmetry and gradient alpha values (α^*), the stationary phases can be evaluated.

Two gradient times were used as inputs for a retention time model, using the conditions described in *Section 2.9.2*. The gradient time for the SST was determined

using modelling software (LC Simulator*, Equation 10*), where full resolution was achieved for all analytes on the five stationary phases evaluated.

$$ln\,k' = a + bX \qquad \textit{Equation 10}$$

Where *a* and *b* are analyte specific parameters and *X* the percent of organic modifier in the mobile phase. The equation is valid for isocratic conditions. The modelling software employs *Equation 10* and numerical calculations in order to mimic gradient conditions.

The starting composition was set to 5% to account for any stationary phase prone to dewetting in 100% aqueous (i.e. long chain alkyl phases and phases with high hydrophobicity) [54-56]. The flow rate was set to 0.3 mL/min to account for the increased back-pressure due to smaller particle sizes and the column oven set to 40 °C in order to minimise ambient temperature fluctuations and increase mass transfer whilst minimising column instability.

The test was performed on each column before first use and then periodically to ensure performance was maintained. An example of a column which is performing well and a column which is no longer fit for purpose can be observed in *Figure 7*. The Acquity HSS C18 can be seen to have split peaks caused by a contaminated inlet frit.

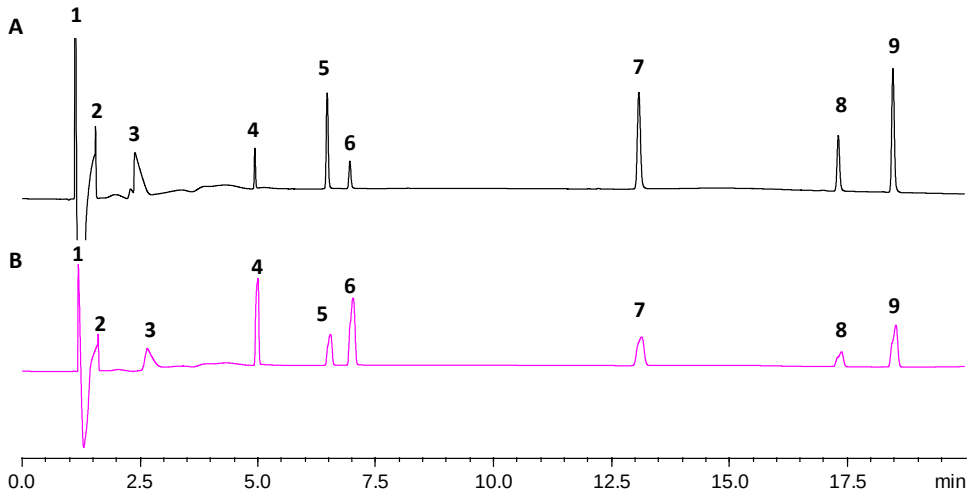

Figure 7 Example chromatograms of the SST mixture on the Acquity HSS C18 using the 0.1% v/v formic acid mobile phase conditions. Chromatogram A illustrates a column performing well whilst chromatogram B demonstrates a column with a blocked inlet frit. Performed on the Shimadzu Nexera X2 LC instrument. Mobile phase A: 0.1% v/v formic acid in water, mobile phase B: 0.1% v/v formic acid in acetonitrile, gradient: 5-100%B over 20 mins, flow rate: 0.3 mL/min, column oven: 40 °C, UV detection: 215 nm, injection volume: 1 µL. Peak 1: Uracil, Peak 2: Benzene sulfonic acid, Peak 3: Benzylamine, Peak 4: Caffeine, Peak 5: Benzylalcohol, Peak 6: Phenol, Peak 7: Toluene, Peak 8: Butylbenzene, Peak 9: Pentylbenzene

3.3 Rationale for Peptides to be Evaluated for the Peptide Base Column Characterisation Protocol

3.3.1 Selection of the Parent Peptide to be Modified

The peptide was selected to probe the characteristics of the stationary phase. To be relevant for the biopharma industry, the peptide requires certain relevant properties, such as typical degradation sites, suitable stability, representative size and chain length. Experience and modelling of peptides from within Novo Nordisk suggested a suitable probe for the study was Bovine GLP-2 (*Table 22*), as discussed below.

Table 22 Bovine GLP-2 peptide chain.

Amino Acid #	1	2	3	4	5	6	7	8	9	10	11	12	13	14	15	16	17	18	19	20	21	22	23	24	25	26	27	28	29	30	31	32	33
Bovine GLP-2	H	A	D	G	S	F	S	D	E	M	N	T	V	L	D	S	L	A	T	R	D	F	I	N	W	L	I	Q	T	K	I	T	D

Bovine GLP-2 has the necessary properties to investigate multiple interactions such as degradation sites for racemisation, oxidation and deamidation, hydrophobicity, aromatic and steric interactions, and electrostatic forces. The peptide is also pharmaceutically relevant, being close in sequence to glucagon, whilst also being small enough to reduce the cost of synthesis.

However, at this size, there is the potential to form secondary structures (i.e. alpha helix or beta sheets), which could potentially inhibit any interaction which is attempted to be studied [57]. As such, ideally the chain length should be reduced to avoid these complications, where Hearn suggested a defined secondary structure would be absent for residues of up to 15 amino acids [58]. This was confirmed using Far-UV circular dichroism which shall be described in greater detail in *Section 3.3.5*.

The sequence in *Table 22* highlights two segments which make this peptide ideal as a probe, where the left-hand chain has slightly more hydrophilic character (amino acid number 1-15), whilst the right-hand side is slightly more hydrophobic (amino acid number 16-33). Thus, two separate segments of the 33 amino acid chain were synthesised in order to investigate the various retention mechanisms. These two separate segments served as the base sequence for a series of peptides to be synthesised. In total 26 peptides were synthesised based on these two sequences.

The peptide does not contain the amino acid cysteine (C) as it is prone to covalent aggregate formation (i.e. disulfide bridges formed by oxidative coupling of thiols) or disulfide bond scrambling. Omitting cysteine should minimise these instability problems.

Table 23 contains a list of the 26 peptides selected to probe the stationary phase characteristics, which were synthesised using the Wang resin before cleavage. d corresponds to D-Asp, iD to L-isoAsp, id to D-isoAsp, h and s correspond to D-His and D-Ser respectively and oM corresponds to Met(O). Marked in grey within the table represents the amino acid change. It also contains a summary for the change in the sequence.

Table 23 Summary of changes in the peptide sequence and their rationale. Marked in grey within the table represents the amino acid change.

Peptide Number	Peptide	Rationale	Sequence																																
			1	2	3	4	5	6	7	8	9	10	11	12	13	14	15	16	17	18	19	20	21	22	23	24	25	26	27	28	29	30	31	32	33
1	Bovine GLP-2 (1-15)	Original sequence	H	A	D	G	S	F	S	D	E	M	N	T	V	L	D																		
2	[D-His1]-Bovine GLP-2 (1-15)	Racemisation	h	A	D	G	S	F	S	D	E	M	N	T	V	L	D																		
3	[D-Asp3]-Bovine GLP-2 (1-15)	Racemisation	H	A	d	G	S	F	S	D	E	M	N	T	V	L	D																		
4	[L-isoAsp3]-Bovine GLP-2 (1-15)	Isomerisation	H	A	iD	G	S	F	S	D	E	M	N	T	V	L	D																		
5	[D-isoAsp3]-Bovine GLP-2 (1-15)	Racemisation / Isomerisation	H	A	id	G	S	F	S	D	E	M	N	T	V	L	D																		
6	[D-Ser5]-Bovine GLP-2 (1-15)	Racemisation	H	A	D	G	s	F	S	D	E	M	N	T	V	L	D																		
7	[D-Ser7]-Bovine GLP-2 (1-15)	Racemisation	H	A	D	G	S	F	s	D	E	M	N	T	V	L	D																		
8	[Met(O)10]-Bovine GLP-2 (1-15)	Oxidation	H	A	D	G	S	F	S	D	E	oM	N	T	V	L	D																		
9	[L-Asp11]-Bovine GLP-2 (1-15)	Deamidation / Negative charge	H	A	D	G	S	F	S	D	E	M	D	T	V	L	D																		
10	[D-Asp11]-Bovine GLP-2 (1-15)	Deamidation / Racemisation / Negative charge	H	A	D	G	S	F	S	D	E	M	d	T	V	L	D																		
11	[L-isoAsp11]-Bovine GLP-2 (1-15)	Deamidation / Isomerisation / Negative charge	H	A	D	G	S	F	S	D	E	M	iD	T	V	L	D																		
12	[D-isoAsp11]-Bovine GLP-2 (1-15)	Deamidation / Isomerisation / Racemisation / Negative charge	H	A	D	G	S	F	S	D	E	M	id	T	V	L	D																		
13	Bovine GLP-2 (16-33)	Original sequence																S	L	A	T	R	D	F	I	N	W	L	I	Q	T	K	I	T	D
14	[D-Ser16]-Bovine GLP-2 (16-33)	Racemisation																s	L	A	T	R	D	F	I	N	W	L	I	Q	T	K	I	T	D
15	[Ile26,Leu27]-Bovine GLP-2 (16-33)	Switch in AA sequence																S	L	A	T	R	D	F	I	N	W	I	L	Q	T	K	I	T	D
16	[L-Asp21,Gly22]-Bovine GLP-2 (16-33)	Loss of aromatic group																S	L	A	T	R	D	G	I	N	W	L	I	Q	T	K	I	T	D
17	[D-Asp21,Gly22]-Bovine GLP-2 (16-33)	Loss of aromatic group / Racemisation																S	L	A	T	R	d	G	I	N	W	L	I	Q	T	K	I	T	D
18	[L-isoAsp21,Gly22]-Bovine GLP-2 (16-33)	Loss of aromatic group / Isomerisation																S	L	A	T	R	iD	G	I	N	W	L	I	Q	T	K	I	T	D
19	[D-isoAsp21,Gly22]-Bovine GLP-2 (16-33)	Loss of aromatic group / Racemisation / Isomerisation																S	L	A	T	R	id	G	I	N	W	L	I	Q	T	K	I	T	D
20	[Val26]-Bovine GLP-2 (16-33)	Aliphatic effect																S	L	A	T	R	D	F	I	N	W	V	I	Q	T	K	I	T	D
21	[Ile26]-Bovine GLP-2 (16-33)	Steric effect																S	L	A	T	R	D	F	I	N	W	I	I	Q	T	K	I	T	D
22	[Phe26]-Bovine GLP-2 (16-33)	Aromatic effect																S	L	A	T	R	D	F	I	N	W	F	I	Q	T	K	I	T	D
23	[Trp26]-Bovine GLP-2 (16-33)	Aromatic effect																S	L	A	T	R	D	F	I	N	W	W	I	Q	T	K	I	T	D
24	[Tyr26]-Bovine GLP-2 (16-33)	Aromatic / Phenolic effect																S	L	A	T	R	D	F	I	N	W	Y	I	Q	T	K	I	T	D
25	[Lys20]-Bovine GLP-2 (16-33)	Polarity effect																S	L	A	T	K	D	F	I	N	W	L	I	Q	T	K	I	T	D
26	[Lys26]-Bovine GLP-2 (16-33)	Positive charge																S	L	A	T	R	D	F	I	N	W	K	I	Q	T	K	I	T	D

3.3.2 "Hydrophilic" Segment – Bovine GLP-2 (1-15)

The "hydrophilic" segment of the Bovine GLP-2 sequence can be seen in *Table 24*. This section of the sequence was designed to illustrate the effect of common degradation products. There were 11 different peptides produced to demonstrate racemisation, oxidation and deamidation products caused by chemical instability, where the variations are described in the table.

Table 24 The "hydrophilic" segment of the Bovine GLP-2 peptide, with the sequence of potential degradation products. Where h denotes D-His, d denotes D-Asp, i denotes iso, s denotes D-Ser, oM denotes oxidised Met. Marked in grey within the table represents the amino acid change

Peptide Number	Peptide	Sequence														
		1	2	3	4	5	6	7	8	9	10	11	12	13	14	15
1	Bovine GLP-2 (1-15)	H	A	D	G	S	F	S	D	E	M	N	T	V	L	D
2	[D-His1]-Bovine GLP-2 (1-15)	h	A	D	G	S	F	S	D	E	M	N	T	V	L	D
3	[D-Asp3]-Bovine GLP-2 (1-15)	H	A	d	G	S	F	S	D	E	M	N	T	V	L	D
4	[L-isoAsp3]-Bovine GLP-2 (1-15)	H	A	iD	G	S	F	S	D	E	M	N	T	V	L	D
5	[D-isoAsp3]-Bovine GLP-2 (1-15)	H	A	id	G	S	F	S	D	E	M	N	T	V	L	D
6	[D-Ser5]-Bovine GLP-2 (1-15)	H	A	D	G	s	F	S	D	E	M	N	T	V	L	D
7	[D-Ser7]-Bovine GLP-2 (1-15)	H	A	D	G	S	F	s	D	E	M	N	T	V	L	D
8	[Met(O)10]-Bovine GLP-2 (1-15)	H	A	D	G	S	F	S	D	E	oM	N	T	V	L	D
9	[L-Asp11]-Bovine GLP-2 (1-15)	H	A	D	G	S	F	S	D	E	M	D	T	V	L	D
10	[D-Asp11]-Bovine GLP-2 (1-15)	H	A	D	G	S	F	S	D	E	M	d	T	V	L	D
11	[L-isoAsp11]-Bovine GLP-2 (1-15)	H	A	D	G	S	F	S	D	E	M	iD	T	V	L	D
12	[D-isoAsp11]-Bovine GLP-2 (1-15)	H	A	D	G	S	F	S	D	E	M	id	T	V	L	D

All proteinogenic amino acids, except glycine, contain a chiral centre at the α-carbon and as such, have the ability to produce enantiomers. Amino acids in biological systems are in the L- form but can convert into the D- form if racemisation (the formation of an optically inactive product) occurs. If one chiral centre is inverted in a peptide, it creates diastereoisomers. As diastereoisomers possess different physicochemical properties, these compounds can be resolved in an achiral system. However, the diastereoisomers often prove difficult to fully resolve using typical reversed-phase conditions used in industry, therefore it is critical to be able to optimise selectivity differences. The rate of racemisation can depend on the reaction parameters (i.e. pH, temperature and solvents) and the amino acid side chain and its ability to withdraw electrons from the α-carbon [59-

61]. Histidine (H) and serine (S) are known to be particularly susceptible to racemisation, thereby producing [D-His1]-, [D-Ser5]- and [D-Ser7]-Bovine GLP-2 (1-15) (Peptide Numbers 2, 6 and 7 respectively, *Figure 8*).

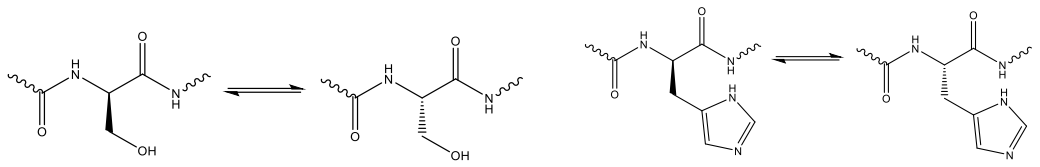

L-Serine D-Serine L-Histidine D-Histidine

Figure 8 Racemised structures of serine and histidine.

The D- and L- nomenclature describe the relative configuration of the molecule by relating the molecule to glyceraldehyde. It describes the relative relationship between amino acids whereas *R / S* nomenclature describes the absolute configuration, which is discussed in more detail below. Racemisation of histidine can occur during synthesis, typically by enolization. This is most likely facilitated by the inductive effect of the imidazole ring. Serine has the ability to racemise in solution as well as during synthesis [59]. The D- version of the peptides were produced by introducing the D- isomer into the synthetic pathway. The racemised amino acid forms diastereoisomeric peptides, which are possible to separate in an achiral separation system such as RPC.

Oxidation is one of the most common pathways for chemical degradation, as demonstrated by the probe [Met(O)10]-Bovine GLP-2 (1-15) (Peptide Number 8, *Figure 9*). Oxidation of the sulfur in methionine (i.e. by Oxone®, potassium peroxymonosulfate [62]) results in two diastereoisomeric sulfoxide peptide species, by means of the lone pair of electrons on the sulfur. These diastereoisomers will have different physicochemical properties which RPC should be capable of separating. The Oxone® is small which allows the oxidising agent to approach without steric hindrance thus the diastereoisomeric species exist in a 1:1 ratio. The diastereoisomers are assigned the nomenclature *R* and *S* configuration, by following the Cahn-Ingold-Prelog priority rules [22]. The *R/S* nomenclature rule is used to name the enantiomers of a chiral compound, where the substituents are prioritised

based on atomic mass, with the largest atomic mass given highest priority. The nomenclature is attributed on the spatial orientation of the prioritised substituents. A clockwise rotation is notated as "*R*" (*rectus*, right) whilst counter clockwise rotation is classed as "*S*" (*sinister*, left). Furthermore, there is also the potential to undergo additional oxidation to form the sulfone [63].

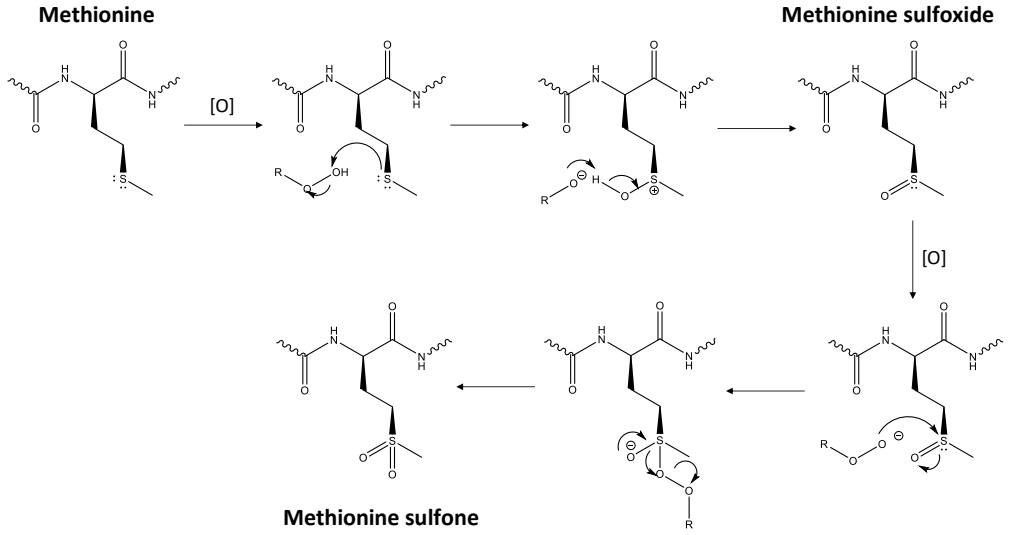

Figure 9 Schematic of oxidation pathway for methionine to methionine sulfoxide and methionine sulfone.

Deamidation is a chemical instability process of removing an amide functionality from an organic compound [63-73]. This occurs predominantly in the amino acids asparagine and glutamine as the side chains contain amide groups. Deamidation occurs more readily when an amino acid in a peptide chain is followed by a small, flexible amino acid such as glycine which has little steric hindrance which leaves the peptide group open for attack. The relatively small polar side chains for serine and threonine also facilitate deamidation. Deamidation occurs at amino acid 11 to form [L-Asp11]-, [D-Asp11]-, [L-isoAsp11]- and [D-isoAsp11]-Bovine GLP-2 (1-15) (Peptide Numbers 9-12), using the pathway described in *Figure 10*. As the asparagine side chain attacks the peptide bond, it forms a cyclic succinimide intermediate, which can ring open to form the aspartate or isoaspartate via hydrolysis. The formation of D- or L-aspartate / isoaspartate is dictated by the enolation reaction, where the nucleophile can attack either from above or below the molecule [66]. A D-

asparagine variant is not produced as the ring requires a nucleophile (i.e. ammonia) to open. The process of deamidation can proceed more readily when using elevated pH (alkaline pH increases the rate of succinimide formation due to greater deprotonation of the peptide bond) or temperature. Glutamine deamidation can occur but at a lower rate [71]. This tendency to isomerise at a lower rate than asparagine is attributed to the higher energy barrier for the six-membered ring formed for Glu / Gln conversion in comparison to the five-membered ring formed by Asp / Asn conversion.

The aspartic acid at position 3 in the peptide chain can undergo racemisation and isomerisation to form [D-Asp3]-, [L-isoAsp3]- and [D-isoAsp3]-Bovine GLP-2 (1-15) (Peptide Numbers 3-5). This transformation is facilitated by the glycine in amino acid position 4 on the peptide chain and follows the same reaction pathway as demonstrated in *Figure 10*. The asparagine derivative is not formed as the ring cannot be opened without the presence of ammonia.

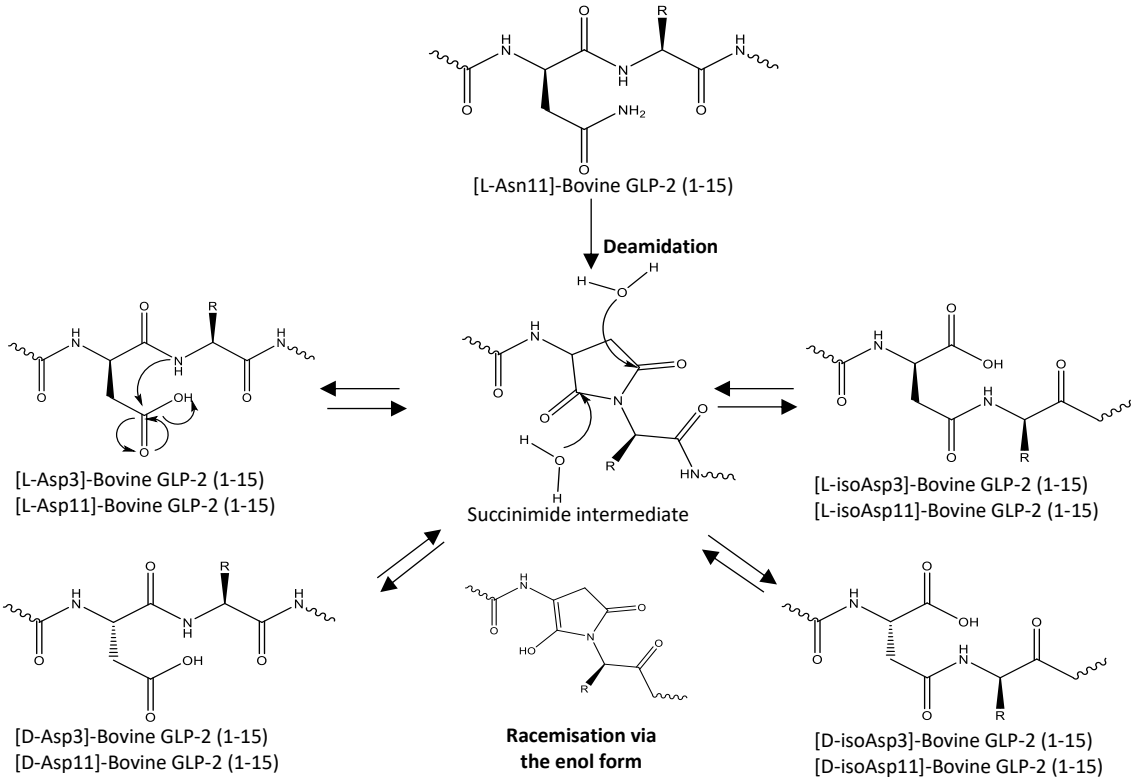

Figure 10 Schematic of deamidation, isomerisation and racemisation of [L-Asn11]- and [L-Asp3]-Bovine GLP-2 (1-15) via the succinimide intermediate.

3.3.3 "Hydrophobic" Segment – Bovine GLP-2 (16-33)

The "hydrophobic" segment of the bovine peptide can be seen in *Table 25*. This section of the peptide underwent various modifications to determine the effects of properties such as branching, aliphatic and aromatic interactions, charge and hydrophobicity. These are changes that do not take place during degradation but which are relevant for probing peptide-column interactions.

Table 25 The "hydrophobic" segment of the Bovine GLP-2 peptide, with the sequences of peptide with various modifications. Where s denotes D-Ser, d denotes D-Asp, i denotes iso. Marked in grey within the table represents the amino acid change.

Peptide number	Peptide	Sequence																	
		16	17	18	19	20	21	22	23	24	25	26	27	28	29	30	31	32	33
13	Bovine GLP-2 (16-33)	S	L	A	T	R	D	F	I	N	W	L	I	Q	T	K	I	T	D
14	[D-Ser16]-Bovine GLP-2 (15-33)	s	L	A	T	R	D	F	I	N	W	L	I	Q	T	K	I	T	D
15	[Ile26,Leu27]-Bovine GLP-2 (15-33)	S	L	A	T	R	D	F	I	N	W	I	L	Q	T	K	I	T	D
16	[L-Asp21,Gly22]-Bovine GLP-2 (15-33)	S	L	A	T	R	D	G	I	N	W	L	I	Q	T	K	I	T	D
17	[D-Asp21,Gly22]-Bovine GLP-2 (15-33)	S	L	A	T	R	d	G	I	N	W	L	I	Q	T	K	I	T	D
18	[L-isoAsp21,Gly22]-Bovine GLP-2 (15-33)	S	L	A	T	R	iD	G	I	N	W	L	I	Q	T	K	I	T	D
19	[D-isoAsp21,Gly22]-Bovine GLP-2 (15-33)	S	L	A	T	R	id	G	I	N	W	L	I	Q	T	K	I	T	D
20	[Val26]-Bovine GLP-2 (15-33)	S	L	A	T	R	D	F	I	N	W	V	I	Q	T	K	I	T	D
21	[Ile26]-Bovine GLP-2 (15-33)	S	L	A	T	R	D	F	I	N	W	I	I	Q	T	K	I	T	D
22	[Phe26]-Bovine GLP-2 (15-33)	S	L	A	T	R	D	F	I	N	W	F	I	Q	T	K	I	T	D
23	[Trp26]-Bovine GLP-2 (15-33)	S	L	A	T	R	D	F	I	N	W	W	I	Q	T	K	I	T	D
24	[Tyr26]-Bovine GLP-2 (15-33)	S	L	A	T	R	D	F	I	N	W	Y	I	Q	T	K	I	T	D
25	[Lys20]-Bovine GLP-2 (15-33)	S	L	A	T	K	D	F	I	N	W	L	I	Q	T	K	I	T	D
26	[Lys26]-Bovine GLP-2 (15-33)	S	L	A	T	R	D	F	I	N	W	K	I	Q	T	K	I	T	D

This section of the peptide has one serine site in position 16 which can undergo racemisation to produce [D-Ser16]-Bovine GLP-2 (16-33) (Peptide Number 14). The serine diastereoisomers can be seen in *Figure 8*.

Leucine and isoleucine are isomeric species – they possess the same molecular formula but different spatial arrangement of atoms. Within Bovine GLP-2 (16-33), leucine occupies position 26 whilst isoleucine is in position 27 of the peptide chain. By reversing the order of leucine and isoleucine (*Figure 11*), the peptide can be used to probe the subtle effect of amino acid position (Peptide Number 15). It is

expected to be difficult to separate due to the peptide having very similar physicochemical properties.

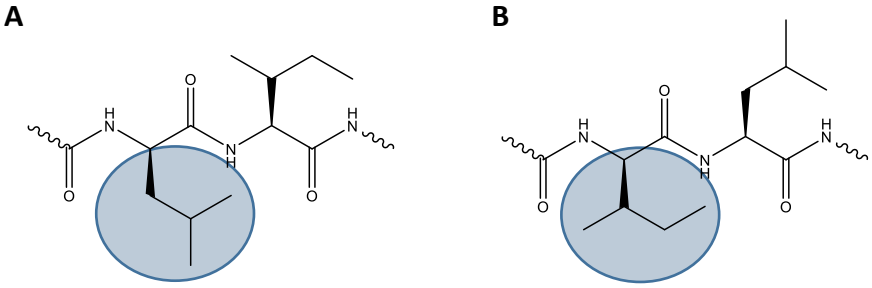

Figure 11 Chemical structure of positions 26 and 27 of Bovine GLP-2 (16-33) (A) [Leu26,Ile27]- and (B) [Ile26,Leu27]-Bovine GLP-2 (16-33).

The amino acid at position 22 was changed from phenylalanine (F) to glycine (G) to be adjacent to aspartic acid (D) (Peptide Number 16, *Figure 12*). Glycine is known to facilitate instability due to its small size when beside the aspartate amino acid. A cyclic intermediate enables four isomeric products to be generated: [L--Asp21,Gly22]-, [D-Asp21,Gly22]-, [L-isoAsp21,Gly22]- and [D-isoAsp21,Gly22]-Bovine GLP-2 (16-33) (Peptide Numbers 16-19), following the pathway demonstrated in *Figure 10*.

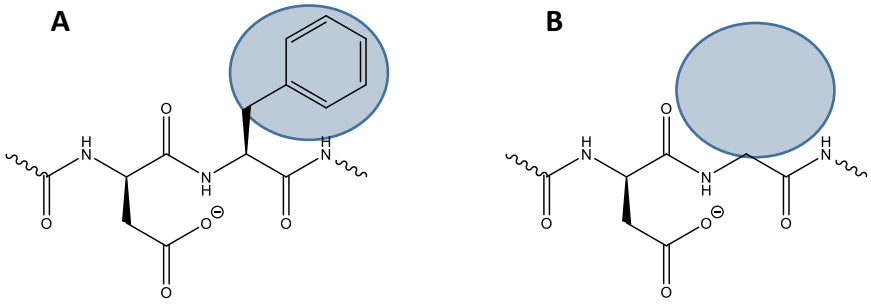

Figure 12 Chemical structure of positions 21 and 22 of (A) [L-Asp21,Phe22]- and (B) [L-Asp21,Gly22]-Bovine GLP-2 (16-33).

The amino acid at position 26 was changed to valine (V, [Val26]-), isoleucine (I, [Ile26]-), phenylalanine (F, [Phe26]-), tryptophan (W, [Trp26]-) and tyrosine (Y, [Tyr26]-Bovine GLP-2 (16-33)) (Peptide Numbers 20-24, respectively). A comparison of L, V and I might probe the aliphatic effect (*Figure 13)*, whilst F and Y can establish

the impact of changes in phenolic character (*Figure 14*). F, W and Y can examine the effect of aromaticity (*Figure 15*). Small molecules are highly influenced by aromatic and phenolic effects, however, it is uncertain how the change of a single amino acid in a peptide will impact on selectivity, since this is a relatively subtle modification of the peptide compared to a small molecule. Mant *et al.* did observe selectivity differences on a range of peptides similar in size which differed by one amino acid [20, 21, 74], however, their peptides had several glycine residues throughout the sequence to prevent any secondary structure. This might not be the case for biologically active peptides which typically are more heterogenic.

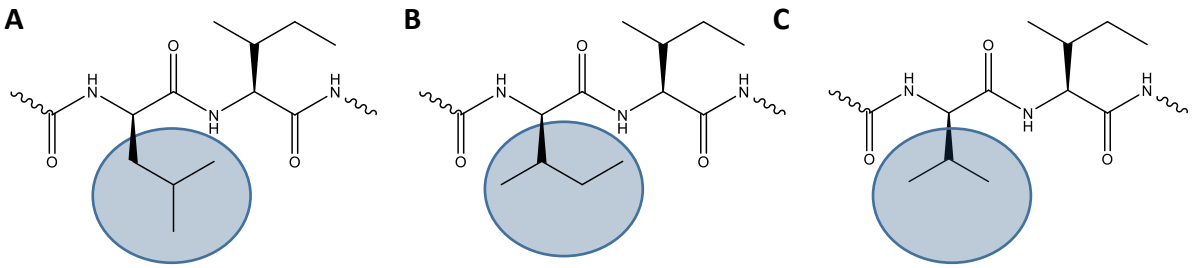

Figure 13 Chemical structure of positions 26 of (A) [Leu26]- (B) [Ile26]- and (C) [Val26]-Bovine GLP-2 (16-33) to investigate the aliphatic effect.

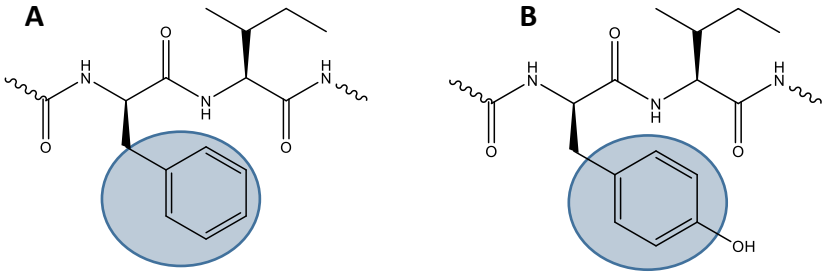

Figure 14 Chemical structure of positions 26 and 27 of (A) [Phe26]- and (B) [Tyr26]-Bovine GLP-2 (16-33) to investigate π-π electron interactions and phenolic effects.

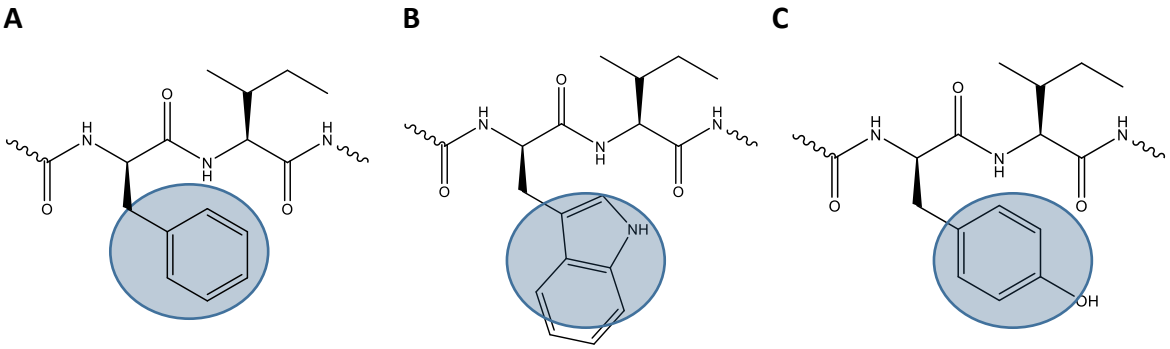

Figure 15 Chemical structure of positions 26 and 27 of (A) [Phe26]- (B) [Trp26]- and (C) [Tyr26]-Bovine GLP-2 (16-33) to investigate aromaticity effects.

The amino acid at position 20 was changed from arginine (R) to lysine (K, [Lys20]-Bovine GLP-2 (16-33)) (Peptide Number 25, *Figure 16*). This modification investigates the effect of a small change in polarity and basicity of the peptide with the same charge (from pK_a 12.48 to 10.35 for the substituted amino acid).

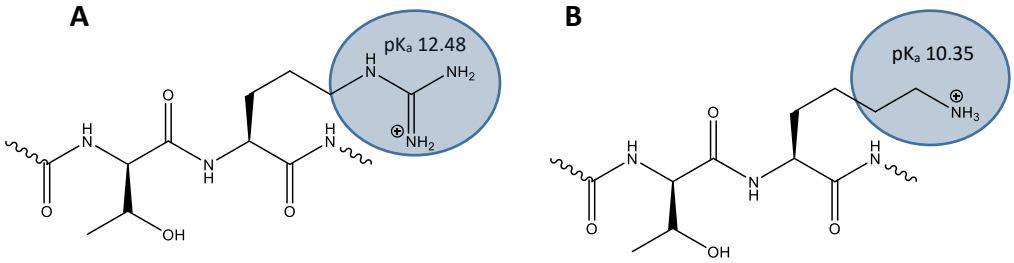

Figure 16 Chemical structure of positions 20 and 21 of (A) [Arg20]- and (B) [Lys20]-Bovine GLP-2 (16-33) to investigate polarity effects.

The amino acid at position 26 was changed from leucine (L) to lysine (K, [Lys26]-Bovine GLP-2 (16-33) (Peptide Number 26)) to assess the effect of changing from a neutral to a positive species (*Figure 17*).

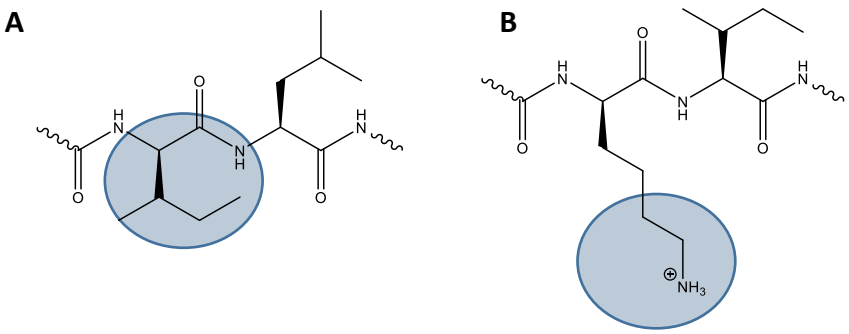

Figure 17 Chemical structure of positions 26 and 27 of (A) [Leu26]- and (B) [Lys26]-Bovine GLP-2 (16-33) to investigate effects of charge.

3.3.4 Solubility and Stability of Bovine GLP-2

Solubility studies were conducted by Novo Nordisk on the unmodified hydrophilic and hydrophobic Bovine GLP-2 chains (Peptide Number 1 and 13, respectively). The two peptides were dissolved in 100% distilled water, DMSO / H_2O (80:20 v/v) or pH 7 phosphate buffer before evaluation on Day 0, 7 and 14 at 8 °C. The pH was measured in the aqueous organic mixtures in order to ascertain how acidic the conditions were. The measured pH was lower for the water sample than the DMSO and phosphate diluents. This can be attributed to the freeze-dried peptides which are supplied in the TFA salt form (*Table 26*). Visual inspections were also conducted at these time intervals, where clear solutions were observed for Peptide Number 1 (hydrophilic chain) dissolved in 80% DMSO or phosphate buffer and Peptide Number 13 (hydrophobic chain) dissolved in water or 80% DMSO. The hydrophilic Bovine GLP-2 (1-15) produced a gel like structure when dissolved in 100% water, whilst precipitation was observed between Bovine GLP-2 (16-33) and phosphate buffer. It is common practice within Novo Nordisk to use a DMSO based diluent when analysing peptide samples, which is corroborated by these results.

Table 26 Solubility study for peptides Bovine GLP-2 (1-15) and Bovine GLP-2 (16-33) in either distilled water, 80% DMSO or pH 7 phosphate. Samples stored at 8 °C when not being analysed.

	Peptide Number 1 Bovine GLP-2 (1-15)			Peptide Number 13 Bovine GLP-2 (16-33)		
	Distilled Water	**80% DMSO**	**pH 7 phosphate**	**Distilled Water**	**80% DMSO**	**pH 7 phosphate**
Day 0, 8 °C	Clear, small particles (like "gel")	Clear	Clear	Clear	Clear	Precipitates
Day 7, 8 °C	Clear, small particles (like "gel")	Clear	Clear	Clear	Clear	Precipitates
Day 14, 8 °C	Clear, small particles (like "gel")	Clear	Clear	Clear	Clear	Precipitates
pH @ Day 14	3.10	5.13	5.97	2.99	5.76	6.65

The stability of both peptides in relation to sample diluent was evaluated for all sample diluents (i.e. the presence of additional peaks / changes in chromatographic profile), except Bovine GLP-2 (16-33) in phosphate buffer which caused precipitation. Stability was assessed by gradient chromatography where peak profiles and area were compared using a mobile phase of water with 90% MeCN with 0.09% TFA.

The profiles were similar over the course of the investigation, with no growth in impurity peaks. The area of the main peak was integrated and compared for increase in impurities. The highest and most consistent area was produced from the 80% DMSO sample diluent, suggesting the peptides had superior stability under those conditions (*Figure 18*). The level of impurities also remained consistent from day 0 to 14 at 8 °C.

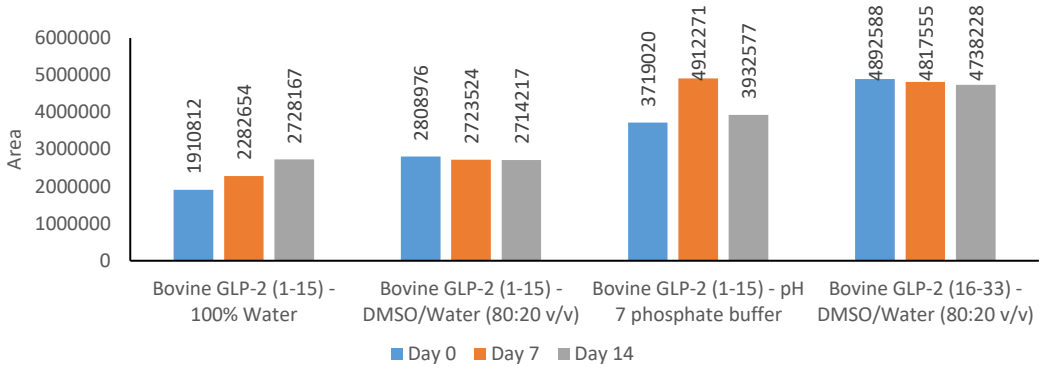

Figure 18 Comparison of peak area for peptides Bovine GLP-2 (1-15) and Bovine GLP-2 (16-33) using different diluents. Data provided by Novo Nordisk.

3.3.5 Use of Circular Dichroism to Estimate Peptide Secondary Structure

Circular dichroism (CD) is a well-used tool to help elucidate structural information for peptides. Multiple samples can be evaluated in physiological buffers within a couple of hours to provide information on stability, changes in conformation and binding properties of the peptide. This rapid technique enables simple determination of the presence or absence of a secondary structure within the peptide probes used for the characterisation. For a greater understanding of any specific residue involved in the binding however, additional techniques would need to be employed such as NMR or x-ray crystallography [75-77].

CD measures the difference in absorbed left-handed circularly polarised light (L-CPL) and right-handed circularly polarised light (R-CPL) of a chiral molecule with chromophores. The molecule is exposed to a range of wavelengths which will absorb to differing degrees to produce a spectrum with either positive or negative signals. The spectrum produced depends on which light is absorbed to a greater extent (i.e. a positive signal is produced for greater absorbed L-CPL whilst negative is absorbed to a lesser extent than R-CPL).

CD uses the far UV region to gather information on secondary structure, by focussing on the peptide bond absorbing group. There is a weak, broad characteristic $n \rightarrow \pi^*$ transition at 210 nm and $\pi \rightarrow \pi^*$ transition observed at 190 nm, which intimates certain secondary structures [77]. These distinctive transitions enable one to identify the presence of α-helixes, β-sheets and β-turns within a peptide, or alternatively, a lack of higher order structure (i.e. random coil). CD can also be used to assess peptide structure quantitatively with various protocols available to aid determination [77].

CD was performed within Novo Nordisk on four peptides which were either representative of the peptide probes, or the amino acid sequence highlighted potential sites for binding (i.e. a moiety in close proximity to a terminus). These peptides and the sample preparation can be seen in *Table 27*. Each sample was dissolved in acetonitrile / water mixtures with either formic acid or ammonium

formate. The conditions corresponded to the average conditions the peptides would be exposed to during the column characterisation protocol (described in *Section 2.10.5*). Where there were potential solubility issues, the concentration of acetonitrile and the volume were increased. Measurements were made at both 20 and 40 °C *(Figure 19* and *Figure 20*, respectively), where the lower temperature corresponded to ambient temperature and the higher temperature coincided with the operating conditions for the column characterisation (the development of the column characterisation can be found in *Section 3.5*).

Table 27 Preparation of peptides for circular dichroism analysis.

Peptide Number	Peptide	Conc. of Peptide (mg/mL)	Conc. of MeCN (%)	Conc. of TFA* (mM)	Conc. of Formic Acid (%)	Conc. of Ammonium Formate (mM)
1	Bovine GLP-2 (1-15)	0.41	30	0.6	0.9	
		0.44	23	1.2		20
9	[L-Asp11]-Bovine GLP-2 (1-15)	0.41	30	0.6	0.9	
		0.55	23	1.2		20
13	Bovine GLP-2 (16-33)	0.69	23	1.4	0.10	
		0.3	30	0.7		18
26	[Lys26]-Bovine GLP-2 (16-33)	0.95	23	1.8	0.10	
		0.91	23	1.8		20

** Neutralised with sodium hydroxide solution.*

A Jasco J1500 instrument (S/N A023261638) was used with a measured range of 260 – 190 nm, data pitch of 0.5 nm, band width 2.00 nm, scanning speed of 50 nm/min and a 0.2 mm cell length. Three repeat measurements were made at temperatures set at either 20 or 40 °C (±0.10 °C). Blank samples (i.e. the sample diluent) were run to determine any background noise or other artefacts within the spectra not related to the peptide.

Random coils were observed under both temperature and sample diluent conditions for Bovine GLP-2 (1-15), [L-Asp11]-Bovine GLP-2 (1-15) and [Lys26]-Bovine GLP-2 (16-33) (Peptide Numbers 1, 9 and 26, respectively), with a negative

maximum at approximately 200 nm (*Figure 19* and *Figure 20*). This was determined by a lack of artefacts in the CD spectra which denote higher order structures [77]. Thus, there is no evidence of a secondary structure for these peptides under these conditions, and it could be expected that these peptides would possess a random coil under the chromatographic conditions of the column characterisation protocol.

Bovine GLP-2 (16-33) (Peptide Number 13) differed, however, with a negative signal at ~220 nm which is characteristic of a part helical conformation or aggregation. The response is dissimilar for the two different diluent conditions where the signal is more pronounced under the ammonium formate conditions, which could be induced by changes in pH, solvent or concentration, and therefore could be the cause of some self-association. Molecular modelling suggested that the amino acid residue region "FNWLI" within Bovine GLP-2 (16-33) could explain any aggregation, if it was observed.

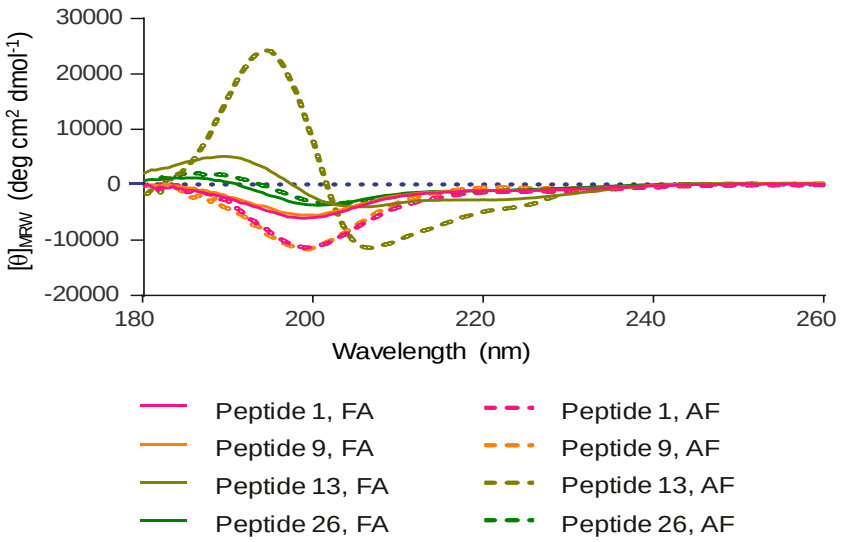

Figure 19 CD spectra for Peptides 1, 9, 13 and 26 dissolved in formic acid (solid line) or ammonium formate (dashed line) diluent at 20 °C. Data provided by Novo Nordisk.

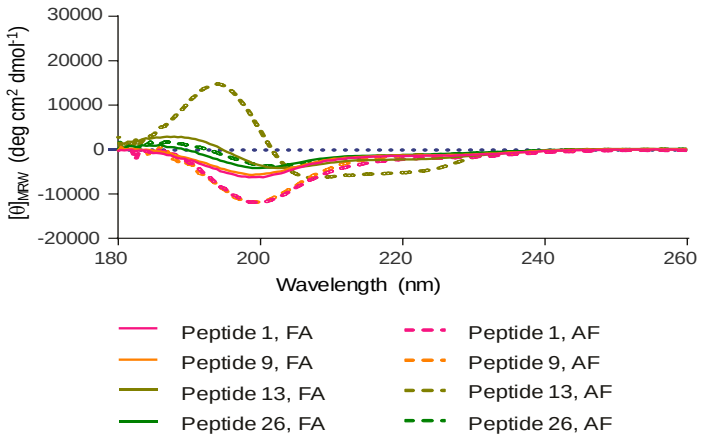

Figure 20 CD spectra for Peptides 1, 9, 13 and 26 dissolved in formic acid (solid line) or ammonium formate (dashed line) diluent at 40 °C. Data provided by Novo Nordisk.

The potential for self-association was further studied by diluting the sample and re-evaluating by CD, where a reduction of the response at 220 nm would suggest aggregation rather than a helical structure. A dilution would not remove the signal if there was a secondary structure. The artefact at 220 nm at 40 °C was reduced, which therefore indicates the peptide does not possess a secondary structure, but does have the potential to self-associate (*Figure 21*). This has ramifications for the protocol where it is important to minimise the concentration of the peptides to ensure all peptides are random coils within the characterisation process.

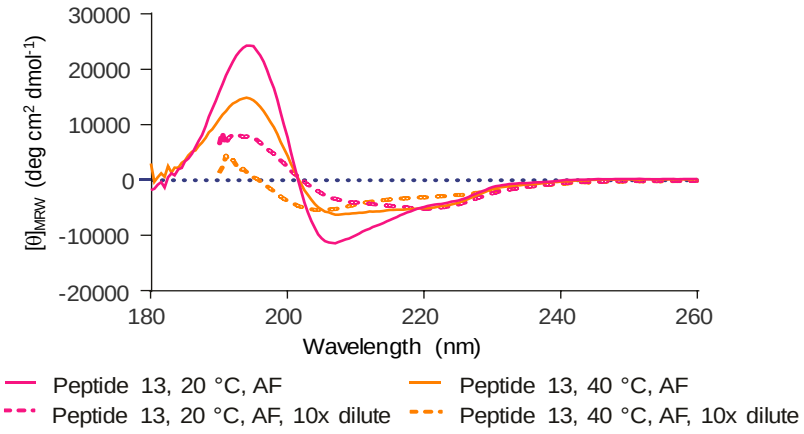

Figure 21 CD spectra for Peptide 13 at 20 and 40 °C using the original sample concentration (solid lines) and a 10x dilution (dashed lines). Data provided by Novo Nordisk.

3.4 Rationale for Performing Column Characterisation using Small Molecules

There are numerous stationary phases available on the market, all possessing different properties depending on parameters such as pore size, ligand chemistry and bonding density. Column characterisation is a standardised approach used to assess the chromatographic properties of these HPLC phases. Many protocols can be found in literature using small test solutes to evaluate the stationary phase for common retention mechanisms, such as hydrophobicity or hydrogen bonding, which allows for comparison between different column manufacturers, ligand chemistry and LC instrumentation [13-19, 49, 78-91].

The Snyder approach, known as the Hydrophobic Subtraction model (HSM), measures the hydrophobicity, steric interactions, acidic and basic hydrogen bonds and the cation exchange capacity at low and intermediate pH. Some simple schematic diagrams highlight the different interactions measured by the model (*Figure 22*). RPC utilises a non-polar stationary phase which is capable of forming hydrophobic interactions with analytes. The degree of this interaction depends on the logD (i.e. a measure of hydrophobicity at a specific pH value which looks at the concentration of an analyte distributed between *n*-octanol and water, *Equation 11*) of the analyte as well as the ligand on the stationary phase, i.e. a C18 stationary phase is more hydrophobic than a C8, whilst pentylbenzene is more hydrophobic than butylbenzene. The more hydrophobic analyte has a greater propensity for the non-polar stationary phase than the polar mobile phase, thus elutes later than the less hydrophobic solute (*Figure 22(A)*).

$$LogD = \frac{Neutral+ionised\ in\ octanol}{Neutral+ionised\ in\ water}\ at\ a\ specific\ pH \qquad \textit{Equation 11}$$

The HSM investigates the resistance of the stationary phase to bulky molecules (*Figure 22(B)*). The larger molecule cannot penetrate the stationary phase, therefore elutes before the smaller molecule, which can be drawn further towards the surface of the phase. The density of the bonded phase can also be critical to this

parameter, where a more densely bonded phase excludes a molecule whilst a lower coverage can accept the same molecule.

Silanol groups possess a dipole which can form an electrostatic attraction to a nearby electronegative atom such as nitrogen or oxygen, via a hydrogen bond (*Figure 22(C)*). Additionally, ionised silanols are negatively charged, which can retain positively charged species such as bases via cation exchange interactions (*Figure 22(D)*). However, any negatively charged species such as ionised acids will be repelled from the stationary phase by the electrostatic repulsion [13, 14, 45].

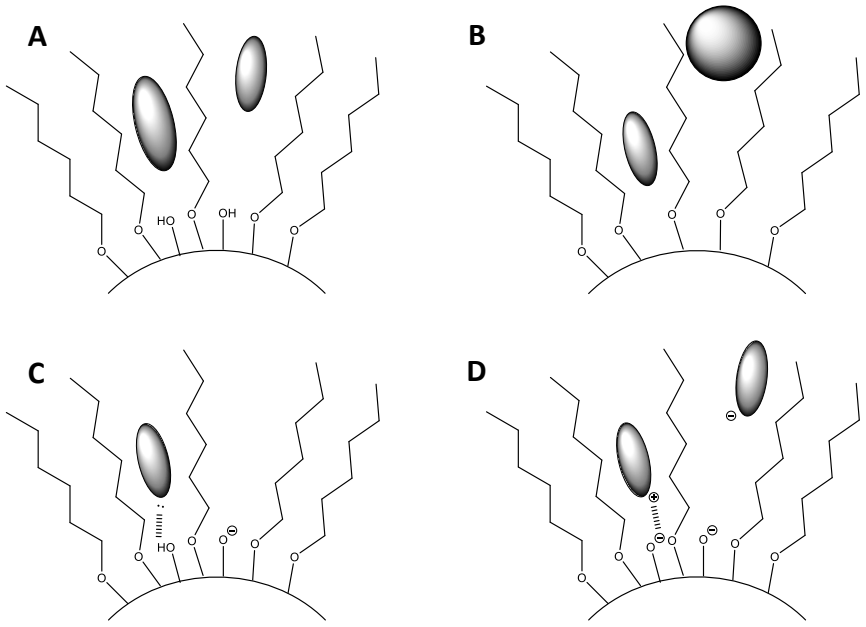

Figure 22 Schematic diagrams for (A) hydrophobicity, (B) steric interactions (C) hydrogen bonding and (D) ionic attraction and repulsion. Structures drawn using Chem3D Pro (Version 16.0.0.82 based on [45]).

The Euerby *et al.* protocol is an extension of the Tanaka protocol, which investigates the above properties, however, under different conditions and alternative probes. The aromatic characteristics of the phase are also investigated with markers for π-π and dipole-dipole interactions and phenolic activity. There are also extensions on the protocols which probe the acidic and basic character, thereby providing more information on other key retention mechanisms [17-19].

The NIST SRM 870 tests consists of five probes which are used to identify hydrophobicity, silanol activity and metal content. Various authors have commented that tests for surface metal activity is highly dependent on the history of the column. Factors such as shipping and storage solvent can be extremely influential on the metal activity, thus is only valid for that column at that particular moment in time which thereby reduces its usefulness as a characterisation measure [84, 85, 92, 93].

By collating data from a large set of stationary phases using column characterisation protocols, a database can be created for comparison between different vendors and ligand chemistry. They allow the end user to not only check the most similar stationary phase for "back-up" columns, but also the most different phases, useful for method development purposes.

The PQRI database and Stoll's database, which is based on Snyder's Hydrophobic Subtraction model, contains >730 entries, whilst ACD's database, based on the work of Tanaka and Euerby *et al.*, contains >340. One of the smaller records is the USP database constructed using NIST SRM 870, which contains 124 entries (information was correct as of July 2019) [82, 86, 94]. Both the PQRI and ACD database contain common type B silica stationary phases in addition to type A silica and more unusual phases such as polymer coated alumina and zirconium oxide. The type A and B nomenclature refers to the purity of the silica, where type A silicas possess lower purity, less uniform particle structure and greater metal content than the type B silicas. The majority of modern stationary phases use type B silicas as the support [88]. The USP database based on the NIST SRM 870 protocol is limited to type B silica with some type A silica.

Borges *et al.* compared these three databases to ascertain their applicability and identify any weaknesses in the column selection process [88]. Borges evaluated the chromatographic descriptors used for characterising the stationary phase for each methodology; six descriptors are used by PQRI and ACD, and three descriptors used by USP. He determined each were independent of the other descriptors based on

the percentage relative standard deviation (%RSD), which signified each descriptor was necessary to describe the phase. Borges also stated the Tanaka and HSM approaches had similar discriminating power for differentiating between diverse stationary phases (%RSD range of 38-421% and 22-439% respectively), whilst the USP was significantly lower (41-69%) [88].

Borges' study also compared the Hydrophobic Subtraction Model and the Extended Tanaka protocol to establish if they identified similar or dissimilar columns. In general, the two databases provided subtle differences in rankings of similarity, however, they both successfully highlighted similar or dissimilar columns. The two databases cannot be directly compared as Snyder uses regressions whilst Euerby uses selectivity values [88].

The Euerby *et al.* methodology was used to characterise several commercially available stationary phases. Past experience has provided significant knowledge into the technique which will be highly beneficial for extracting influential retention mechanisms. The commercial columns were donated by Waters, Agilent, Fortis, Phenomenex and Supelco (*Table 28*). The Thermo columns were purchased directly from the manufacturer. The PLRP-S stationary phase was not characterised as the conditions produced excessive retention times for the test probes.

Table 28 Extended Tanaka characterisation results for HPLC columns to be used in the study.

Description	k_{PB}	$\alpha_{(CH2)}$	$\alpha_{(T/O)}$	$\alpha_{(C/P)}$	$\alpha_{(B/P\ pH\ 7.6)}$	$\alpha_{(B/P\ pH\ 2.7)}$	$\alpha_{(TNB/T)}$	$\alpha_{(BSA/T)}$	$\alpha_{P/BA}$	$\alpha_{(1,2/1,4\text{-}DNB)}$	Particle Size (µm)	Pore Size (nm)
Acquity UPLC BEH C4 300	0.28	1.24	0.88	1.48	0.40	0.22	0.39	0.13	1.00	1.42	1.7 [2]	300
Acquity BEH C8	1.16	1.34	0.86	0.59	0.31	0.13	0.24	0.02	1.00	1.18	1.7 [2]	130
Acquity UPLC BEH C18 130 [3]	3.99	1.47	1.38	0.37	0.23	0.09	0.17	0.00	1.00	1.00	1.7 [2]	130
Acquity UPLC BEH C18 300 [3]	1.97	1.48	1.41	0.38	0.22	0.11	0.17	0.02	1.00	1.00	1.7 [2]	300
Acquity BEH Shield RP18	2.08	1.41	2.36	0.30	0.27	0.13	0.31	0.04	1.35	1.11	1.7 [2]	130
Acquity CSH C18 [3]	3.53	1.44	1.35	0.40	0.38	0.09	0.21	0.03	0.98	1.00	1.7 [2]	130
Acquity CSH Fluoro Phenyl [3]	0.46	1.00	3.10	1.72	1.24	-0.06	0.48	0.74	0.96	1.48	1.7 [2]	130
Acquity CSH Phenyl Hexyl [3]	1.47	1.31	1.13	0.70	0.42	0.07	0.85	0.16	0.94	1.22	1.7 [2]	130
Acquity HSS C18	7.38	1.48	1.47	0.37	0.24	0.11	0.14	0.01	1.00	0.97	1.8 [2]	100
Acquity HSS C18-SB	2.57	1.39	1.94	1.86	4.99	0.16	0.24	0.01	0.88	1.23	1.8 [2]	100
Acquity HSS T3 [3]	6.02	1.50	1.19	0.50	0.34	0.12	0.22	0.01	1.00	0.94	1.8 [2]	100
Cortecs UPLC T3	2.87	1.47	1.20	0.51	0.26	0.13	0.22	0.02	1.00	0.96	1.6 [1]	120
Polaris Amide C18	2.87	1.43	2.43	0.20	0.15	-0.02	0.20	2.39	1.50	1.28	3.0 [2]	200
Poroshell 120 PFP	1.06	1.26	2.80	0.67	0.67	0.04	0.52	0.07	1.29	2.16	2.7 [2]	120
Poroshell 120 Bonus-RP	1.73	1.34	1.57	0.39	0.31	0.01	0.28	1.60	1.27	1.31	2.7 [2]	120
Poroshell 120 Phenyl Hexyl	1.98	1.33	1.21	0.86	0.44	0.14	0.98	0.01	1.00	1.00	2.7 [2]	120
Poroshell 120 SB-AQ	0.55	1.30	1.11	0.36	1.14	0.18	0.42	0.09	1.00	1.09	2.7 [2]	120
Poroshell HPH-C8 [3]	1.82	1.36	0.91	0.33	0.37	0.08	0.20	0.04	1.00	1.11	2.7 [2]	120
Poroshell HPH-C18	3.83	1.49	1.26	0.45	0.38	0.10	0.18	0.01	1.00	0.92	2.7 [2]	120
Agilent SB-C8	2.23	1.37	0.93	1.32	1.26	0.14	0.25	0.00	0.89	1.11	3.5 [2]	80
Agilent SB-C18	5.37	1.49	1.24	0.64	0.94	0.10	0.17	0.01	1.00	0.89	3.5 [2]	80
Zorbax SB-C18 300 [3]	1.23	1.44	1.22	0.76	1.00	0.12	0.21	0.01	1.00	0.87	3.5 [2]	300
PLRP-S [4]											3.0 [2]	100
Ascentis Express Biphenyl	1.69	1.29	1.53	2.30	0.96	0.16	1.89	0.01	0.87	0.75	2.7 [1]	90
Ascentis Express C18	5.39	1.50	1.42	0.42	0.70	0.10	0.14	0.01	1.00	0.89	2.7 [1]	90
Ascentis Express C8	2.61	1.39	0.93	0.30	0.39	0.09	0.19	0.01	1.00	1.11	2.7 [1]	90
Ascentis Express F5	1.40	1.27	2.53	0.69	1.65	0.48	0.51	0.01	1.20	2.62	2.7 [1]	90
Ascentis Express Phenyl-Hexyl	2.30	1.35	1.17	0.83	0.54	0.11	1.02	0.02	1.00	0.96	2.7 [1]	90
Ascentis Express RP-Amide	3.20	1.43	1.79	0.22	0.38	0.04	0.19	0.05	1.49	1.22	2.7 [1]	90
BIOshell A160 Peptide C18	2.26	1.45	1.21	0.75	1.00	0.13	0.22	0.01	1.00	0.93	2.7 [1]	160
BIOshell A160 Peptide CN	0.20	1.15	1.82	0.88	1.37	0.22	0.92	-0.14	1.00	1.12	2.7 [1]	160
Acclaim Mixed Mode WAX	0.77	1.29	2.45	0.06	0.09	-0.10	0.24	0.00	1.93	1.49	5 [2]	120
Acclaim Mixed Mode WCX	0.66	1.16	3.33	0.48	1.84	0.05	0.43	0.05	1.48	1.83	5 [2]	120
Acclaim Mixed Mode HILIC	0.55	1.25	1.90	1.19	2.18	0.06	0.24	0.02	1.11	1.75	5 [2]	120
Chromolith® Performance RP-18e	2.36	1.47	1.43	0.43	0.63	0.09	0.17	0.01	1.00	0.95	N/A [2]	130 [5]
Kinetex Evo C18	3.08	1.44	1.12	0.42	0.37	0.09	0.19	0.03	1.00	1.09	2.6 [1]	100
Kinetex Biphenyl	1.36	1.31	1.52	2.14	0.80	0.16	1.97	0.02	0.87	0.72	2.6 [1]	100
Kinetex C8	1.84	1.36	1.16	0.36	0.42	0.09	0.20	0.01	1.00	1.26	2.6 [1]	100
Kinetex C18	3.67	1.46	1.25	0.45	0.43	0.11	0.18	0.01	1.00	1.05	2.6 [1]	100
Kinetex F5	1.36	1.32	2.29	0.77	0.71	0.13	0.43	0.00	1.11	1.47	2.6 [1]	100
Luna Omega C18	5.42	1.46	1.11	0.53	0.42	0.11	0.20	0.00	1.00	1.03	1.6 [2]	100
Luna Omega Polar C18	3.58	1.43	1.14	0.67	0.66	0.13	0.26	0.01	1.00	1.00	1.6 [2]	100
Luna Omega PS C18	3.84	1.43	1.11	0.53	0.51	0.08	0.22	0.14	1.00	1.12	1.6 [2]	100
Fortis Diphenyl	1.54	1.31	0.93	0.81	0.56	0.07	0.41	0.32	1.00	1.11	1.7 [3]	110

[1]SPP, [2]TPP, [3]Data acquired from M. Euerby and P. Petersson, [4]Conditions not suitable for analysis due to excessive retention, [5]Average mesopore size.

The Extended Tanaka characterisation protocol can provide significant quantities of data, with 21 selectivity values (α) which can be generated by the extended protocol and a further 23 α values provided by the acidic and basic characterisation [17-19, 50, 79, 95]. To perform the entire characterisation protocol on all the stationary phases would take significant resources, therefore only the most applicable descriptors were selected. The most meaningful chromatographic descriptors for this study were considered to be k_{PB} and $\alpha_{(CH2)}$ (ligand density and hydrophobicity / ability to differentiate between methylene groups), $\alpha_{(T/O)}$ (steric selectivity), $\alpha_{(C/P)}$ (hydrogen bonding capacity), $\alpha_{(B/P)}$ (cation exchange capacity at pH 2.7 and 7.6 i.e. acidic and total silanol activity), $\alpha_{(P/BOH)}$ (phenolic selectivity), $\alpha_{(1,3,5\text{-}TNB/T)}$ (aromatic π-π interactions between a π-acid and π-base), $\alpha_{(1,2\text{-}/1,4\text{-}DNB)}$ (dipole-dipole interactions) and $\alpha_{(BSA/T)}$ (anion exchange capacity, *Figure 23*). The reduced probe sample set allows for a greater number of columns to be included in the study which will enhance its applicability across a greater number of stationary phases.

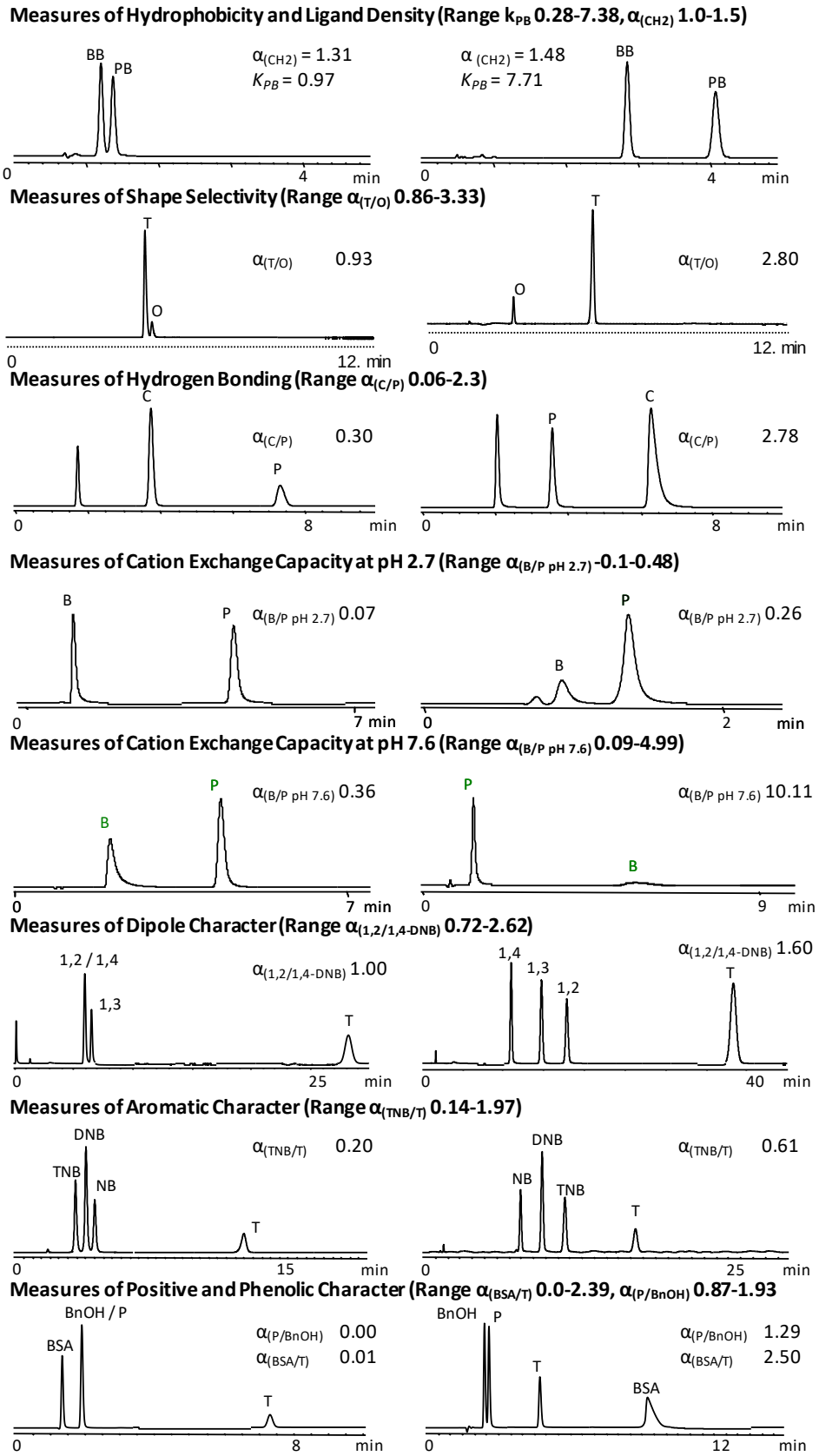

Figure 23 Example chromatograms for each alpha value to be determined in the Extended Tanaka protocols. See Section 2.7 for specific LC operating conditions.

Test solutes are complex molecules which can possess several moieties which make it possible for multiple retention mechanisms to be at play. This can make it difficult to rationalise chromatographic results. For example, $\alpha_{T/O}$ is a measure of shape selectivity between the puckered *o*-terphenyl and planar triphenylene. The volume of *o*-terphenyl restricts its accessibility into the stationary phase, whilst there isn't such a steric resistance for triphenylene. However, triphenylene also has the ability to perform strong π-π interactions with pentafluorophenyl phases, as a π-acid and π-base, which could also affect the alpha value [89]. Caffeine is also known to undergo mixed mode interactions (i.e. *π-π* and hydrogen bonding) which can influence the respective alpha value. Although the alpha values may represent mixed mode retention mechanisms, they can still be used for the purpose of identifying similar and dissimilar columns. The ability to critically assess the alpha values is extremely important in order to understand characterisation results. It is therefore advantageous that the ACD database only accepts column entries provided solely by the Euerby / Petersson research group on virgin columns, where the results are also critically assessed before uploading. By only accepting results from within the research group, the validity of the database is maintained.

The robustness of the extended Tanaka characterisation tests is also well described in literature, where statistical tools such as reduced factorial design, principal component analysis (PCA) and multiple linear regression highlighted the critical parameters to obtain reliable results [95].

Reduced factorial design, which is discussed in much greater detail in *Section 3.7.1* and *3.7.2,* is a tool which investigates the key chromatographic parameters and critically assesses their contribution to the methodology. Euerby *et al.* [95] evaluated the robustness for each of the parameters in the Tanaka column characterisation protocol. These parameters include methanol content, temperature, pH and buffer concentration. They determined that methanol content was the most critical parameter for all the test conditions, then temperature. They suggest mobile phases should ideally be prepared by weight and not by volume (content should be controlled ±0.5% v/v), however, the experience of the analyst

suggests volumes can be determined accurately without detriment to the results. The column oven temperature should be obtained using a calibrated column thermostat (within ±3 °C of the setpoint) and mobile phases sufficiently preheated. The total ion exchange parameters are influenced by the pH of the mobile phase, thus must be controlled in order to obtain reliable results (pH ±0.1 and buffer concentration within ±2 mM) [95].

The chemometric analysis tool PCA is used to describe large datasets which contain several dimensions and reduce it to typically two dimensions known as principal components which is visually simpler to comprehend [96]. This is particularly beneficial for column characterisation databases, which contain considerable quantities of data. The reduced data can be displayed in score and loading plots. A score plot presents observations (in this circumstance, the stationary phases evaluated) in a 2-dimensional space along two axes where principal component 1 (PC1) is along the x axis and principal component 2 (PC2) is along the y axis. The position of the observations allows the analyst to detect trends. Observations which are separated horizontally are influenced predominantly by PC1, which those separated vertically are influenced predominantly by PC2. The variables used to describe the stationary phases are placed in a loading plot similar to that of a score plot. The position of the variables in the loading plot suggest that region is influenced by that variable. By superimposing the score and loading plot, a biplot can be produced.

PCA is extremely efficient at handling large datasets but requires dedicated software to analyse the results which limits the user if they do not possess the appropriate software. A criticism of PCA is that by using two PCs the amount of variability described can be relatively low which suggests a loss of information. This can be placated by utilising more PCs, which will increase the variability described. Also, PCA in this circumstance is being used to describe trends and patterns, not to predict, thus the variability described in the column PCA is sufficient. The column database is ever changing with additions of new stationary phases, which can affect the weighting of the variables. Outlying results can also affect the variable

weighting, but as the tool is used for trends or visualising dissimilar phases, the chemometric tool is fit for purpose.

PCA was applied to the data in *Table 28* to highlight the benefit of the technique, producing a biplot (*Figure 24*). The first PC described approximately 35% of the variability whilst the second PC described an additional 29%. In total, 64% of the variables are described by the model which is satisfactory for looking at observations and trends. The key chromatographic parameters evaluated are denoted by purple, star markers – k_{PB}, $\alpha_{(CH2)}$, $\alpha_{(T/O)}$, $\alpha_{(C/P)}$, $\alpha_{(B/P \text{ at pH } 2.7 \text{ and } 7.6)}$, $\alpha_{(TNB/T)}$, $\alpha_{(1,2\text{-}1,4\text{-}DNB)}$, $\alpha_{(P/BA)}$ and $\alpha_{(BSA/T)}$. The stationary phases are categorised based on prior knowledge into alkyl, mixed mode, PEG, PFP and phenyl groupings. The largest collection is based on alkyl phases, which range in alkyl lengths C4-C18, and differ in degree of endcapping, ligand density, or silica type (i.e. purity). The vast majority of alkyl phases are based in the second quadrant and are dominated by hydrophobic retention mechanisms (e.g. k_{PB} and $\alpha_{(CH2)}$). There are also some alkyl phases in the first quadrant, which are typically alkyl linkers which have reduced ligand density or are non endcapped, therefore can undergo hydrogen bonding and silanophilic interactions (e.g. $\alpha_{(C/P)}$ and $\alpha_{(B/P \text{ at pH } 2.7 \text{ and } 7.6)}$). The phenyl type phases are also positioned in the same direction, which could be due to potential silanophilic interaction, interactions between the caffeine and the aromatic rings, or alternatively drawn in that direction by the $\alpha_{(TNB/T)}$. The polar embedded group (PEG) consists of amide functionalities and carbamates. These phases are typically in the third quadrant, and are dominated by either phenolic interactions or possess positive character (e.g. $\alpha_{(P/BA)}$ and $\alpha_{(BSA/T)}$). The mixed mode or PFP moieties were collated in the fourth quadrant, where retention mechanisms could be based on shape or dipole-dipole interactions with the test probes (e.g. $\alpha_{(T/O)}$ and $\alpha_{(1,2\text{-}/1,4\text{-}DNB)}$). The scatter of phases suggests the stationary phases used in this study are representative of the most common phases available on the market, and cover a range of retention mechanisms. This chemometric technique will be further demonstrated in *Section 3.5.2.1* and *3.6.3*.

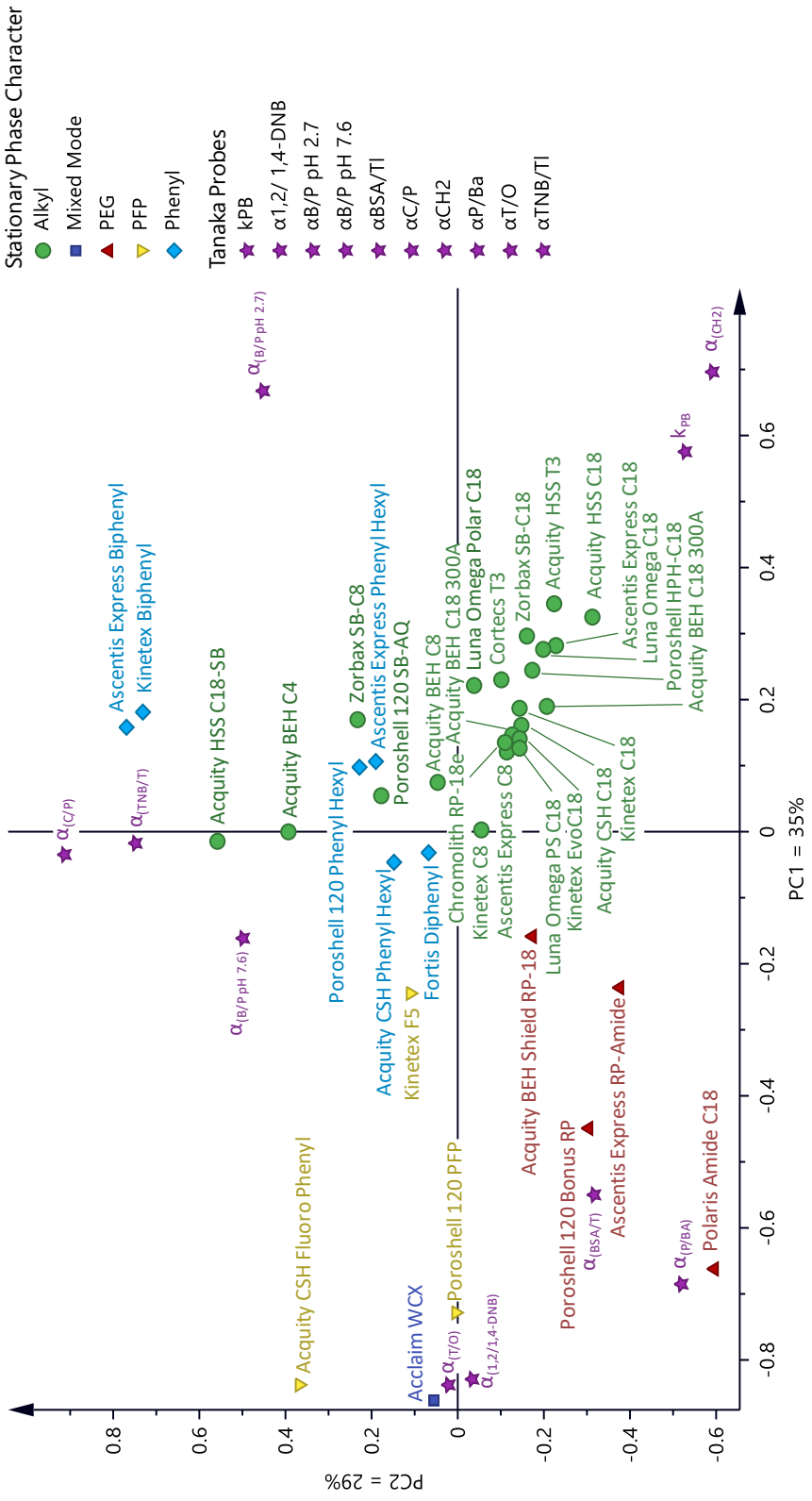

Figure 24 Biplot of the chromatographic parameters investigated by the Extended Tanaka protocol and the stationary phases assessed.

Despite there being a plethora of information on reversed phase stationary phase characterisation using small molecules, the validity of the results is uncertain when applied to peptide chromatography. The physicochemical properties of small molecules compared to peptides are certainly different, such as the ability to partition into the stationary phase which will have a particular influence on selectivity. Thus, the best suited probes for column characterisation when studying peptides should be peptide standards. Although there are a number of publications which are intended to predict peptide retention times based primarily on hydrophobicity and sequence, literature is more limited on characterising stationary phases with peptides [7, 8, 10-12]. The success of these predictions is based on an understanding of the role of hydrophobicity based on amino acid side chain differences as well as the secondary structure of the peptide.

Hodges *et al.* [20] investigated the use of small peptides as probes for reversed phase columns and compared the findings against the PQRI database. The peptide standards were designed and synthesised to produce chains with 12 amino acids which were modified at the same position along the chain. The position was modified with alanine, valine, isoleucine, tyrosine and phenylalanine, in order to assess the effect of increased hydrophobicity and aromaticity whilst in the same environment to reduce any nearest neighbour influence. By only investigating the effect of those five amino acids, however, it doesn't take into account other common retention mechanisms, such as phenolic activity or effect of charge, which is quite limiting. The design of the peptides also has limited relevance to what analysts are working on (i.e. structurally related species and no degradation products).

The peptides contained glycine periodically along the chain in order to disrupt secondary structure formation. Secondary structures provide another level of complexity, which the study wished to avoid in order to look at the effect of altering a single amino acid in the residue. They state no secondary structures were formed as confirmed using circular dichroism (CD) in the presence of TFA (aq), TFA in MeCN and TFA in trifluoroethanol (TFE - a known helix-inducing solvent).

The peptides were assessed on six different ligand functionalities from the same manufacturer, but on different base silicas. The study was quite limited in sample size by only assessing six stationary phases thereby reducing the applicability of the study to a wider array of stationary phases. There was also little discussion about the properties of the columns (i.e. surface coverage, pore size etc) which are known to influence peptide retention. The study compared the stationary phases using two different solvents, which highlighted selectivity differences. There are very limited examples of methanol used for the analysis of peptides, however, this study shows there are benefits to utilising this solvent.

The PQRI database suggested the stationary phases all possessed quite varied properties with a wide range in ranking (known as *F* values). The peptide standards, however, indicated greater similarity between columns, which led the authors to conclude there was very little correlation between small molecule and peptide characterisation protocols [20]. This is a significant driver for the present work, as it suggests the use of small molecule protocols is not beneficial in developing methods for peptides and highlights a need for a peptide-based column characterisation protocol.

It is the intention that this research should build upon this work, using biologically active peptides which are more representative of the samples that would be analysed. These peptides will be used to develop a column characterisation protocol which will evaluate a greater number of stationary phases to develop a database. Chemometric statistical analysis such as PCA could help to distil the key variables which influence the stationary phases.

3.5 Development of the Peptide RPC Column Characterisation Protocol

3.5.1 Rationale for Mobile Phase to be Evaluated for the Peptide Base Column Characterisation Protocol

Peptide analysis at low pH typically includes either of the following mobile phase additives: phosphate salts, trifluoroacetic acid (TFA), ammonium formate, ammonium acetate or formic acid [47, 48]. Phosphate salts are frequently used within the biopharmaceutical industry for peptide separations as they often provide a favourable selectivity and peak shape, however, they were not favoured in the protocol due to their lack of volatility which prohibits peak identification using MS detection. TFA is a frequently used additive as it is a good compromise, i.e. it gives both acceptable chromatographic and MS performance, however, it typically demonstrates greater tailing than phosphate salts. It was not selected for the protocol as it was shown to mask electrostatic and more subtle polar interactions between the peptides and the stationary phases hence reducing the discriminating power of the column characterisation protocol (see S*ection 3.7.12*). As it can also irreparably modify the stationary phase surface, it would be impractical for the protocol, in that once exposed to TFA the column could not be used with other additives in the characterisation protocol [97]. The intention of this present study was to develop a simple and robust column characterisation protocol, by differentiating the subtle interactions of peptides with the stationary phase surface and not to develop optimum LC methods. Although TFA is often used as an additive in peptide separations, it is not the most commonly used within industry, therefore it is important to characterise stationary phases using appropriate mobile additives. TFA and other interesting or commonly used mobile phases will however be characterised in a subsequent study which could potentially aid the chromatographer in the selection of the most appropriate mobile phases for method development (see *Section 3.9*).

The primary rationale for selecting formic acid as the mobile phase additive for the column characterisation protocol was its lack of masking subtle interactions

(compared to TFA) and hence enhance the discriminating power of the protocol. Additional benefits included its ease of tracking peaks using MS detection, volatility and lack of signal suppression in positive electrospray ionisation. Within Novo Nordisk, formic acid is used in approximately 70% of methodologies because of the increased MS sensitivity and the fact that TFA not only reduces the MS signal but also takes 2-3 days to be removed from the MS. Formic acid would not normally be used for LC-UV due to the poor peak shapes that it typically generates but is advantageous in that it permits the user to understand the purer interactions of the stationary phase.

Historically, peptide analysis was performed at low pH in order to minimise the interaction of peptides with deprotonated residual silanols at intermediate pH, which can cause detrimental band broadening and excessive tailing for ionised species. However, intermediate pH should still be considered due to the alternative selectivity which it confers by changing the physicochemical properties of both the stationary phase and the peptides.

Ammonium acetate and ammonium formate are commonly used salts at their native pH (pH 6.5 in water), although they have limited buffering capacity at that pH. Both salts can be used under MS conditions, which is advantageous for early studies for peak tracking compared to other salts which can buffer at intermediate pH but are not MS compatible (e.g. potassium phosphate). Thus, two studies were performed to ascertain which salt was the most suitable for the study of these peptides. Both ammonium salts are known to be hygroscopic (absorb water), therefore a humidity chamber was installed using a saturated salt solution with sodium chloride to determine which had the greater hygroscopicity. In addition, the ion suppression of both salts was observed under MS conditions.

3.5.1.1 Hygroscopic Study

Hygroscopicity can be problematic for consistent results. This often manifests as clumping in the salt container but it is frequently ignored despite its effect on buffer concentration.

A humidity chamber was set up following the schematic in *Figure 25*. A saturated salt solution was established using sodium chloride at a relative humidity of 75.47% ±0.14 at 20 °C [98]. Relative humidity is the ratio between water vapour present in air against the vapour pressure of water at a given temperature. Accurately, 0.5 g ±0.05 g of ammonium formate and ammonium acetate salts (LC-MS grade) was weighed into weighing boats before being placed in the humidity chamber. The salts were weighed periodically to determine water uptake.

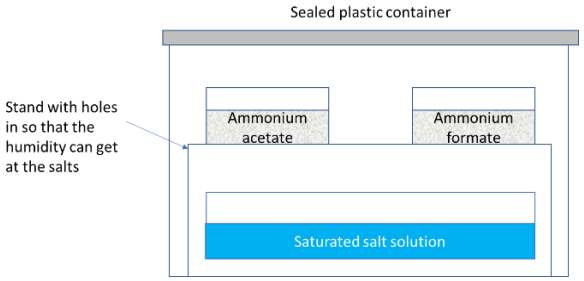

Figure 25 Schematic of the humidity chamber.

The mass and appearance of each salt was compared over 6 hours. The study has shown the ammonium acetate had a greater uptake of water when compared to the ammonium formate, where mass increased by 32.9% and 24.8% respectively. The acetate salt also liquified within 4 hours using the 75% relative humidity, whilst the formate salt remained crystalline. A less exacerbated scenario was set up at ambient humidity using a magnesium chloride salt chamber (RH 33.07% ±0.18 [98, 99]). This saw a mass increase of 7.9% for ammonium acetate and 3.3% for ammonium formate over 6 hours, which was in agreement with the sodium chloride chamber. The results indicate that the most suitable salt, as determined using hygroscopicity, is ammonium formate. However, it should be noted that these

buffers should be satisfactory if stored in desiccators [100]. The robustness of ammonium formate will be further investigated in *Section 3.7.2.2* and *3.7.3.*

3.5.1.2 Ion Suppression Study

Anecdotal evidence suggested that the acetate salt can produce significant adducts in the MS and ion suppression however, there is very little literature which corroborates this. Both LC-MS grade salts were assessed for ion suppression using the MS, in order to determine which salt provided the greatest sensitivity. Four peptides of different molecular weights were injected onto an Acquity HSS C18 column (150 x 2.1 mm, 1.8 µm particle) using a 40 minute gradient from 5-55% B, where line A1 was 20 mM ammonium formate in H_2O, A2 was 20 mM ammonium acetate in H_2O, line B1 was 20 mM ammonium formate in MeCN/H_2O (90:10 v/v) and line B2 was 20 mM ammonium acetate in MeCN/H_2O (90:10 v/v). The formate and acetate salts were at native pH values, respectively. The flow rate was set to 0.3 mL/min and the column oven temperature set to 40 °C. The MS had the following operating conditions: desolvation line (DL) temperature and heat block set to 350 and 300 °C respectively, nebulising gas flow set at 0.5 L/min, and drying gas flow at 5 L/min. The two salts were compared using both Selected Ion Monitoring (SIM) and profile in positive mode on the MS, where SIM monitored *m/z* 820, 1069, 1076 and 1105. Profile mode scanned a range of *m/z* 400-2000 with a scan speed of 10,000 u/sec and event time of 0.2 sec.

The response for ammonium formate using SIM for the four peptides was up to 2x greater than that for the ammonium acetate chromatogram (*Figure 26*).

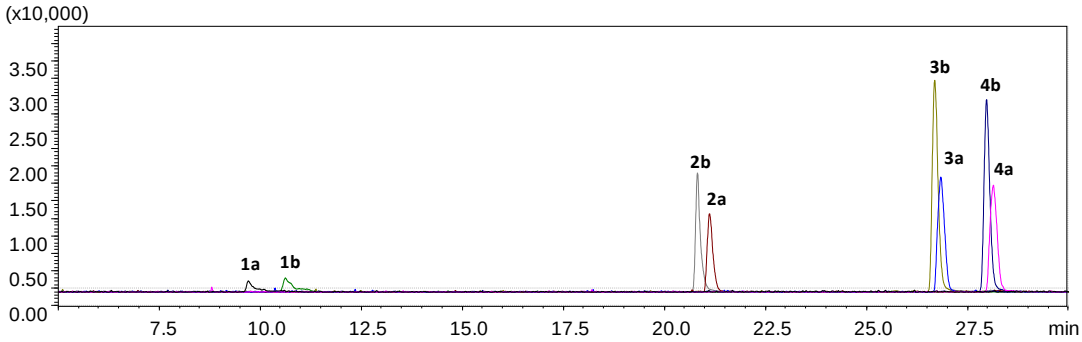

Figure 26 SIM response for four peptides using (a) ammonium acetate and (b) ammonium formate gradients. Analyses were performed on the Nexera X2 coupled to the 2020 single quadrupole MS. The gradient was 5-55%B over 40 minutes, flow rate was 0.3 mL/min, column oven temperature was 40 °C, and ESI source in positive mode. (1) Bovine GLP-2 (1-15) (m/z 820), (2) [Lys26]- (m/z 1076), (3) [Phe26]- (m/z 1105) and (4) Bovine GLP-2 (16-33) (m/z 1069).

There were also concerns regarding the cleanliness of the buffer salt, which were inspected in the total ion chromatogram (TIC). The TIC and extracted average spectra did not illustrate any adduct formation. Nor did it suggest a significant degree of impurities which could affect the cleanliness of the spectra. Thus, the results cannot influence the decision for buffer type.

From the intensity, hygroscopicity and anecdotal evidence, the buffer to be used through this study is ammonium formate.

3.5.2 Rationale for Column and Peptide Selection for Peptide Screen

A gradient screen was used as a basis for the characterisation protocol using peptide standards. A gradient was used to encompass all 26 peptides under one chromatographic condition within a certain timeframe. This would not be possible under isocratic conditions, given the wide physicochemical properties of the peptides to be analysed, as well as the differences exhibited by the stationary phases to be evaluated. The protocol must utilise the same chromatographic conditions for every column in order to compare the properties of the stationary phase. To achieve this in a rational design, a reduced number of columns and

peptides were modelled using two different t_G to ascertain the most appropriate gradient conditions. A PCA of the column characterisation data using small molecules determined complementary stationary phases appropriate for this task, whilst a comparison of physicochemical properties determined the most diverse peptides. Thus, a method which is applicable for a significant proportion of stationary phases with suitable retention for many of the peptides was established.

3.5.2.1 Column Selection

The protocol was developed on a reduced number of stationary phases which were deemed to represent a large range of column functionalities. The selection of the stationary phases was based on prior knowledge of the columns and it was presumed would offer a wide range in selectivity to be representative of a larger collection of stationary phases, ideal for a characterisation database. This was corroborated by the positioning of the stationary phases within the score plot in *Figure 25*, where the stationary phases were spread across all four quadrants, and illustrated different retention mechanisms (i.e. hydrophobic, steric, phenolic, etc) which would be of interest to investigate. Some columns possessed a large positive charged surface whilst others had a high degree of residual silanol groups in order to characterise a wide array of column functionalities. Some of the columns chosen would not normally have been selected when developing state of the art peptide methods, due to potential batch to batch variability issues for certain phases, but were essential to establish a database.

All columns assessed were new as supplied by the manufacturer and were standardised in the 150 x 2.1 mm column format, with particle size (d_p) varying between 1.7 to 3 µm (*Table 28*). The peak apex of a water injection was used as the dead time marker for each column [101]. All stationary phases were assessed using Extended Tanaka characterisation protocols which are well described in literature [17, 95] and the Tanaka results can be accessed via the free ACD website [86]. The extended characterisation results were supplied by either Euerby and Petersson or

were characterised in this study. The integrity of the stationary phases was ensured before and after usage by an SST (*Section 2.8*) which assessed the column for changes in hydrophobicity, hydrogen bonding, positive charge and negative charge (silanol activity).

An array of C18 phases were selected which differed by base silica (i.e. Acquity BEH C18, Acquity CSH C18 and Acquity HSS C18). In addition to selecting columns which could offer different selectivity, it is of interest to investigate the subtleties between similar phases to be able to identify back up columns. The ligand density was also evaluated which could impact on selectivity by changing the architecture of the particle and accessibility to the silica surface (i.e. Acquity HSS C18 SB and Acquity HSS T3).

A preliminary study on the effect of chain length could be evaluated to assess the effect of varying hydrophobicity where observed selectivity differences could possibly be explained as a function of chain length differences (i.e. Acquity BEH C8 and the Acquity BEH C18). The Acquity BEH C4 could not be used to assist in chain length characterisation as the phase was a 300 Å material and monofunctionally bonded whereas the C8 and C18 variants have a smaller pore size and are trifunctionally bonded.

A commonly used range of columns include polar embedded group (PEG) and phenyl phases, which can offer alternative selectivity. A carbamate ligand (Acquity BEH Shield RP18) and an amide ligand (Polar Amide C18) were selected to represent two styles of PEG functionalities and synthetic routes, where the amide phase is prepared via a two-step synthetic route which generates positive character to the phase due to residual amino groups, whilst the carbamate is a one-step synthetic route thus can be considered neutral [18]. The phenyl phases (i.e. Acquity CSH Fluoro Phenyl, Acquity CSH Phenyl Hexyl, Ascentis Express Biphenyl and Fortis Diphenyl) vary by alkyl linker based on manufacturer information (i.e. C0-C6), fluoro-substitutions and the number of aromatic rings, which all impact on the available interactions with probes.

The final phase selected to develop the characterisation protocol was the Acclaim Mixed Mode WCX, which is a weak cation exchange phase based on a carboxylic acid moiety. This phase can offer hydrogen bonding interactions at low pH with the protonated carboxylic acid moiety and substantial electrostatic interactions at intermediate pH via the negatively charged dissociated carboxylic acid. Both types of interactions might provide selectivity differences for polar and charged peptide species.

Table 29 Extended Tanaka Characterisation results for the stationary phases to be used in the development of the Peptide RPC Column Characterisation Protocol, with the grey highlighted phases used to develop the experimental conditions for the Peptide RPC Column Characterisation Protocol due to exhibiting the most extreme characteristics.

Description	k_{PB}	α_{CH2}	$\alpha_{T/O}$	$\alpha_{C/P}$	$\alpha_{B/P\ pH\ 7.6}$	$\alpha_{B/P\ pH\ 2.7}$	$\alpha_{TNB/T}$	$\alpha_{BSA/T}$	$\alpha_{P/BA}$	$\alpha_{1,2/\ 1,4\text{-}DNB}$
Acquity BEH C8	1.16	1.34	0.86	0.59	0.31	0.13	0.24	0.02	1.00	1.18
Acquity BEH Shield RP18	2.08	1.41	2.36	0.30	0.27	0.13	0.31	0.04	1.35	1.11
Acquity CSH C18 [1]	3.53	1.44	1.35	0.40	0.38	0.09	0.21	0.03	0.98	1.00
Acquity CSH Fluorophenyl [1]	0.46	1.00	3.10	1.72	1.24	-0.06	0.48	0.74	0.96	1.48
Acquity CSH Phenyl hexyl [1]	1.47	1.31	1.13	0.70	0.42	0.07	0.85	0.16	0.94	1.22
Acquity HSS C18	7.38	1.48	1.47	0.37	0.24	0.11	0.14	0.01	1.00	0.97
Acquity HSS C18 SB	2.57	1.39	1.94	1.86	4.99	0.16	0.24	0.01	0.88	1.23
Acquity HSS T3 [1]	6.02	1.50	1.19	0.50	0.34	0.12	0.22	0.01	1.00	0.94
Acquity UPLC BEH C4 300	0.28	1.24	0.88	1.48	0.40	0.22	0.39	0.13	1.00	1.42
Acquity UPLC BEH C18 [1]	3.99	1.47	1.38	0.37	0.23	0.09	0.17	0.00	1.00	1.00
Polaris Amide C18	2.87	1.43	2.43	0.20	0.15	-0.02	0.20	2.39	1.50	1.28
Ascentis Express Biphenyl	1.69	1.29	1.53	2.30	0.96	0.16	1.89	0.01	0.87	0.75
Fortis Diphenyl	1.54	1.31	0.93	0.81	0.56	0.07	0.41	0.32	1.00	1.11
Acclaim Mixed Mode WCX	0.66	1.16	3.33	0.48	1.84	0.05	0.43	0.05	1.48	1.83

[1]Data acquired from M. Euerby and P. Petersson

Five stationary phases were selected from the initial 12 columns to determine the experimental conditions. As previously demonstrated in *Section 3.4*, column characterisation is extremely data rich and requires careful analysis to determine the subtle interactions within the column. A smaller PCA was performed on the data in *Table 29*, to produce the biplot in *Figure 27*. A biplot is a loading plot combined with a score plot which aids identification of parameters which influence the observations. The first PC has a R2X[1] value of 0.345, which describes ~35% of the

variability whilst the second PC has a R2X[2] of 0.286, describing a further ~29%. In total, ~63% of the variability is described by the model which is satisfactory for looking at observations and trends. The purple, star markers are the key chromatographic parameters used in the Extended Tanaka protocols. The other markers are the subset of stationary phases, classified into either alkyl, mixed mode, PFP, PEG or phenyl groups. Based on the position of the chromatographic parameters k_{PB} and α_{CH2}, it is possible to suggest the Acquity HSS C18 retention is predominantly dictated by hydrophobic mechanisms, whilst the Acquity BEH C4 and Acquity HSS C18 SB have significantly more silanophilic and hydrogen bonding capabilities, as suggested by the position of the chromatographic measures $\alpha_{(C/P)}$, $\alpha_{(B/P\ pH\ 7.6\ and\ 2.7)}$. The Acquity CSH Fluorophenyl retention is largely influenced by dipole-dipole interactions due to the electron rich fluorinated ring ($\alpha_{(1,2/1,4\text{-}DNB)}$) and steric interactions, possibly due to the ligand architecture and accessibility into the stationary phase ($\alpha_{(T/O)}$). The Polaris Amide C18 has significant positive charge on the stationary phase and phenolic retention ($\alpha_{(BSA/T)}$ and $\alpha_{(P/BA)}$, respectively).

The evaluation using PCA suggest those five stationary phases possess significant differences in hydrophobicity, positive charge and accessibility to silanol groups, and as such, would represent a large proportion of columns. The Acquity BEH C4 and the Acquity HSS C18-SB, although positioned close in the biplot, were both included as the five most extreme stationary phases. Their position in the plot is probably due to silanophilic activity, however, this interaction will be different on both of these phases, given the low ligand coverage for the Acquity HSS C18-SB compared to the Acquity BEH C4, whilst the BEH phase has significantly less hydrophobicity (see *Table 29*).

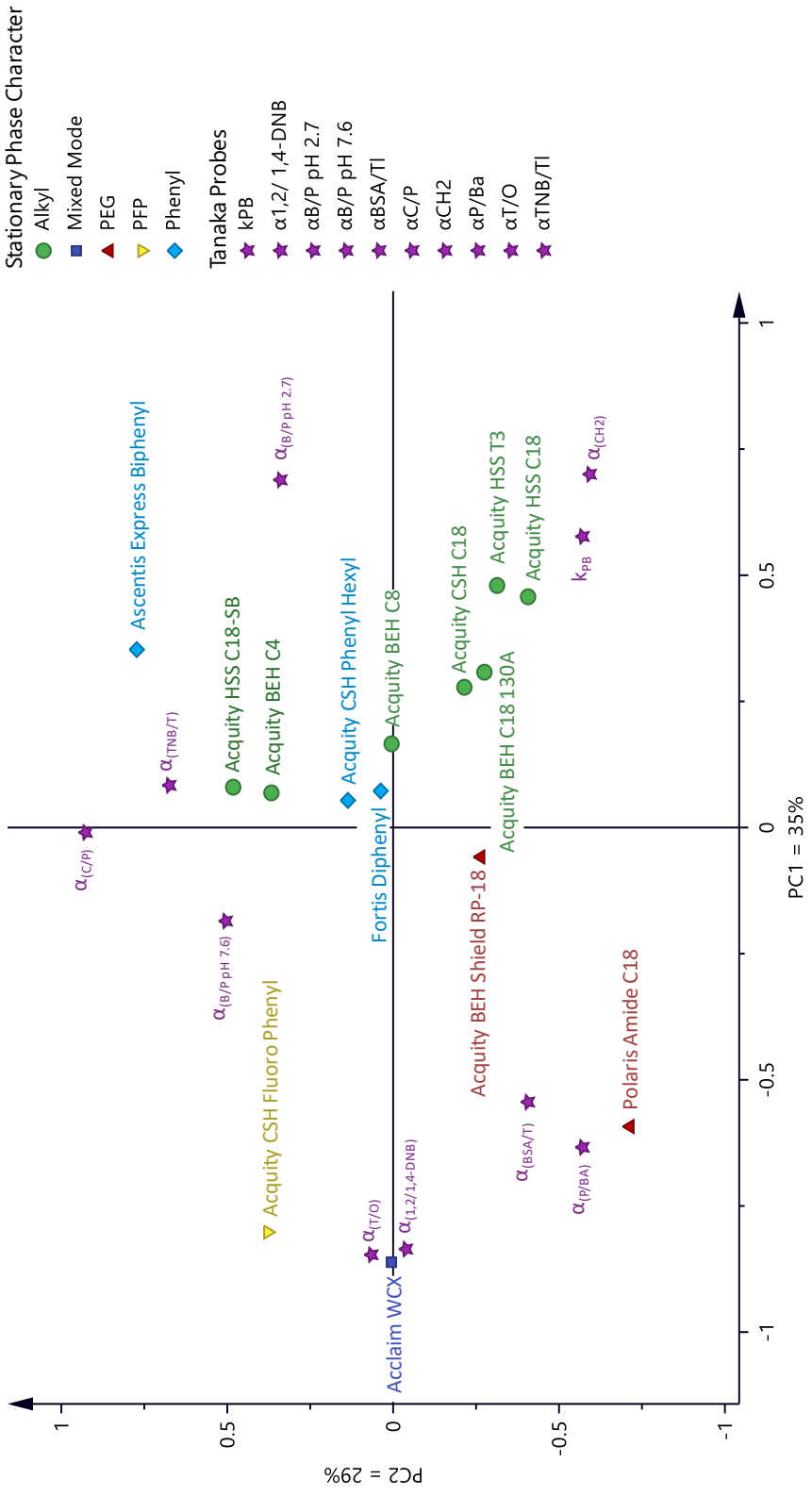

Figure 27 Biplot of the Extended Tanaka protocol chromatographic parameters (purple stars) and the stationary phases used to develop the protocol.

3.5.2.2 Peptide Selection

The physicochemical properties of the peptide were evaluated to determine the two most extreme probes to define a suitable workspace for all peptides. This included markers for isoelectric point (pI – the pH at which the peptide has a net neutral charge), partition coefficient for the zwitterion (logP – the ratio of the concentration of a compound between an aqueous (e.g. water) and lipophilic (e.g. n-octanol) phase which is a measure of hydrophobicity) and the polar surface area (PSA – the sum of surface contributions of polar atoms in a molecule (i.e. oxygen and nitrogen (*Table 30*)).

As there are a few isomeric species with the same physicochemical properties described, they have been removed from the table. Based on their extreme differences, the peptides highlighted are the probes used to determine the gradient range for the peptide tests. These peptides cover the low, intermediate and high response to each of the parameters shown in *Table 30*. This should demonstrate the range of polarity, isoelectric point and hydrophobicity and provide an adequate workspace for the other peptides to be analysed.

Table 30 Comparison of parameters for peptide probes. pI: Isoelectric point. LogP: Partition coefficient. PSA: Polar surface area.

	Name	Mass	pI	LogP	PSA
1	Bovine GLP-2 (1-15)	1638	3.9	-12.18	778
4	[L-isoAsp3]-Bovine GLP-2 (1-15)	1638	3.7	-12.18	778
11	[L-isoAsp11]-Bovine GLP-2 (1-15)	1639	3.6	-11.55	772
13	Bovine GLP-2 (16-33)	2135	5.4	-10.21	903
15	[Ile26,Leu27]-Bovine GLP-2 (16-33)	2135	5.4	-10.21	903
16	[Gly22]-Bovine GLP-2 (16-33)	2045	5.4	-12.24	903
18	[L-isoAsp,Gly22]-Bovine GLP-1(16-33)	2045	5.3	-12.24	903
20	[Val26]-Bovine GLP-2 (16-33)	2121	5.4	-10.59	903
21	[Ile26]-Bovine GLP-2 (16-33)	2135	5.4	-10.14	903
22	[Phe26]-Bovine GLP-2 (16-33)	2169	5.4	-9.88	903
23	[Trp26]-Bovine GLP-2 (16-33)	2208	5.4	-9.59	919
24	[Tyr26]-Bovine GLP-2 (16-33)	2185	5.4	-10.12	924
25	[Lys20]-Bovine GLP-2 (16-33)	2107	5.4	-12.09	868
26	[Lys26]-Bovine GLP-2 (16-33)	2150	8.2	-13.99	929

3.5.2.3 Peptide Screen

The peptide screen was performed on the five diverse stationary phases, using the most extreme peptides in terms of physicochemical properties to ascertain a suitable workspace for the majority of stationary phases and peptides. The screen was performed using the conditions described in *Section 2.9.3*, at both low (formic acid at pH 2.5) and intermediate pH (ammonium formate at native pH, pH 6.45), to provide interesting selectivity differences based on the change in ionisation state of both the analytes and the stationary phases. The gradient Two gradients times (t_G) of 10 and 30 minutes were used as input runs for the retention time model for both ammonium formate and formic acid mobile phase conditions. The models were created using ACD LC simulator, which was used for numerical calculations and based on simple linear isocratic retention models defined using *Equation 12*.

$$ln\, k^{'} = a + bX \qquad \textit{Equation 12}$$

Where *a* and *b* are analyte specific parameters and *X* the percent of organic modifier in the mobile phase.

The resolution map (t_G *versus* resolution of the critical pair) for the Acquity HSS C18, which was typical of the other phases assessed, can be seen in *Figure 28*. Ample resolution was seen between each of the four peaks for all of the phases assessed as demonstrated by the Acquity HSS C18 in *Figure 28*. As the methodology must accommodate 26 peptides with varying physicochemical properties, it was imperative to select operating conditions with suitable resolving power.

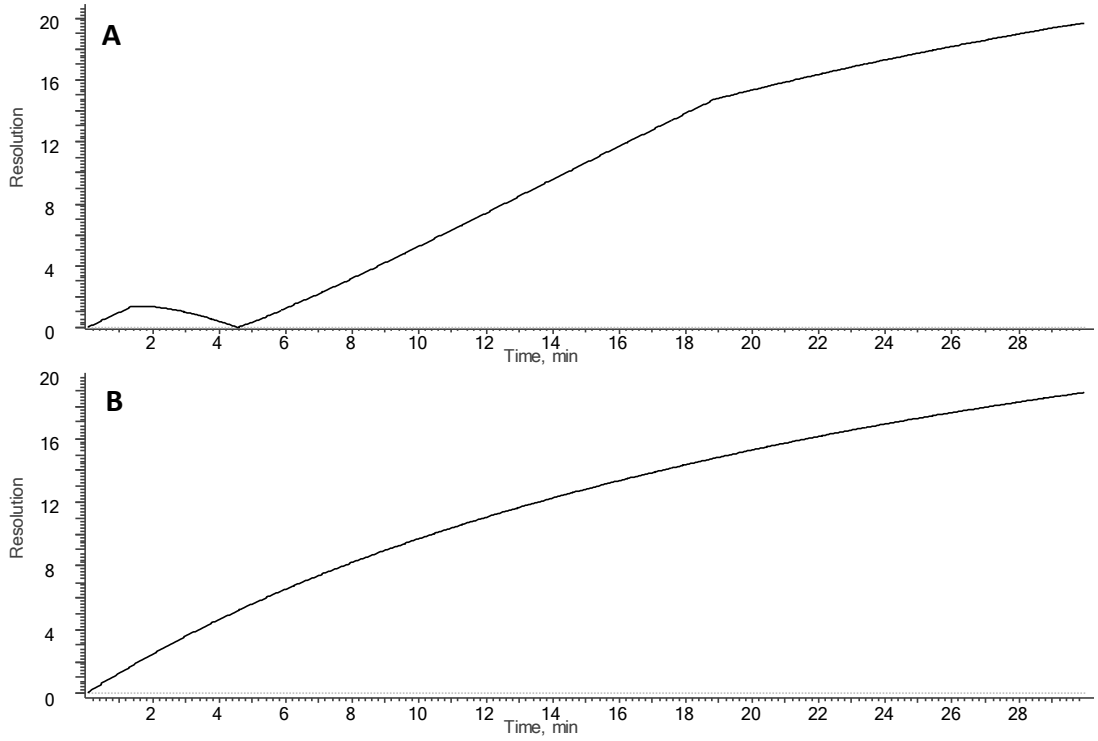

Figure 28 Resolution map comparing time (t_G) versus resolution of the critical pair for the Acquity HSS C18 using (A) formic acid and (B) ammonium formate mobile phase conditions. Analyses were formed on the Waters H-class binary system described in Section 2.9.2.1. The formic acid conditions utilised a mobile phase of 0.1% formic acid in water and 0.1% formic acid in acetonitrile. The ammonium formate conditions utilised a mobile phase of 20 mM ammonium formate native pH in water and 20 mM ammonium formate in acetonitrile / water (80:20 v/v). The gradients assessed were 10-50%B using either a 10 minute or 30 minute t_G with a 20 minute t_G used to validate the model. Flow rate was 0.3 mL/min, column oven temperature was 40 °C, detection used a combination of UV at 215 nm and MS for peak confirmation.

The conditions derived from the retention time model at low pH suggested a 40-minute gradient (extrapolated) with a change in %B of 10-50% which provided adequate *k** (gradient retention factor i.e. the instantaneous retention factor as the analyte passes the midpoint of the column) for the five stationary phases (lowest *k** was 1.6 on the Polaris Amide whilst the highest was 5.6 on the Acquity HSS C18-SB). Ideally, *k** should be between 2-10, however, a compromise was required between *k** and run time length. *k** was calculated using Snyder's approximation (*Equation 13* [102]) which utilised the retention model *m* term constant. The conditions determined using the retention time model at intermediate pH were 5-55% B over a

40-minutes t_G, which also provided suitable *k** with a reasonable run time. The full chromatographic conditions can be seen in the experimental section.

$$k^* = \frac{t_G F}{1.15 v_M m \Delta\phi} \qquad \textit{Equation 13}$$

Where t_G is gradient time (minutes), *F* is flow rate (mL/min), v_M is the column volume (mL), $\Delta\phi$ is the change in organic expressed as a decimal and *m* is calculated from the b term fitted by LC Simulator using *Equation 14*.

$$m = \frac{100\, b}{ln\, 10} \qquad \textit{Equation 14}$$

3.5.3 Rationale for Defining Peptide Cocktails for the Development of the Peptide RPC Column Characterisation Protocol

Cocktails of peptides are the most efficient means to evaluate all 26 peptides in a time efficient manner. The gradient cycles defined in *Section 2.9.3* are 54 minutes each, thus the need to reduce the overall run time per column. Each test mix should contain two peptides as reference to indicate if there has been a shift in retention time through the course of the experiment. These peptides should have different *m/z* from the other peptides in the mixture and represent both hydrophilic and the hydrophobic peptides.

Each peptide was individually injected using the two peptide gradients on the Acquity HSS C18 to establish the most abundant *m/z*, which might facilitate groupings. The Acquity HSS C18 was presumed to be the most stable due to the functionality of the ligand and limited ligand bleed in the MS therefore should produce cleaner spectra. The *m/z* range for the Shimadzu single quad MS 2010 is 50-2000, therefore the peptides with a *m/z* of above 2000 cannot be detected (i.e. typically z=1 charge). However, with a z=2 charge, the *m/z* becomes less than 2000 and the peptides can be observed. The z=2 charge was observed for all peptides and was typically the most abundant, although the z=3 charge using formic acid as the

mobile phase additive did prove more abundant for a number of peptides (*Table 31*).

Peptide mixtures can be defined using a number of methods, such as different *m/z*, logical groupings based on the property the peptide is intended to investigate or based on the separation on the Acquity HSS C18.

Basing the cocktails on the retention on the Acquity HSS C18 should be used as a low priority selection criterion as the peptides may coelute on other stationary phases.

Logical groupings would include racemisation products, deamidation products, increase in hydrophobicity, aliphatic *versus* aromatic, linear *versus* branched. However, the racemisation and deamidation products would all possess the same MW which would make peak identification for those groups difficult if based solely on mass. A combination of logical groupings and *m/z* is the best compromise to define the test mixes.

The cocktails contain between 5-6 peptides, including the two reference peptides. Most of the early eluting peptides have a *m/z* of 820 which would be difficult to differentiate from other peptides with the same mass, therefore unsuitable as a reference. However, [Met(O)10]-Bovine GLP-2 (Peptide Number 8) is also an early eluting peptide and *m/z* is higher at 828. Although, as a diastereoisomer there are two peaks which would reduce the peak height, it was determined to be the most appropriate reference standard. [Trp26]-Bovine GLP-2 (Peptide Number 23) is one of the more retained peptides and is the only peptide to have a MW of 2208 and [M/2]+2H of 1105. These two candidates are excellent as references to ensure the integrity of the data. Each test mix can be seen in *Table 31*. The test mixes were validated on the Acquity HSS C18 using both gradients.

Table 31 Peptide Test Mixtures used for the Development of the Peptide RPC Column Characterisation Protocol. The predominant charge was [M/2]+2H.

Peptide Name	Peptide Number	Test Mix	MW	Formic Acid		Ammonium Formate	
				[M/2]+2H	Net charge	[M/2]+2H	Net charge
[Met(O)10]-Bovine GLP-2 (1-15)	8	1,2,3,4,5,6,7,8	1654	828	1.2	828	-3.7
[Trp26]-Bovine GLP-2 (16-33)	23	1,2,3,4,5,6,7,8	2208	1105	2.2	1105	0.0
Bovine GLP-2 (1-15)	1	1	1638	820	1.2	820	-3.7
Bovine GLP-2 (16-33)	13	1	2135	1069	2.2	1069	0.0
[D-isoAsp,gly22]-Bovine GLP-2 (16-33)	19	1	2045	1024	2.2	1024	0.0
[L-Asp11]-Bovine GLP-2 (1-15)	9	2	1638	820	1.1	820	-4.7
[Val26]-Bovine GLP-2 (16-33)	20	2	2121	1062	2.2	1062	0.0
[Ile26]-Bovine GLP-2 (16-33)	21	2	2135	1069	2.2	1069	0.0
[D-Asp11]-Bovine GLP-2 (1-15)	10	3	1638	820	1.1	820	-4.7
[L-isoAsp11]-Bovine GLP-2 (1-15)	11	3	1638	820	1.1	820	-4.7
[D-isoAsp11]-Bovine GLP-2 (1-15)	12	3	1638	820	1.1	820	-4.7
[D-His1]-Bovine GLP-2 (1-15)	2	4	1638	820	1.2	820	-3.7
[Phe26]-Bovine GLP-2 (16-33)	22	4	2169	1086	2.2	1086	0.0
[Tyr26]-Bovine GLP-2 (16-33)	24	4	2185	1094	2.2	1094	0.0
[D-Asp3]-Bovine GLP-2 (1-15)	3	5	1638	820	1.2	820	-3.7
[Lys20]-Bovine GLP-2 (16-33)	25	5	2107	1055	2.2	1055	0.0
[Lys26]-Bovine GLP-2 (16-33)	26	5	2150	1076	3.2	1076	1.0
[D-Ser5]-Bovine GLP-2 (1-15)	6	6	1638	820	1.2	820	-3.7
[D-Ser16]-Bovine GLP-2 (16-33)	14	6	2135	1069	2.2	1069	0.0
[D-Ser7]-Bovine GLP-2 (1-15)	7	6	1638	820	1.2	820	-3.7
[L-isoAsp3]-Bovine GLP-2 (1-15)	4	7	1638	820	1.2	820	-3.7
[D-isoAsp3]-Bovine GLP-2 (1-15)	5	7	1638	820	1.2	820	-3.7
[Ile26,Leu27]-Bovine GLP-2 (16-33)	15	7	2135	1069	2.2	1069	0.0
[Gly22]-Bovine GLP-2 (16-33)	16	7	2045	1024	2.2	1024	0.0
[D-Asp21,Gly22]-Bovine GLP-2 (16-33)	17	8	2045	1024	2.2	1024	0.0
[L-isoAsp,gly22]-Bovine GLP-2 (16-33)	18	8	2045	1024	2.2	1024	0.0

3.6 Initial Results on the Subset of Stationary Phases on all Peptides

The 14 columns described in *Section 3.5.2.1* were assessed with all 26 peptides described in *Section 3.3.1.* The retention time, peak area, peak width at 50% (w_h) and symmetry were recorded for each peptide in the eight test mixtures (data not shown). Peak area was used to aid peak identification where mass could not differentiate between peptides (i.e. racemisation species). w_h was converted to peak width at base (w or 4σ) using *Equation 15* [101]. This was in turn used to determine peak capacity which will be further discussed in *Section 3.6.7*.

$$w = \frac{4w_h}{2.35}$$ *Equation 15*

3.6.1 Defining Normalised Retention

A normalised retention time approach was used to compensate for instrumentation and column differences using *Equation 16*, with the use of two reference peptides. These peptides were [Met(O)10]-Bovine GLP-2 (1-15) (Peptide Number 8a, t_{gRef8a}) and [Trp26]-Bovine GLP-2 (16-33) (Peptide Number 23, t_{gRef23}), which were both present in all eight test mixtures. Thus, in theory, the values for each peptide ranged from 0 to 1.

$$t_g^x = \frac{t_g - t_{gRef8a}}{t_{g\,Ref23} - t_{g\,Ref8a}}$$ *Equation 16*

However, it was noted that [Trp26]-Bovine GLP-2 (16-33) (Peptide Number 23) was often not the most retained peptide, which meant that some peptides eluted outside of this range. The most retained peptide was considered to be [Ile26,Leu27]-Bovine GLP-2 (16-33) (Peptide Number 15), hence the hydrophobic reference was changed to produce a new normalised retention for the 14 columns assessed, $t_g^{''}$ using *Equation 17.* The final definition for normalised retention (t_g^*) for any new characterised stationary phase can be seen in *Equation 18*.

$$t_g^{"} = \frac{t_g^x}{t_{gRef15}}$$ *Equation 17*

$$t_g^* = \frac{t_g - t_{gRef8a}}{t_{gRef15} - t_{gRef8a}}$$ *Equation 18*

The normalised retention time for all 26 peptides on the 14 stationary phases ($t_g^{''}$) can be seen in *Table 32* & *Table 33* for formic acid and *Table 34* & *Table 35* ammonium formate, firstly displaying the hydrophilic normalised retention times, then the hydrophobic normalised retention times.

Table 32 Normalised retention time for the hydrophilic peptides determined on the 14 initial stationary phases using formic acid additives.

Formic Acid														
	Acquity CSH Fluorophenyl	Fortis Diphenyl	Ascentis Express Biphenyl	Acclaim WCX	Acquity BEH C18 130 A	Acquity HSS T3	Acquity CSH C18	Acquity CSH Phenyl Hexyl	Acquity BEH Shield RP-18	Acquity BEH C8	Acquity BEH C4	Acquity HSS C18-SB	Acquity HSS C18	Polaris Amide C18
Peptide Number	Peptide	t_g''	t_g''	t_g''	t_g''	t_g''	t_g''	t_g''	t_g''	t_g''	t_g''	t_g''	t_g''	t_g''
1	Bovine GLP-2 (1-15)	0.264	0.292	0.271	0.212	0.289	0.290	0.329	0.348	0.314	0.285	0.253	0.243	0.297	0.355
2	[D-His1]-Bovine GLP-2 (1-15)	0.287	0.304	0.275	0.215	0.296	0.295	0.338	0.354	0.324	0.298	0.258	0.248	0.304	0.373
3	[D-Asp3]-Bovine GLP-2 (1-15)	0.260	0.302	0.274	0.220	0.294	0.291	0.330	0.345	0.319	0.298	0.261	0.252	0.302	0.353
4	[L-isoAsp3]-Bovine GLP-2 (1-15)	0.339	0.303	0.260	0.198	0.289	0.291	0.358	0.394	0.337	0.296	0.252	0.242	0.301	0.405
5	[D-isoAsp3]-Bovine GLP-2 (1-15)	0.363	0.331	0.286	0.198	0.310	0.314	0.382	0.423	0.361	0.317	0.274	0.259	0.323	0.433
6	[D-Ser5]-Bovine GLP-2 (1-15)	0.286	0.300	0.282	0.204	0.295	0.295	0.338	0.365	0.320	0.294	0.261	0.246	0.304	0.368
7	[D-Ser7]-Bovine GLP-2 (1-15)	0.220	0.253	0.241	0.191	0.256	0.252	0.287	0.307	0.272	0.260	0.220	0.208	0.263	0.305
8a	[Met(O)10]-Bovine GLP-2 (1-15)	0.000	0.000	0.000	0.000	0.000	0.000	0.000	0.000	0.000	0.000	0.000	0.000	0.000	0.000
8b	[Met(O)10]-Bovine GLP-2 (1-15)	0.000	0.003	0.000	0.000	0.006	0.007	0.008	0.008	0.006	0.006	0.000	0.006	0.007	0.023
9	[L-Asp11]-Bovine GLP-2 (1-15)	0.375	0.353	0.315	0.270	0.339	0.337	0.391	0.433	0.374	0.331	0.299	0.282	0.341	0.430
10	[D-Asp11]-Bovine GLP-2 (1-15)	0.360	0.330	0.302	0.268	0.319	0.324	0.369	0.405	0.357	0.317	0.290	0.278	0.331	0.400
11	[L-isoAsp11]-Bovine GLP-2 (1-15)	0.302	0.203	0.173	0.150	0.224	0.177	0.237	0.358	0.223	0.166	0.152	0.137	0.179	0.269
12	[D-isoAsp11]-Bovine GLP-2 (1-15)	0.360	0.259	0.224	0.183	0.172	0.240	0.300	0.294	0.285	0.213	0.207	0.185	0.242	0.347

Table 33 Normalised retention time for the hydrophobic peptides determined on the 14 initial stationary phases using formic acid additives.

Formic Acid														
	Peptide Number	Peptide	Acquity CSH Fluorophenyl t_g''	Fortis Diphenyl t_g''	Ascentis Express Biphenyl t_g''	Acclaim WCX t_g''	Acquity BEH C18 130 A t_g''	Acquity HSS T3 t_g''	Acquity CSH C18 t_g''	Acquity CSH Phenyl Hexyl t_g''	Acquity BEH Shield RP-18 t_g''	Acquity BEH C8 t_g''	Acquity BEH C4 t_g''	Acquity HSS C18-SB t_g''	Acquity HSS C18 t_g''	Polaris Amide C18 t_g''
	13	Bovine GLP-2 (16-33)	0.956	0.942	0.955	0.979	0.950	0.952	0.946	0.940	0.957	0.940	0.947	0.979	0.949	0.948
	14	[D-Ser16]-Bovine GLP-2 (16-33)	0.969	0.952	0.955	0.968	0.956	0.960	0.961	0.956	0.965	0.950	0.953	0.975	0.959	0.964
	15	[Ile26,Leu27]-Bovine GLP-2 (16-33)	1.000	1.000	1.000	1.000	1.000	1.000	1.000	1.000	1.000	1.000	1.000	1.000	1.000	1.000
	16	[Gly22]-Bovine GLP-2 (16-33)	0.373	0.552	0.584	0.595	0.590	0.577	0.533	0.482	0.566	0.581	0.579	0.590	0.577	0.505
	17	[D-Asp,gly22]-Bovine GLP-2 (16-33)	0.365	0.550	0.582	0.596	0.584	0.576	0.524	0.476	0.560	0.579	0.582	0.586	0.576	0.493
	18	[L-isoAsp,gly22]-Bovine GLP-2 (16-33)	0.443	0.590	0.607	0.608	0.619	0.610	0.577	0.550	0.600	0.611	0.604	0.608	0.606	0.561
	19	[D-isoAsp,gly22]-Bovine GLP-2 (16-33)	0.451	0.564	0.575	0.576	0.589	0.584	0.568	0.538	0.588	0.585	0.584	0.586	0.585	0.556
	20	[Val26]-Bovine GLP-2 (16-33)	0.817	0.862	0.838	0.842	0.836	0.840	0.823	0.802	0.843	0.828	0.839	0.871	0.836	0.829
	21	[Ile26]-Bovine GLP-2 (16-33)	0.913	0.919	0.908	0.931	0.919	0.924	0.915	0.902	0.925	0.911	0.921	0.949	0.921	0.917
	22	[Phe26]-Bovine GLP-2 (16-33)	0.947	0.951	0.955	0.975	0.933	0.928	0.913	0.869	0.928	0.914	0.914	0.949	0.932	0.907
	23	[Trp26]-Bovine GLP-2 (16-33)	0.947	0.919	0.955	1.000	0.878	0.876	0.861	0.869	0.900	0.847	0.865	0.906	0.871	0.868
	24	[Tyr26]-Bovine GLP-2 (16-33)	0.751	0.727	0.758	0.808	0.687	0.696	0.676	0.657	0.743	0.666	0.715	0.754	0.682	0.722
	25	[Lys20]-Bovine GLP-2 (16-33)	0.947	0.919	0.915	0.941	0.942	0.941	0.938	0.932	0.946	0.936	0.941	0.980	0.952	0.940
	26	[Lys26]-Bovine GLP-2 (16-33)	0.109	0.382	0.432	0.440	0.419	0.399	0.344	0.250	0.397	0.411	0.437	0.420	0.400	0.283

Table 34 Normalised retention times for the hydrophilic peptides determined on the 14 initial stationary phases using ammonium formate additives.

Ammonium Formate															
	Peptide Number	Peptide	Acquity CSH Fluorophenyl	Fortis Diphenyl	Ascentis Express Biphenyl	Acclaim WCX	Acquity BEH C18 130 A	Acquity HSS T3	Acquity CSH C18	Acquity CSH Phenyl Hexyl	Acquity BEH Shield RP-18	Acquity BEH C8	Acquity BEH C4	Acquity HSS C18-SB	Acquity HSS C18	Polaris Amide C18
			t_g''	t_g''	t_g''	t_g''	t_g''	t_g''	t_g''	t_g''	t_g''	t_g''	t_g''	t_g''	t_g''	t_g''
	1	Bovine GLP-2 (1-15)	0.137	0.160	0.162	0.004	0.146	0.146	0.150	0.164	0.153	0.156	0.158	0.106	0.242	0.278
	2	[D-His1]-Bovine GLP-2 (1-15)	0.131	0.182	0.183	0.004	0.165	0.164	0.169	0.176	0.174	0.172	0.178	0.121	0.253	0.301
	3	[D-Asp3]-Bovine GLP-2 (1-15)	0.112	0.162	0.158	0.004	0.149	0.149	0.154	0.169	0.154	0.158	0.154	0.111	0.243	0.280
	4	[L-isoAsp3]-Bovine GLP-2 (1-15)	0.095	0.152	0.155	0.004	0.147	0.147	0.151	0.163	0.149	0.157	0.136	0.100	0.232	0.265
	5	[D-isoAsp3]-Bovine GLP-2 (1-15)	0.225	0.162	0.160	0.004	0.147	0.147	0.151	0.167	0.151	0.167	0.136	0.100	0.242	0.274
	6	[D-Ser5]-Bovine GLP-2 (1-15)	0.142	0.179	0.190	0.004	0.163	0.161	0.169	0.183	0.170	0.171	0.167	0.117	0.257	0.303
	7	[D-Ser7]-Bovine GLP-2 (1-15)	0.108	0.163	0.177	0.004	0.160	0.156	0.161	0.172	0.167	0.166	0.156	0.104	0.218	0.257
	8a	[Met(O)10]-Bovine GLP-2 (1-15)	0.000	0.000	0.000	0.000	0.000	0.000	0.000	0.000	0.000	0.000	0.000	0.000	0.000	0.000
	8b	[Met(O)10]-Bovine GLP-2 (1-15)	0.000	0.006	0.008	0.000	0.002	0.002	0.002	0.008	0.000	0.002	0.000	0.000	0.005	0.000
	9	[L-Asp11]-Bovine GLP-2 (1-15)	0.063	0.103	0.098	0.002	0.089	0.094	0.100	0.121	0.088	0.107	0.083	0.051	0.224	0.292
	10	[D-Asp11]-Bovine GLP-2 (1-15)	0.024	0.074	0.080	-0.003	0.062	0.056	0.101	0.071	0.078	0.101	0.013	0.034	0.197	0.268
	11	[L-isoAsp11]-Bovine GLP-2 (1-15)	-0.009	0.005	0.027	-0.003	0.040	0.038	0.080	0.099	0.063	0.077	-0.019	0.008	0.094	0.172
	12	[D-isoAsp11]-Bovine GLP-2 (1-15)	0.016	0.074	0.080	-0.003	0.077	0.078	0.043	0.055	0.038	0.046	0.022	0.034	0.143	0.224

Table 35 Normalised retention times for the hydrophobic peptides determined on the 14 initial stationary phases using ammonium formate additives.

Ammonium Formate															
	Peptide Number	Peptide	Acquity CSH Fluorophenyl t_g''	Fortis Diphenyl t_g''	Ascentis Express Biphenyl t_g''	Acclaim WCX t_g''	Acquity BEH C18 130 A t_g''	Acquity HSS T3 t_g''	Acquity CSH C18 t_g''	Acquity CSH Phenyl Hexyl t_g''	Acquity BEH Shield RP-18 t_g''	Acquity BEH C8 t_g''	Acquity BEH C4 t_g''	Acquity HSS C18-SB t_g''	Acquity HSS C18 t_g''	Polaris Amide C18 t_g''
	13	Bovine GLP-2 (16-33)	0.971	0.949	0.957	0.984	0.945	0.945	0.946	0.952	0.951	0.937	0.945	0.973	0.943	0.948
	14	[D-Ser16]-Bovine GLP-2 (16-33)	0.976	0.961	0.968	1.002	0.958	0.959	0.961	0.965	0.961	0.951	0.953	0.977	0.962	0.965
	15	[Ile26,Leu27]-Bovine GLP-2 (16-33)	1.000	1.000	1.000	1.000	1.000	1.000	1.000	1.000	1.000	1.000	1.000	1.000	1.000	1.000
	16	[Gly22]-Bovine GLP-2 (16-33)	0.225	0.695	0.704	0.680	0.678	0.671	0.673	0.687	0.694	0.663	0.675	0.670	0.635	0.585
	17	[D-Asp,gly22]-Bovine GLP-2 (16-33)	0.714	0.689	0.702	0.635	0.672	0.664	0.669	0.682	0.689	0.668	0.681	0.646	0.646	0.590
	18	[L-isoAsp,gly22]-Bovine GLP-2 (16-33)	0.728	0.706	0.716	0.681	0.690	0.683	0.687	0.702	0.704	0.686	0.694	0.651	0.651	0.610
	19	[D-isoAsp,gly22]-Bovine GLP-2 (16-33)	0.706	0.695	0.704	0.684	0.681	0.676	0.677	0.689	0.696	0.668	0.676	0.662	0.662	0.589
	20	[Val26]-Bovine GLP-2 (16-33)	0.899	0.888	0.886	0.891	0.862	0.863	0.862	0.870	0.874	0.856	0.871	0.894	0.894	0.851
	21	[Ile26]-Bovine GLP-2 (16-33)	0.946	0.935	0.938	0.951	0.924	0.924	0.925	0.929	0.930	0.916	0.927	0.950	0.950	0.925
	22	[Phe26]-Bovine GLP-2 (16-33)	0.971	0.958	0.979	0.959	0.934	0.931	0.895	0.927	0.941	0.914	0.918	0.943	0.943	0.923
	23	[Trp26]-Bovine GLP-2 (16-33)	0.971	0.935	0.963	0.976	0.889	0.888	0.895	0.927	0.911	0.860	0.882	0.914	0.914	0.885
	24	[Tyr26]-Bovine GLP-2 (16-33)	0.862	0.805	0.819	0.860	0.747	0.751	0.761	0.790	0.795	0.724	0.777	0.806	0.806	0.749
	25	[Lys20]-Bovine GLP-2 (16-33)	0.958	0.943	0.950	0.936	0.943	0.942	0.943	0.947	0.945	0.935	0.938	0.963	0.963	0.943
	26	[Lys26]-Bovine GLP-2 (16-33)	0.725	0.697	0.706	0.961	0.633	0.625	0.632	0.657	0.651	0.612	0.648	0.738	0.738	0.454

3.6.2 Defining Selectivity

The response required in the model will be based on selectivity (α). Isocratic separations are simpler to define using the ratio between solute retention factors, which is under constant proportions of eluent and not affected by dwell volume. The means by which selectivity in gradient chromatography is defined has been debated in various publications (i.e. Snyder *et al.*, Jandera, [102, 103]). Gradient chromatography presents a far more complex scenario than isocratic separations where the changing eluent composition, dwell volume, column dead volume and complexity of the gradient can all be influential parameters.

Snyder describes the selectivity factor for gradients (α^*, *Equation 19*) as the ratio between the gradient retention factor for the band pair at the column midpoint. k^* can be calculated using *Equation 13*, which is an approximation. A detailed description of how to calculate k^* can be found by Lundell [104].

$$\alpha^* = \frac{k^*_2}{k^*_1} \qquad \textit{Equation 19}$$

Jandera [103] suggested an alternate means of evaluating selectivity, suggesting α_g, the relative retention in gradient chromatography, might be more applicable (*Equation 20*), where V_g is the retention volume (i.e. retention time x flow).

$$\alpha_g = \frac{V_{g2}}{V_{g1}} \qquad \textit{Equation 20}$$

This was further advanced in *Equation 21* and *Equation 23,* where the effect from differences in dwell volume between different systems is compensated. *Equation 22* was used to determine V'_g used in both *Equation 21* and *Equation 23*, where V_g is subtracted by the column volume (V_m) and the dwell volume (V_d)

$$\alpha^* = \frac{V'_{g2}}{V'_{g1}} \qquad \textit{Equation 21}$$

$$V'_g = V_g - V_m - V_d \qquad \textit{Equation 22}$$

$$\alpha^* = 1 + \frac{\Delta V'_g}{V'_{g1}} \qquad \textit{Equation 23}$$

The four methods (*Equation 19, 20, 21* and *23*) were theoretically simulated to evaluate the effect of common changes i.e. change in dwell volume, change in flow and change in mobile phase composition (*Appendix 1*). The results suggested *Equation 19* provided the most robust result but required significant work to practically determine *a* and *m*. *Equation 20* was affected by the slope of the gradient and therefore was manipulated if the dwell volume was adjusted. *Equation 21* is more intuitive than *Equation 23*, as the equation shows similarities to the isocratic selectivity equation which is more familiar to the majority of chromatographers, therefore suggests the most suitable method to define selectivity is *Equation 21*. *Equation 21* can also be converted from volume into time, where V_g can be converted into t_g which is the retention time in gradient elution and V_m and V_d converted to t_m and t_d (column dead time and dwell time), which would also increase the familiarity for chromatographers (*Equation 24* and *Equation 25)*.

$$\alpha^* = \frac{t'_{g2}}{t'_{g1}} \qquad \textit{Equation 24}$$

$$t'_g = t_g - t_m - t_d \qquad \textit{Equation 25}$$

However, upon generating the alpha values for the 14 stationary phases, it was noted that two peaks which had the same spacing but different normalised retention times produced different alpha values. This shouldn't be the case, as it would suggest greater selectivity differences despite both pairs having the same degree of separation. The point at which the compounds elute should not be represented in the selectivity term.

A better representation could be to use delta (Δt_g^*) to describe selectivity, which is the difference between two peaks. Chromatographers are familiar with the concept of alpha values, however, it isn't usual to use delta to define selectivity, which could present an issue. Another disadvantage of this approach is that the number will be between 0 and 1 which is not intuitive for a chromatographer to understand the relevance of the value. However, an advantage is that the approach gives the same weighting to an early eluting parameter compared to a later eluting parameter. It is also simple to perform. Another advantage is that Δt_g^* does not require the determination of t_m and t_d and thereby the reproducibility should improve.

The use of delta is supported by *Figure 29.* In *Figure 29(A)*, t_{gA1}^* and t_{gA2}^* equal 0.69 and 0.79, respectively. In *Figure 29(B)*, t_{gA1}^* equals 0.32 whilst t_{gA2}^* equals 0.42. An alpha value would suggest *(A)* equalled 1.15 whilst *(B)* equalled 1.33. However, the delta value for both cases is 0.10, giving the separation between the peaks equal weighting than the retention time which impacts on alpha. Thus, selectivity was defined using *Equation 26*.

$$\Delta t_g^* = t_{g2}^* - t_{g1}^* \qquad \textit{Equation 26}$$

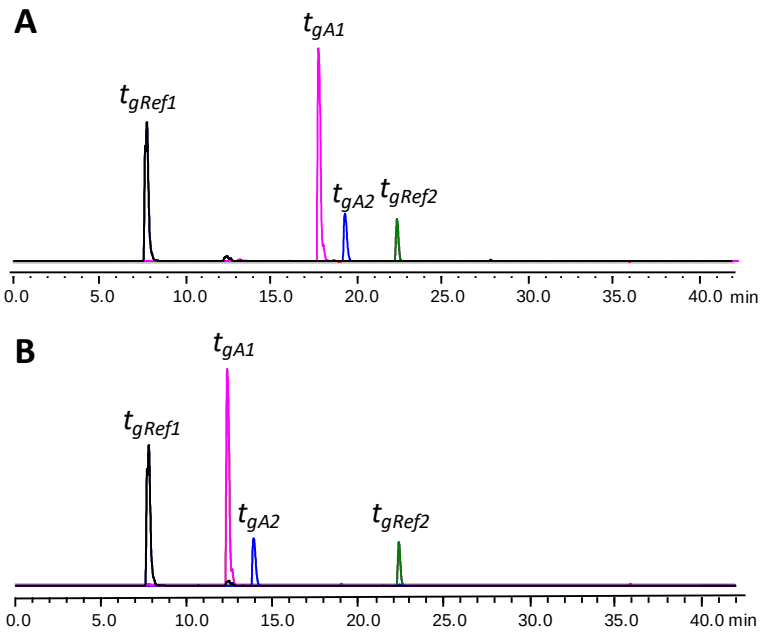

Figure 29 Example of alpha affected by the point of elution where (A) αt_g^* equalled 1.15 and Δt_g^* equalled 0.10 and (B) αt_g^* equalled 1.33 and Δt_g^* equalled 0.10.

A total of 33 delta values were generated per mobile phase based on the rationale in *Section 3.3.2* and *3.3.3* and were calculated using *Equation 26* (*Table 36).* These include racemisation, oxidation and changes in phenolic or aliphatic character.

Table 36 List of delta values and their rationale

Delta	Change	Rationale
Δ(2,1)	[L-His1] → [D-His1]	Steric - racemisation
Δ(3,1)	[L-Asp3] → [D-Asp3]	Steric - racemisation
Δ(4,1)	[L-Asp3] → [L-isoAsp3]	Steric - isomerisation
Δ(5,1)	[L-Asp3] → [D-isoAsp3]	Steric- isomerisation
Δ(5,4)	[L-isoAsp3] → [D-isoAsp3]	Steric - racemisation
Δ(6,1)	[L-Ser5] → [D-Ser5]	Steric - racemisation
Δ(7,1)	[L-Ser7] → [D-Ser7]	Steric - racemisation
Δ(8a,1)*	[Met10] → [Met(O)10]	Oxidation
Δ(8b,1)*	[Met10] → [Met(O)10]	Oxidation
Δ(8b,8a)*	[Met(O)10] → [Met(O)10]	Steric - racemisation
Δ(9,1)	[L-Asn11] → [L-Asp11]	Increase in negative charge
Δ(10,1)	[L-Asn11] → [D-Asp11]	Increase in negative charge
Δ(10,9)	[L-Asp11] → [D-Asp11]	Steric - racemisation
Δ(11,1)	[L-Asn11] → [L-isoAsp11]	Increase in negative charge
Δ(12,1)	[L-Asn11] → [D-isoAsp11]	Increase in negative charge
Δ(12,11)	[L-isoAsp11] → [D-isoAsp11]	Steric - racemisation
Δ(14,13)	[L-Ser16] → [D-Ser16]	Steric - racemisation
Δ(15,13)	[Leu26,Ile27] → [Ile26,Leu27]	Steric – switch in amino acid sequence
Δ(16,13)	[L-Asp21,Phe22] → [L-Asp21,Gly22]	Aromatic – removal of aromatic group
Δ(17,16)	[L-Asp21,Gly22] → [D-Asp21,Gly22]	Steric - racemisation
Δ(18,16)	[L-Asp21,Gly22] → [L-isoAsp21,Gly22]	Increase in negative charge
Δ(19,16)	[L-Asp21,Gly22] → [D-isoAsp21,Gly22]	Increase in negative charge
Δ(19,18)	[L-isoAsp21,Gly22] → [D-isoAsp21,Gly22]	Steric - racemisation
Δ(20,13)	[Leu26] → [Val26]	Alkyl – removal of $-CH_2$
Δ(21,13)	[Leu26] → [Ile26]	Alkyl – change of $-CH_3$ position
Δ(22,13)	[Leu26] → [Phe26]	Aromatic – addition of aromatic group
Δ(23,13)	[Leu26] → [Trp26]	Aromatic – addition of aromatic group
Δ(23,22)	[Phe26] → [Trp26]	Aromatic – addition of aromatic group
Δ(24,13)	[Leu26] → [Tyr26]	Phenolic – addition of hydroxyl group
Δ(24,22)	[Phe26] → [Tyr26]	Phenolic – addition of hydroxyl group
Δ(24,23)	[Trp26] → [Tyr26]	Phenolic – addition of hydroxyl group
Δ(25,13)	[Arg20] → [Lys20]	Change in polarity
Δ(26,13)	[Leu26] → [Lys26]	Increase in positive charge

The results for the hydrophilic peptides on the Acclaim WCX in ammonium formate are highlighted in red (*Table 34*). The Acclaim WCX is a mixed mode stationary

phase with a carboxylic acid moiety. Under the formic acid conditions (*Figure 30(A)*), the acidic moiety is unionised, whilst the peptides all possess a positive net charge, thus all the peptides have some retention. However, under ammonium formate conditions (*Figure 30(B)*), the Acclaim WCX is ionised, which can form electrostatic interactions with the peptides. The hydrophobic peptides all possess a positive charge, hence have a greater retention under intermediate pH conditions. The hydrophilic peptides, however, are all negatively charged which created a mutual repulsion on the stationary phase thus the hydrophilic peptides are eluted before the void. As such, the results under ammonium formate conditions would heavily skew any data interpretation, therefore the decision was made to exclude the Acclaim WCX when used with ammonium formate from any chemometric analysis.

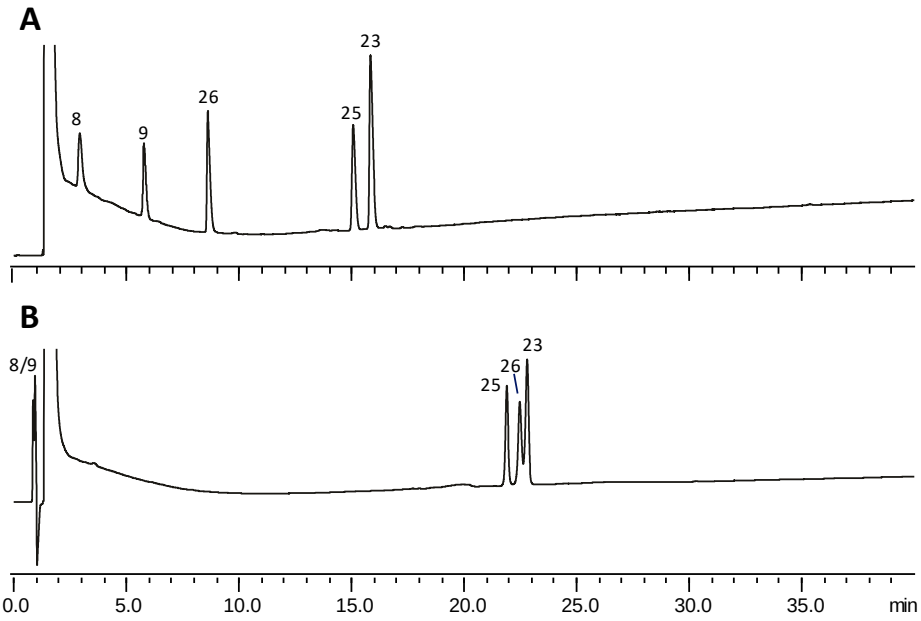

Figure 30 UV chromatogram displaying the peptides eluting on the Acclaim WCX using either (A) formic acid or (B) ammonium formate mobile phase conditions. Analyses were performed on the Nexera X2 coupled to the 2020 single quadrupole system. The formic acid conditions utilised a mobile phase of 0.1% formic acid in water and 0.1% formic acid in acetonitrile with 10-50%B over 40 minutes. The ammonium formate conditions utilised a mobile phase of 20 mM ammonium formate native pH in water and 20 mM ammonium formate in acetonitrile / water (80:20 v/v) with 5-55%B over 40 minutes. Flow rate was 0.3 mL/min, column oven temperature was 40 °C, and detection used a combination of UV at 215 nm and MS for peak confirmation. Peak 8: [Met(O)10]-, Peak 9: [L-Asp11]-Bovine GLP-2 (1-15), Peak 23: [Trp26]-, Peak 25: [Lys20]-, Peak 26: [Lys26]-Bovine GLP-2 (16-33)

All delta values described in *Table 36* can be seen in *Table 37* & *Table* 38 and *Table 39* & *Table* 40 in formic acid and ammonium formate, respectively. The sign in front of the Δt_g^* result is indicative of the elution order for the separation e.g. [Leu26] → [Lys26] with a Δt_g^* of -0.848 means that [Lys26] elutes earlier than [Leu26]. The largest average difference was observed using formic acid between [Leu26]- and [Lys26]-Bovine GLP-2 (Peptide Number 13 and 26, respectively), which could be expected due to the changes in charge. The smallest average differences (i.e. Δt_g^* values close to zero) were typically racemic in nature, which highlights the difficulty in separating these closely related species. The difference in responses for the position of the racemisation also accentuates the issue of analysing racemates, where [L-Ser5] → [D-Ser5] and [L-Ser7] → [D-Ser7]-Bovine GLP-2 (1-15) differ at position 5 and 7 respectively in the residue chain, but produced some signficant differences in Δt_g^* for both formic acid and ammonium formate (Peptide Number 1, 6 and 7).

Table 37 Delta values for the hydrophilic peptides determined on the 14 initial stationary phases using formic acid additives.

Formic Acid		Acquity CSH Fluorophenyl	Fortis Diphenyl	Ascentis Express Biphenyl	Acclaim WCX	Acquity BEH C18 130 A	Acquity HSS T3	Acquity CSH C18	Acquity CSH Phenyl Hexyl	Acquity BEH Shield RP-18	Acquity BEH C8	Acquity BEH C4	Acquity HSS C18-SB	Acquity HSS C18	Polaris Amide C18
	[L-His1]-> [D-His1]	Δ(2,1)	0.012	0.004	0.003	0.007	0.005	0.009	0.006	0.010	0.013	0.005	0.006	0.007	0.018
	[L-Asp3] -> [D-Asp3]	Δ(3,1)	0.009	0.003	0.009	0.005	0.001	0.001	-0.003	0.005	0.012	0.008	0.010	0.005	-0.001
	[L-Asp3] -> [L-isoAsp3]	Δ(4,1)	0.011	-0.011	-0.014	0.001	0.001	0.030	0.047	0.023	0.011	-0.001	-0.001	0.003	0.050
	[L-Asp3] -> [D-isoAsp3]	Δ(5,1)	0.039	0.015	-0.014	0.022	0.024	0.053	0.075	0.047	0.031	0.021	0.016	0.026	0.078
	[L-isoAsp3] -> [D-isoAsp3]	Δ(5,4)	0.027	0.026	0.000	0.021	0.023	0.024	0.029	0.024	0.021	0.023	0.017	0.022	0.028
	[L-Ser5] -> [D-Ser5]	Δ(6,1)	0.008	0.010	-0.008	0.006	0.005	0.009	0.017	0.006	0.009	0.008	0.003	0.006	0.013
	[L-Ser7] -> [D-Ser7]	Δ(7,1)	-0.039	-0.030	-0.021	-0.033	-0.038	-0.042	-0.041	-0.042	-0.025	-0.033	-0.034	-0.035	-0.050
	[Met10]->[Met(O)10]	Δ(8a,1)	-0.292	-0.271	-0.212	-0.289	-0.290	-0.329	-0.348	-0.314	-0.285	-0.253	-0.243	-0.297	-0.355
	[Met10]->[Met(O)10]	Δ(8b,1)	-0.289	-0.271	-0.212	-0.282	-0.283	-0.321	-0.340	-0.308	-0.279	-0.253	-0.237	-0.290	-0.332
	[Met(O)10]->[Met(O)10]	Δ(8b,8a)	0.003	0.000	0.000	0.006	0.007	0.008	0.008	0.006	0.006	0.000	0.006	0.007	0.023
	[Asn11] -> [L-Asp11]	Δ(9,1)	0.061	0.044	0.059	0.050	0.047	0.062	0.085	0.060	0.046	0.046	0.039	0.043	0.076
	[Asn11] -> [D-Asp11]	Δ(10,1)	0.038	0.031	0.056	0.031	0.034	0.040	0.057	0.043	0.032	0.037	0.036	0.034	0.046
	[L-Asp11] -> [D-Asp11]	Δ(10,9)	-0.023	-0.013	-0.002	-0.019	-0.014	-0.023	-0.028	-0.017	-0.014	-0.008	-0.003	-0.009	-0.030
	[Asn11] -> [L-isoAsp11]	Δ(11,1)	-0.089	-0.098	-0.062	-0.064	-0.113	-0.092	0.011	-0.091	-0.119	-0.101	-0.106	-0.119	-0.086
	[Asn11] -> [D-isoAsp11]	Δ(12,1)	-0.034	-0.047	-0.028	-0.117	-0.050	-0.029	-0.054	-0.029	-0.072	-0.046	-0.058	-0.055	-0.008
	[L-isoAsp11] -> [D-isoAsp11]	Δ(12,11)	0.056	0.051	0.034	-0.052	0.063	0.063	-0.064	0.061	0.047	0.055	0.048	0.063	0.078

Table 38 Delta values for the hydrophobic peptides determined on the 14 initial stationary phases using formic acid additives.

Formic Acid	Acquity CSH Fluorophenyl	Fortis Diphenyl	Ascentis Express Biphenyl	Acclaim WCX	Acquity BEH C18 130 A	Acquity HSS T3	Acquity CSH C18	Acquity CSH Phenyl Hexyl	Acquity BEH Shield RP-18	Acquity BEH C8	Acquity BEH C4	Acquity HSS C18-SB	Acquity HSS C18	Polaris Amide C18
[L-Ser16] -> [D-Ser16]	Δ(14,13)	0.012	0.010	0.000	-0.010	0.006	0.008	0.015	0.016	0.008	0.010	0.006	-0.004	0.010	0.016
[Leu26,Ile27] -> [Ile26,Leu27]	Δ(15,13)	0.044	0.058	0.045	0.021	0.050	0.048	0.054	0.060	0.043	0.060	0.053	0.021	0.051	0.052
[Phe22] -> [Gly22]	Δ(16,13)	-0.584	-0.390	-0.372	-0.384	-0.360	-0.376	-0.413	-0.458	-0.391	-0.359	-0.368	-0.389	-0.372	-0.443
[L-Asp,Gly22] -> [D-Asp,Gly22]	Δ(17,16)	-0.008	-0.002	-0.001	0.001	-0.006	-0.001	-0.009	-0.007	-0.006	-0.002	0.003	-0.003	-0.001	-0.011
[L-Asp,Gly22] -> [L-isoAsp,Gly22]	Δ(18,16)	0.070	0.038	0.023	0.013	0.030	0.034	0.043	0.067	0.035	0.030	0.025	0.018	0.029	0.056
[L-Asp,Gly22] -> [D-isoAsp,Gly22]	Δ(19,16)	0.078	0.012	-0.008	-0.019	-0.001	0.007	0.034	0.056	0.022	0.004	0.004	-0.004	0.008	0.051
[L-isoAsp,Gly22] -> [D-isoAsp,Gly22]	Δ(19,18)	0.008	-0.026	-0.031	-0.032	-0.031	-0.027	-0.009	-0.012	-0.013	-0.026	-0.021	-0.021	-0.021	-0.005
[Leu26] -> [Val26]	Δ(20,13)	-0.139	-0.080	-0.117	-0.137	-0.114	-0.112	-0.123	-0.138	-0.114	-0.112	-0.108	-0.108	-0.114	-0.119
[Leu26] -> [Ile26]	Δ(21,13)	-0.043	-0.023	-0.047	-0.048	-0.030	-0.028	-0.031	-0.038	-0.031	-0.029	-0.026	-0.030	-0.028	-0.031
[Leu26] -> [Phe26]	Δ(22,13)	-0.010	0.008	0.000	-0.004	-0.016	-0.024	-0.033	-0.071	-0.028	-0.027	-0.033	-0.030	-0.017	-0.041
[Leu26] -> [Trp26]	Δ(23,13)	-0.010	-0.023	0.000	0.021	-0.071	-0.077	-0.085	-0.071	-0.056	-0.094	-0.082	-0.073	-0.079	-0.080
[Phe26] -> [Trp26]	Δ(23,22)	0.000	-0.032	0.000	0.025	-0.055	-0.052	-0.052	0.000	-0.028	-0.067	-0.050	-0.043	-0.061	-0.039
[Leu26] -> [Tyr26]	Δ(24,13)	-0.206	-0.216	-0.197	-0.171	-0.263	-0.256	-0.270	-0.283	-0.214	-0.275	-0.231	-0.225	-0.268	-0.226
[Phe26] -> [Tyr26]	Δ(24,22)	-0.196	-0.224	-0.197	-0.167	-0.246	-0.232	-0.237	-0.212	-0.186	-0.248	-0.199	-0.195	-0.250	-0.185
[Trp26] -> [Tyr26]	Δ(24,23)	-0.196	-0.192	-0.197	-0.192	-0.191	-0.179	-0.184	-0.212	-0.158	-0.181	-0.149	-0.153	-0.189	-0.146
[Arg20] -> [Lys20]	Δ(25,13)	-0.010	-0.023	-0.040	-0.038	-0.007	-0.011	-0.008	-0.008	-0.010	-0.005	-0.006	0.001	0.002	-0.008
[Leu26] -> [Lys26]	Δ(26,13)	-0.848	-0.561	-0.523	-0.539	-0.531	-0.553	-0.602	-0.690	-0.560	-0.530	-0.510	-0.559	-0.549	-0.665

Table 39 Delta values for the hydrophilic peptides determined on the 14 initial stationary phases using ammonium formate additives.

Ammonium Formate		Polaris Amide C18	Acquity HSS C18	Acquity HSS C18-SB	Acquity BEH C4	Acquity BEH C8	Acquity BEH Shield RP-18	Acquity CSH Phenyl Hexyl	Acquity CSH C18	Acquity HSS T3	Acquity BEH C18 130 A	Ascentis Express Biphenyl	Fortis Diphenyl	Acquity CSH Fluorophenyl
	[L-His1]-> [D-His1]	Δ(2,1)	0.023	0.011	0.015	0.020	0.015	0.021	0.012	0.019	0.018	0.018	0.020	0.022	-0.005
	[L-Asp3] -> [D-Asp3]	Δ(3,1)	0.002	0.001	0.005	-0.004	0.002	0.002	0.005	0.004	0.003	0.003	-0.005	0.001	-0.025
	[L-Asp3] -> [L-isoAsp3]	Δ(4,1)	-0.013	-0.010	-0.006	-0.022	0.001	-0.003	-0.001	0.000	0.001	0.001	-0.007	-0.008	-0.042
	[L-Asp3] -> [D-isoAsp3]	Δ(5,1)	-0.004	0.000	-0.006	-0.022	0.010	-0.002	0.002	0.000	0.001	0.001	-0.002	0.002	0.088
	[L-isoAsp3] -> [D-isoAsp3]	Δ(5,4)	0.009	0.010	0.000	0.000	0.009	0.002	0.004	0.000	0.000	0.000	0.005	0.010	0.130
	[L-Ser5] -> [D-Ser5]	Δ(6,1)	0.025	0.016	0.011	0.009	0.015	0.017	0.019	0.018	0.015	0.017	0.028	0.018	0.005
	[L-Ser7] -> [D-Ser7]	Δ(7,1)	-0.021	-0.024	-0.002	-0.002	0.010	0.014	0.008	0.010	0.010	0.014	0.015	0.003	-0.029
	[Met10]->[Met(O)10]	Δ(8a,1)	-0.278	-0.242	-0.106	-0.158	-0.156	-0.153	-0.164	-0.150	-0.146	-0.146	-0.162	-0.160	-0.137
	[Met10]->[Met(O)10]	Δ(8b,1)	-0.278	-0.237	-0.106	-0.158	-0.155	-0.153	-0.156	-0.148	-0.144	-0.145	-0.155	-0.154	-0.137
	[Met(O)10]->[Met(O)10]	Δ(8b,8a)	0.000	0.005	0.000	0.000	0.002	0.000	0.008	0.002	0.002	0.002	0.008	0.006	0.000
	[Asn11] -> [L-Asp11]	Δ(9,1)	-0.073	-0.018	-0.055	-0.075	-0.049	-0.064	-0.043	-0.051	-0.052	-0.058	-0.064	-0.058	-0.073
	[Asn11] -> [D-Asp11]	Δ(10,1)	-0.113	-0.045	-0.072	-0.145	-0.055	-0.075	-0.093	-0.049	-0.090	-0.084	-0.083	-0.086	-0.113
	[L-Asp11] -> [D-Asp11]	Δ(10,9)	-0.040	-0.027	-0.017	-0.070	-0.006	-0.010	-0.050	0.002	-0.038	-0.027	-0.019	-0.028	-0.040
	[Asn11] -> [L-isoAsp11]	Δ(11,1)	-0.146	-0.148	-0.098	-0.177	-0.079	-0.090	-0.065	-0.070	-0.108	-0.106	-0.135	-0.155	-0.146
	[Asn11] -> [D-isoAsp11]	Δ(12,1)	-0.120	-0.099	-0.072	-0.136	-0.111	-0.115	-0.109	-0.108	-0.067	-0.070	-0.083	-0.086	-0.120
	[L-isoAsp11] -> [D-isoAsp11]	Δ(12,11)	0.025	0.049	0.026	0.041	-0.031	-0.025	-0.043	-0.038	0.041	0.037	0.053	0.069	0.025

Table 40 Delta values for the hydrophobic peptides determined on the 14 initial stationary phases using ammonium formate additives.

Ammonium Formate		Acquity CSH Fluorophenyl	Fortis Diphenyl	Ascentis Express Biphenyl	Acquity BEH C18 130 A	Acquity HSS T3	Acquity CSH C18	Acquity CSH Phenyl Hexyl	Acquity BEH Shield RP-18	Acquity BEH C8	Acquity BEH C4	Acquity HSS C18-SB	Acquity HSS C18	Polaris Amide C18
	Δ(14,13)	0.005	0.011	0.011	0.013	0.014	0.015	0.013	0.010	0.014	0.008	0.005	0.019	0.017
[L-Ser16] -> [D-Ser16]	Δ(15,13)	0.029	0.051	0.043	0.055	0.055	0.054	0.048	0.049	0.063	0.055	0.027	0.057	0.052
[Leu26,Ile27] -> [Ile26,Leu27]	Δ(16,13)	-0.746	-0.255	-0.253	-0.268	-0.274	-0.274	-0.265	-0.257	-0.275	-0.270	-0.302	-0.308	-0.363
[Phe22] -> [Gly22]	Δ(17,16)	0.489	-0.005	-0.002	-0.006	-0.007	-0.004	-0.005	-0.004	0.006	0.006	-0.024	0.011	0.005
[L-Asp,Gly22] -> [D-Asp,Gly22]	Δ(18,16)	0.503	0.011	0.012	0.013	0.012	0.014	0.014	0.010	0.023	0.019	-0.019	0.016	0.025
[L-Asp,Gly22] -> [L-isoAsp,Gly22]	Δ(19,16)	0.481	0.001	0.000	0.004	0.005	0.005	0.002	0.003	0.005	0.001	-0.008	0.027	0.004
[L-Asp,Gly22] -> [D-isoAsp,Gly22]	Δ(19,18)	-0.023	-0.010	-0.011	-0.009	-0.007	-0.009	-0.012	-0.008	-0.018	-0.018	0.010	0.010	-0.021
[L-isoAsp,Gly22] -> [D-isoAsp,Gly22]	Δ(20,13)	-0.072	-0.062	-0.071	-0.083	-0.082	-0.084	-0.082	-0.077	-0.082	-0.074	-0.079	-0.049	-0.097
[Leu26] -> [Val26]	Δ(21,13)	-0.024	-0.014	-0.019	-0.021	-0.021	-0.021	-0.023	-0.021	-0.022	-0.018	-0.023	0.007	-0.024
[Leu26] -> [Ile26]	Δ(22,13)	0.000	0.009	0.022	-0.012	-0.014	-0.051	-0.026	-0.010	-0.024	-0.027	-0.030	-0.001	-0.025
[Leu26] -> [Phe26]	Δ(23,13)	0.000	-0.014	0.007	-0.056	-0.057	-0.051	-0.026	-0.039	-0.077	-0.063	-0.059	-0.029	-0.063
[Leu26] -> [Trp26]	Δ(23,22)	0.000	-0.023	-0.015	-0.045	-0.043	0.000	0.000	-0.029	-0.054	-0.036	-0.029	-0.029	-0.038
[Phe26] -> [Trp26]	Δ(24,13)	-0.109	-0.144	-0.138	-0.198	-0.194	-0.185	-0.162	-0.156	-0.214	-0.168	-0.167	-0.137	-0.199
[Leu26] -> [Tyr26]	Δ(24,22)	-0.109	-0.153	-0.160	-0.186	-0.180	-0.134	-0.136	-0.146	-0.190	-0.142	-0.137	-0.137	-0.174
[Phe26] -> [Tyr26]	Δ(24,23)	-0.109	-0.130	-0.145	-0.142	-0.138	-0.134	-0.136	-0.117	-0.136	-0.106	-0.108	-0.108	-0.136
[Trp26] -> [Tyr26]	Δ(25,13)	-0.013	-0.007	-0.007	-0.002	-0.003	-0.003	-0.005	-0.006	-0.003	-0.007	-0.010	0.019	-0.006
[Arg20] -> [Lys20]	Δ(26,13)	-0.246	-0.253	-0.250	-0.312	-0.320	-0.314	-0.295	-0.300	-0.325	-0.296	-0.235	-0.206	-0.494
[Leu26] -> [Lys26]														

3.6.3 Chemometric Analysis

The databases are extremely data rich and as such needs to be mined to observe trends and patterns. In tabular form, it is often difficult to distinguish trends, thus the data was used to construct a PCA score and loading plot of the stationary phases and the delta values which might indicate a possible rationale for the positioning of the stationary phase.

The results from *Table 37* to *Table 40* were all centred by autoscaling (i.e. subtracting the average for each variable and dividing with its standard deviation) before generating the loading and score plots in *Figure 31* and *Figure 32*, respectively. The variables were autoscaled in order to give each parameter the same importance. The loading plot (*Figure 31*) contains all 66 delta values in both formic acid and ammonium formate. Each delta value was categorised based on the property that delta was investigating. Category 1 and 2 investigated an addition of a positive or a negative charge, respectively, whilst category 3 investigated changes in phenolic character. Category 4 investigated changes in aromatic character and category 5 investigated the simple effect of changing a methylene group. Category 6 investigated steric effects (i.e. racemisation) whilst category 7 investigated the effect of oxidation of methionine. From the results, it suggests there are clusters of parameters, for example, the yellow diamond markers denote an increase in phenolic character, whilst the dark blue pentagons denote an addition of a negative charge in the 1st and 2nd quadrants. The plots corresponded to approximately 56% of the variables, which is a good start for developing the Peptide RPC Column Characterisation Protocol.

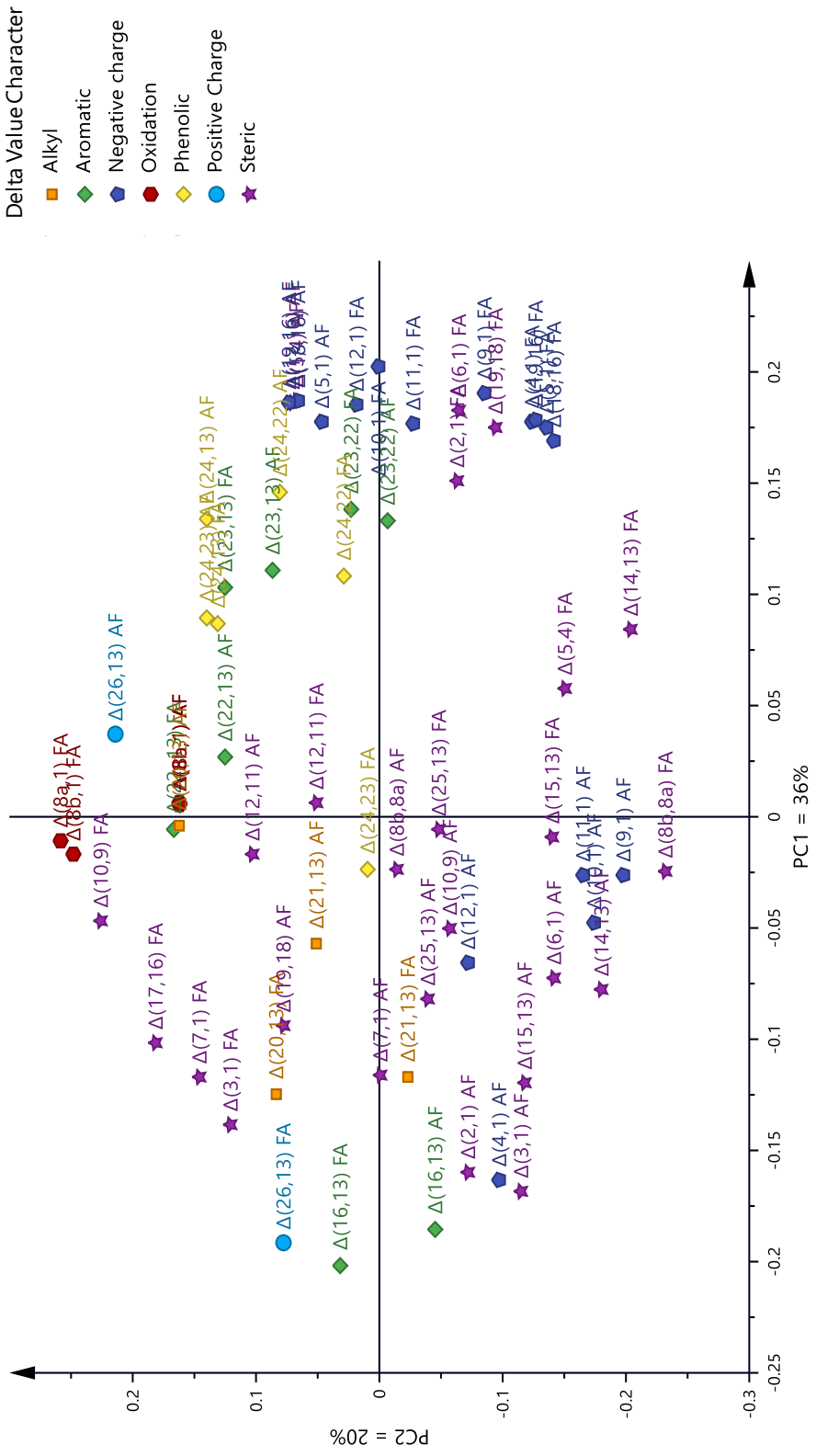

Figure 31 Loading plot of the 66 delta values generated by peptides.

The score plot (*Figure 32*) shows the placement for the stationary phases evaluated, excluding the Acclaim WCX. Each column was colour coded based on a reduce number of parameters from the Extended Tanaka protocols (*Table 41*). The parameters were k_{PB}, $\alpha_{(C/P)}$ and $\alpha_{(BSA/T)}$, in order to differentiate based on hydrophobicity, hydrogen bonding and positive character, respectively. The Acquity BEH C8, Acquity BEH C18, Acquity HSS C18 and Acquity HSS T3 are known to use hydrophobic retention mechanisms, thus were all grouped. The Acquity BEH Shield RP18 was also included in this group, however it is known to have additional polarity due to the amide functionality but was not represented by a parameter in this table ($\alpha_{(P/BA)}$ was calculated as 1.35, whilst a standard C18 phase is typically 1.00). The Acquity CSH C18, Acquity CSH Fluorophenyl, Acquity CSH Phenyl Hexyl and Polaris Amide C18 all possess positive character on the surface of the stationary phase and it is thought that electrostatic interactions could provide a key retention mechanism for the peptides. The final group of columns were the Acquity HSS C18-SB, Acquity BEH C4, Ascentis Express Biphenyl and Fortis Diphenyl which are all known to possess negative character, thus were grouped.

Table 41 Comparison of k_{PB}, $\alpha_{(C/P)}$ and $\alpha_{(BSA/T)}$ on the 14 stationary phases to define column groupings. Green = alkyl, blue = negative charge, red = positive charge.

Description	k_{PB}	$\alpha_{(C/P)}$	$\alpha_{(BSA/T)}$
Acquity BEH C8	1.16	0.59	0.02
Acquity BEH Shield RP18	2.08	0.30	0.04
Acquity CSH C18	3.53	0.40	0.03
Acquity CSH Fluorophenyl	0.46	1.72	0.74
Acquity CSH Phenyl hexyl	1.47	0.70	0.16
Acquity HSS C18	7.38	0.37	0.01
Acquity HSS C18 SB	2.57	1.86	0.01
Acquity HSS T3	6.02	0.50	0.01
Acquity UPLC BEH C4 300	0.28	1.48	0.13
Acquity UPLC BEH C18	3.99	0.37	0.00
Polaris Amide C18	2.87	0.20	2.39
Ascentis Express Biphenyl	1.69	2.30	0.01
Fortis Diphenyl	1.54	0.81	0.32

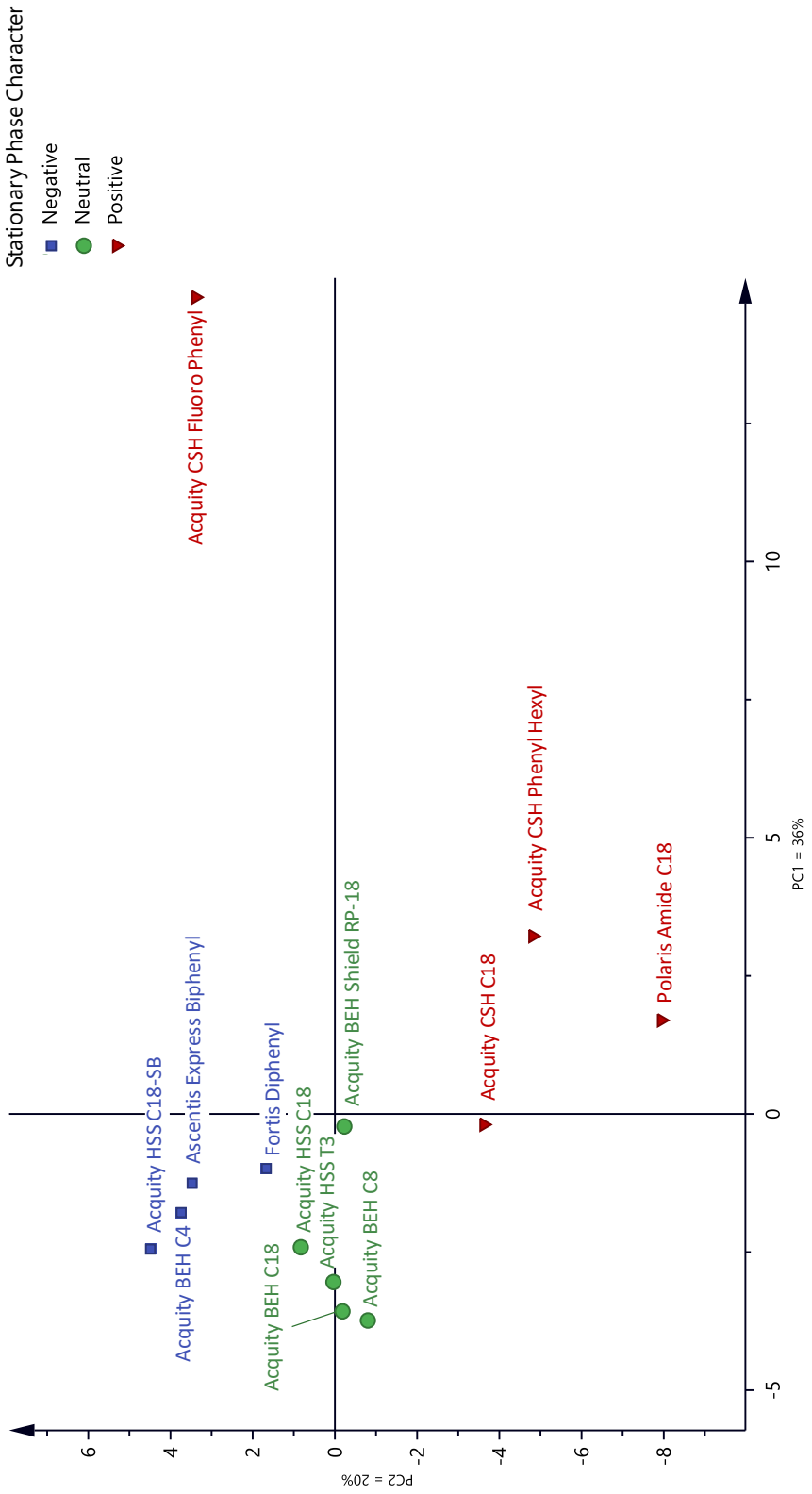

Figure 32 Score plot of the stationary phases characterised using peptides with colour coding defined by Table 41.

From the score plot in *Figure 32* it is clear to see that groups are forming, and the categories based on the Extended Tanaka protocol results were based on rational thought. There is also a good degree of scatter suggesting the peptide test compounds are discriminating between different stationary phases and probing the selectivity of each phase. Encouragingly, the stationary phases with positive character are in the opposite quadrant to the phases with negative character. These also correspond nicely to the loading plot, where markers for increase in positive charge on the peptides (light blue circle markers) are in the 1st and 4th quadrant in *Figure 31*, which correlates to the stationary phases with negative charge in the score plot in *Figure 32* and vice versa for increases in negative charge on the peptide and stationary phases with positive charge.

The Acquity CSH Fluorophenyl is located furthest from the other stationary phases assessed which suggests the chemistry is different to the other stationary phases evaluated thus far. The alkyl phases are quite closely clustered together when tested using peptides, suggesting a high degree of similarity in selectivity. This is in slight contrast with the small molecule score plot in *Figure 24,* where the length of alkyl chain can have a large impact on hydrophobicity, hence selectivity.

Stationary phases from other manufacturers will be assessed using the Peptide RPC Column Characterisation Protocol chromatographic conditions, where the results will be added to the database and the score plot. However, to characterise each stationary phase using two mobile phases with all 26 peptides would be time consuming. The loading plot also would suggest that some probes were duplicating results, thus unnecessary for the test. It would be advantageous to reduce the number of peptides required which would reduce the number of test mixtures.

The number of probes can be reduced in an array of ways, following an iterative process. Firstly, parameters which are close to the origin are said to be insignificant to the PCA, so consequently can be removed from the model. Examples of such parameters include Δ(8b,8a) and Δ(24,23), which were probes looking at the difference in retention between the methionine diastereoisomers and difference in

the amino acids tyrosine (phenolic) and tryptophan (aromatic). In addition, variables with small Δt_g^* and variables with similar meanings can be removed, provided the structure of the loading plot is preserved. This requires an iterative process where the removal of certain probes from the model are compared against the original loading and score plots to maintain the integrity of the model. A sufficient number of parameters must be kept in the model otherwise only noise is modelled. The suggested peptide probes for the protocol, delta values, score and loading plots can be seen in *Section 3.6.5*.

3.6.4 Assessment of Peptide-Column Interactions

The peptides probes were designed to investigate peptide-column interactions, both in terms of common degradants and impurities but also specific changes to evaluate differences in hydrophobicity, electrostatic interactions, aromatic and hydrogen bonding interactions and steric interactions.

3.6.4.1 Hydrophobic Interactions

Hydrophobic interaction, which is the primary retention mechanism in reversed phase chromatography, could be evaluated by investigating the effect of probes possessing differing hydrophobicity (i.e. changing leucine to valine) and by changing the hydrophobicity of the stationary phase (i.e. different alkyl length).

Mant *et al*. deduced the order of hydrophobicity for amino acids when there were no nearest neighbour effects, where the order corresponding for the peptides investigated in this study were Trp > Phe > Leu > Ile > Tyr > Val [105]. A purely hydrophobic interaction without nearest neighbour effects would suggest the elution order in this study should be Peptide 20 < 24 < 21 < 13 < 22 < 23, however, this was not the case as seen in *Figure 33*. It is possible the peptides used in Mant's study possess a random coil within the stationary phase as well as the mobile phase since they observe an expected retention order whereas the peptides within this

study do not follow the expected order due to a secondary structure induced in the stationary phase but not present in the mobile phase as shown with CD.

[Leu26]- and [Val26]-Bovine GLP-2 (16-33) (Peptides 13 and 20) differ by just one methyl group, which represents a subtle change in the peptide's overall hydrophobicity, however, when compared on a range of C18 phases (Acquity BEHs, HSSs and CSHs) there were substantial selectivity differences between the two probes (*Figure 33 (A), (D)* and *(G)*). This is in agreement with Mant *et al.* who witness greater retention for a peptide modified with a leucine compared to one modified with a valine [105]. [Ile26,Ile27]- and [Leu26,Ile27]-Bovine GLP-2 (16-33) (Peptides 21 and 13, respectively) only differ by the position of a methylene group on the side chain, however, they have substantial selectivity differences on the C18 phases during gradient elution. Literature suggests it is reasonable to expect retention differences between these two peptides, as the β-branched chain on the isoleucine is closer to the peptide backbone, thus less able to interact with the stationary phase [105]. This is again in agreement with the previous study, where the peptide modified with leucine had greater retention than the peptide modified with isoleucine.

[Ile26,Leu27]- possesses the same overall hydrophobicity as [Leu26,Ile27]-Bovine GLP-2 (16-33) (Peptides 15 and 13, respectively), but have substantial selectivity differences on the C18 phases during gradient elution (*Figure 33* and *Figure 34*), which suggests an alternative mechanism. One possible explanation could be that the change in position of the methyl group changes the shape of the peptide in the hydrophobic acetonitrile layer on the stationary phase and that results in differences in the interactions which can take place [106-108].

The more hydrophobic molecules [Phe26]-, [Trp26]- and [Tyr26]- (Peptides 22, 23 and 24) were then compared against [Leu26]-Bovine GLP-2 (16-33) (Peptide 13). Based on retention data obtained by Mant *et al.*, although they possess bulkier, aromatic side chains, a hydrophobic retention mechanism should preferentially retain [Phe26]- and [Trp26]- over [Leu26]-Bovine GLP-2 (16-33) (*Figure 33*). [Tyr26]-

Bovine GLP-2 (16-33) should be the least retained of the four peptides described. However, on all of the C18 phases, [Phe26]-, [Trp26]- and [Tyr26]- eluted earlier, which confirms that a hydrophobic retention mechanism must be acting in combination with an alternative mechanism.

The same phenomenon was experienced on the Acquity BEH alkyl range of stationary phases, where a lack of pure hydrophobic mechanism was observed (*Figure 33 (A), (B)* and *(C)*). There was a subtle change in elution order for the Acquity BEH C8 and C4, however, where [Ile26]- and [Phe26]- (Peptides 21 and 22) switched in elution order. One possible explanation could be that the aromatic groups change the shape of the peptide in the adsorbed acetonitrile layer and thereby expose other groups which can participate in polar / electrostatic interactions [106-108]. It may also not be possible to draw too many conclusions from this comparison as the C4 phase had a different pore size (300 *versus* 130 Å) and used monofunctional bonding compared to trifunctional bonding.

There are subtle selectivity differences between the stationary phases, however, to a large extent, the type and length of the ligand (C4-C18) does not appear to be critical for the separation of these probes.

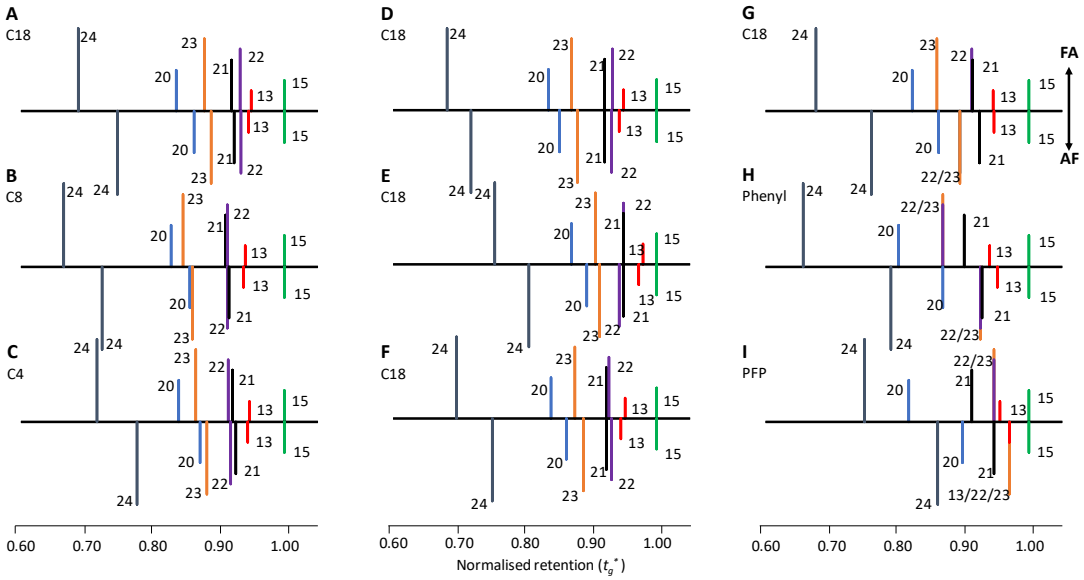

Figure 33 Comparison of (A) Acquity BEH C18 (B) Acquity BEH C8 (C) Acquity BEH C4 (D) Acquity HSS C18 (E) Acquity HSS C18-SB (F) Acquity HSS T3 (G) Acquity CSH C18 (H) Acquity CSH Phenyl Hexyl (I) Acquity CSH Fluoro Phenyl to invesitgate hydrophobic interactions (Peptide 13: [Leu26,Ile27]-, 15: [Ile26,Leu27]-, 20: [Val26,Ile27]-, 21: [Ile26,Ile27]-, 22: [Phe26,Ile27]-, 23: [Trp26,Ile27]-Bovine GLP-2 (16-33)). Data with bars above the retention axis correspond to low pH whereas below the axis correspond to intermediate pH (pH 6.45).

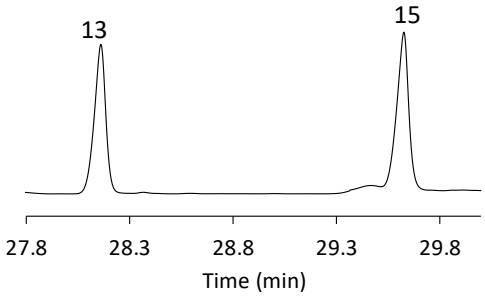

Figure 34 [Leu26,Ile27]- and [Ile26,Leu27]-Bovine GLP-2 (Peptides 13 and 15) on the Acquity BEH C8 chromatographed using the ammonium formate gradient

3.6.4.2 Electrostatic Interactions

The addition of negative charge was evaluated using peptides [L-Asp11]- and [Asn11]-Bovine GLP-2 (1-15) (Peptides 9 and 1 respectively). Their retentions were compared on stationary phases with negative and positive character (*Figure 35*) where in formic acid, on both sets of columns the asparagine peptide was eluted before the aspartic acid variant. The net charge for [L-Asp11]- and [Asn11]-Bovine GLP-2 (1-15) under formic acid conditions were 1.1 and 1.2, respectively, thus very

similar. In ammonium formate, however, the elution order was reversed, and the aspartic acid containing peptide eluted first. Under intermediate pH conditions (pH 6.45) the aspartic acid peptide has a net charge of -4.7 whilst the asparagine peptide has a net charge of -3.7, and as such, [L-Asp11]- would be expected to elute last on the phases with positive character due to enhanced electrostatic interactions. However, as the more acidic species [L-Asp11]- eluted first it suggests that despite having a greater negative charge than [Asn11]-, it is the position of the charge and accessibility in the adsorbed peptides secondary structure that is important rather than the overall net charge of the peptide hence the more charged / hydrophilic [L-Asp11]- elutes first.

The addition of positive charge was then investigated using the probes [Lys26]- and [Leu26]-Bovine GLP-2 (16-33) (Peptides 26 and 13, respectively). [Lys26]- eluted first on all stationary phases and mobile phases, however, there was increased retention under ammonium formate conditions (pH 6.45) due to increased electrostatic interactions compared to the formic acid gradient conditions (pH 2.5). The difference is most pronounced for the Acclaim Mixed Mode WCX which contains a carboxylic acid functionality. At pH 6.45, the carboxylic acid on the stationary phase ligand is deprotonated and thus the positively charged [Lys26]- becomes strongly retained. Due to repulsion, columns with a positive character (the CSH series and the Polaris Amide C18 columns) elute [Lys26]- earlier at low pH than columns with a negative character (i.e. more accessible silanol groups).

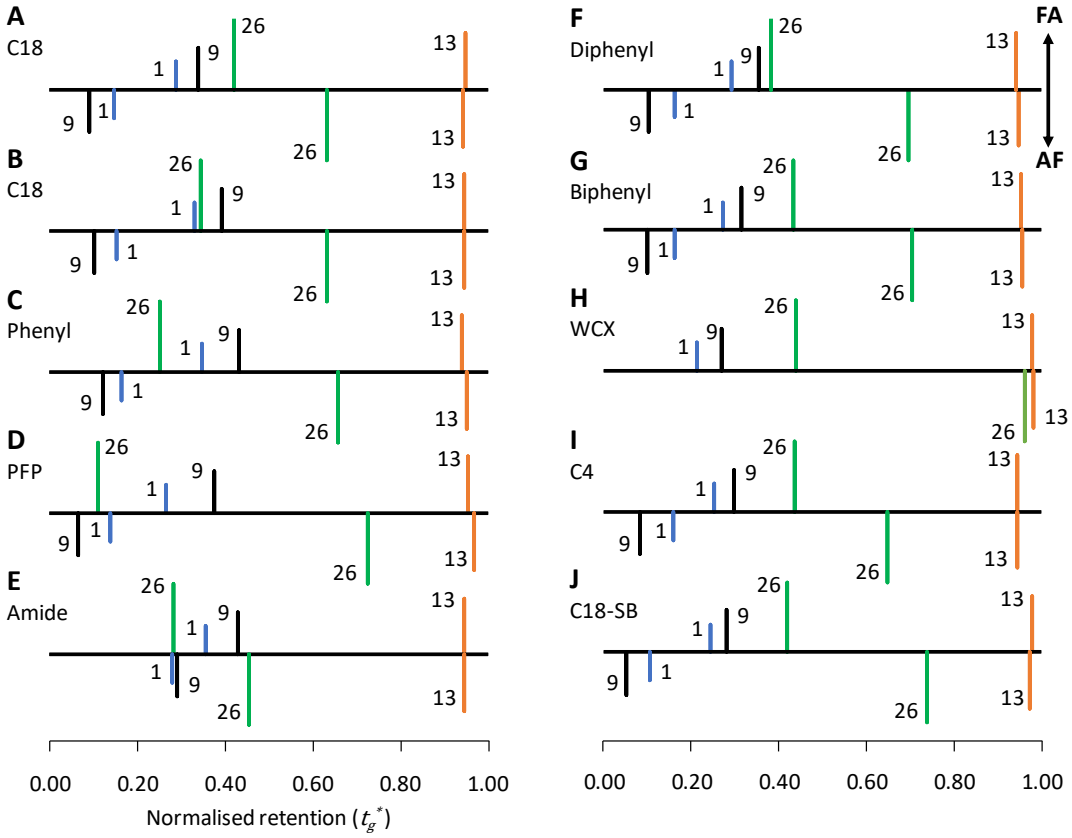

Figure 35 Comparison of (A) Acquity BEH C18, (B) Acquity CSH C18 (C) Acquity CSH Phenyl Hexyl (D) Acquity CSH Fluoro Phenyl (E) Polaris Amide C18 (F) Fortis Diphenyl (G) Ascentis Express Biphenyl (H) Acclaim Mixed Mode WCX (I) Acquity BEH C4 (J) Acquity HSS C18-SB to investigate electrostatic interactions (Peptide 1: [Asn11]-, 9: [L-Asp11]-Bovine GLP-2 (1-15), 13: [Leu26]-, 26: [Lys26]-Bovine GLP-2 (16-33)). Data with bars above the retention axis correspond to low pH whereas below the axis correspond to intermediate pH (pH 6.45).

3.6.4.3 Aromatic Interactions

Phenyl containing phases (Acquity CSH Phenyl Hexyl, Fortis Diphenyl and Ascentis Biphenyl) and the pentafluorophenyl phase (Acquity CSH Fluoro Phenyl) were compared against the Acquity BEH C18 and CSH C18 to assess for potential aromatic interactions. The probes used were [Leu26]-, [Phe26]-, [Trp26]- and [Tyr26]-Bovine GLP-2 (16-33) (Peptides 13, 22, 23 and 24, respectively).

The CSH phases all possessed the same elution order in both formic acid and ammonium formate, highlighting minimal aromatic retention which suggests the stationary phase ligand becomes less important for these separations (*Figure 36*).

The diphenyl and biphenyl phases on the other hand were able to resolve the aromatic species and also had different elution orders compared to the CSH phases. [Phe26]- elutes after [Leu26]- and there is a significantly larger retention of [Phe26]- at mid pH suggesting that this is due to electrostatic interaction and not due to π-π interactions. The diphenyl and biphenyl phases suggest a more negative character due to accessible silanol groups whereas the CSH phases have a more positive character due to positively charged groups in the stationary phase, as indicated within the PCA (*Figure 32*).

There is the potential that the acetonitrile within the mobile phase could reduce any subtle aromatic interactions of the peptides with the stationary phase due to competing π-π interactions [109-111]. The elution order based on hydrophobicity alone using Hodges's work would suggest [Tyr26]- elute first, then [Leu26]-, [Phe26]- and then finally [Trp26]-Bovine GLP-2 (16-33) (Peptide Number 24, 13, 22, and 23, respectively) [112]. However, this was not the case here where [Trp26]- typically eluted before [Phe26] and [Leu26]-Bovine GLP-2 (16-33). This is highly suggestive that an alternative retention mechanism must be introduced, such as the formation of a second order structure of the peptide in the stationary phase exposing certain functional groups and hiding others.

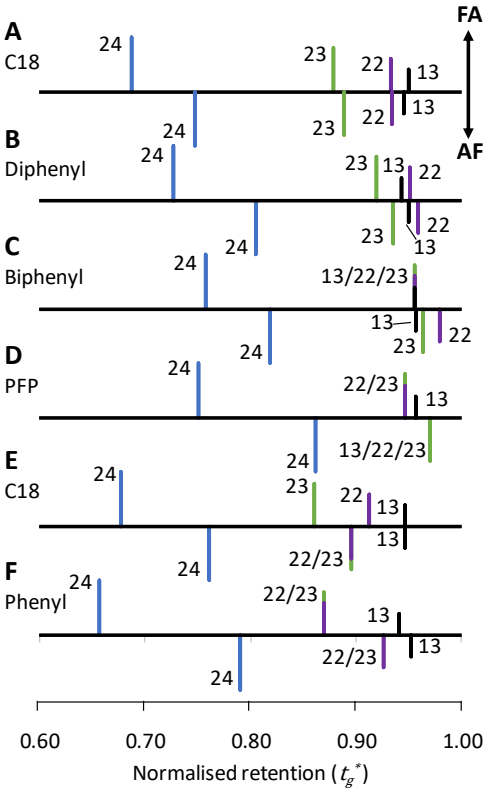

Figure 36 Comparison of (A) Acquity BEH C18 (B) Fortis Diphenyl (C) Ascentis Express Biphenyl (D) Acquity CSH Fluoro Phenyl (E) Acquity CSH C18 (F) Acquity CSH Phenyl Hexyl to investigate aromatic interactions (Peptide 13: [Leu26]-, 22: [Phe26]-, 23: [Trp26]-, 24: [Tyr26]-Bovine GLP-2 (16-33)). Data with bars above the retention axis correspond to low pH whereas below the axis correspond to intermediate pH (pH 6.45).

3.6.4.4 Hydrogen Bonding Interactions

Prior knowledge of the stationary phases suggested those phases which are likely to form hydrogen bonding interactions are the Polaris Amide C18 via the amide functionality, the Acquity BEH Shield RP-18 via the embedded carbamate moiety, the Acquity BEH C4 via the short alkyl ligand which promotes greater accessibility to residual silanol groups on the silica surface, Acquity HSS C18-SB via low ligand surface coverage and lack of end-capping and thus more silanol groups, and the Acclaim Mixed Mode WCX via the carboxylic acid moiety. The Acquity BEH C18 was used as a baseline since it is based on hybrid silica, is end-capped and thus should have minimal potential to form hydrogen bonds. The peptides [Phe26]- and [Tyr26]-Bovine GLP-2 (16-33) (Peptide Numbers 22 and 24) were assessed for hydrogen

bonding interactions with the stationary phases as they only differ due to the presence of the hydroxyl group on the tyrosine. The phenylalanine derivative eluted last on all the stationary phases and mobile phases although with greater retentivity in ammonium formate for the tyrosine variant (data not shown). The trend seems to suggest that polarity is more dominant than hydrogen bonding capabilities. The extra retentivity in ammonium formate of the tyrosine peptide could indicate that the stationary phase is becoming more polar. The lack of hydrogen bonding could be due to the position of the amino acid change in the peptide residue. It is possible hydrogen bond interactions could be more pronounced if tyrosine was located closer to the terminal amino acids.

There are large selectivity differences observed between the two peptides considering only a 16 Da difference in their ~2300 Da structures, which indicates the addition of the hydroxyl group has caused some significant changes in the interactions within the chromatographic system.

The position of the Acquity BEH Shield RP-18 at the origin in the score plot is highly suggestive that the carbamate group masks any underlying silanol groups and the carbamate is not involved in any pronounced hydrogen bonding interactions with [Tyr26]-Bovine-GLP-2 (16-33) (Peptide Number 24).

3.6.4.5 Interactions Related to Degradation of Peptides

Purity profiling methods developed for biopharmaceutical peptides should be able to separate degradation products. Consequently, an important aspect of the protocol was to evaluate selectivity for common degradants and racemisation products. Racemisation and isomerisation often produce peptides which are diastereoisomers of the original peptides, which have very similar physiochemical properties. An investigation of the retention order of diastereoisomeric peptides containing the D- and L-forms of a particular amino acid residue indicate that the retention order often is the same at both low and mid pH. This was the case for 78% of the 117 combinations of delta values and columns in the current study. A

comparison of which pH typically generates a higher delta value for racemates did not show any trend. In 54% of the cases mid pH gave a larger delta value. A similar result was obtained for isomeric delta values, where 73% of the 26 combinations often gave the same elution order in both low and mid pH. However, there was a trend where low pH gave a large delta value (85% of the combinations).

The score plot (*Figure 32*) was used to identify phases which were deemed chromatographically similar and dissimilar with regard to their ability to separate racemised amino acid residues. The Acquity CSH Phenyl Hexyl and Acquity HSS C18-SB were selected as phases with large differences in selectivity for the separation of [D-Ser16]- and [L-Ser16]-Bovine GLP-2 (16-33) (Peptide Numbers 14 and 13, respectively), whilst the Acquity HSS T3 and Acquity BEH C18 were compared as phases which provide similar selectivity, i.e. these phases are located at the extremes and close to origin when projected on to a line through the origin and $\Delta(14,13)$.

The diverse columns with formic acid (*Figure 37 (A)* and *(B)*) exhibit a difference in the degree of resolution, where there is coelution but a switch in elution order on the Acquity HSS C18-SB and resolution achieved on the Acquity CSH Phenyl Hexyl. By switching to ammonium formate (*Figure 37 (E)* and *(F)*), baseline resolution was achievable on the Acquity CSH Phenyl Hexyl, whilst the Acquity HSS C18-SB has a switched elution order. For difficult separations such as resolving racemic species, it is essential to have large peak capacity which is typical for mobile phases such as ammonium formate, whereas solvents which have low ionic strength, such as formic acid, typically failed to resolve the two species due to poor peak shape.

In *Figure 37 (C), (D), (G)* and *(H)*, the Acquity HSS T3 and Acquity BEH C18 all produced similar looking chromatograms irrespective of stationary or mobile phase, with similar selectivity and normalised retention times.

This comparison has provided an early indication that this protocol could show differentiation between the phases, even for challenging separations such as resolving racemic species. The example above was selected using $\Delta(14,13)$. In order

to select columns from the score plot (*Figure 32*) likely to give large differences in selectivity for any racemates the selection would have been Acquity BEH C8, Acquity HSS C18-SB, Acquity CSH Fluoro Phenyl, Acquity CSH Phenyl Hexyl and Polaris Amide C18

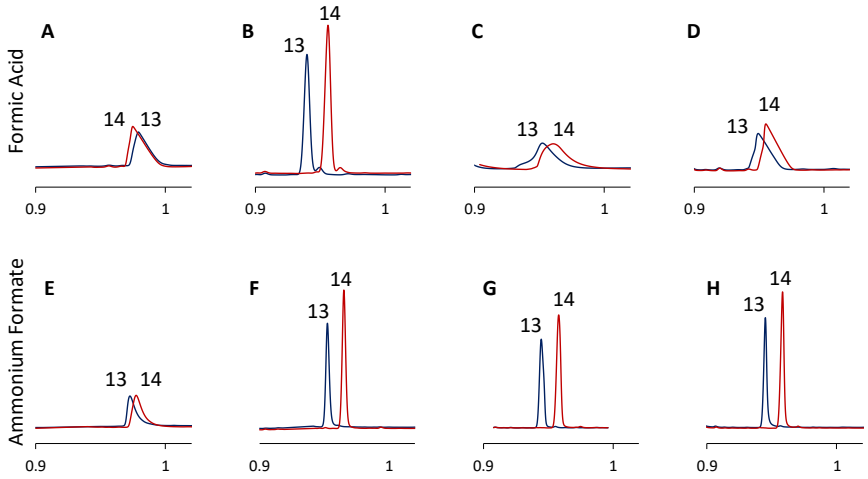

Figure 37 Chromatograms of (13) [L-Ser16]- and (14) [D-Ser16]-Bovine GLP-2 (16-33) on phases predicted to be similar or dissimilar based on the score plot in Figure 34. From L-R: Acquity HSS C18-SB, Acquity CSH Phenyl Hexyl, Acquity HSS T3, Acquity BEH C18, A-D in formic acid, E-H in ammonium formate

[Met(O)10]- and [Met10]-Bovine GLP-2 (1-15) (Peptide Numbers 8 and 1, respectively) were compared to investigate the effect of oxidation. Peptides containing the more hydrophilic, oxidised methionine eluted first on all the stationary phases irrespective of the mobile phase conditions, with ample degree of separation achieved between the two species in either formic acid or ammonium formate gradient conditions.

3.6.5 Suggested Probes Selected for the Peptide RPC Column Characterisation Protocol Robustness

After careful analysis of the Peptide RPC Column Characterisation Protocol development results and the effect of each delta value, the probes were selected for the final Peptide RPC Column Characterisation Protocol. The number of peptides

was reduced from 26 down to 11 peptides, which generated 11 delta values which cover a range of interactions (*Table 42*). These interactions included the effect of oxidation, steric effects, changes in negative or positive charge and changes in aromatic or phenolic character.

Table 42 Selection of peptides and delta values used in the Peptide RPC Column Characterisation Protocol.

Delta	Mobile Phase	Rationale	Peptides
(3,1)	Ammonium formate (pH 6.45)	Steric	(3) [D-Asp3]-Bovine GLP-2 (1-15) (1) Bovine GLP-2 (1-15)
(8a,1)	Formic acid (pH 2.5)	Oxidation	(8a) [Met(O)10]-Bovine GLP-2 (1-15) (1) Bovine GLP-2 (1-15)
(9,1)	Formic acid (pH 2.5) and ammonium formate (pH 6.45)	Addition of a negative charge	(9) [L-Asp11]-Bovine GLP-2 (1-15) (1) Bovine GLP-2 (1-15)
(10,9)	Ammonium formate (pH 6.45)	Steric	(10) [D-Asp11]-Bovine GLP-2 (1-15) (9) [L-Asp11]-Bovine GLP-2 (1-15)
(14,13)	Formic acid (pH 2.5)	Steric	(14) [D-Ser16]-Bovine GLP-2 (16-33) (13) Bovine GLP-2 (16-33)
(15,13)	Ammonium formate (pH 6.45)	Steric	(15) [Ile26,Leu27]-Bovine GLP-2 (16-33) (13) Bovine GLP-2 (16-33)
(16,13)	Formic acid (pH 2.5)	Aromatic to alkyl	(16) [Gly22]-Bovine GLP-2 (16-33) (13) Bovine GLP-2 (16-33)
(24,13)	Ammonium formate (pH 6.45)	Alkyl to aromatic	(24) [Tyr26]-Bovine GLP-2 (16-33) (13) Bovine GLP-2 (16-33)
(26,13)	Formic acid (pH 2.5) and ammonium formate (pH 6.45)	Addition of a positive charge	(26) [Lys26]-Bovine GLP-2 (16-33) (13) Bovine GLP-2 (16-33)

Base sequence for Bovine GLP-2 (1-15) "HADGSFSDEMNTVLD" and Bovine GLP-2 (16-33) "SLATRDFINWLIQTKITD"

The loading plot (*Figure 38*) contained parameters in all four quadrants, thus describing all of the workspace, with distinct areas for positive character and silanophilic interactions at the top and the bottom of the loading plot, respectively. The score plot (*Figure 39*) also contained stationary phases in all four quadrants, but with distinct regions for the different categories of phases. Approximately 76% of the variables were described by the final Peptide RPC Column Characterisation Protocol probes, which was adequate for observing trend.

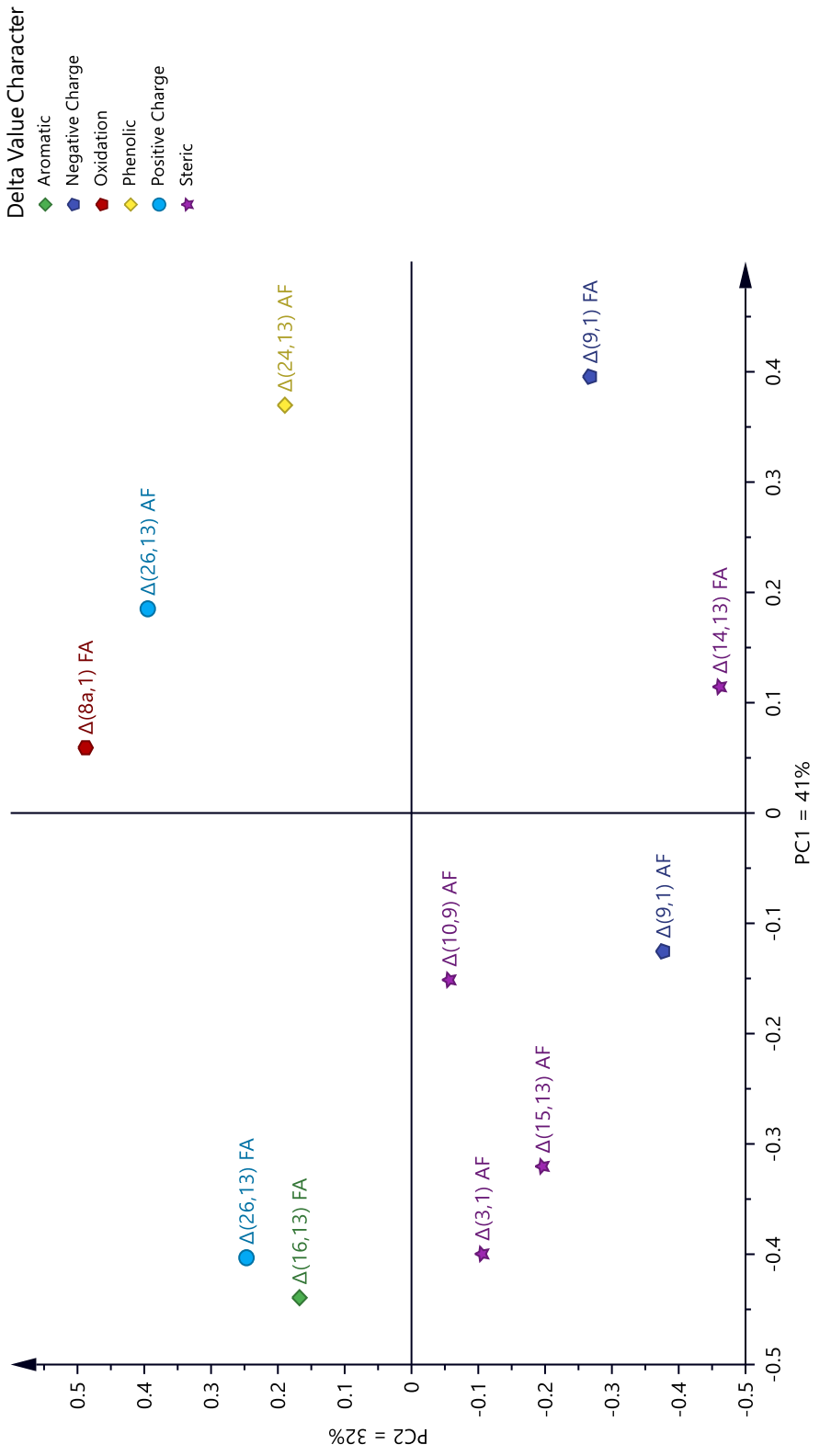

Figure 38 Loading Plot of the Delta Value to be Included in the Peptide RPC Column Characterisation Protocol.

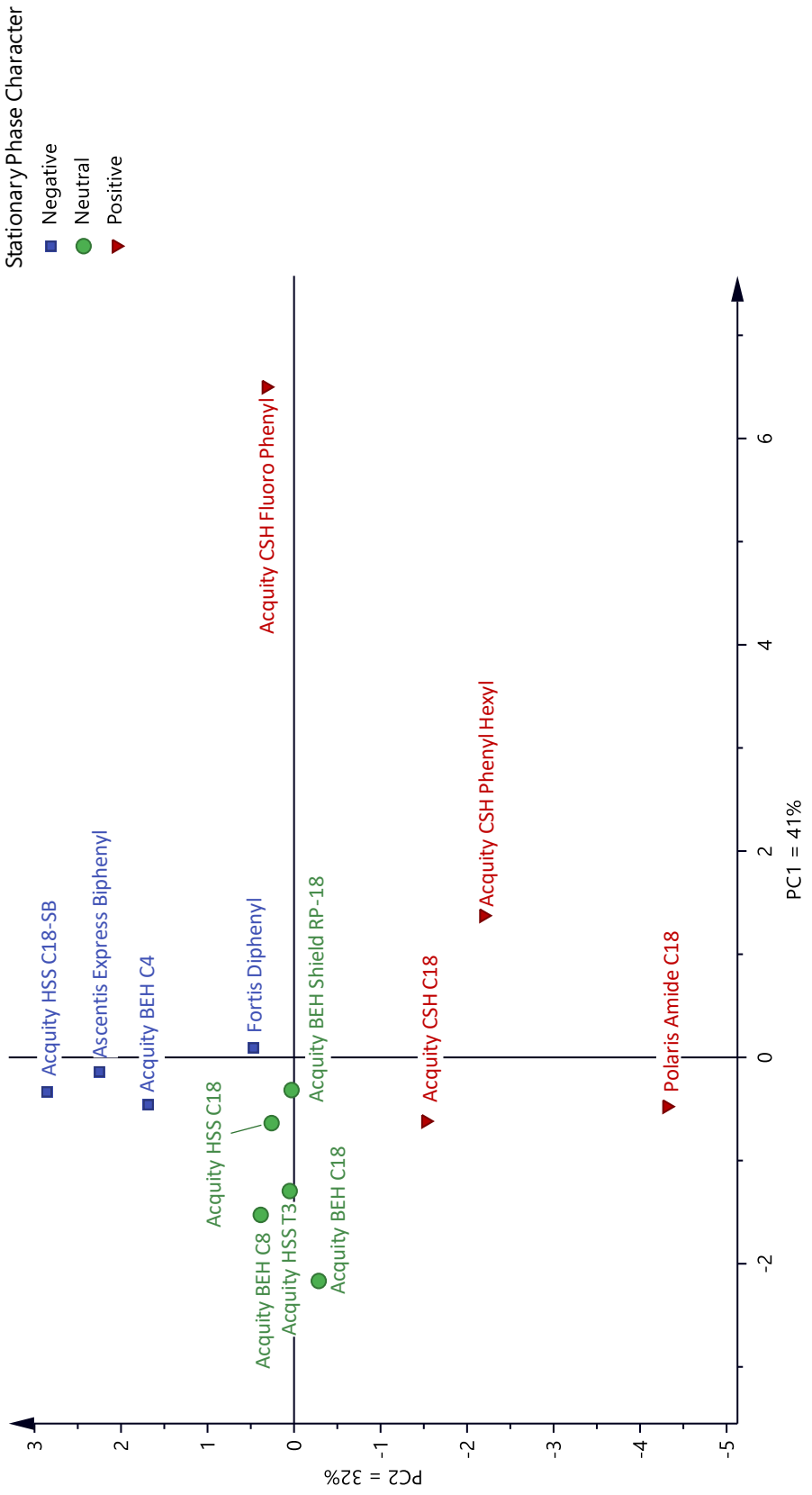

Figure 39 Score Plot Using the Delta Values to be Included in the Peptide RPC Column Characterisation Protocol.

3.6.6 Defining the Peptide RPC Column Characterisation Protocol Mixtures

Three new test mixtures were devised for the peptides in the Peptide RPC Column Characterisation Protocol (*Table 43*).Each mixture contained the two reference peptides [Met(O)10]-Bovine GLP-2 (1-15) (Peptide Number 8) and [Ile26,Leu27]-Bovine GLP-2 (16-33) (Peptide Number 15) in order to normalise the results.

The test mixtures contained both peptides used to calculate the delta value to prevent the influence of different injections and drifts in retention, thus maximising robustness. The first test mixture (TM1) contained a total of seven peptides to calculate five delta values. The second and third test mixtures (TM2 and TM3, respectively) contained six peptides each to calculate two delta values. Peaks were identified based on either their mass or differentiated by peak area where the same mass was present (i.e. L-/D- isomers).

Table 43 Test mixtures for the Peptide RPC Column Characterisation Protocol.

TM1			TM2			TM3		
Peptide	**Peptide Number**	**Delta**	**Peptide**	**Peptide Number**	**Delta**	**Peptide**	**Peptide Number**	**Delta**
[Met(O)10]-Bovine GLP-2 (1-15)	8	Δ(8a,1)	[Met(O)10]-Bovine GLP-2 (1-15)	8	Δ(10,9)	[Met(O)10]-Bovine GLP-2 (1-15)	8	Δ(3,1)
Bovine GLP-2 (1-15)	1	Δ(9,1)	[D-Asp11]-Bovine GLP-2 (1-15)	10	Δ(26,13)	Bovine GLP-2 (1-15)	1	Δ(14,13)
[L-Asp11]-Bovine GLP-2 (1-15)	9	Δ(15,13)	[L-Asp11]-Bovine GLP-2 (1-15)	9		[D-Asp3]-Bovine GLP-2 (1-15)	3	
[Gly22]-Bovine GLP-2 (16-33)	16	Δ(16,13)	[Lys26]-Bovine GLP-2 (16-33)	26		Bovine GLP-2 (16-33)	13	
[Tyr26]-Bovine GLP-2 (16-33)	24	Δ(24,13)	Bovine GLP-2 (16-33)	13		[D-Ser16]-Bovine GLP-2 (16-33)	14	
Bovine GLP-2 (16-33)	13		[Ile26,Leu27]-Bovine GLP-2 (16-33)	15		[Ile26,Leu27]-Bovine GLP-2 (16-33)	15	
[Ile26,Leu27]-Bovine GLP-2 (16-33)	15							

The three test mixtures were injected on the Kinetex Evo C18 to assess the suitability of the proposed compositions (*Figure 40*) with successful results. The peaks response was similar between each injection and peptides which appeared in multiple mixtures gave the same retention and normalised retention times. As such, the proposed test mixtures were approved for the Peptide RPC Column Characterisation Protocol.

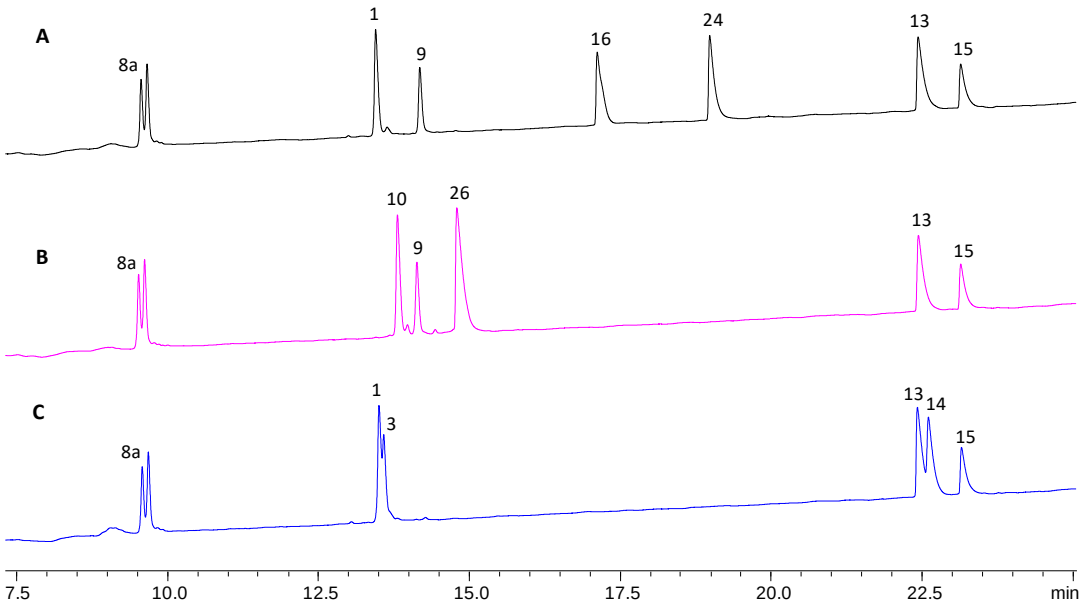

Figure 40 Example chromatograms at 215 nm of the (A) TM1 (B) TM2 (C) TM3 mixtures using the 0.1% v/v formic acid conditions described in Section 2.10.5. Peak 1: Bovine GLP-2 (1-15), 3: [D-Asp3]-Bovine GLP-2 (1-15), 8a: [Met(O10]-Bovine GLP-2 (1-15), 9: [L-Asp11]-Bovine GLP-2 (1-15), 10: [D-Asp11]-Bovine GLP-2 (1-15), 13: Bovine GLP-2 (16-33), 14: [D-Ser16]-Bovine GLP-2 (16-33), 15: [Ile26,Leu27]-Bovine GLP-2 (16-33), 16: [Gly22]-Bovine GLP-2 (16-33), 24: [Tyr26]-Bovine GLP-2 (16-33), 26: [Lys26]-Bovine GLP-2 (16-33).

3.6.7 Defining Peak Capacity

Sample peak capacity (*PC***) is a measure of separation power in gradient elution and is defined as the total number of peaks within a chromatogram which can be resolved with R_s = 1. The *PC*** value (*Equation 27*) should ideally be large for method development purposes in order to have a greater chance for resolving all compounds. The value can be reduced for optimised separations. Snyder *et al.* suggested that for a separation of compounds where n=10, peak capacity would

have to be greater than 80 to resolve all peaks, however, an optimised method could reduce the peak capacity to around 40 [102].

$$PC^{**} = \frac{t_{Rf} - t_{Ri}}{w_{Ave}} + 1 \qquad \textit{Equation 27}$$

t_{Rf} and t_{Ri} where the retention time for the final and initial peak, respectively, and w_{Ave} was the average width at base for all peaks in the first peptide test mixture (TM1), excluding the oxidised methionine peaks. The oxidised methionine was excluded as the diastereoisomers were unable to be resolved on all the stationary phases evaluated, which could potentially skew the results.

The above approach was used as the conventional peak capacity defined by Snyder [102] is a hypothetical measurement based on the gradient time divided by the peak width, which often overestimates the capacity of the separation. The sample peak capacity approach used in *Equation 27* calculates the peak capacity for the fraction of the gradient which is being used to separate all the compounds of interest, which is bracketed by the retention of the first and last peak of elution. Although the value of peak capacity by this measurement will be smaller than by the conventional measurement, it is more practically relevant to chromatographic separations.

Peak capacities can be improved by utilising high efficiency RP stationary phases, such as superficially porous particles (SPP) or sub-2 µm totally porous particles (TPP). The majority of the stationary phases within this project can be classed as either SPP or sub-2 µm TPP to improve chromatographic separations. Alternatively, peak capacity can be affected by the mobile phase additive.

The peak capacities for the 14 columns used to develop the Peptide RPC Column Characterisation Protocol were determined in both formic acid and ammonium formate (*Figure 41*) using the peptides from TM1 described in *Section 3.6.5*. Typically, the peak capacities were improved in ammonium formate in comparison to formic acid, with a few exceptions (i.e. Acquity CSH Phenyl Hexyl and Acquity CSH

Fluorophenyl). The poor performance could be due to the low ionic strength for formic acid solutions. Separations in formic acid are also more susceptible to overloading effects, which could reduce the performance [113, 114]. Poor peak shape at low pH is often attributed to silanophilic interactions, however, with the increase in modern silicas which do not possess a significant degree of strongly acidic silanols, this cannot be the cause of exaggerated peak shapes for basic species. McCalley *et al*. hypothesised that poor peak shape can often be ascribed to overloading for basic species due to mutual repulsion effects between adsorbed ions of the same charge [48, 115, 116]. This effect is increased further when low ionic strength mobile phases are used, such as 0.1% formic acid. Further research by McCalley, which used positively charged peptide probes also supported this theory where he compared the responses of four multiply positively charged peptides in phosphate buffer, formic acid and TFA [48]. The phosphate buffer gave significantly better peak shape and chromatographic performance compared to the formic acid due to a significantly higher ionic strength which reduces mutual repulsion.

Although formic acid can result in poor peak shape, this was not the case for the Acquity CSH range of stationary phases which were specifically designed to provide an improved peak shape for basic species due to the presence of a small permanent positive character on the surface of the phase [117, 118]. The Polaris Amide C18, which also possessed a positive character, additionally provided good chromatographic performance in formic acid.

The peak capacity for the Acclaim WCX in ammonium formate was excluded as the hydrophilic peptides eluted before the void, thus peak width could not be determined for those peptides.

It was also noted that the more retentive columns tended to have greater PC^{**} values, such as the C18 phases, compared to less retentive phases such as the C4 or fluoro phenyl phases. This could be due to the greater elution window for the C18 type phases, which should be taken into consideration when observing PC^{**}.

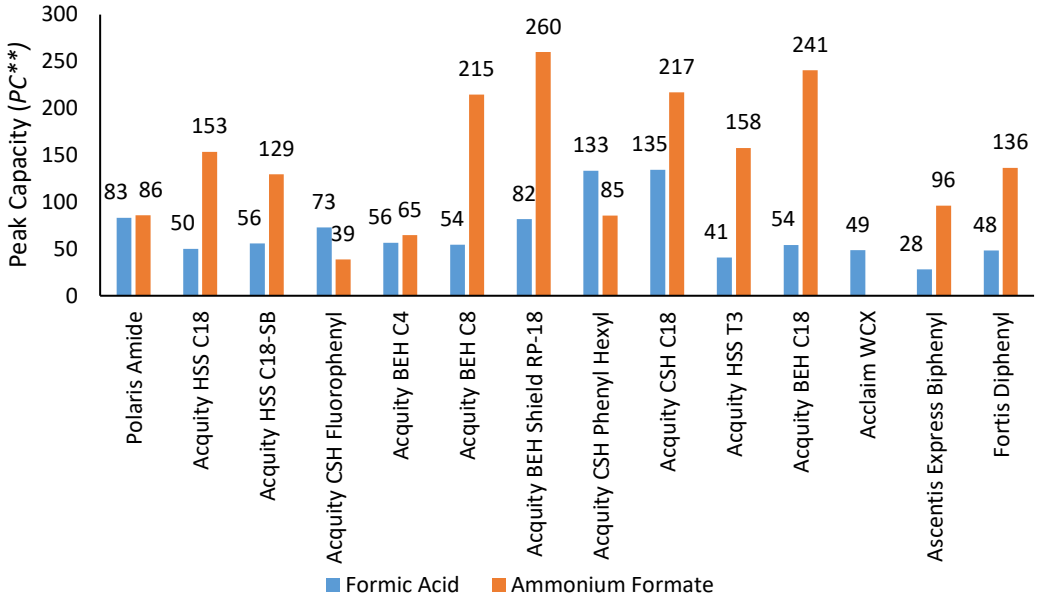

Figure 41 Peak capacities determined for the 14 stationary phases using the formic acid and ammonium formate gradient conditions described for the Peptide RPC Column Characterisation Protocol.

3.7 Robustness of the Peptide RPC Column Characterisation Protocol using Factorial Design

The Peptide RPC Column Characterisation Protocol was evaluated to ensure the integrity of the results generated. This required an in-depth analysis of the methodology, by performing a factorial design (otherwise known as Design of Experiment (DoE)) for both the formic acid and the ammonium formate conditions. In addition, the intermediate precision, the effect of loading on a hydrophilic peptide and the effect of pH switching were assessed, which has been known to cause drifts in retention [48, 115, 116, 119].

DoE is a statistical tool composed typically of two or more parameters known as factors. It is particularly advantageous for gaining a greater precision for estimating the main factor effects and exploring the interactions between those different factors. It can also contribute towards conclusions of further studies [120, 121].

DoE is particularly advantageous over an alternative approach; changing one factor at a time (OFAT). OFAT requires significantly more experiments and data than DoE, which can utilise a significant amount of resource in both cost and time. Even so, OFAT poorly understands the joint influence of parameters, as only one variable is considered in one experiment [122].

DoE is an extremely organised approached. It is an ideal tool to investigate whether a variable is an observed effect or if in fact it is purely noise. Modelling data is an oversimplification of the data, however, by selecting the most appropriate model, a small aspect of reality can be described.

3.7.1 Factorial Design

There are numerous models available depending on the objective of the factorial design. Some common examples include Plackett Burman and reduced factorial design [95, 120, 123, 124]. The most typical objective used to evaluate the robustness of a methodology is the screening design, where a reduced factorial design can provide sufficient information regarding the influencing factors. A 2^3 factorial design identifies eight experimental conditions and three centre points which act as validation runs to describe the variability and deduce the random effect within the workspace. Some common parameters for chromatographic robustness studies include wavelength, temperature, flow rate and mobile phase preparation. The levels for each parameter are typically selected based on instrument specification and expected error associated with equipment (i.e. glassware).

The column batch to batch variation is not typically included in the robustness test. It is categorical / discreet variable which typically is accounted for in the validation of intermediate precision. Note that it is of critical importance to get columns from different base silica batches. Just different batches of packing or attachment of ligands to the silica will not reflect the true batch to batch variation. When ordering the columns, one must stress the need for columns from different base silica batches.

3.7.2 Rationale for the Design of Experiment Levels

3.7.2.1 Formic Acid Method DoE Levels

Wavelength is typically investigated within a DoE as a change can affect the area of the integrated peak and the signal to noise ratio. This was less important within this study as the data was qualitative and peak confirmation was ascertained by MS data therefore was excluded from the DoE.

Temperature is often used to improve speed of separations, reduce back pressure by reducing mobile phase viscosity and increase column performance due to faster analyte molecular diffusion and reduced mass transfer term in the van Deemter equation. It is a critical variable requiring adjustments to meet the acceptance criteria in the system suitability test. In several cases reversal of elution order is observed for a temperature difference of less than 3 °C [125]. Furthermore, due to differences in the construction of column thermostats the actual temperature in the column differs from one instrument to another despite identical set-point / read-back, with deviations recorded as large as 5 °C [126]. Radial and axial temperature gradients are two contributing factors which should be evaluated [127-133]. Radial temperature gradients (i.e. changes in temperature across the cross section of the column) can lead to band broadening and poor chromatographic performance. This is typically a result of heat dissipation from the outer parts of the columns. The discrepancy in the temperature cross section affects the solvent viscosity, where there is a divergence in solvent viscosity across the cross section of the column which therefore affects the linear velocity. Thus, a parabolic band is generated where the band migrates faster at the walls than at the centre of the column, as demonstrated in *Figure 42(A)* [125]. Axial temperature gradients, on the other hand, are changes in temperature along the length of the stationary phase (i.e. the outlet is warmer than the inlet). This can be as a result of frictional heating, where the incoming solvent rubs against the column bed which converts the friction into heat. The degree of heating can be dependent on particle size, column dimensions,

pressure, temperature and flow rate. With frictional heating, the solute migrates along the length of the column with minimised band spreading under adiabatic conditions (i.e. no transfer of heat between a system and its surroundings), therefore the chromatographic performance is unaffected by axial temperature gradients. If there is efficient dissipation of heat from the column wall in a system such as in a water bath, then frictional heating can also result in radial gradients. Frictional heating will also cause changes in temperature which alters the solvent viscosity and linear velocity along the length of the column, which affects retention and selectivity, as demonstrated in *Figure 42(B)* [125].

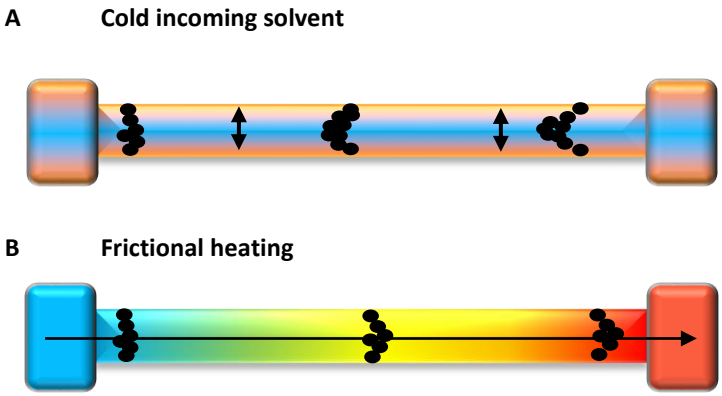

Figure 42 Schematic of a column undergoing (A) radial and (B) axial temperature gradients as a result of insufficient solvent preheating and frictional heating, respectively. Blue = cooler temperatures, red = hotter temperatures.

The most critical parameter for column characterisation using peptides is to maintain retention and selectivity, therefore, the column oven should ideally exhibit limited frictional heating / axial temperature gradients. Thus, it was deemed necessary to evaluate the actual column temperature for different column ovens for the robustness of the Peptide RPC Column Characterisation Protocol using a set protocol.

The average temperature within the column can be measured as a function of retention time *versus* temperature. The retention time of caprylophenone (20 µg/mL in MeCN) was used as a relative measure of the average temperature within

the column [53]. Two thermostat designs (Shimadzu CTO-30A still air oven and Shimadzu CTO-20A forced air oven) were compared against a water bath where temperature was determined using a calibrated thermometer with an accuracy of ±0.5 °C, defined as ±95% confidence interval, between 0 to 100 °C. The sample was injected at 4 µL with a flow rate set to 0.3 mL/min. The mobile phase was MeCN / H_2O (45:55 w/w), where solvents were weighed and premixed to eliminate instrument to instrument %MeCN variation. The sample was injected at 30 to 60 °C in 5 °C intervals to plot (retention time – system dead time) *versus* temperature to determine a deviation in temperature for the LC system (i.e. ΔT at a certain retention time). System dead time was subtracted from the retention time to allow for comparison between the three ovens and was determined by the retention time of uracil dissolved in water, where the column was replaced with a ZDV union.

It can be assumed that the retention time obtained from a column submerged in a bath with circulating water will correspond to an accurate average column temperature. A 1 m x 0.1 mm steel tubing was submerged in the water bath to provide adequate solvent preheating. An XBridge C18, 3.5 µm, 50 x 2.1 mm column was first evaluated to assess the average column temperature without frictional heating as an influence (*Figure 43*). Frictional heat is minimal due to the reduced column length and greater than 3 µm particle size. Any deviation from the water bath trend (orange markers) suggests a deviation between the temperature of the column and the set point of the oven. The Shimadzu CTO-20A oven (forced air, green markers) matches the water bath closely, within experimental error, however, the Shimadzu CTO-30A oven (still air, blue markers) exhibits a greater deviation from the average column temperature, particularly at higher temperatures. At 40 °C, the temperature used in the Peptide RPC Column Characterisation Protocol and system suitability tests, the forced air oven is +0.13 °C from the set point, whilst the still air oven is -1.77 °C lower than the set point, *Table 44*.

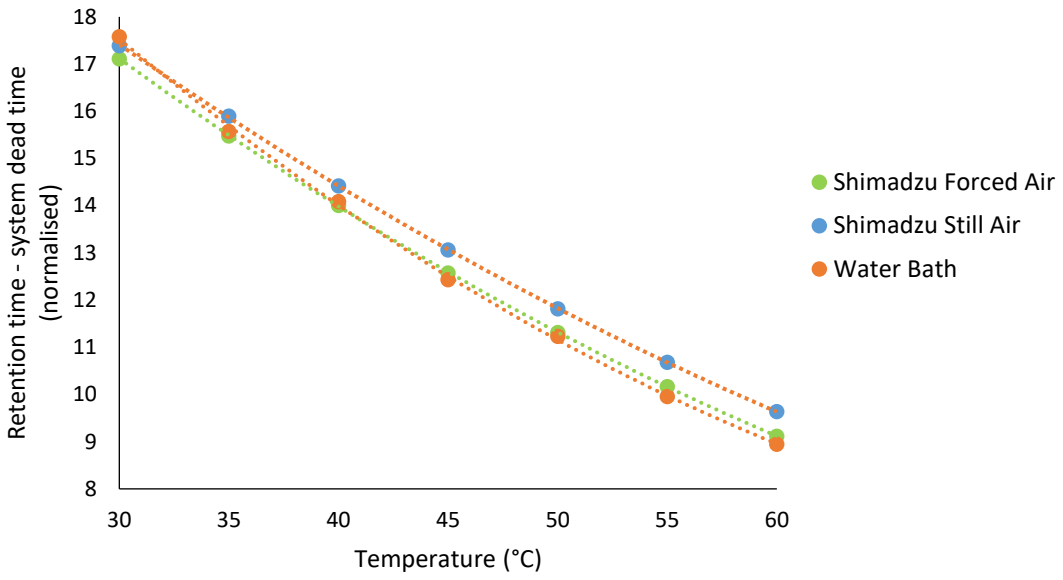

Figure 43 Plot of (t_R-System dead time) versus Temperature for caprylophenone using the XBridge C18, 3.5 µm, 50 x 2.1 mm column. Flow rate was 0.3 mL/min using MeCN / H_2O (45:55 w/w). All data was normalised to make a valid comparison.

A second column was used to assess the average column temperature with heat of friction (Acquity UPLC BEH C18, 1.7 µm, 150 x 2.1 mm column). The graph in *Figure 44* displays both the deviation in average column temperature from the oven set point. At the lowest temperature, the caprylophenone eluted earliest on the CTO-30A (still air), then CTO-20A (forced air). This suggests there is frictional heating in the column. The forced air oven provides similar retention to the water bath, which suggests the set point of the oven is accurate. The still air oven deviates from the water bath at the higher temperatures, which suggests the column isn't at 60 °C, as suggested by the oven set point. This could indicate insufficient preheating, or a pressure effect. However, at 40 °C, the forced air oven and still air oven are both within 0.8 °C of the set point. In fact, the still air oven is actually closer to the set point at 0.35 °C, however, the column in the still air oven must be experiencing different influencing factors where the retention is lower at lower temperatures and higher at higher temperatures than the baseline provided by the water bath which would reduce the reproducibility of the separation, whilst the forced air oven overlays the majority of the water bath trace.

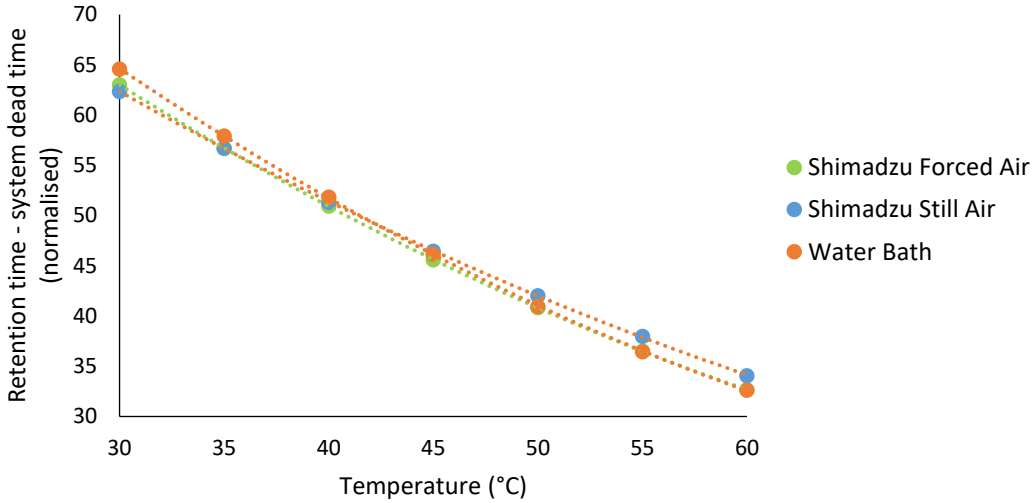

Figure 44 Plot of (t_R-System dead time) versus Temperature for caprylophenone using the XBridge BEH C18, 1.7 µm, 150 x 2.1 mm column. Flow rate was 0.3 mL/min using MeCN / H_2O (45:55 w/w). All data was normalised to make a valid comparison.

Table 44 Comparison of measured temperature against set point of the oven.

Oven Design	Measured Temperature (°C)		Set Point – Measured (°C)		Percentage of Set Point (%)	
	50 x 2.1 mm	150 x 2.1 mm	50 x 2.1 mm	150 x 2.1 mm	50 x 2.1 mm	150 x 2.1 mm
Water Bath	40		-		-	
CTO-30A Still Air	41.77	39.65	-1.77	+0.35	104.4	99.1
CTO-20A Forced Air	39.87	39.25	+0.13	+0.75	99.7	98.1

Peptide RPC Column Characterisation Protocols utilises 40 °C, which based on these results, suggest the Shimadzu forced air oven can provide the same temperature in the column as a water bath controlled using a certified thermometer. The deviation between oven design on the two different column formats, however, suggests it is important to check the temperature of the column before characterising columns using the Peptide RPC Column Characterisation Protocol or any other protocol. It is thought that for minimised radial temperature gradients in the column and to achieve high efficiencies, a still air oven should be used. However, this result

focused on the effect of retention time as this could impact on selectivity which is the main focus of the main study.

It is important for the user to check the temperature of their oven with the water bath approach as previous experience has observed some column ovens can deviate significantly more than this [134]. Despite this, the limits for the formic acid DoE was ±2 °C as the Shimadzu forced air column oven produced an actual column oven temperature close to the programmed value. The difference in column oven temperature was evaluated during intermediate precision where different column ovens were used.

The specification provided by various instrument manufacturers for flow rate typically is ±1% which probably corresponds to 3x SD, which would suggest a range of 0.3 mL/min ± 0.003. Tests produced by Novo Nordisk on eight instruments identified a 99% confidence interval (CI) of 0.5% at 0.1 mL/min, thus would suggest a limit of 0.3 mL/min ± 0.0015. The limit was actually set to 0.3 mL/min ± 0.005 as it was deemed a more practical value which may have the potential to see a practical effect and would allow for aging instrumentation.

The original development conditions used a starting %B of 10% for the formic acid gradient. However, it was noticed that on some of the stationary phases, the more hydrophilic peptides were sometimes poorly retained and had interference from the DMSO solvent front. As such, it was decided to reduce the starting %B from 10% to 5% and adjust the gradient conditions accordingly to generate the same selectivity, which was confirmed via chromatographic experiments. It would be ill-advised to have the starting %B any lower than 5% due to potential de-wetting of pores resulting in a reduced accessible surface in the column and thus poor retention for hydrophobic stationary phases under low organic conditions. De-wetting is most critical when the pressure is removed on hydrophobic stationary phases when saturated in water and as such, to ensure the integrity and robustness of the separation, the initial conditions were set to 5%. The gradient accuracy is dependent on the accuracy of the pump which is typically specified to ±0.4%

(averaged from three different instrument manufacturers). It is assumed the specifications are 3x SD, thus the average SD would be 0.14%. This was in reasonable agreement with data determined by Novo Nordisk on 16 instruments where SD was 0.16% which provided a 99% CI of 0.46% which is comparable to the average specification for composition accuracy. The level selected for the DoE was ±0.4%, where the entire gradient was adjusted as it was assumed to be a systematic error in the accuracy of the pump.

Significant errors can be generated by preparing volumes using glassware, therefore solvents were prepared by weight to eliminate these errors. The pan balance has a random error of < 0.01 g which is assumed to be 3x SD.

In experimental work, it can be more appropriate to combine random errors which are associated as the combined error can be larger than the individual therefore more relevant [135]. For example, it could be more prudent to combine the errors associated with the weighing of solvents in conjunction with dispensing formic acid.

The pipette was specified to have a systematic error of < 0.8% and a random error of < 0.3% for dispensing 1000 µL which would correlate to 3x SD. An assessment of the pipette by weighing 1000 µL of water determined the systematic error was -0.05% and the random error was 0.1% (SD) which would suggest the pipette is in line with the specifications. The repeatability of the pan balance was 0.01 g (3x SD) whilst the analytical balance was $5e^{-5}$ g (3x SD).

By assessing the propagation of errors, the most appropriate approach would be to use multiplicative expressions, as shown in *Equation 28*, where a, b, c and d are measured variables and y is the final value. The equation can be rearranged to allow the determination of the errors associated with the formic acid mobile phase preparation. The sum of the random and systematic errors associated with the pipette and pan balance were determined to be <0.0013%, which would give a concentration of 0.10% ± 0.001% (*Figure 45*). However, the purity of the formic acid accounts for another error, which gives a maximum and minimum content of 0.101% and 0.097%. In order to make the model symmetrical, the levels should be

set to a minimum of 0.10% ± 0.003%. It is good working practice to use an additive in both the weak (aqueous) and strong (organic) solvents in reversed phase chromatography, and as such, should both be considered within the DoE.

$$\frac{\sigma_y}{y} = \sqrt{\frac{\sigma_a}{a}^2 + \frac{\sigma_b}{b}^2 + \frac{\sigma_c}{c}^2 + \frac{\sigma_d}{d}^2} \qquad \textit{Equation 28}$$

Random Error		
Pipette	0.3	%
Pan Balance	0.01	g

Variable	**Calculation**		
[FA]	0.001	0.1	%
$\sigma_{Numerator}$	$1 \times \frac{0.3}{100}$	0.003	g or mL
Numerator		1	g or mL
$\sigma_{Denominator/Denominator}$	$\sqrt{\frac{0.01}{999}^2 + \frac{0.003}{1}^2}$	0.003000	
Denominator	$999 + 1$	1000	g or mL
$\sigma_{Denominator}$	$\frac{\sigma_D}{D} \times D$	3.000017	g or mL
$\sigma_{C/C}$	$\sqrt{\frac{\sigma_N}{N}^2 + \frac{\sigma_D}{D}^2}$	0.004243	
C	0.001	0.1	%
σ_C	$\frac{\sigma_C}{C} \times C$	0.000424	%
Pipette Systematic Error	0.8 %	0.0008	%
Sum of random and systematic errors		0.001224	%
Purity of Formic Acid	98-100%		
Max	$0.1 + sum\ of\ errors \times 1.00$	0.101	%
Min	$0.1 - sum\ of\ errors \times 0.98$	0.097	%

Figure 45 Propagation of errors associated with preparing the formic acid mobile phase. N = numerator, D = denominator, C = concentration

The concentration of the formic acid can impact on pH, which can be critical for selectivity of ionisable species. Formic acid acts as a reasonable buffer as doubling the concentration of the acid hardly affects the pH. A separate experiment was performed which looked at the effect of using 0.05%, 0.10% and 0.15% v/v formic acid in the aqueous and organic components in order to rationalise the limits for the DoE. The pH determined in the aqueous was 2.89, 2.70 and 2.63, respectively, which was in close agreement with the expected values of 2.91, 2.73 and 2.65 (estimated by ChemBuddy). The delta values were determined using t_g^* and compared using %RSD and the difference between the maximum and minimum. The most affected variables were Δ(3,1) and Δ(14,13) (*Table 45*).

Table 45 Δt_g^* values associated with different concentrations of formic acid.

					Δtg*				
FA%	**Δ(3,1)**	**Δ(8a,1)**	**Δ(9,1)**	**Δ(10,9)**	**Δ(14,13)**	**Δ(15,13)**	**Δ(16,13)**	**Δ(24,13)**	**Δ(26,13)**
0.05%	0.000	-0.294	0.057	-0.026	0.017	0.054	-0.402	-0.257	-0.575
0.10%	0.006	-0.286	0.053	-0.024	0.013	0.051	-0.394	-0.253	-0.560
0.15%	0.008	-0.280	0.052	-0.022	0.010	0.048	-0.39	-0.251	-0.554
Diff	0.008	0.014	0.005	0.004	0.007	0.006	0.012	0.006	0.021
%RSD	90.504	-2.442	4.892	-9.228	25.589	6.011	-1.484	-1.304	-1.907

The limits for the concentration of formic acid in the aqueous or organic was debated between 0.1% v/v ± 0.005 or ±0.010. The data above in *Table 45* was used to aid this decision by determining the potential delta differences one could expect at different concentrations. The delta values were plotted against the concentration of formic acid, where the polynomial equation was used to determine y at specific formic acid concentrations (*Table 46*). The results indicate that the difference expected for most of the delta values would be relatively small, apart from Δ(3,1) and Δ(14,13). At 0.1% v/v ± 0.005, one could expect a difference of approximately 7 and 3% respectively, whilst at 0.1% v/v ± 0.010 a difference of approximately 15 and 5% respectively could be expected. As such, the limits for the concentration of formic acid in the aqueous and organic components should be 0.1% v/v ± 0.005 to minimise the sensitivity of the two most susceptible probes to changes in formic acid concentration.

Table 46 Polynominal equations for each Δt_g^* value in formic acid to determine the impact of formic acid concentration.

Δt_g^*	Polynomial Equation	Y=					Expected Difference			
		0.090%	0.095%	0.100%	0.105%	0.110%	0.090%	0.095%	0.105%	0.110%
Δ(3,1)	$-0.6457x^2+0.2091x-0.0088$	0.005	0.005	0.006	0.006	0.006	-15.287	-7.358	6.787	13.002
Δ(8a,1)	$-0.2743x^2+0.1947x-0.303$	-0.288	-0.287	-0.286	-0.286	-0.285	0.498	0.247	-0.242	-0.479
Δ(9,1)	$0.5473x^2-0.16x+0.0637$	0.054	0.053	0.053	0.053	0.053	1.053	0.501	-0.450	-0.848
Δ(10,9)	$-0.2392x^2+0.0916x-0.0304$	-0.024	-0.024	-0.024	-0.023	-0.023	1.953	0.951	-0.901	-1.751
Δ(14,13)	$0.1024x^2-0.0886x+0.021$	0.014	0.014	0.013	0.013	0.012	5.253	2.607	-2.568	-5.097
Δ(15,13)	$0.0213x^2-0.0656x+0.0574$	0.052	0.051	0.051	0.051	0.050	1.206	0.602	-0.600	-1.197
Δ(16,13)	$-0.7823x^2+0.2715x-0.4131$	-0.395	-0.394	-0.394	-0.393	-0.393	0.312	0.151	-0.141	-0.272
Δ(24,13)	$-0.49x^2+0.1627x-0.2644$	-0.254	-0.253	-0.253	-0.253	-0.252	0.275	0.133	-0.123	-0.236
Δ(26,13)	$-1.7193x^2+0.5528x-0.5982$	-0.562	-0.561	-0.560	-0.559	-0.558	0.404	0.194	-0.179	-0.342

Dwell volume is one of the most overlooked parameters when considering gradient chromatography. The dwell volume is the volumetric contribution from the point at which the solvents mix up to the head of the column. Isocratic chromatography is unaffected by the dwell volume as a constant mobile phase composition is used. However, as the proportion of solvents change in gradient chromatography, the dwell volume can play a pivotal role in selectivity [51]. The dwell volume of modern LC instrumentation can be as low as 100 µL up to roughly 500 µL, assuming a low volume mixer is in place, therefore the dwell volume was adjusted to compare the chromatographic results provided under these conditions. It is also a necessity to have larger mixers when TFA is employed in LC systems to produce a satisfactory baseline without oscillation due to poor mixing. This was performed by either having an isocratic hold before the gradient to recreate a larger dwell volume or a delayed injection, which was injected on the gradient to represent a smaller dwell volume.

A summary of the factorial design specification can be seen in *Table 47*, which will be applied to the formic acid peptide gradient using the three test mixtures described in *Section 2.10.3.* The experimental conditions and run order can be seen in *Table 48*. The original chromatographic conditions can be seen in *Section 2.10.4.*

Table 47 Summary of the robustness range required for each factor for the formic acid DoE study.

Parameter	-1 Level	0 Level	+1 Level
Temperature (°C)	38	40	42
Flow Rate (mL/min)	0.295	0.300	0.305
Systematic Shift in Gradient (%B)	-0.4	0.0	0.4
%FA in Aqueous	0.095	0.100	0.105
%FA in Organic	0.095	0.100	0.105
Dwell Volume Difference (µL)	100	300	500

Table 48 DoE conditions for the formic acid peptide gradient.

Exp No	Exp Name	Run Order	Column Temperature (°C)	Systematic Shift in Gradient (%B)	Flow Rate (mL/min)	Volume of Formic Acid in Aqueous (% v/v)	Volume of Formic Acid in Organic (% v/v)	Dwell Volume (µL)
1	N1	3	38	-0.4	0.295	0.105	0.105	500
2	N2	8	42	-0.4	0.295	0.095	0.095	500
3	N3	4	38	0.4	0.295	0.095	0.105	100
4	N4	9	42	0.4	0.295	0.105	0.095	100
5	N5	11	38	-0.4	0.305	0.105	0.095	100
6	N6	1	42	-0.4	0.305	0.095	0.105	100
7	N7	10	38	0.4	0.305	0.095	0.095	500
8	N8	7	42	0.4	0.305	0.105	0.105	500
9	N9	5	40	0.0	0.300	0.100	0.100	300
10	N10	6	40	0.0	0.300	0.100	0.100	300
11	N11	2	40	0.0	0.300	0.100	0.100	300

3.7.2.2 Ammonium Formate Method DoE Levels

The same levels and rationales for temperature, flow rate, initial %B concentration and dwell volume were applied to the ammonium formate DoE as those described in *Table 47.* However, in addition to these levels, the mobile phase preparation for the ammonium formate experiments was considered.

A similar approach was used as in the formic acid DoE which looked at the cumulative effect of mobile phase preparation. Both the ammonium formate and the solvents were weighed out, on the analytical balance with a random error of $5e^{-5}$ g (3x SD) and pan balance with a random error of 0.01 g (3x SD). The sum of the variances indicated a very low uncertainty for the ammonium formate content in both the A and B solvents, where the concentration would be 20 mM ± 0.0004 mM. This would be impractical to measure thus concentration should not be considered in the DoE.

At intermediate pH, the chromatography is more susceptible to subtle changes in the pH which could have profound effects on the retention of the peptides, where it could change the net charge of the peptides as well as alter the ionisation state of silanols. There were also concerns regarding the reproducibility from different batches with different histories (i.e. the length of time a bottle is open). The hygroscopicity of ammonium formate was assessed under artificially high humid conditions which saw both ammonium formate and acetate increase in mass as water was absorbed (*Section 3.5.1.1*). A second study was conducted where 1.26 g of ammonium formate was dispensed into scintillation vials, where one was capped and the other left exposed under standard conditions in the laboratory. The capped vial increased by 0.79% in weight whilst the uncapped increased by 1.59% in 24 hours. The two vials were then made up to 200 mM solutions where the pH was measured. The electrode was calibrated using pH 7.00 and 2.00 calibrants. The pH of the capped solution was 6.44 whilst the uncapped solution was lower at 6.25. It was hypothesised that the loss in pH could be due to loss of ammonia. Carefully stored ammonium formate should be used to avoid such a shift in pH.

The reproducibility of different batches of ammonium formate (n=6) with different histories were assessed in both Shimadzu and Novo Nordisk. The pH of 16 solutions of 200 mM ammonium formate was measured with an average response of 6.45 (95% CI 6.42-6.47). The solutions were then diluted to 20 mM and measured again with an average response of 6.30 (95% CI 6.25-6.35). An additional study looked at the repeatability of pH measurements, where three readings were recorded. The average pH for a 200 mM solution (n=27) was 6.43 (95% CI 6.40-6.46), whilst a 20 mM solution (n=17) was 6.31 (95% CI 6.28-6.34). These results were in keeping with the above results and suggest that the batch of ammonium formate does not seem critical, however, being exposed to the atmosphere would be critical.

It was noted the measured pH values for 200 mM and 20 mM solutions were different from the predicted values in *Figure 46*, which suggested the solutions between 10-200 mM should have a pH of 6.5. The pH was mostly affected by low concentrations of buffer (i.e. 0.1 mM had a pH of 6.69). Thus, it was decided to measure the pH for 15 – 25 mM solutions in 5 mM intervals. The results were similar to those above where there was a decrease of approx. 0.11 pH units between the stock solution and the 15-25 mM solutions (*Table 49*). The pH for the 15-25 mM were all very similar, thus corroborating pH should be considered in the DoE, and not buffer concentration.

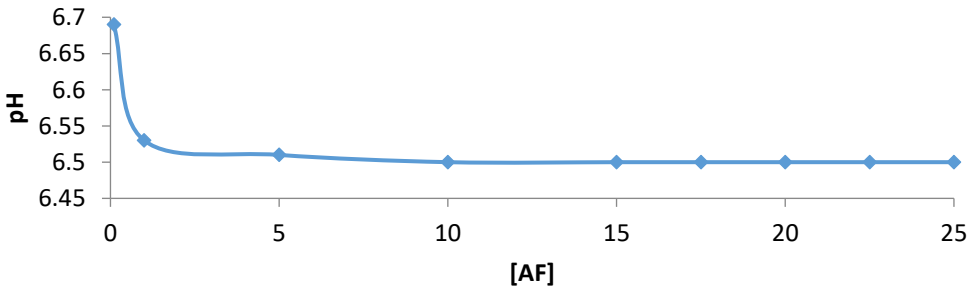

Figure 46 Plot of predicted pH against ammonium formate concentration (mM).

Table 49 Measured pH of different concentration ammonium formate solutions.

Concentration (mM)	pH Range (n=3)	Average pH
200	6.39-6.42	6.41
25	6.29-6.32	6.31
20	6.28-6.31	6.30
15	6.28-6.3	6.29

The level for the DoE should be set to 6.39 to 6.51, as the 99% CI based on the n=27 results above should expect a value between 6.35-6.51, whilst the 99% CI based on the n=16 results should expect a value between 6.39-6.50. If the pH is outside of this interval there is a problem with the stock solution, such as a loss of ammonia or formic acid.

The content of acetonitrile in the B solvent had quite wide levels in the original DoE, however, preparations based on weight is more accurate than volume therefore the limits should be reduced to accommodate the greater accuracy. Originally, the B solvent contained 90% acetonitrile, however, it was decided to reduce the concentration to 80% in order to reduce any influence from poor mixing. At 90%, a turbid solution formed, which was improved by stirring and slight heat. However, this could lead to potential robustness issues if the solution wasn't properly mixed, thus the concentration was lowered. The chromatography was assessed using either 20 mM ammonium formate (native pH) in MeCN / H_2O (90:10 w/w) or (80:20 w/w). Selectivity was maintained when the gradient was adjusted using *Equation 13.* The accumulation of errors would suggest very small deviations for acetonitrile (density 0.786 g/cm^3) where the concentration is 80 ± 0.01% (*Figure 47*). In order to see an effect, the levels should be set to 80 ± 0.1%.

Random Error		
Analytical balance	0.00005	%
Pan balance	0.01	g

Variable	**Calculation**		
[MeCN]	$\frac{628.8/0.786}{200 + 628.8/0.786}$	80	%
$\sigma_{\text{Numerator}}$	$\sqrt{\frac{0.01}{0.786}^2}$	0.01272265	mL
Numerator		800	mL
$\sigma_{\text{Denominator/Denominator}}$	$\sqrt{\frac{0.01^2}{100} + \frac{0.01^2}{100} + \frac{0.01}{628.8}^2}$	0.00014231	
Denominator	$200 + \frac{628.8}{0.786}$	1000	mL
$\sigma_{\text{Denominator}}$	$\frac{\sigma_D}{D} \times D$	0.14231274	mL
$\sigma_{\text{C/C}}$	$\sqrt{\frac{\sigma_N}{N}^2 + \frac{\sigma_D}{D}^2}$	0.00014320	
c	0.8	80	%
σ_{C}	$\frac{\sigma_C}{C} \times C$	0.01146	%

Figure 47 Propagation of errors associated with preparing the ammonium formate mobile phase. N = numerator, D = denominator, C = concentration

A summary of the factorial design specification can be seen in *Table 50*, which will be applied to the ammonium formate peptide gradient using the three test mixtures described in *Section 3.6.5*. The experimental conditions and run order can be seen in *Table 51*. The original chromatographic conditions can be seen in *Section 2.9.*

Table 50 Summary of the robustness range required for each factor.

Parameter	-1 Level	0 Level	+1 Level
Temperature (°C)	38	40	42
Flow Rate (mL/min)	0.295	0.300	0.305
Systematic Shift in Gradient (%B)	-0.4	0.0	0.4
pH of the Stock Solution	6.39	6.45	6.51
Concentration of MeCN in the B Solvent (%)	79.9	80.0	80.1
Dwell Volume Difference (µL)	100	300	500

Table 51 DoE conditions for the ammonium formate peptide gradient.

Exp No	Exp Name	Run Order	Column Temperature (°C)	Systematic Shift in Gradient (%B)	Flow Rate (mL/min)	pH of 200 mM Stock Solution	MeCN (w/w) Composition in the B Line	Dwell Volume (µL)
1	N1	3	38	-0.4	0.295	6.51	80.1	500
2	N2	8	42	-0.4	0.295	6.39	79.9	500
3	N3	4	38	0.4	0.295	6.39	80.1	100
4	N4	9	42	0.4	0.295	6.51	79.9	100
5	N5	11	38	-0.4	0.305	6.51	79.9	100
6	N6	1	42	-0.4	0.305	6.39	80.1	100
7	N7	10	38	0.4	0.305	6.39	79.9	500
8	N8	7	42	0.4	0.305	6.51	80.1	500
9	N9	5	40	0	0.300	6.45	80.0	300
10	N10	6	40	0	0.300	6.45	80.0	300
11	N11	2	40	0	0.300	6.45	80.0	300

3.7.3 DoE Results

Both DoE's contained three repeat experiments named N9-11, which had the 0 level parameters and were randomly allocated in the run order (*Table 48* and *Table* 51). Ideally three different mobile phases should be created for each method, however, there were practical constraint in the number of solvent lines. This meant the same batch of formic acid or ammonium formate mobile phase was utilised for N9-11 during the main study, and a repeat study of just methods N9-11 with different batches of solvent was conducted post DoE. The results for the same batch and the different batches all matched up but only the different batches of solvents were included in the results for the DoE.

All the delta values used in the Peptide RPC Column Characterisation Protocol were recorded in *Table 52* and *Table* 53 for the different. The robustness of each delta value was assessed by fitting a first order polynomial model to the data obtained using Modde. The delta values used to build the Peptide RPC Column Characterisation Protocol in formic acid are Δ(8a,1), Δ(9,1), Δ(14,13), Δ(16,13) and Δ(26,13). The delta values measured in ammonium formate are Δ(3,1), Δ(9,1), Δ(10,9), Δ(15,13), Δ(24,13) and Δ(26,13). The delta values which are not used to characterise the stationary phases were also included. As those delta values were in the test mixtures, it is important to assess the robustness so as to avoid interference with any critical peptide.

Table 52 Input Δt_g^* results under various experimental conditions in formic acid to invesitgate the robustness of the methodology in Modde.

Exp Name	Run Order	T	%B	F	%FA A	%FA B	Vd	Δ(3,1)	Δ(8a,1)	Δ(9,1)	Δ(10,9)	Δ(14,13)	Δ(15,13)	Δ(16,13)	Δ(24,13)	Δ(26,13)
N1	3	38	-0.4	0.295	0.105	0.105	500	0.006	-0.289	0.054	-0.023	0.013	0.050	-0.395	-0.248	-0.566
N2	8	42	-0.4	0.295	0.095	0.095	500	0.004	-0.285	0.055	-0.024	0.013	0.050	-0.395	-0.252	-0.569
N3	4	38	0.4	0.295	0.095	0.105	100	0.006	-0.291	0.055	-0.023	0.013	0.052	-0.394	-0.247	-0.567
N4	9	42	0.4	0.295	0.105	0.095	100	0.005	-0.284	0.055	-0.024	0.013	0.050	-0.394	-0.251	-0.566
N5	11	38	-0.4	0.305	0.105	0.095	100	0.006	-0.289	0.054	-0.023	0.012	0.048	-0.396	-0.250	-0.568
N6	1	42	-0.4	0.305	0.095	0.105	100	0.004	-0.284	0.054	-0.024	0.013	0.049	-0.395	-0.254	-0.568
N7	10	38	0.4	0.305	0.095	0.095	500	0.005	-0.291	0.055	-0.023	0.013	0.049	-0.398	-0.251	-0.571
N8	7	42	0.4	0.305	0.105	0.105	500	0.005	-0.285	0.053	-0.023	0.013	0.049	-0.393	-0.252	-0.565
N9	5	40	0.0	0.300	0.100	0.100	300	0.006	-0.286	0.054	-0.023	0.012	0.049	-0.395	-0.250	-0.564
N10	6	40	0.0	0.300	0.100	0.10	300	0.005	-0.286	0.054	-0.023	0.013	0.049	-0.395	-0.250	-0.568
N11	2	40	0.0	0.300	0.100	0.100	300	0.005	-0.286	0.054	-0.023	0.013	0.049	-0.395	-0.251	-0.567
							Max	0.006	-0.284	0.055	-0.023	0.013	0.052	-0.393	-0.247	-0.564
							Min	0.004	-0.291	0.053	-0.024	0.012	0.048	-0.398	-0.254	-0.571
							Deviation Between Max and Min (%)	52.166	-2.601	2.705	-4.196	8.348	7.817	-1.135	-2.528	-1.259

Table 53 Input Δt_g^* results under various experimental conditions in ammonium formate to invesitgate the robustness of the methodology in Modde.

Exp Name	Run Order	T	%B	F	pH	[MeCN]	Vd	Δ(3,1)	Δ(8a,1)	Δ(9,1)	Δ(10,9)	Δ(14,13)	Δ(15,13)	Δ(16,13)	Δ(24,13)	Δ(26,13)
N1	3	38	-0.4	0.295	6.51	80.1	500	0.002	-0.089	0.061	-0.025	0.011	0.050	-0.271	-0.181	-0.304
N2	8	42	-0.4	0.295	6.39	79.9	500	0.052	-0.115	0.108	-0.040	0.012	0.056	-0.314	-0.214	-0.353
N3	4	38	0.4	0.295	6.39	80.1	100	0.002	-0.084	0.062	-0.025	0.011	0.050	-0.271	-0.181	-0.306
N4	9	42	0.4	0.295	6.51	79.9	100	0.055	-0.112	0.108	-0.037	0.011	0.056	-0.312	-0.211	-0.343
N5	11	38	-0.4	0.305	6.51	79.9	100	0.048	-0.110	0.110	-0.037	0.011	0.056	-0.312	-0.209	-0.346
N6	1	42	-0.4	0.305	6.39	80.1	100	0.000	-0.091	0.056	-0.024	0.011	0.049	-0.276	-0.187	-0.311
N7	10	38	0.4	0.305	6.39	79.9	500	0.051	-0.113	0.109	-0.039	0.013	0.057	-0.313	-0.209	-0.349
N8	7	42	0.4	0.305	6.51	80.1	500	0.003	-0.084	0.063	-0.025	0.010	0.047	-0.268	-0.182	-0.299
N9	5	40	0	0.3	6.45	80.0	300	0.003	-0.076	0.063	-0.026	0.009	0.047	-0.265	-0.178	-0.294
N10	6	40	0	0.3	6.45	80.0	300	0.003	-0.074	0.063	-0.027	0.009	0.048	-0.264	-0.178	-0.294
N11	2	40	0	0.3	6.45	80.0	300	0.003	-0.076	0.063	-0.025	0.009	0.048	-0.267	-0.180	-0.296
							Max	0.055	-0.074	0.110	-0.024	0.013	0.057	-0.264	-0.178	-0.294
							Min	0.000	-0.115	0.056	-0.040	0.009	0.047	-0.314	-0.214	-0.353
							Deviation Between Max and Min (%)	-	-36.267	94.757	-40.228	48.567	22.045	-15.888	-16.593	-16.874

The results from the Modde model, which are based on multiple linear regression (MLR), can be seen in *Figure 48-Figure* 54*.* The Summary of Fit graphs provides an overview as to the validity of the model and how well the model is described (*Figure 48Figure* 49 for the formic acid results and *Figure 50Figure* 51 for the ammonium formate).

The quality of the model is measured using a regression coefficient from fitting the model (R^2) and one from a cross validation of the model (Q2) [136, 137]. The cross validation is an iterative process which removes each experiment once to observe its contribution to the model fit. For a good model, both values are close to 1. However, in a robustness evaluation an ideal outcome would be a for a poor model, i.e. low R^2 and Q2 values. Model validity is another measure used to determine the fit of the model, where a value of 1 indicates a perfect fit and a value of less than 0.25 suggests a significant error with the model. Finally, reproducibility is an observation of the variation caused by pure error compared to the total variation provided by the response. A value of 1 suggests there is no random error associated with the measurements whilst a value of less than 0.5 indicates large error and poor experimental control with significant noise.

The average R^2 and Q2 for the delta values in formic acid were 0.761 (standard deviation SD 0.208) and -0.133 (SD 0.151), respectively, whilst for the ammonium formate delta values, R^2 and Q2 measured 0.750 (SD 0.080) and -0.200 (SD 0.000), respectively. The centre point experiments (N9-11) provide an indication into the reproducibility of the procedure, where the average difference for the delta probes was 0.001 (ranged from 0.000 to 0.004 for the relevant delta values).

The parameters were assessed using residual normal probability plots where the results were all within the ±2 bracket, where any variable outside that bracket is seen as atypical (data not shown).

The reproducibility results (yellow bar) were excellent for all the responses, with results ranging between 0.98 and 1.00, indicating the methodology has little pure

error associated with it. The result gives an early indication that the Peptide RPC Column Characterisation protocol should be robust.

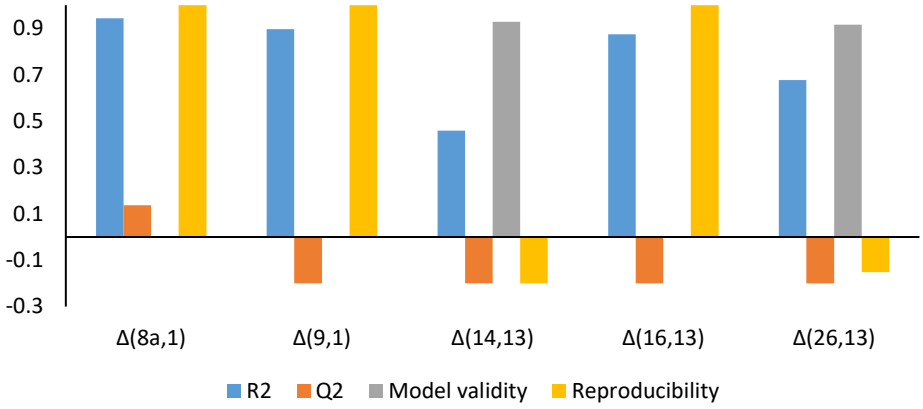

Figure 48 Summary of fit for Δ(8a,1), Δ(9,1), Δ(14,13), Δ(16,13) and Δ(26,13) in formic acid.

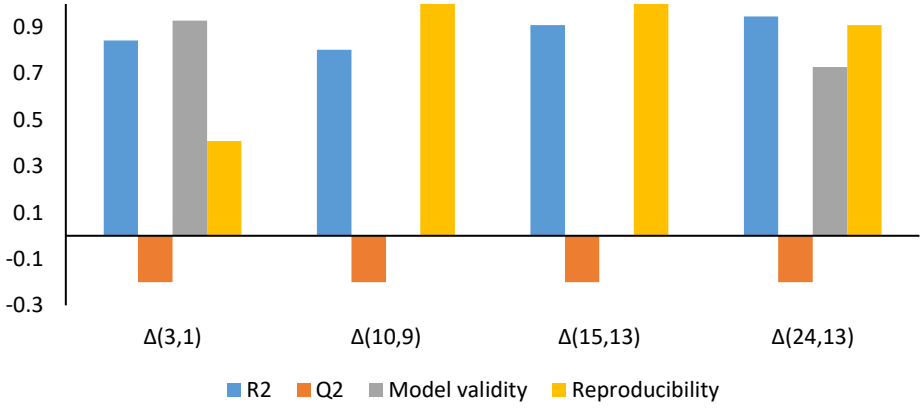

Figure 49 Summary of fit for Δ(3,1), Δ(10,9), Δ(15,13), and Δ(24,13) in formic acid.

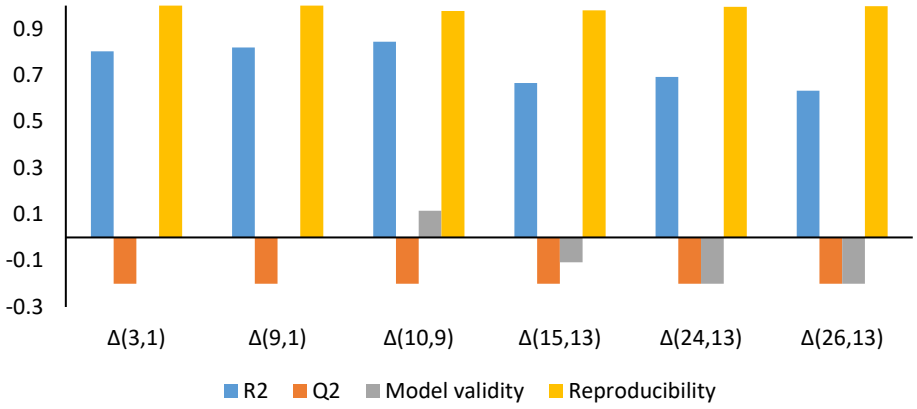

Figure 50 Summary of fit for Δ(3,1), Δ(9,1), Δ(10,9), Δ(15,13), Δ(24,13) and Δ(26,13) in ammonium formate.

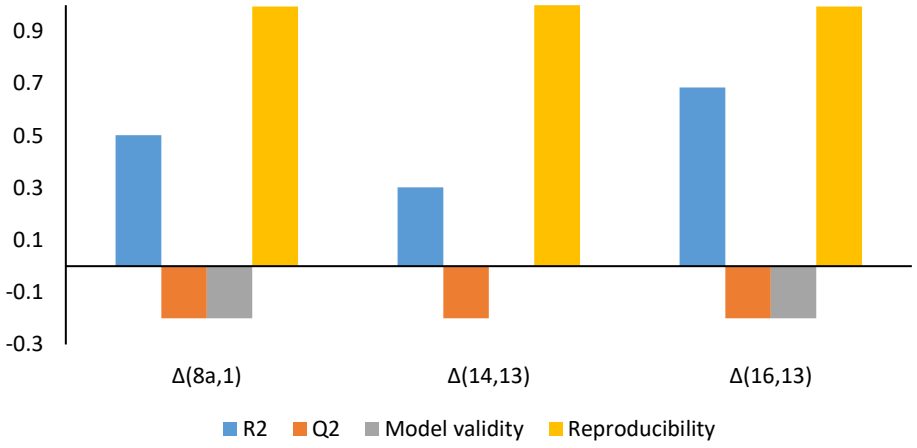

Figure 51 Summary of fit for Δ(8a,1), Δ(14,13) and Δ(16,13) in ammonium formate

Another stronger tool for evaluating the factorial design results is by confidence plots which display regression coefficients and confidence intervals (*Figure 52-Figure* 55). The coefficients are scaled and centred to allow the coefficients to be comparable. The confidence intervals are indicative of the significance of the coefficient, where an error bar which crosses zero is an insignificant parameter. The height of the bar indicates its degree of influence. A narrow confidence interval suggests a greater certainty for the result.

Temperature had no discernible effect on any of the responses in ammonium formate and the majority in formic acid, however, there was a statistical response

for Δ(8a,1) and Δ(16,13) in formic acid (*Figure 52*). The height of the bars however would indicate that the practical significance on these two delta results would be minimal. Although for these probes it has a minimal effect, it is recommended that the actual temperature of the column is determined, as it is known that the column oven design, oven manufacturer and even column position within the oven can change the actual temperature within the column.

The responses in formic acid and ammonium formate were all unaffected by the systematic shift in the gradient (*Figure 52-Figure* 55). This systematic shift in the gradient assumes the same degree of error will apply across the length of the gradient.

A change of flow rate also corresponds to a change in gradient slope. Flow rate only presented a small statistical response for Δ(9,1) in formic acid (*Figure 52*), whilst all other responses in both ammonium formate and formic acid were unaffected. Similar to temperature, the actual practical effect of this variable would be quite minimal, thus this parameter can be assumed to be robust within the methodology.

Dwell volume was statistically insignificant for all responses in either mobile phase, indicating this variable does not impact on the robustness of either the formic acid or ammonium formate gradient. This is to a large extent due to the normalisation of the retention times which removes the effect of dwell volume, allowing direct comparison between different instrumentation. The dwell volume range selected for evaluation (100-500 µL) should cover UHPLC instrumentation.

Differences in formic acid levels could impact on the robustness of the protocol as different levels would result in a different pH which would affect the overall net charge on the peptides. However, differences in formic acid volume were observed to be insignificant, the Δ(9,1) and Δ(16,13) values exhibited a very small statistical significance but this was deemed to be of little practical relevance (*Figure 52*). It is recommended that formic acid volumes should be dispensed volumetrically from a pre-calibrated pipette which is checked each time a solvent is prepared to ensure the integrity of the chromatographic results. Although there would be a greater

accuracy in weighing formic acid, it was deemed unnecessary by these results which demonstrated the pipette was sufficiently accurate and weighing could reduce the practicality of the method.

The stationary phase environment at intermediate pH is somewhat unpredictable due to the range of pK_a values for the residual silanols [138-140]. It is believed the majority of silanols should be ionised at pH 6.45 (the native pH of ammonium formate), however, this uncertainty can potentially lead to a greater degree of variation in results and hence can contribute to the lack of robustness. The ammonium formate can also be a source of error, where the age of the buffer, its storage environment and its resultant pH range were investigated. The pH was measured for 16 different 200 mM solutions where the average pH was 6.45 (SD 0.03). The levels in the DoE (pH 6.45 ±0.06) were set based on a 99% CI based on triplicate determinations of the pH. The age of the ammonium formate did not appear to greatly affect the overall pH of the solution, where the pH measured was within the range tested in the DoE. There was, however, a change in pH based on salts which were inappropriately stored, which resulted in a lower pH for a poorly capped container which indicates a loss of ammonia. This could impact on the degree of silanol ionisation and hence affect retention and the delta values. Ideally, the formate salt should be stored in a desiccator to reduce water uptake but firmly replacing the cap should reduce the risk of ammonia loss.

The responses in ammonium formate were all stable within the upper and lower pH limits in the DoE, with no statistical significance (*Figure 54*). The pH of the stock buffer solution should be measured using appropriately calibrated standards to ensure the pH is within this range to ensure the integrity of the protocol. It is also advised that if the ammonium formate exhibits any considerable signs of hygroscopicity in addition to changes in pH then it should not be used. Alternatively, storing the ammonium formate in a desiccator would remove such issues [100].

To avoid microbial growth which could contaminate the LC system and potentially block the column inlet frit, causing split peaks and higher back pressures, it is recommended to limit the storage of stock buffer solution to 4 weeks at 5 °C.

Experience has shown that the same chromatographic results can be obtained from the stock solution after this storage period.

The selectivity of Δ(3,1), Δ(9,1), Δ(10,9) and Δ(24,13) were particularly susceptible to the change in acetonitrile content in the B solvent in the ammonium formate gradients (*Figure 54*). The effect was actually significant enough that it would have practical relevance, unlike previous variables, and thus warranted further investigation.

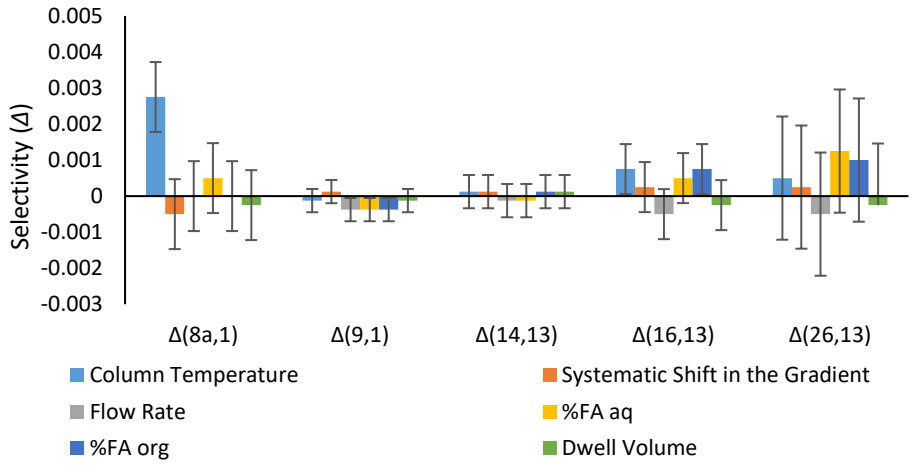

Figure 52 Confidence plots for Δ(8a,1), Δ(9,1), Δ(14,13), Δ(16,13) and Δ(26,13) with confidence intervals under formic acid conditions

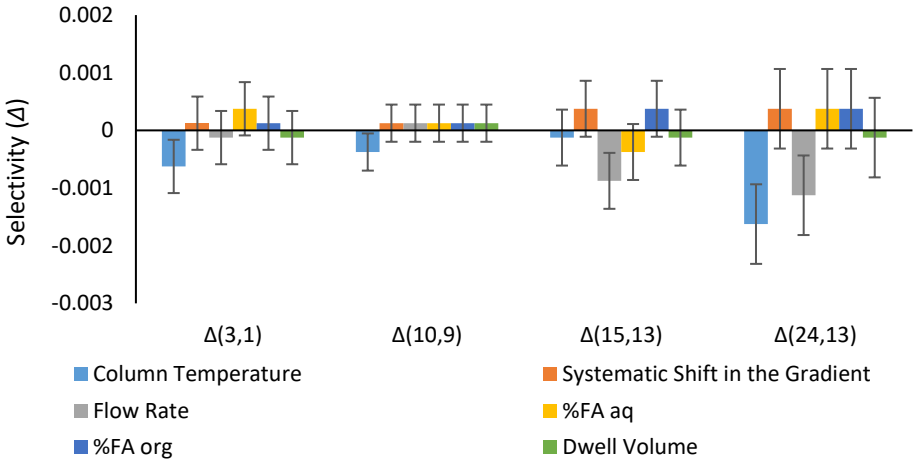

Figure 53 Confidence plots for Δ(3,1), Δ(10,9), Δ(15,13), and Δ(24,13) with confidence intervals under formic acid conditions

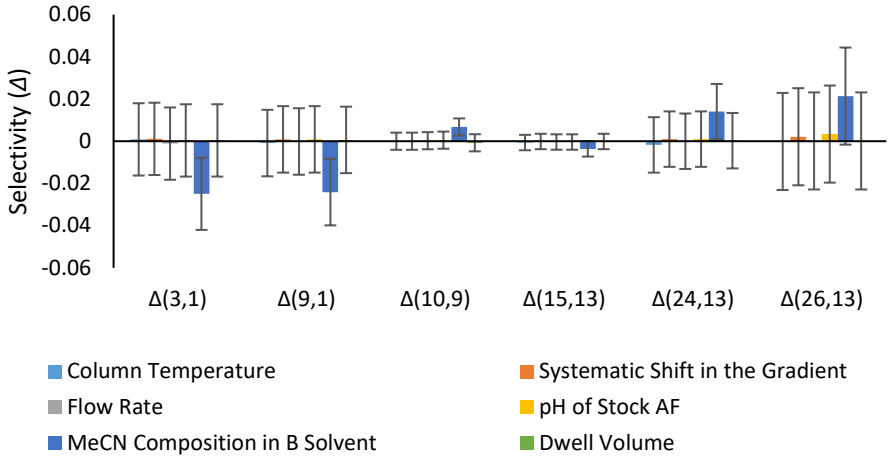

Figure 54 Confidence plots for Δ(3,1), Δ(9,1), Δ(10,9), Δ(15,13), Δ(24,13) and Δ(26,13) with confidence intervals under ammonium formate conditions

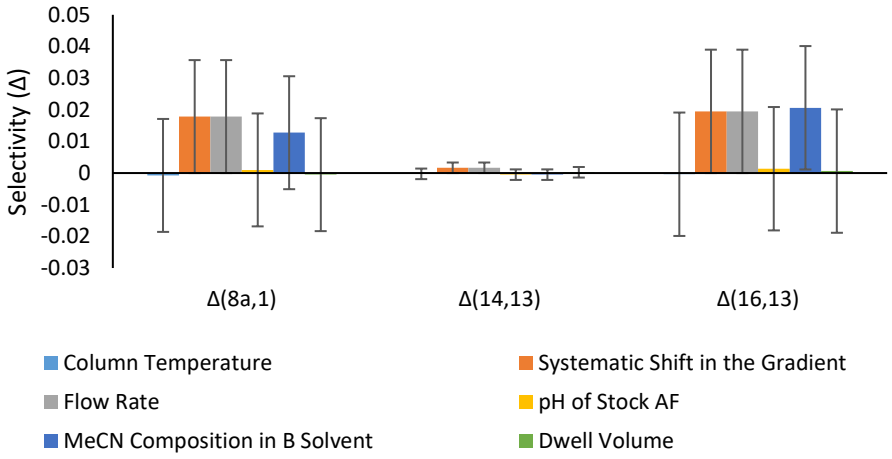

Figure 55 Confidence plots for Δ(8a,1), Δ(14,13) and Δ(16,13) with confidence intervals under ammonium formate conditions

The data was placed in a biplot (*Figure 56*) in order to ascertain the degree of scatter that was produced from the robustness data. The results revealed two distinct groups. The results from only formic acid were evaluated using PCA, which showed a small cluster of points, whilst a similar plot containing only ammonium formate data possessed the two distinct groups. This indicated that the results in *Figure 56* were related to the intermediate pH conditions. The only common theme to the smaller group containing N2, N4, N5 and N7 was the -1 level for the acetonitrile content in the B solvent (i.e. corresponds to a loss of acetonitrile).

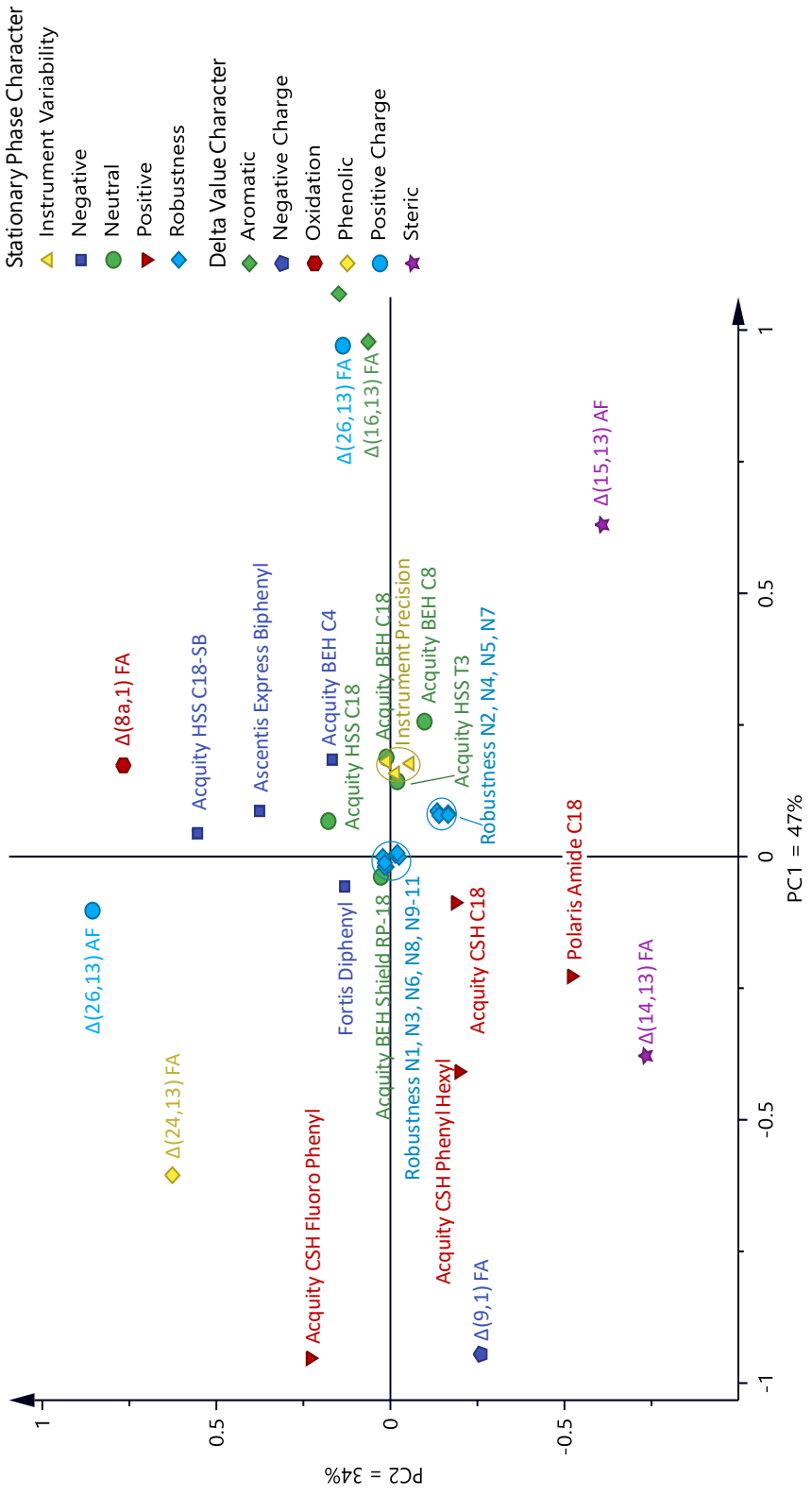

Figure 56 Biplot to demonstrate the scatter produced from the robustness and instrument precision

The results suggested that a loss of acetonitrile is critical. It was therefore decided to conduct an evaporation study to ascertain what could be reasonably lost via the LC solvent caps in the mobile phase reservoirs (*Table 54*). An Agilent Valve cap (Waldbronn, Germany) and a SCAT safety cap (Mörfelden-Walldorf, Germany) were compared against a closed cap used for solvent storage. There was 0.00% loss in weight for the closed cap over 30 days, suggesting acetonitrile is not lost during storage, however, it was calculated that losses of 0.04 and 0.03% for the Agilent and SCAT caps, respectively, could be expected per day, which could prove to be a practical problem. Although the loss of acetonitrile would be significantly less with either cap and valve compared to no such measure, the small loss in organic could still potentially cause large problems with consistency in results which would affect robustness.

Table 54 Evaporation of acetonitrile study over 36 days using different types of solvent caps

	Loss after 36 days		**Loss per day**	
	G	**%**	**g**	**%**
Agilent	5.51	1.26	0.15	0.04
SCAT	4.67	1.08	0.13	0.03
Capped	0.00	0.00	0.00	0.00

In order to combat this the approach was taken to change the B solvent from 20 mM ammonium formate in MeCN/H_2O (80:20 w/w) to 100% MeCN. The gradient was adjusted accordingly to achieve the same volume fraction of MeCN and compared against the original method, with similar chromatographic results, regardless of the reduced buffer concentration in the B solvent (the ammonium formate concentration is reduced from 18 to 12 mM during the part of the gradient where peptides typically elute).

3.7.4 Reduced Intermediate Precision

Intermediate precision is a measure of the degree of scatter for a set of conditions which have been applied to different instrumentation to account for within laboratory variation. This parameter allows one to analyse the effect of different analysts, days, solvents and instrumentation. In this study, only the instrument to instrument variation was established.

An Acquity HSS C18 was used to assess the intermediate precision using formic acid first then ammonium formate. The instruments used were a Waters H Class (quaternary, low pressure mixing system), Waters I Class and Agilent 1290 (both binary, high pressure mixing systems). The same mobile phase, stationary phase and peptides standards were used on all three systems.

The delta values were added to the database and a biplot produced (*Figure 56*) after centring the data. The three instruments were clustered together, and circled using a 95% CI, indicating a high reproducibility of the Peptide RPC Column Characterisation Protocol between instrumentation.

The Peptide RPC Column Characterisation Protocol was assessed with different column ovens which can create large differences in selectivity due to the actual temperature exposed to the stationary phase. The clustered results are encouraging for achieving reproducible results within different laboratories and instruments.

3.7.5 Column Batch to Batch Variation

The column batch to batch variability was assessed using six Ascentis Express C18 columns. All columns differed by silica, whilst three columns contained the same batch of silane with three additional silane batches used for the remaining columns (*Table 55*).

All batch to batch columns were tested using the new protocol with the reduced number of probes (i.e. removal of probes susceptible to changes in MeCN) on the same occasion and mobile phases to remove their contribution to any variability.

The batch to batch observations can be seen encircled within the biplot (*Figure 57*) where the scatter seen is due to the batch to batch variation as the data was collected on the same day using the same instrument and solvents to eliminate their contribution from the results. The results are also in keeping with previous batch to batch studies performed on other columns using various protocols [95, 141-146]. This highlights that any deviation between columns within the biplot is caused by selectivity differences, thus it is feasible to distinguish stationary phases which are chromatographically similar or dissimilar using this approach.

Table 55 Column batch information for the batch to batch study

Column	Pore Size (Å)	Particle Size (µm)	Dimensions (mm)	Batch	Serial Number	Silane
1	90	2.7	150 x 2.1	S17018	USWM003480	1
2	90	2.7	150 x 2.1	S16105	USWM003472	1
3	90	2.7	150 x 2.1	S16104	USWM003468	1
4	90	2.7	150 x 2.1	S17138	USWM003477	2
5	90	2.7	150 x 2.1	S18095	USWM003488	4
6	90	2.7	150 x 2.1	S18058	USWM003484	3

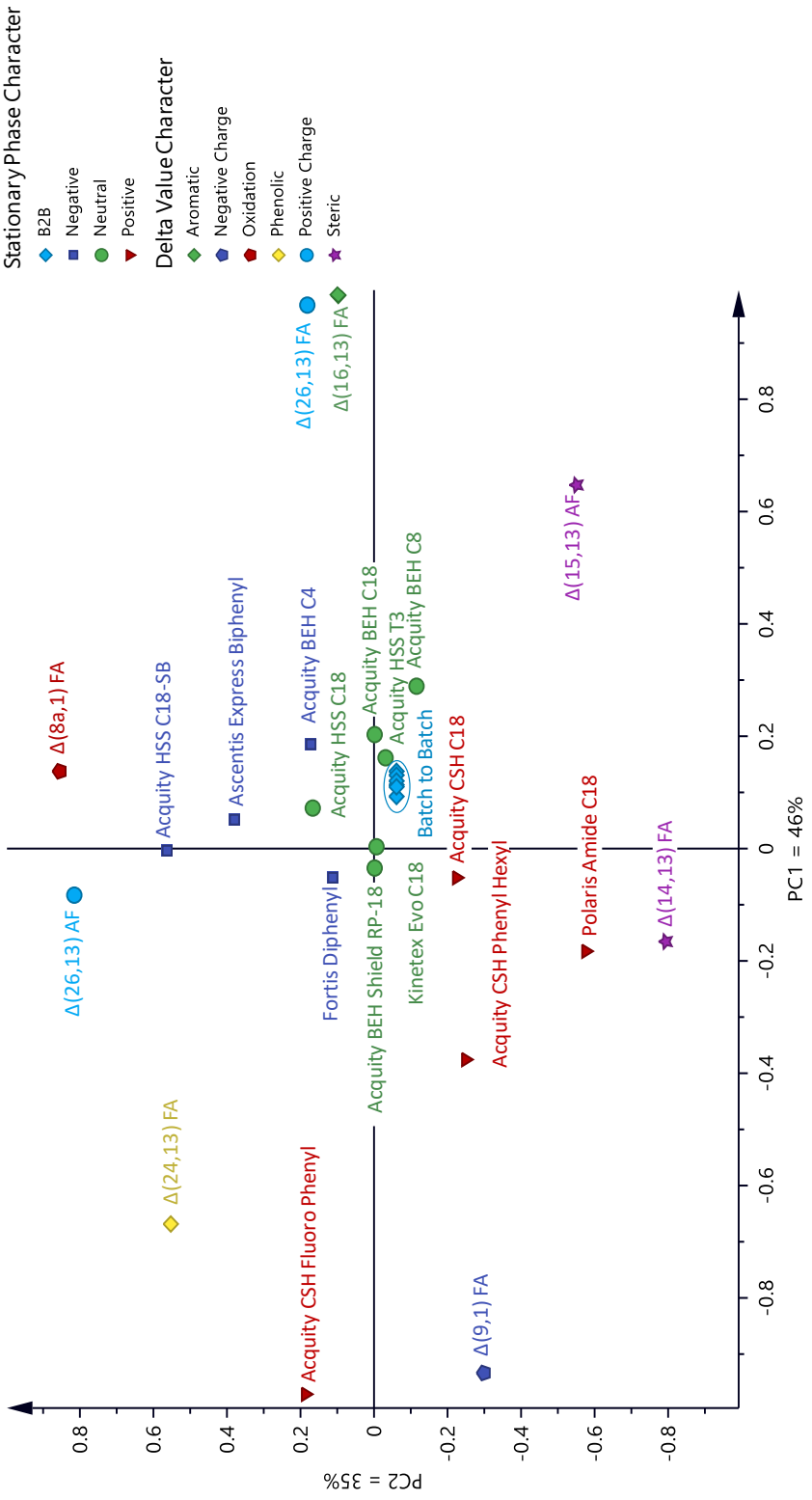

Figure 57 Biplot of the Peptide RPC Column Characterisation Protocol chromatographic parameters and the intermediate precision for different batches of stationary phases with a 95% CI.

3.7.6 Analyte Loading Studies

Poor peak shape of ionisable species is often attributed to interactions with deprotonated silanols, where ionised basic species form electrostatic interactions which leads to band broadening and tailing. However, modern type B silicas are often designed to reduce these electrostatic interactions by using extensive endcapping on the stationary phase, which suggests the number of silanols is often reduced, and low metal content of the new generation silica, yet poor peak shape is still observed.

Chromatographic efficiency can be highly susceptible to overloading of compounds which contributes to poor peak shape. The permissible load before chromatographic performance is affected is often substantially lower for peptides and protein separations. A study has shown that the basic peptide Angiotensin II had approximately 60 times lower column saturation capacity than a non-ionogenic compound [116, 147], which led to significantly more tailing with increased loading. This is often attributed to residual silanol interactions, however, work by Buckenmaier *et al*. suggested that silanol overload could be more problematic for older, type A silica which is typically impure, rather than modern type B silica. Buckenmaier compared the loading response given by alkyl silica columns (i.e. contain silanol groups) against polymer columns (i.e. no silanol groups present) which allowed the authors to assess the silanophilic interactions. They established that cation exchange sites were present at pH 7.0 to interact with basic solutes, despite a lack of silanols on the polymeric phases. The basic solutes were retained by a hydrophobic mechanism at low and high pH, where the basic solute was ionised at low pH, but the column sites uncharged, whilst at high pH, the basic solute was unionised whilst the column sites were charged.

A stock solution of [D-Asp3]-Bovine GLP-2 (1-15) (1 mg/mL, Peptide Number 3) underwent a series of dilutions using DMSO/H_2O (80:20 v/v). Each solution was reproducibly injected onto the Kinetex Evo C18 (150 x 2.1 mm, 2.6 µm) using the formic acid gradient chromatographic conditions. The low ionic strength of formic

acid is a worst-case scenario; thus, it was selected to observe the effects of loadability and overloading.

Eight dilutions were made in total (*Figure 58*) with the resulting chromatograms overlaid. The hydrophilic peptide, which has a net charge of +1.2 at pH 2.5, displayed the characteristic “shark fin” peak shape with increased load for a positively charged species in acidic conditions i.e. a typical right-angled front and extreme tailing. The time for the apex of the peak, which is used to measure the retention time, decreased with increased load on the column and as such, would affect the normalised retention times used to calculate delta values. The degree to which this effect occurs could be different for each peptide, hence the load for each peptide must be well described in order to maintain consistent delta values. The peak shape for this study is not of critical concern as it is the retention time which must be consistent, hence the necessity to keep the load constant. A well-defined load is necessary to obtain reproducible retention times in the protocol. When devising chromatographic methods, it would be crucial to select mobile phases which can provide better peak shape, with the biopharmaceutical industry typically utilising phosphate salt-based systems.

The loading profile could also be different depending on the type of stationary phase used. For example, the Acquity CSH range of stationary phases were optimised to provide improved peak shape and efficiency for basic species to provide linear isotherms, rather than typical Langmuir isotherm. Overloading behaviour is thought to be due to variations in the surface charge, where the balanced surface charge of the CSH range counteracts that issue to produce symmetrical, efficient peaks [117].

The sample solubility also is critical when it comes to sample load. The net charge of the hydrophilic peptides at pH 2.5 and 6.5 are +1.1 to +1.2 and -4.7 to -3.7, respectively. The hydrophobic peptides have a net charge of +2.2 at pH 2.5, whilst at pH 6.5 the net charge is 0.0. A pI of 0.0 may highlight potential solubility problems and the possibility of precipitation and clogging of the inlet frit. Pressure increases and decreased column performance were observed after prolonged

exposure to intermediate pH conditions. Replacement of the inlet frit and scanning electron microscopy proved that particulates had been deposited onto the frit. Hence, in order to minimise the likelihood of this happening the load of the peptides was reduced, and inline filters installed between the injector and the column.

The impurity observed after the tail of the main peak was only observed at high concentrations, thus efforts were not made to identify the peak, however the *m/z* was identical to the main peak (*m/z* 820).

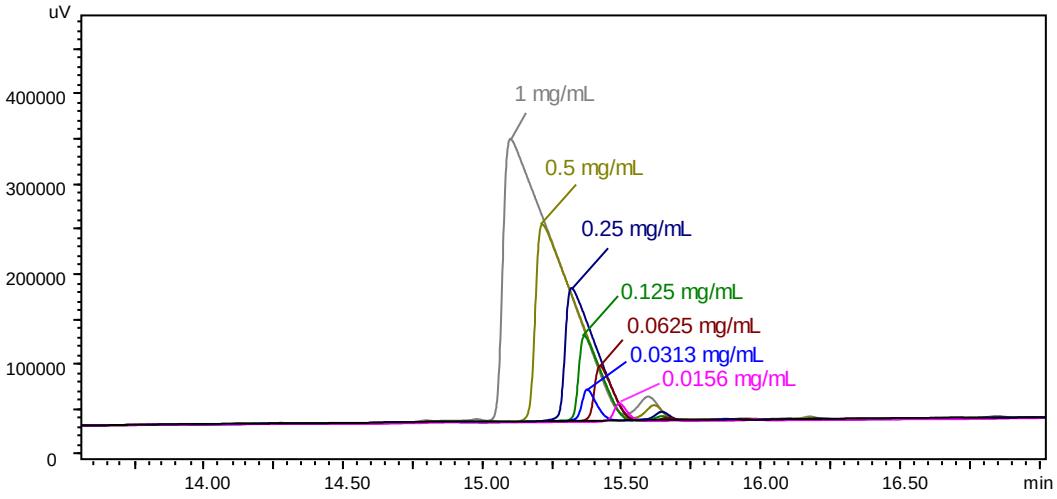

Figure 58 Loadability of the hydrophilic peptide [D-Asp3]-Bovine GLP-2 (1-15) on the Kinetex Evo C18 using formic acid Peptide RPC Column Characterisation Protocol conditions. Analyses were performed on the Nexera X2 coupled to the 2020 single quadrupole system. The formic acid conditions utilised a mobile phase of 0.1% formic acid in water and 0.1% formic acid in acetonitrile with 10-50%B over 40 minutes. Flow rate was 0.3 mL/min, column oven temperature was 40 °C, and detection was UV at 215 nm.

3.7.7 On-Column Degradation Studies

Conditions within the column (e.g. pH and temperature) can be a source of analyte degradation. It is also possible for analytes to undergo oxidation induced by metals adsorbed to the column. Thus, it was deemed appropriate to assess the test mixtures for any increases in impurities. A series of gradients were performed for all the test mixtures, which all possessed the same t_G (40 minutes) and %B/min change, however, an initial isocratic hold was utilised before the gradient of 0, 10,

20 and 30 minutes. The same approach was employed to monitor the on-column degradation reaction of a corticosteroid initiated by metal contamination of the RP column [92, 93].

The three peptide test mixtures were injected using the four different isocratic hold methods in both formic acid and ammonium formate on the Kinetex Evo C18. The normalised retention times (t_g^*), peak areas and heights were all consistent between the different methods and there were no additional peaks caused by degradation in the chromatograms. This is promising that the residency time on the stationary phase does not cause instability of the peptide probes.

3.7.8 Slow Equilibration

Marchand *et al*. observed that ionised solutes could have pronounced retention time drifts when switching from non-buffered solvents to low pH, buffered mobile phases [119]. This was not the case for non-ionised species, which were stable within the typical 10-20 column volumes. In comparison, the ionised species could take upwards of several hours to equilibrate. Marchand also stated the re-equilibration was substantially longer when converting from high to low pH. Their research suggested the re-equilibration was unaffected by volume, which is often considered the most important parameter, thus an increase in flow rate had little impact. They discovered time had greater importance, hence a column could be stored in the buffered mobile phase and the column would be equilibrated upon use. However, this could notably decrease the lifetime of the stationary phase by causing ligand cleavage. McCalley alternatively overcame slow-equilibration b flushing the stationary phase for 10-12 hours [48, 115].

The Marchand research group tested 19 stationary phases from eight different column manufacturers and found approximately 40% of phases tested exhibited slow equilibration for ionised species when tested between high and low pH [119]. The exact mechanism for this phenomenon is not known, but it is speculated that with the advent of modern silica with low surface charge, changes in pH can require

significant time to re-equilibrate which is displayed as retention drift for ionisable species. This may have a significant impact on the current research where it is expected some of the stationary phases in this study could have issues with re-equilibration.

To investigate the issue of slow equilibration, a selection of C18 type phases was assessed using the peptides as probes to determine any practical constraints for the Peptide RPC Column Characterisation protocol, which utilises both low and intermediate pH. The peptide test mixture was repeatedly injected on a C18 stationary phase using the formic acid gradient conditions with consistent results (*Figure 59*). The stationary phase was then exposed to the ammonium formate gradient conditions, which saw quick equilibration of the peptide mixture within duplicate injections, suggesting consistent results can be achieved when moving from low to intermediate pH conditions.

However, when the same column was then re-exposed to the formic acid gradient, it failed to yield results comparable to those prior to exposure to intermediate pH (slow reduction in retention – see *Figure 59(B)*). The retention times for all peaks had increased but were consistently decreasing in retention between injections.

Even overnight static equilibration in low pH conditions failed to restore the stationary phase to its original chromatographic retentivity (*Figure 59(C)*).

Although there are stationary phases which have been devised to combat this issue such as the Acquity CSH range of phases [117], there are a number of commercially available columns which do exhibit this phenomenon. Previous knowledge of these types of columns and demonstration in this study have shown that several of the new generation non-positive character columns exhibited this pronounced slow equilibration effect when moving from intermediate to low pH. As such, it is better to remove this issue than examine for it every time a new stationary phase is evaluated. Thus, this was removed as a potential problem by testing under low pH conditions initially, before testing at intermediate pH using ammonium formate in order to avoid any detrimental retention drifts.

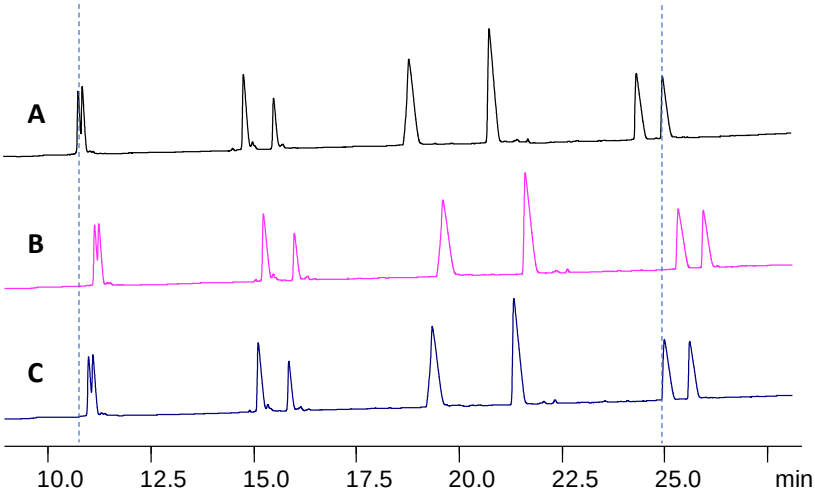

Figure 59 Chromatograms demosntrating the effect of slow equilibration. (A) the original chromatogram in formic acid prior to exposure to ammonium formate at intermediate pH, (B) re-evaluation of the same column in formic acid after exposure to intermediate pH, (C) re-evaluation after static equilibration in formic acid to attempt to restore the original chroamtography. Exact column details are not disclosed for confidential reasons. Analyses were performed on the Nexera X2 coupled to the 2020 single quadrupole system. The formic acid conditions utilised a mobile phase of 0.1% formic acid in water and 0.1% formic acid in acetonitrile with 10-50%B over 40 minutes. The ammonium formate conditions utilised a mobile phase of 20 mM ammonium formate native pH in water and 20 mM ammonium formate in acetonitrile / water (80:20 v/v) with 5-55%B over 40 minutes. Flow rate was 0.3 mL/min, column oven temperature was 40 °C, and detection used a combination of UV at 215 nm and MS for peak confirmation.

3.7.9 Stability of Peptides

Over the course of the robustness studies, it was noted that columns were reducing in chromatographic performance quicker than anticipated and increased in pressure. This was observed on a number of columns, before pinpointing that it specifically occurred on columns tested repeatedly in ammonium formate at its native pH, not in formic acid.

Within 6,000 column volumes, the stationary phases would reduce in efficiency before split peaks were observed. The issue was raised with Waters R&D in Milford, MA, USA, who retested the columns using their SST, which confirmed the decrease in performance. Examination of the inlet frit of each column by Scanning Electron Microscopy (SEM) highlighted an issue with particulates forming on the head of the

column. A replacement inlet frit brought the efficiency of the column back in line with specification, which highlights the column packing material was not an issue, but purely the material on the inlet frit.

These particulates (*Figure 60*) contained organic matter and were not seen on columns which had not been exposed to ammonium formate. Further discussions suggested the hydrophobic peptides within the test mixtures possessed a net charge of 0.0 at pH 6.5, which would be the lowest point of solubility and could explain the presence of particulates where it began to precipitate upon meeting the mobile phase and collected on the head of the column. This would block channels through to the column and create poor chromatographic performance and split peaks where the solute band is dispersed.

In order to prevent stationary phases from experiencing these issues, the load of each peptide injected was reduced and a 0.2 µm inline filter was introduced prior to the column to collect any precipitated peptide. The inline filter was disposed before any detrimental peak shapes could be observed from the column (approximately after every 30 columns evaluated based on experimental data).

Figure 60 Scanning Electron Microscopy (SEM) images of two inlet frits from two separate columns exhibiting high pressure and split peaks. Top row: Image of the entire inlet frit. Bottom row: Image zoomed in on particulate matter.

3.7.10 Recommendations

The two Design of Experiments were used to highlight any practical constraints required for the methodology [148]. The formic acid methodology indicated a robust method with limited statistical impact based on the parameters tested. Thus, the procedures which were already in place such as weighing solvents and ensuring the pipette dispensed 1 g of water accurately prior to delivery of formic acid were sufficient. The ammonium formate methodology required greater constraints which was expected as the effect of electrostatic interactions can be extremely subtle and affected by small deviations.

The intermediate precision indicated the methods provided similar profiles regardless of instrument type, which highlights its applicability across laboratories

and indicates characterisation can be performed on instruments other than the Shimadzu Nexera X2.

The concentration of the peptides used is extremely important to avoid overloading which changes the peak shape and width to affect peak capacity but most importantly for the Peptide RPC Column Characterisation Protocol, changes the retention time. This is the most critical as the retention time is used to produce t_g^* which in turn creates various delta values which are used to develop the database and score plots.

The order of exposure to the mobile phases also needs to be carefully considered. Ideally, dedicated columns should be used for different pH evaluations in order to avoid drifts in retention, however, this may not be entirely practically. In such circumstances, the stationary phase should be first exposed to formic acid then ammonium formate to reduce the effect of pH slow equilibration which can affect approximately 40% of commercially available columns. Experiments have shown that there is a small effect from low to intermediate pH which was considered minimal.

A summary of the mitigation put in place to ensure robustness and reliability can be found in *Table 56*. The full protocol and test mixtures are described in *Table 57*-*Table 58*. A summary of the delta values measured in each mobile phase is described in *Table 59*.

Table 56 Mitigation to increase the robustness and reliability of the Peptide RPC Column Characterisation protocol, including the rationale for each action

Mitigating Action	**Rationale**
Prepare solvents by weight rather than volume	There are greater errors associated with glassware, thus more reproducible mobile phases can be prepared by weight.
Store mobile phases in the fridge when not in use. Mobile phases to be disposed within 4 week at 5 °C.	Bottles should be capped and appropriately stored to minimise evaporation and prevent microbial growth.
Assess the accuracy of the pipette before each use	To ensure the pipette can accurately dispense formic acid.
Measure the pH of the stock ammonium formate solution (6.39-6.51).	The salt container should be carefully capped to avoid loss of ammonia which can result in a lower pH. In addition, measures should be put in place to reduce the effect of hygroscopicity (i.e. use a desiccator, avoid using salt which has significant clump formation).
Use 100% MeCN instead of 20 mM ammonium formate in MeCN/H_2O (80:20 w/w) in the B solvent combined with a corresponding change in gradient slope.	The loss of acetonitrile in the B solvent causes significant differences for certain delta values. Changing to 100% MeCN addresses this problem.
Remove Δ(3,1), Δ(9,1) and Δ(10,9) measured in ammonium formate	Improve the robustness of the procedure as they were sensitive to changes in MeCN. Although these delta values had some influence within the loading plot, they can be removed with minimal effect on the score plot and the remaining probes cover the range of interactions which should be investigated.
Use reference peptides in each test mixture	Allows retention times to be normalised for direct comparison between different batches of solvent, different analysts and removes the contribution from the dwell volume and column volume.

Each test mixture should contain the two peptides used to create the delta value	Removes any random injection to injection variation of retention time in addition to fluctuations in temperature or mobile phase composition.
Characterise the stationary phase in formic acid prior to ammonium formate	Removes the effect of slow equilibration and retention drifts.
Use a specific load for each peptide	Changing the load on the column can cause changes in retention which will impact on the delta value produced.
Assess the actual temperature of the column	Column oven designs can create as much as ±5 °C difference [125, 126], which can impact significantly on selectivity. Obtaining the actual temperature of the oven enables the end-user to adjust the temperature appropriately for direct comparisons of different column oven designs.
Mobile phase bottles should be stored correctly with a cap and stored at 5 °C. When stored on the system, a good vapour valve should be installed	Storage of capped solvent bottles in the fridge reduces microbial growth in the aqueous mobile phase and evaporation, whilst the vapour valve prevents dust / microbes entering the chromatographic system and acetonitrile losses [149].
Reduce load of the peptides and add an inline filter to induce mixing and trapping of particles prior to column	The hydrophobic peptides have a pI of 0.0 in ammonium formate at pH 6.45, which could cause solubility issues such as precipitation on the frit at the head of the column. This can cause bad peak shapes, increased pressures and reduced column lifetime. By reducing the load and introducing an inline filter, it will reduce the risk for precipitation and increase the robustness of the protocol.
Use a reference column to act as a system suitability test	This provides a baseline for the instrument to detect any differences in any asymmetrical shifts in the gradient (as well as other problems).

3.7.11 Definitive Protocol for the Peptide RPC Column Characterisation Protocol

If different column dimensions are employed, it is recommended that the user employs method translation tools [51].

Table 57 Description of the Peptide RPC Column Characterisation Protocol for 150 x 2.1 mm columns formats

Parameter	Protocol
Mobile Phase	A1: 0.1% (±0.005%) v/v formic acid in water – Add 1.000 mL formic acid to 999.0 g (±0.01 g) water B1: 0.1% (±0.005%) v/v formic acid in acetonitrile – Add 1.000 mL formic acid to 785.2 g (±0.01 g) acetonitrile A2: 20 mM Ammonium formate in water – Add 100.0 g (±0.01 g) 200 mM ammonium formate stock solution to 900.0 g (±0.01 g) water B2: Acetonitrile
Stock Buffer	200 mM Ammonium formate pH 6.45 (±0.06) – Dissolve 1.261 g (±0.1 mg) in 100.0 g (±0.01 g) water and measure the pH using an appropriately calibrated probe
Gradient	**Time** / **%B** 0.0 / 4.5 40.0 / 50.0 42.0 / 50.0 42.1 / 4.5 54.1 / 4.5
Flow Rate	0.3 mL/min (±0.005 mL/min)
Column Oven Temperature	40 °C (±2 °C)
Autosampler Temperature	Recommend 10 °C
Wavelength	215 nm Ref 360 nm (band width 8 and 100 nm)
MS	Selected Ion Monitoring (z=2)
Dwell Volume	100 – 500 µL
Stock Peptide Concentration & Diluent	0.25 mg/mL in DMSO/H_2O (80:20 v/v)

The run order is of great importance and should be first assessed at low pH then intermediate pH.

Table 58 Test mixtures with their rationale, m/z and load to ensure consistent results

Test Mixture	Peptide Number	Peptide	Rationale	*m/z*	Load (µg)
TM1	1	Bovine GLP-2 (1-15)	Original sequence	820	0.250
	8a	[Met(O)10]-Bovine GLP-2 (1-15)	Oxidation	828	0.250
	9	[L-Asp11]-Bovine GLP-2 (1-15)	Deamidation / Negative charge	820	0.125
	13	Bovine GLP-2 (16-33)	Original sequence	1069	0.25
	15	[Ile26,Leu27]-Bovine GLP-2 (16-33)	Switch in AA sequence	1069	0.075
TM2	8a	[Met(O10]-Bovine GLP-2 (1-15)	Oxidation	828	0.250
	13	Bovine GLP-2 (16-33)	Original sequence	1069	0.250
	15	[Ile26,Leu27]-Bovine GLP-2 (16-33)	Switch in AA sequence	1069	0.075
	24	[Tyr26]-Bovine GLP-2 (16-33)	Phenolic effect	1076	0.125
	26	[Lys26]-Bovine GLP-2 (16-33)	Positive charge	1094	0.250
TM3	8a	[Met(O)10]-Bovine GLP-2 (1-15)	Oxidation	828	0.250
	13	Bovine GLP-2 (16-33)	Original sequence	1069	0.250
	14	[D-Ser16]-Bovine GLP-2 (16-33)	Racemisation	1069	0.125
	15	[Ile26,Leu27]-Bovine GLP-2 (16-33)	Switch in AA sequence	1069	0.075
	16	[L-Asp21,Gly22]-Bovine GLP-2 (16-33)	Loss of aromatic group / Racemisation	1024	0.125

Table 59 Description of which mobile phase is used to measure the delta value

Test Mixture	Delta	Measured in Formic Acid	Measured in Ammonium Formate
TM1	Δ(8a,1)	✓	
	Δ(9,1)	✓	
	Δ(15,13)		✓
TM2	Δ(24,13)		✓
	Δ(26,13)	✓	✓
TM3	Δ(14,13)	✓	
	Δ(16,13)	✓	

3.7.12 Comparison of TFA versus Formic Acid

In order to investigate the hypothesis that TFA masks certain interactions between the column and the peptide, a study was conducted where 0.1% v/v formic acid was substituted with 0.1% v/v TFA in both the aqueous and organic phase on the reduced number of delta values. Thirteen columns were tested using the more robust version of the protocol described in *Section 3.7.11*, which used 8 of the 11 probes to increase the reliability of the methodology. Distinct groups can be observed in the formic acid biplot plot (*Figure 61A*) with 87% of the variability described, where the position of the columns can be rationalised based on what is known about the column characters. With TFA, it is no longer possible to see these distinct groupings, and only 68% of the variability is described, which suggests a less clear structure for that dataset (*Figure 61B*). This would appear to confirm the hypothesis that TFA will mask peptide-column interactions and thus columns become more similar. Stationary phases such as the Acquity HSS C18-SB with no end-capping and low surface coverage appear similar to columns with end-capping and positive charge like Acquity CSH Fluoro Phenyl and Polaris Amide C18 which are very different. As such, to describe the interactions of the columns, it is important to assess each column using formic acid, rather than TFA. Although TFA is used for peptide analysis, formic acid is often used within industry methodologies due to its enhanced signal in the MS. A further evaluation of TFA as an additive will be described in a subsequent section where mobile phases are characterised (*Section 3.9*).

The PC^{**} was measured for both the formic acid, ammonium formate and TFA gradient conditions on the reduced number of delta values. The greater performance, as shown by increased PC^{**} values, was typically achieved using intermediate pH (*Table 60*). Formic acid characteristically provides poorer performance, whilst TFA usually produced good values of peak capacity. Despite poorer performance, the peak performance for formic acid was within 25% (average) of the TFA performance and 37% (average) in ammonium formate.

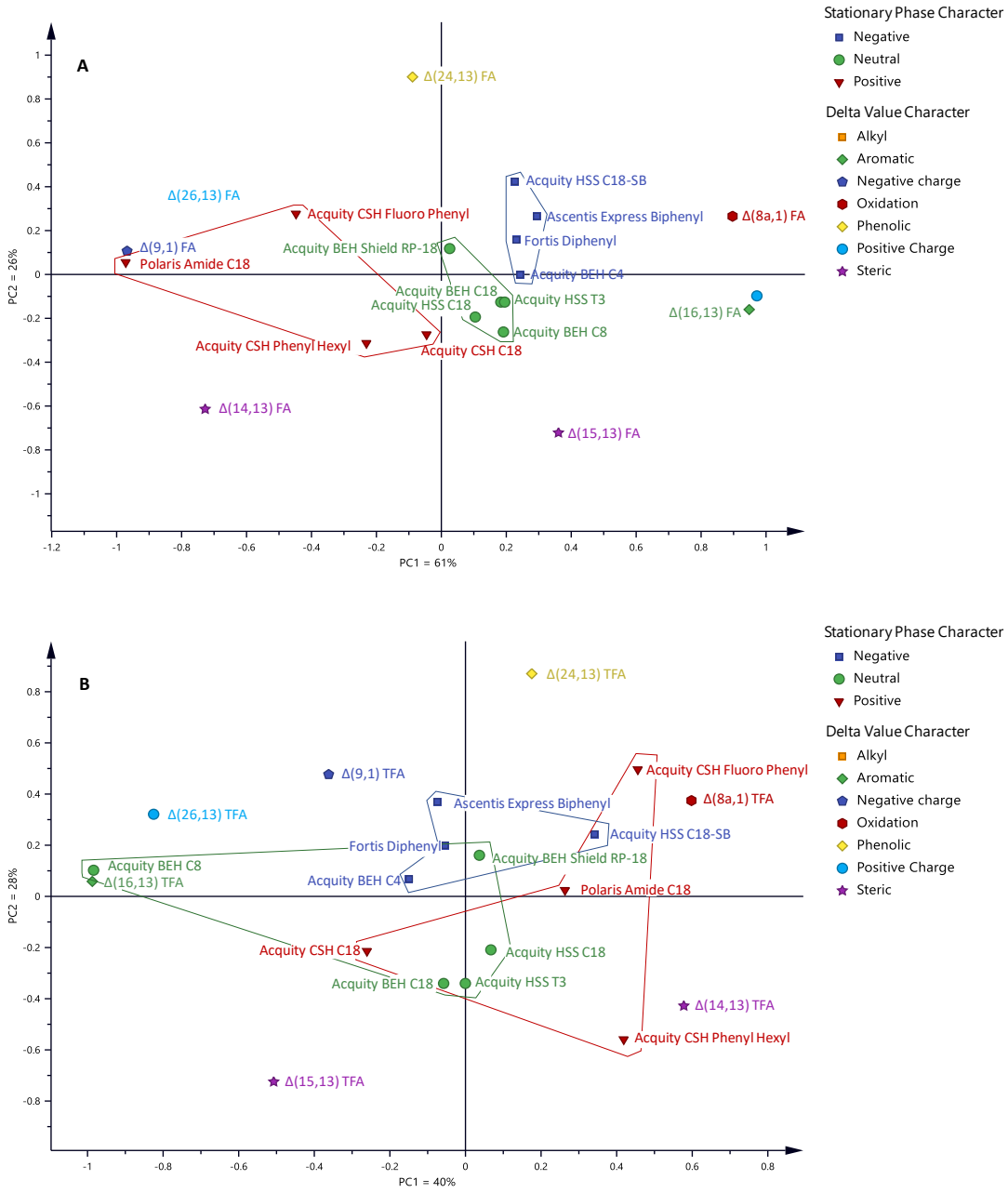

Figure 61 Biplots of the reduced number of delta values on the 13 stationary phases in (A) formic acid and (B) TFA. The different stationary phases have been grouped and colour coded based on prior knowledge of the stationary phase properties.

Table 60 Peak capacity measured for each stationary phase using both the formic acid, TFA and ammonium formate gradients

PC**	Acquity BEH C4	Acquity BEH C8	Acquity BEH C18	Acquity BEH Shield RP-18	Acquity CSH C18	Acquity CSH Fluoro Phenyl	Acquity CSH Phenyl Hexyl	Acquity HSS C18	Acquity HSS C18-SB	Acquity HSS T3	Ascentis Express Biphenyl	Fortis Diphenyl	Polaris Amide C18
Formic Acid	90	121	123	137	146	78	108	80	108	64	66	66	79
Trifluoroacetic Acid	172	137	174	168	173	140	147	142	68	81	129	130	108
Ammonium Formate	129	212	222	229	196	124	180	173	81	183	193	122	96

3.8 Generation of the Peptide RPC Column Characterisation Database

The protocol was applied to 42 columns from seven different column manufacturers. The stationary phases varied in ligand chemistry, bonding procedure and base silica. In addition to conventional silica based stationary phases, some polymeric phases and monolithic columns were characterised. Each stationary phase followed the procedure described in *Section 3.7.11* and any mitigation suggested, such as assessment in formic acid prior to ammonium formate to avoid slow equilibration effects.

3.8.1 Results from the Database

The eight delta values which comprise the RPC Column Characterisation Protocol were collated in formic acid and ammonium formate for each stationary phase (Table 61, for the raw data, see *Table 74-Table* 76 for the formic acid data and *Table 80-Table* 82 for ammonium formate*,* in *Appendix II*). Of the 42 phases assessed, four phases were not suitable where peaks were undetected by either the PDA or SIM. These phases were Ascentis Express F5, BioShell C18, Bioshell CN and AdvancedBio PeptideMap.

It was initially hypothesised that the Ascentis Express F5 retained the multiple positively charged peptides due to the dense electronegative charge associated with the fluorinated aromatic ring in ammonium formate. However, this was not an issue for the Kinetex F5 or Poroshell PFP which possess similar characteristics for aromatic and dipole character to the Ascentis Express F5 based on the Extended Tanaka protocol. There is greater silanophilic activity on the Ascentis Express F5, as highlighted from the Extended Tanaka protocol results for $\alpha_{(B/P\ pH\ 7.6)}$ and $\alpha_{(B/P\ pH\ 2.7)}$, which could possibly help elude to the added retention of the positively net charged peptides in ammonium formate.

The Bioshell CN also experienced issues in ammonium formate conditions, where the more hydrophilic peptides eluted at the solvent front, therefore could not be identified (*Figure 62*). This could be indicative that there is some negative charge, similar to the explanation for the Acclaim WCX repulsion of hydrophilic peptides, or insufficient hydrophobicity to the stationary phase to aid retention. Supporting evidence for increased negative charge on the stationary phase includes the Extended Tanaka protocol measures for silanophilic interactions under intermediate pH conditions, as well as significant retention of the positively charged [Lys26]-(Peptide Number 26), which typically eluted before [Gly22]-Bovine GLP-2 (16-33) (Peptide Number 16) on other stationary phases.

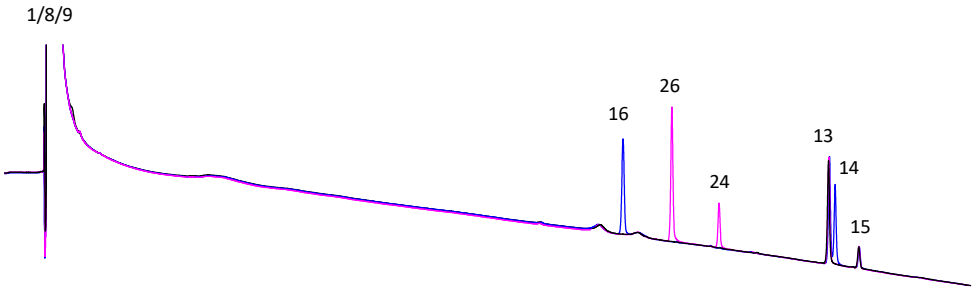

Figure 62 Overlaid UV chromatograms of the three characterisation peptide test mixtures on the Bioshell CN using ammonium formate conditions demonstrating the repulsion of the hydrophilic peptides with the solvent front. Analyses were formed on the Nexera X2 coupled to the 2020 single quadrupole system. The ammonium formate conditions utilised a mobile phase of 20 mM ammonium formate native pH in water and 20 mM ammonium formate in acetonitrile / water (80:20 v/v) with 5-55%B over 40 minutes. Flow rate was 0.3 mL/min, column oven temperature was 40 °C, and detection used a combination of UV at 215 nm and MS for peak confirmation. Peak 1: Bovine GLP-2 (1-15), Peak 8: [Met(O)10]- , Peak 9: [L-Asp11]-Bovine GLP-2 (1-15), Peak 13: Bovine GLP-2 (16-33), Peak 14: [D-Ser16]-, Peak 15: [Ile26,Leu27]-, Peak 16: [Gly22]-, Peak 24: [Tyr26]-, Peak 26: [Lys26]-Bovine GLP-2 (16-33)

The Bioshell C18 could not be characterised using formic acid conditions as neither the SIM or PDA could identify the location of the hydrophobic peptide probes. Peptides could be identified using ammonium formate with typical peak shape responses, thereby suggesting the formic acid conditions are not ideal for this column. The gradient was extended from 50% to 100%MeCN using the same %B/min change as the original gradient, in order to clean the column as well as elute the peptides. However, the peptides remained unidentified, which could suggest they are irreparably bound to the stationary phase (*Figure 63*).

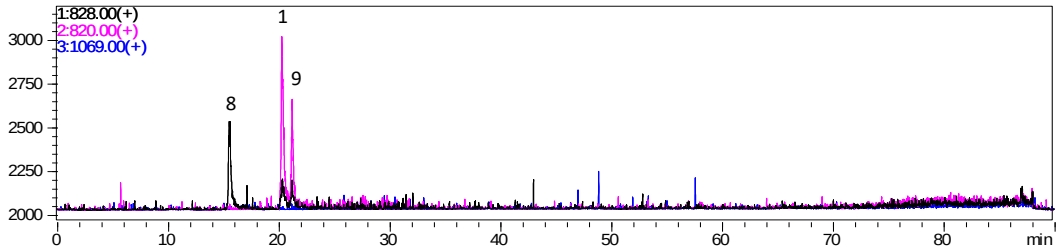

Figure 63 Overlaid SIM spectra of the three characterisation peptide test mixtures on the Bioshell C18 using formic acid conditions demonstrating the hydrophobic peptides failing to elute under gradient conditions which swept to 100% MeCN. Analyses were performed on the Nexera X2 coupled to the 2020 single quadrupole system. The formic acid conditions utilised a mobile phase of 0.1% formic acid in water and 0.1% formic acid in acetonitrile with 10-100%B over 90 minutes. Flow rate was 0.3 mL/min, column oven temperature was 40 °C, and detection used a combination of UV at 215 nm and MS for peak confirmation. Peak 1: Bovine GLP-2 (1-15), Peak 8: [Met(O)10]-, Peak 9: [L-Asp11]-Bovine GLP-2 (1-15), Peak 13: Bovine GLP-2 (16-33), Peak 14: [D-Ser16]-, Peak 15: [Ile26,Leu27]-, Peak 16: [Gly22]-, Peak 24: [Tyr26]-, Peak 26: [Lys26]-Bovine GLP-2 (16-33)

Like the Bioshell C18, the AdvancedBio PeptideMap had retention of peptide probes under ammonium formate conditions, but it was the formic acid which proved problematic for characterisation. The peptide probes could be located on the AdvancedBio PeptideMap with the SIM, but the peaks were extremely unfavourable, with poor peak shape which made it difficult to define a suitable apex for retention time. Therefore, the AdvancedBio PeptideMap was not characterised.

Both the Bioshell C18 and AdvancedBio PeptideMap were evaluated using TFA in place of formic acid to ascertain if the phases were designed with the ion pair in mind for analysis. The results in *Figure 64* demonstrated the improved chromatographic performance on these two problematic stationary phases when using the ion pair TFA. The peak shape on the AdvanceBio PeptideMap has shown significant improvements in comparison to the formic acid conditions.

These four phases were excluded from any further comparisons.

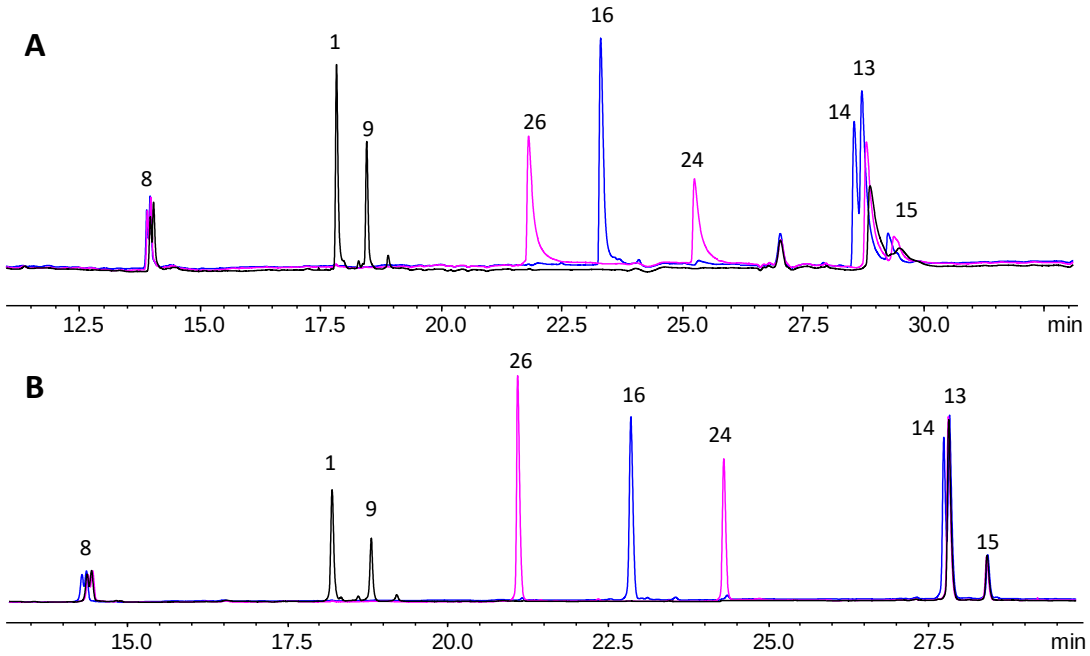

Figure 64 Overlaid chromatograms of TM1-3 on the (A) Bioshell C18 and (B) AdvanceBio PeptideMap columns, using 0.1% v/v TFA in place of formic acid using the Peptide RPC Column Characterisation protocol operating conditions. Analyses were performed on the Nexera X2 coupled to the 2020 single quadrupole system. The formic acid conditions utilised a mobile phase of 0.1% formic acid in water and 0.1% formic acid in acetonitrile with 10-50%B over 40 minutes. Flow rate was 0.3 mL/min, column oven temperature was 40 °C, and detection used a combination of UV at 215 nm and MS for peak confirmation. Peak 1: Bovine GLP-2 (1-15), Peak 8: [Met(O)10]-, Peak 9: [L-Asp11]-Bovine GLP-2 (1-15), Peak 13: Bovine GLP-2 (16-33), Peak 14: [D-Ser16]-, Peak 15: [Ile26,Leu27]-, Peak 16: [Gly22]-, Peak 24: [Tyr26]-, Peak 26: [Lys26]-Bovine GLP-2 (16-33)

Table 61 Delta values determined in formic acid and ammonium formate on 38 stationary phases

Column Name	Classification	Oxidation Δ(8a,1) FA	Negative Charge Δ(9,1) FA	Steric Δ(14,13) FA	Aromatic Δ(16,13) FA	Positive Charge Δ(26,13) FA	Steric Δ(15,13) AF	Phenolic Δ(24,13) AF	Positive Δ(26,13) AF
Ascentis Express C18 480	Neutral	-0.291	0.049	0.015	-0.375	-0.542	0.051	-0.191	-0.297
Ascentis Express C18 472	Neutral	-0.295	0.050	0.015	-0.380	-0.542	0.050	-0.188	-0.295
Ascentis Express C18 468	Neutral	-0.289	0.046	0.015	-0.375	-0.540	0.051	-0.192	-0.302
Ascentis Express C18 477	Neutral	-0.289	0.046	0.015	-0.376	-0.541	0.051	-0.191	-0.300
Ascentis Express C18 488	Neutral	-0.290	0.048	0.015	-0.376	-0.541	0.051	-0.190	-0.299
Ascentis Express C18 484	Neutral	-0.293	0.050	0.014	-0.375	-0.542	0.051	-0.190	-0.298
Ascentis Express RP-Amide	Negative / Polar	-0.282	0.059	0.007	-0.402	-0.586	0.039	-0.136	-0.266
Ascentis Express C8	Neutral	-0.286	0.051	0.015	-0.379	-0.548	0.051	-0.190	-0.299
Ascentis Express Phenyl Hexyl	Negative / Polar	-0.291	0.056	0.008	-0.381	-0.549	0.045	-0.159	-0.263
Ascentis Express Biphenyl	Negative / Polar	-0.267	0.054	0.000	-0.366	-0.520	0.040	-0.130	-0.211
Luna Omega C18	Neutral	-0.296	0.000	0.013	-0.380	-0.566	0.052	-0.184	-0.298
Luna Omega PS C18	Positive	-0.314	0.062	0.015	-0.422	-0.614	0.048	-0.181	-0.316
Luna Omega Polar C18	Neutral	-0.294	0.054	0.012	-0.386	-0.576	0.051	-0.179	-0.287
Kinetex C18	Neutral	-0.262	0.052	0.000	-0.378	-0.531	0.045	-0.161	-0.286
Kinetex Evo C18	Neutral	-0.282	0.054	0.000	-0.412	-0.569	0.049	-0.253	-0.295
Kinetex C8	Neutral	-0.277	0.050	0.013	-0.376	-0.542	0.055	-0.180	-0.291
Kinetex Biphenyl	Negative / Polar	-0.279	0.056	0.000	-0.363	-0.528	0.042	-0.137	-0.137
Kinetex F5	Negative / Polar	-0.263	0.049	0.000	-0.379	-0.529	0.040	-0.148	-0.244
Fortis Diphenyl	Negative / Polar	-0.287	0.056	0.000	-0.387	-0.558	0.048	-0.136	-0.223
Polaris Amide C18	Positive	-0.470	0.205	0.020	-0.569	-0.873	0.024	-0.231	-0.718
Poroshell Bonus-RP	Positive	-0.328	0.083	0.018	-0.438	-0.654	0.043	-0.131	-0.310
Poroshell PFP	Negative / Polar	-0.301	0.067	0.010	-0.453	-0.644	0.042	-0.147	-0.246
Poroshell Phenyl Hexyl	Negative / Polar	-0.288	0.054	0.004	-0.364	-0.523	0.046	-0.160	-0.260

Table 61 Ctd. Delta values determined in formic acid and ammonium formate on 38 stationary phases

Column Name	Classification	Oxidation Δ(8a,1) FA	Negative Charge Δ(9,1) FA	Steric Δ(14,13) FA	Aromatic Δ(16,13) FA	Positive Charge Δ(26,13) FA	Steric Δ(15,13) AF	Phenolic Δ(24,13) AF	Positive Charge Δ(26,13) AF
Poroshell SB-AQ	Negative / Polar	-0.256	0.048	0.000	-0.399	-0.549	0.048	-0.156	-0.264
Poroshell HPH-C8	Neutral	-0.299	0.053	0.014	-0.382	-0.550	0.054	-0.198	-0.310
Poroshell HPH-C18	Neutral	-0.292	0.052	0.013	-0.374	-0.535	0.052	-0.192	-0.310
PLRP-S	Negative / Polar	-0.256	0.055	0.000	-0.400	-0.547	0.029	-0.116	-0.244
Zorbax SB-C18	Neutral	-0.286	0.049	0.012	-0.380	-0.553	0.052	-0.183	-0.269
Zorbax SB-C8	Negative / Polar	-0.273	0.050	0.008	-0.375	-0.559	0.044	-0.170	-0.235
Zorbax 300 SB-C18	Neutral	-0.274	0.044	0.007	-0.356	-0.502	0.046	-0.183	-0.271
Chromolith RP-18e	Neutral	-0.286	0.048	0.012	-0.375	-0.539	0.049	-0.192	-0.300
Acquity BEH C4	Neutral	-0.269	0.048	0.009	-0.364	-0.505	0.055	-0.163	-0.276
Acquity BEH C8	Neutral	-0.297	0.049	0.010	-0.364	-0.540	0.060	-0.207	-0.303
Acquity BEH C18	Neutral	-0.294	0.049	0.009	-0.362	-0.537	0.054	-0.198	-0.303
Acquity BEH C18 300	Neutral	-0.290	0.047	0.009	-0.355	-0.515	0.055	-0.199	-0.303
Acquity BEH Shield RP18	Neutral	-0.310	0.060	0.011	-0.396	-0.572	0.051	-0.153	-0.292
Acquity CSH C18	Positive	-0.325	0.060	0.016	-0.418	-0.613	0.052	-0.181	-0.296
Acquity CSH Fluoro phenyl	Positive	-0.304	0.116	0.012	-0.565	-0.814	0.032	-0.108	-0.192
Acquity CSH Phenyl Hexyl	Positive	-0.346	0.084	0.017	-0.462	-0.695	0.046	-0.154	-0.264
Acquity HSS C18	Neutral	-0.307	0.051	0.012	-0.381	-0.564	0.055	-0.197	-0.312
Acquity HSS C18-SB	Negative / Polar	-0.242	0.042	0.000	-0.384	-0.564	0.024	-0.194	-0.162
Acquity HSS T3	Neutral	-0.283	0.049	0.009	-0.373	-0.553	0.052	-0.191	-0.306
Cortecs T3	Neutral	-0.276	0.047	0.006	-0.371	-0.531	0.051	-0.186	-0.295

The data in *Table 61* was interpreted using PCA, as previously described throughout this thesis. With the increase in columns and more data, the classification of columns was re-evaluated using prior knowledge of the stationary phases and chemical properties to help rationalise their position within the score plot (*Figure 65* and *Table 62*). The classifications were positive ($\alpha_{(BSA/T)}$ >0.1), negative / polar ($\alpha_{(B/P\ pH\ 7.6)}$ >0.8 and $\alpha_{(C/P)}$ >0.8) and neutral character (phases which don't possess any significant silanophilic, hydrogen bonding or positive character).

The $\alpha_{(BSA/T)}$ measure needed to be carefully evaluated as there are a few ways to interpret the data. The Acquity BEH C4 and Fortis Diphenyl results suggest there is positive character to the stationary phase. However, interrogation of the data has shown that the large delta values are caused by reduced retention of toluene on the Acquity BEH C4 (i.e. low hydrophobicity) and increased retention of the BSA on the Fortis Diphenyl due to aromatic interactions between the analyte and the phenyl moiety on the stationary phase.

It is known there is a permanent positive charge on the silica surface of the Acquity CSH C18, which is identical between all of the CSH range of stationary phases [118]. However, the values between the three CSH columns are quite disparate, based on the results in *Table 62*. This is further evidence that it is the accessibility into the stationary phase based on ligand density which can play a crucial role in the retentivity of analytes. The Acquity CSH range of columns have all been classified as phases with positive character based on the manufacturers information and the Extended Tanaka result.

Table 62 Classification of stationary phases characterised using the Peptide RPC Column Characterisation Protocol based on prior knowledge of the phases and information provided by the manufacturer. Classifcation blue = negative, green = neutral and red = postiive character

Column	Endcapped	%C Load*	$\alpha_{(BSA/T)}$ (>0.1)	$\alpha_{(B/P\ pH\ 7.6)}$ (>0.8)	$\alpha_{(C/P)}$ (>0.8)	Classification
Acquity BEH C4	No	8	0.13	0.4	1.5	
Acquity BEH C8	Yes	13	0.02	0.3	0.6	
Acquity BEH C18	Yes	18	0.00	0.2	0.4	
Acquity BEH C18 300	Yes	12	0.02	0.2	0.4	
Acquity BEH Shield RP18	Yes	17	0.04	0.3	0.3	
Acquity CSH C18	Yes	15	0.03	0.4	0.4	
Acquity CSH Fluoro phenyl	No	10	0.74	1.2	1.7	
Acquity CSH Phenyl Hexyl	Yes	14	0.16	0.4	0.7	
Acquity HSS C18	Yes	15	0.01	0.2	0.4	
Acquity HSS C18-SB	No	8.5	0.01	5.0	1.9	
Acquity HSS T3	Yes	11	0.01	0.3	0.5	
Ascentis Express Biphenyl	Yes	-	0.01	1.0	2.3	
Ascentis Express C8	Yes	-	0.01	0.4	0.3	
Ascentis Express C18	Yes	-	0.01	0.7	0.4	
Ascentis Express Phenyl Hexyl	Yes	-	0.02	0.5	0.8	
Ascentis Express RP-Amide	Yes	-	0.05	0.4	0.2	
Chromolith RP-18e	Yes	-	0.01	0.6	0.4	
Cortecs T3	Yes	4.7	0.02	0.3	0.5	
Fortis Diphenyl	Yes	13	0.32	0.6	0.8	
Kinetex Biphenyl	Yes	11	0.02	0.8	2.1	
Kinetex C8	Yes	8	0.01	0.4	0.4	
Kinetex C18	Yes	12	0.01	0.4	0.5	
Kinetex Evo C18	Yes	11	0.03	0.4	0.4	
Kinetex F5	Yes	9	0.00	0.7	0.8	
Luna Omega C18	Yes	11	0.00	0.4	0.5	
Luna Omega Polar C18	Yes	9	0.01	0.7	0.7	
Luna Omega PS C18	Yes	9	0.14	0.5	0.5	
PLRP-S	Yes	-				
Polaris Amide C18	Yes	15	2.39	0.2	0.2	
Poroshell Bonus-RP	Yes	9.5	1.60	0.3	0.4	
Poroshell HPH-C8	Yes	-				
Poroshell HPH-C18	Yes	-	0.01	0.4	0.5	
Poroshell PFP	Yes	5.1	0.07	0.7	0.7	
Poroshell Phenyl Hexyl	Yes	9	0.01	0.4	0.9	
Poroshell SB-AQ	No	-	0.09	1.1	0.4	
Zorbax SB-C8	No	5.5	0.00	1.3	1.3	
Zorbax SB-C18	No	10	0.01	0.9	0.6	
Zorbax 300 SB-C18	No	2.6		1.0	0.8	

The major difference in classifications, as denoted by the first principal component, was based on electrostatic interactions, i.e. positive or negative character on the

stationary phase (*Figure 65)*. The positions of the variables can be located in the loading plot in *Figure 66.*

The 3rd and 4th quadrants of the score plot were dominated by phases with positive character, which is highly influenced by Δ(9,1) FA, a probe with increased negative charge (*Figure 65*, red inverted triangles in the score plot and *Figure 66,* blue pentagon in the loading plot). This group contained the Polaris Amide C18 and Acquity CSH Fluoro Phenyl as the most extreme stationary phases which exhibit alternative selectivity. Also located within the group are the Luna Omega PS C18 and Acquity CSH C18 which are alkyl phases with a small constant positive charge, and the Acquity CSH Phenyl Hexyl and Poroshell Bonus-RP. A previous study performed on the Zorbax Bonus-RP suggested a polar embedded moiety which is produced via a two-step synthetic pathway to create positive character on the stationary phase [18]. This is suggestive that the Poroshell Bonus-RP is also produced in a similar manner, and is also corroborated by the $\alpha_{(BSA/T)}$ results shown in *Table 28.*

Opposite along the x-axis are the probes for increased positive character, Δ(26,13), with phases which are indicative of columns possessing negative character (*Figure 65,* blue squares). This includes stationary phases such as the PLRP-S which is a polymeric stationary phase which is devoid of silanols to participate in silanophilic interactions. There is little literature available regarding the structure of the stationary phase, but it is thought to be similar in structure to other commercially available styrene / divinylbenzene polymeric material phases which can possess residual carboxylate groups on the surface of the polymer, which can introduce a negative charge to the phase [116]. The second principal component, along the y-axis, appeared to be dominated by phenolic interactions, such as hydrogen bonding. The negative group needed greater consideration, as it contained stationary phases which don't possess any negative functionality, such as the Ascentis Express RP-Amide and Poroshell PFP. These phases possess an architecture with greater spacing between the ligands due to the bulky side groups or the ability to form hydrogen bonding interactions. This facilitates a greater accessibility to the silanol

sites on the surface of the silica which permits hydrogen bonding and silanophilic interactions. Phases such as the Poroshell SB AQ and Zorbax SB-C8 are non-endcapped which allow for polar interactions with the free silanols despite having a greater bonding density than the aromatic phases described. Thus, this grouping was described as negative / polar, to encompass the different functionalities capable of forming hydrogen bonds and polar interactions. This group contained polyfluorinated aromatic phases, phenyl phases and alkyl phases with either no endcapping or lower bonding density.

Finally, there was also a distinct grouping of phases which possessed neither positive or negative character, i.e. these phases were neutral (*Figure 65,* green circles). This group typically contained alkyl phases with a high degree of endcapping and high bonding density. These phases usually were C18 type ligand functionalities, although it did contain the Luna Omega Polar C18 and Acquity BEH Shield RP18. These phases might be expected to participate in polar interactions however, based on the chromatographic results exhibited by the peptide probes, they seem to have a more inherent neutral character.

One phase which was unusually positioned within the score plot was the Kinetex C18, which was classified as neutral but located within the negative / polar group. As a C18 phase, it was expected to be located amongst the other long alkyl chains, however, its location prompted further investigation with knowledge from the Tanaka extended protocol. This did not yield any indication of low ligand density or silanophilic interactions which could explain its position. A second column was characterised with similar chromatographic results, suggesting the result was not anomalous. The peptide probes could potentially be more discriminating than the small molecule probes thus highlight the difference in this particularly stationary phase in comparison to other typical C18 ligands.

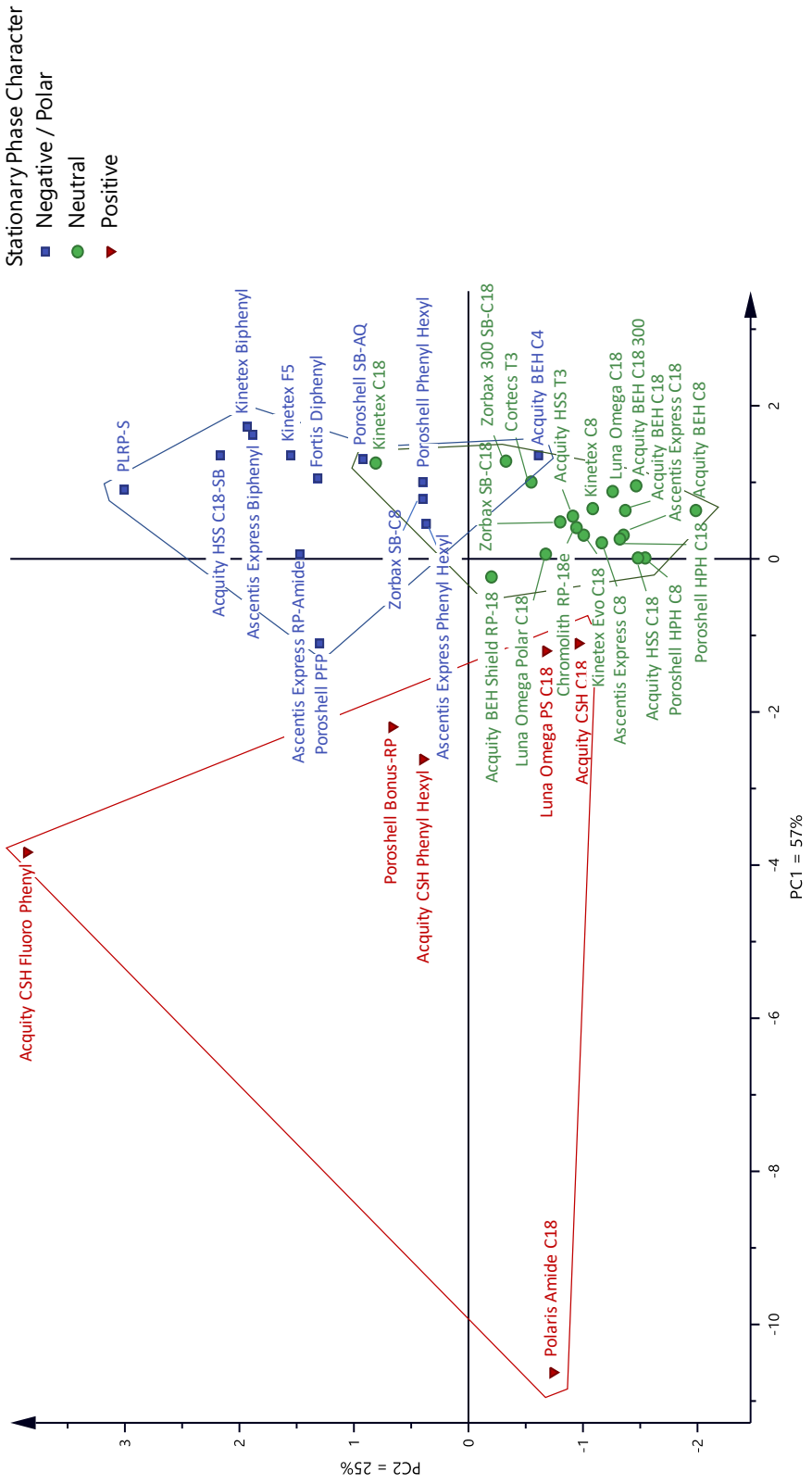

Figure 65 Score plot for the stationary phases characterised using the Peptide RPC Column Characterisation Protocol

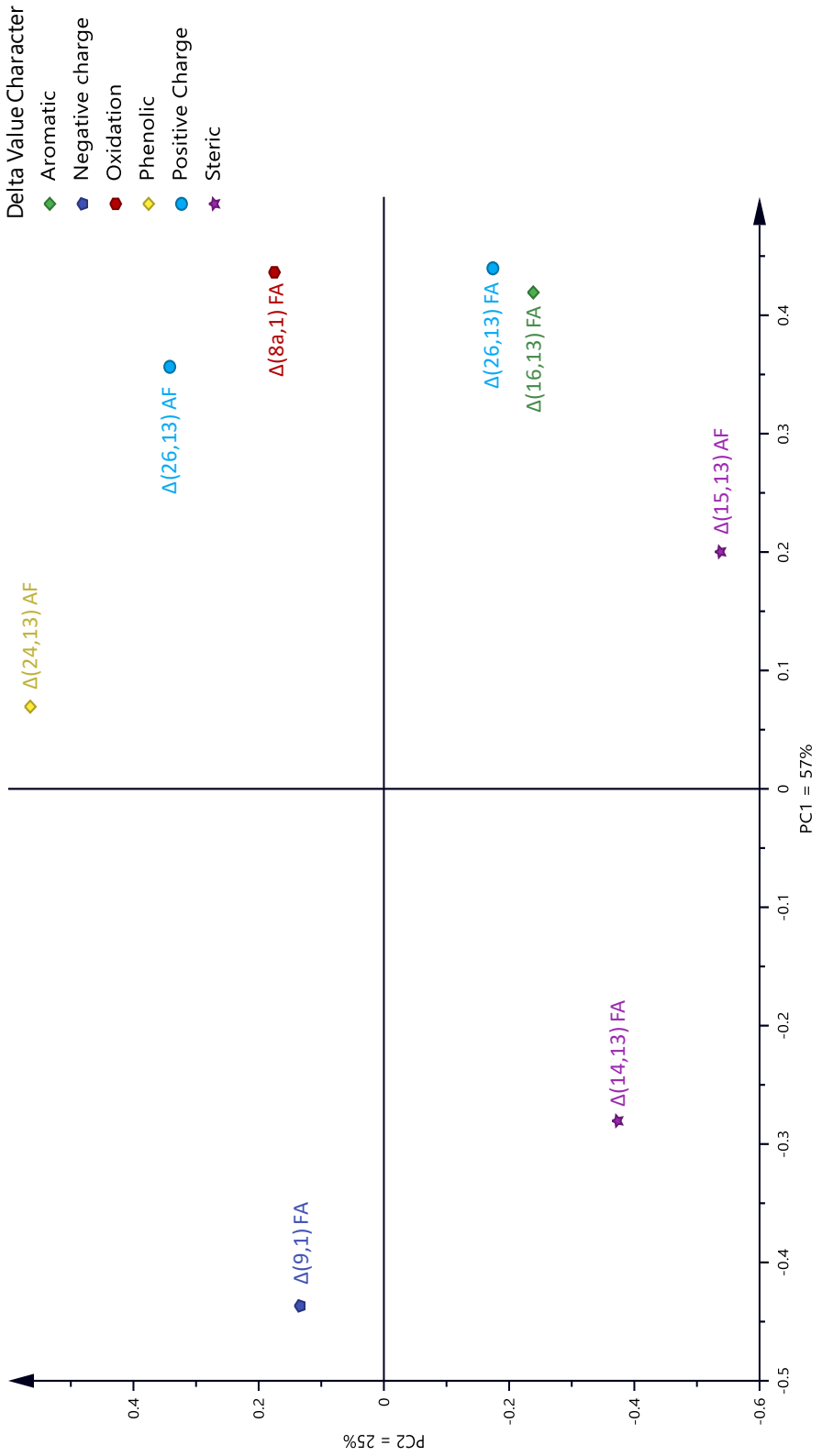

Figure 66 Loading plot for the stationary phases characterised using the Peptide RPC Column Characterisation Protocol

Peak shape was not ideal for the PLRP-S at intermediate pH which could be due to cation exchange sites which exist on the polymer phase at pH 7. This allows for significant tailing caused by the different sites available for the analyte to interact with, with different reaction kinetics leading to peak broadening [116]. This is less of an issue at low pH, and manufacturer literature suggests this type of phase is good for use with formic acid [150].

The *PC*** values, recorded in *Figure 67* (solid bars), demonstrates the increased performance which can be generate when using ammonium formate in comparison to formic acid. The concentration of the ammonium formate in the aqueous portion of the mobile phase was 20 mM which is enough to improve peak shape by reducing mutual repulsion effects. McCalley *et al*. suggested that the poor peak shape often observed for basic species, such as the positively charged peptides used in this study, is related to overloading caused by mutual repulsion between adsorbed ions of the same charge [48, 115, 116]. Mobile phases such as formic acid exacerbate this issue because there is insufficient ion strength, where a 0.1% formic acid v/v solution has approximately 2 mM ion strength in comparison to 20 mM used in the ammonium formate mobile phase. Formic acid mobile phases can, however, produce acceptable levels of peak capacity for phases which possess some positive charge, such as the Polaris Amide C18, the CSH range of stationary phases and the Luna Omega PS C18 [117]. These phases can produce improved peak shapes for basic species, where the peak width at 50% and tailing factor decreased on average by 54 and 22%, respectively between formic acid and ammonium formate. This contrasted with the neutral and negative character stationary phases, which increased in peak width by 32 and 7% on average between formic acid and ammonium formate, and tailing increased by 20 and 21% on average between the two mobile phases.

The *PC*** value observed on the Polaris Amide C18 was lower than expected despite having narrow peak widths. This was attributed to the narrow elution window on the Polaris Amide C18 compared to the other phases assessed, where the elution window was 37 and 46% smaller on average in formic acid and ammonium formate,

respectively. The conventional peak capacity (*PC*) measure was applied to all the stationary phases, where the two different measures complement each other to provide an overview of the chromatographic performance (*Figure 67*, pattern bars). The values of *PC* are superimposed on the *PC***. The values generally follow the same trend, where the ammonium formate conditions generated greater peak capacities than the formic acid, regardless of the measurement method. However, there were some exceptions including the Poroshell PFP, Poroshell Bonus-RP, Luna Omega PS C18, Luna Omega C18, Ascentis Express RP-Amide, Acquity CSH C18, Acquity CSH Fluoro Phenyl, Acquity CSH Phenyl Hexyl, Acquity BEH Shield RP18, Acquity BEH C4 and Acquity BEH C8. For these stationary phases the formic acid conditions generated a greater *PC* value than ammonium formate, whilst the *PC*** was smaller for formic acid than ammonium formate. The Poroshell Bonus-RP, Polaris Amide C18, Acquity CSH C18 Acquity CSH Fluoro Phenyl, Acquity CSH Phenyl Hexyl and Luna Omega PS C18 improved performance can be rationalised based on their positive character, as previously discussed. The remaining phases are perhaps less intuitive to explain. It is most likely due to the narrow elution window measured by the *PC***. It is also important to highlight that phases with * in *Figure 67* have larger particle sizes than typical in this study. It should be expected that the *PC* and *PC*** should increase by x1.4 with a reduction in particle size. This is due to the relationship where N is proportional to $1/d_p$ and w proportional to the square root of N [45, 102].

The sample peak capacities were also calculated for the Acclaim WCX, AdvancedBio Peptide Map, Bioshell Peptide C18 and Bioshell Peptide CN phases, although they were not included in the PCA due to a too low or high retention as explained in *Section 3.8.1*. In addition, it should be noted that the PRLP-S, Polaris Amide C18 and Acclaim WCX were 3 µm thus lower sample peak capacity should be expected in comparison to the smaller particle sizes or the superficially porous particles.

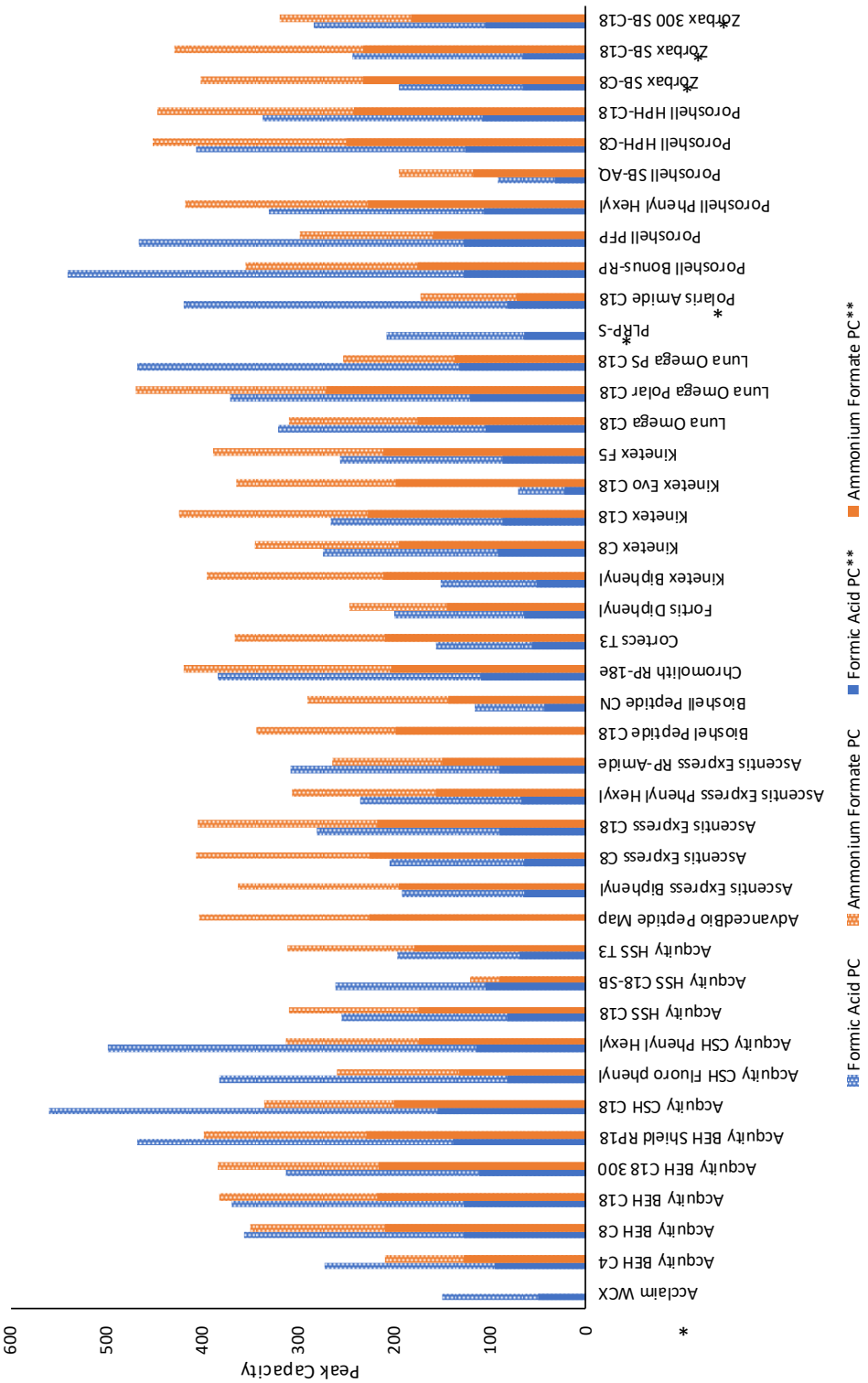

*Figure 67 Peak capacity (PC) and sample peak capacity (PC**) measured in formic acid and ammonium formate for the different columns assessed for the peptide characterisation database. * Columns with larger than 2 µm totally porous particles or 2.7 µm superficially porous particles.*

3.8.2 Comparison of the Peptide RPC Column Characterisation Protocol versus Extended Tanaka Protocols and the Hydrophobic Subtraction Model

The Peptide RPC Column Characterisation Protocol was devised to bridge the deficit in column characterisation approaches for stationary phases used for peptide separations, where it is believed probes which represent the analytes of interest are best suited for characterising the stationary phase. However, it is important to compare and contrast results produced by the peptide protocol against small molecule column characterisation protocols in order to highlight its necessity. As previously stated, the most commonly used protocols with the largest databases are Snyder's Hydrophobic Subtraction Model used in the PQRI database, and the Extended Tanaka protocols in the ACD database [82, 86, 94]. Although 38 columns were characterised using the peptide approach, the comparison was limited to 30 stationary phases which were common between all three databases. The comparison still covered a wide range in ligand functionality for greater applicability. The characterisation data from all 30 columns on the three different protocols were combined into a single loading plot, where the locations of the different variables were observed (*Figure 68*). The closely located terms intimate a greater correlation compared to terms with larger spacing. The potentially similar terms were then analysed using regression coefficients to ascertain the extent of the relationship.

It is known that the two small molecule characterisation approaches have very limited correlation between the probes, despite measuring similar properties [78, 88, 90, 151]. Perhaps unsurprisingly the best correlation is achieved between the two probes which measure hydrophobicity (denoted H in the HSM and $\alpha_{(CH2)}$ for Tanaka). The regression coefficient for this measure on the 30 columns was 0.82, which is similar to the 0.8 value determined by Snyder and Euerby and 0.90 by Borges [88, 151]. The Tanaka approach also uses the retention factor of pentylbenzene to measure ligand density and surface area which is directly linked to hydrophobicity [88]. However, a comparison of H *versus* k_{PB} produced a R^2 value of 0.55. Neue suggested this could be due to the different measurements used (i.e.

alpha *versus* retention factor). The two protocols similarly measure ion exchange capacities at both low and intermediate pH. The position of the HSM's C(2.8) *versus* Tanaka's $\alpha_{(B/P)\ pH\ 2.7}$ were in close proximity within the loading plot, however, the correlation between the two was only 0.55 (*Figure 68*). This was similar to Borges result, however, it was markedly lower than the value determined by Snyder and Euerby, where their value exceeded 0.9. This is probably due to the ligand type assessed. In the Snyder / Euerby study, the majority of phases possessed alkyl moieties which undergo similar retention mechanisms, whereas the phases assessed in this study possessed a more diverse array of ligand functionality which could produce a greater scatter using these sensitive probes. The correlation was lower between C(7.0) and $\alpha_{(B/P)\ pH\ 7.6}$, which had an R^2 of 0.34. Borges correlated the two terms as 0.47 whilst Snyder / Euerby calculated a value of 0.3, which is in close agreement with this study. The differences experienced here could be due to the slightly different pH values used and the pK_a of the basic probes.

The results from the peptide protocol were compared against the two small molecule approaches which highlighted there were some indication of a correlation, particularly for electrostatic types of interactions (i.e. Δ(26,13) FA and C(2.6) or $\alpha_{(B/P)\ pH\ 2.7}$, *Figure 68*). These probes were compared using regression analysis which demonstrated a lack of relationship between the measurements. The R^2 values varied between 0.15 – 0.75 and 0.32 – 0.73 between the delta values and the Tanaka terms, and the delta values and HSM terms, respectively (*Table 63*). The Polaris Amide C18 was typically an extreme column which, once removed, caused the regression coefficient to reduce, as the Polaris phase masked the true extent of the variation. This caused the R^2 values to reduce between 0.10 – 0.45 and 0.20 – 0.41, respectively. These results show essentially the three protocols are uncorrelated.

Figure 68 Loading plot containing the terms from the Peptide RPC Column Characterisation Protocol, Hydrophobic Subtraction Model and Extended Tanaka protocols. Terms which are close together could show potential correlation whilst terms which are at a distance have a limited relationship.

Table 63 The regression coefficients between specific delta values and terms from the Hydrophobic Subtraction Model or Extended Tanaka protocols.

Delta Value	Compared Against	Regression Coefficient (R^2)
Δ(9,1) FA	$\alpha_{(BSA/T)}$	0.75 (0.25)*
Δ(9,1) FA	B	0.55 (0.20)*
Δ(14,13) FA	S	0.32 (0.25)*
Δ(24,13) AF	$\alpha_{(C/P)}$	0.13 (0.10)*
Δ(26,13) FA	$\alpha_{(B/P)\ pH\ 2.7}$	0.55 (0.45)*
Δ(26,13) FA	C(2.8)	0.73 (0.36)*
Δ(26,13) AF	$\alpha_{(B/P)\ pH\ 7.6}$	0.15 (0.36)*
Δ(26,13) AF	C(7.0)	0.41 (0.41)*

* The most extreme column (Polaris Amide C18) was removed and in general reduced the correlation between the different probes.

3.8.3 Validation of the Peptide RPC Column Characterisation Protocol

Tryptic digests of bovine insulin and carbonic anhydrase were made in order to generate peptide fragments which could be tracked for selectivity differences. The aim was to establish if the peptide-based database could select stationary phases with diverse selectivity thus producing a different chromatographic profile. It was previously demonstrated that the protocol can be used to find columns with different and similar selectivity for different purposes. However, the same peptides were used to characterise the stationary phases as well as illustrate differences and similarities with respect to selectivity [152]. In the current study based on the tryptic digests of bovine insulin and carbonic anhydrase, completely different peptides were used for the validation which would be much more appropriate.

The Polaris Amide C18, Zorbax 300 SB-C18, Acquity BEH C8, Ascentis Express C18, Kinetex Biphenyl, Acquity CSH C18 and Acquity CSH Fluoro Phenyl were all identified as very different thus examples of phases which should be chromatographically dissimilar via the score plot in *Figure 65*. Eleven carbonic anhydrase fragments were monitored using extracted ion chromatograms on the six columns using the formic acid gradient used for the Peptide RPC Column Characterisation Protocol (*Figure 69*). There are clear selectivity differences between the six phases, with the elution

order differing between all six phases as well as the degree of resolution between peaks. The Ascentis Express C18, Zorbax 300 C18-SB and Acquity BEH C8 were all categorised as neutral phases, but all demonstrated different elution profiles, which demonstrates that phases within the same classification can bestow alternative selectivity. The peak signals for the Polaris Amide C18 in particular were lower than the other stationary phases which is possibly due to signal suppression caused by coeluting ions not monitored in the EIC. In addition to the different selectivity, the Acquity CSH C18 and Polaris Amide C18 both reveal superb peak shape using formic acid conditions. In *Figure 67*, the Polaris Amide C18 suggested a poor PC^{**} might be expected, however, as demonstrated in *Figure 69*, the peaks are sharp and narrow on the amide phase, which supports the idea that the sample peak capacity underestimated the chromatographic performance of that stationary phase. The smaller *PC*** value is related to the narrower elution window for the protocol peptides on the Polaris Amide C18 in comparison to the other stationary phases. The Polaris Amide C18 retention window was on average 26% smaller in formic acid and 31% smaller in ammonium formate compared to the other phases used to build the column characterisation database. This was confirmed when the *PC* measure was used, where the performance improved significantly for the Polaris Amide C18 (*Table 60*).

Selectivity can also be measured between two chromatographic conditions (i.e. two different columns or mobile phases) by plotting the retention time of a set of compounds to derive the regression coefficient (R^2) [109, 153]. The R^2 value can be inserted into *Equation 29 t*o determine the selectivity correlation, where a S value of 0 signifies identical selectivity, whilst a value of 100 identifies orthogonal selectivity.

$$S = 100 \times \sqrt{1 - R^2} \qquad \textit{Equation 29}$$

This approach was applied to the retention times of 11 digest fragments, where each column in *Figure 69* was compared directly to the Ascentis Express C18, as a

typical C18 phase. Results greater than 10 would typically suggest there are some selectivity differences between the two parameters [109]. The S values (*Figure 69*) were all greater than 11, with the largest differences achieved between the Polaris Amide C18 and the Ascentis Express C18 (S = 33), which is quite significant for the fragments.

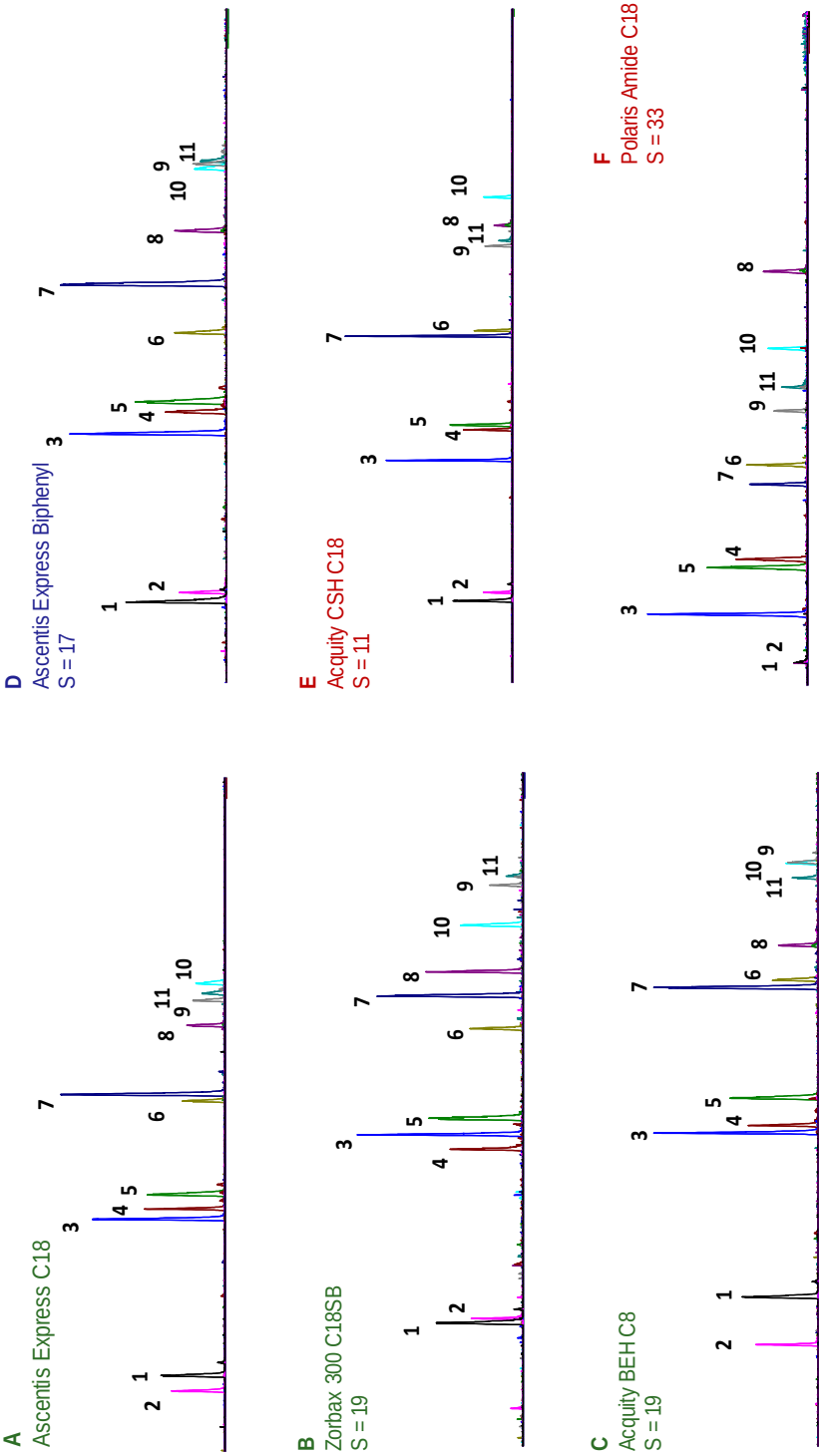

Figure 69 Six stationary phases selected to demonstrate different chromatographic profiles for carbonic anhydrase fragments digested with trypsin. Analyses were performed on the Nexera X2 coupled to the 2020 single quadrupole system. The formic acid conditions utilised a mobile phase of 0.1% formic acid in water and 0.1% formic acid in acetonitrile with 4.5-50%B over 40 minutes. Flow rate was 0.3 mL/min, column oven temperature was 40 °C, and detection used a combination of UV at 215 nm and MS for extracted ions.

As important as choosing stationary phases with different selectivity, it is often crucial to identify phases with similar chromatographic responses. The following phases were identified as potentially providing similar selectivity profiles; Ascentis Express C18 and Poroshell HPH-C18, the Acquity CSH C18 and Luna Omega C18 PS, and finally Kinetex Biphenyl and Ascentis Express Biphenyl. A tryptic digest of carbonic anhydrase was chromatographed using the formic acid gradient conditions described for the peptide characterisation protocol (*Figure 70*). The Poroshell HPH-C18 and Ascentis Express C18 were superimposed in the score plot (*Figure 65*), and clearly demonstrate a similar eluting profile for the peptide fragments. The order of elution as well as the resolution between peaks are extremely similar between the two columns. The Ascentis Express Biphenyl and Kinetex Biphenyl were within proximity to one another in the score plot (*Figure 65*) and contain a similar ligand moiety. In general, the elution profile is very similar, with some subtle differences between the peaks (see peaks 9-11). The final pair, the Luna Omega PS C18 and Acquity CSH C18, have an alkyl moiety with some degree of positive charge on the surface of the phase. Their location within the score plot (*Figure 65*) suggest that some similarity could be expected but also that there are some differences as their positions are not overlaid. The profiles in *Figure 70* confirms that this is the case, where in general, the elution profile is extremely close but there also are selectivity differences between some of the critical pairs. The selectivity correlation was applied to the set of columns, where the Poroshell HPH-C18 was compared to the Ascentis Express C18, the Ascentis Express Biphenyl was correlated against the Kinetex Biphenyl and the Luna Omega PS C18 was evaluated against the Acquity CSH C18. The S-values ranged between 2 and 8, which all demonstrate a close correlation between the predicted pair of similar columns.

Similar selectivity differences were observed for the digest of carbonic anhydrase chromatographed at mid pH and also for the tryptic digest of bovine insulin. Overall, the score plot was successfully used to select stationary phases which could be chromatographically dissimilar with a diverse elution profile or can be used to select phases with similar profiles.

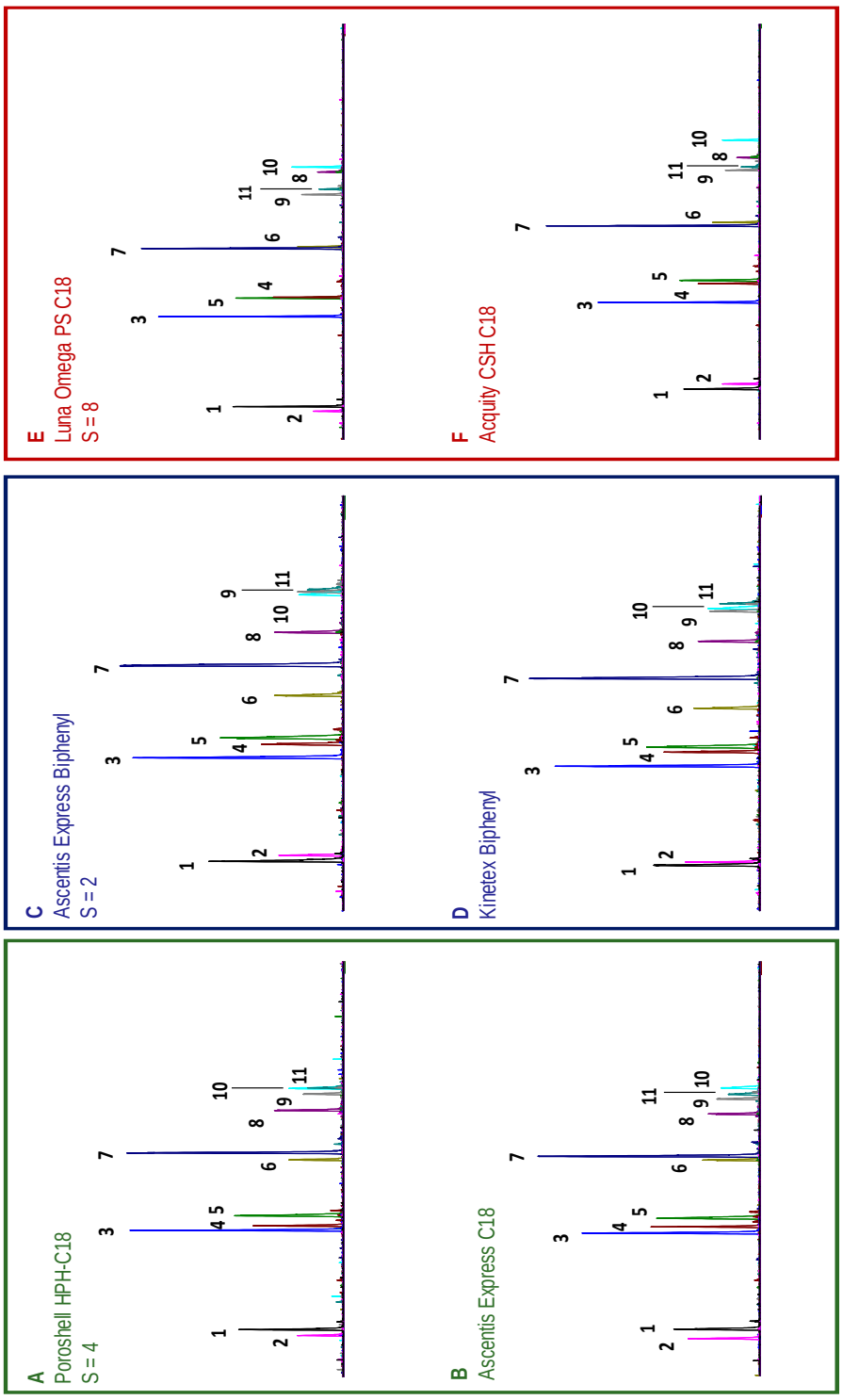

Figure 70 Carbonic anhydrase digest analysed on six stationary phases to demonstrate chromatographic similarities. Analyses were formed on the Nexera X2 coupled to the 2020 single quadrupole system. The formic acid conditions utilised a mobile phase of 0.1% formic acid in water and 0.1% formic acid in acetonitrile with 4.5-50%B over 40 minutes. Flow rate was 0.3 mL/min, column oven temperature was 40 °C, and detection used a combination of UV at 215 nm and MS for extracted ions.

3.8.4 Applying the PCA to Highlight Potential Areas for New Stationary Phase Design

The use of PCA enables the user to visualise the difference or similarities between stationary phases. For example, phases which are located within close proximity are presumed to possess similar chromatographic selectivity, whilst those which are separated can be viewed as chromatographically diverse. This can help to direct the design of new silanes for stationary phases. It is clear that although hydrophobic interactions dominate the retention mechanisms in reversed phase chromatography, there are also other interactions which are important, namely polar and electrostatic interactions.

Phases which could incorporate some form of charge or polar functionality could be of particular interest for peptides and small proteins. Some of the most diverse selectivity was achieved on phases which can incorporate these types of interactions, such as the Polaris Amide C18, Acquity CSH Fluoro Phenyl and the Acclaim WCX. These phases are capable of forming electrostatic and / or polar interactions with the peptides, with different modes of interactions possible depending on the pH conditions. These columns were compared against the neutral Ascentis Express C18 phase, using stick plots of the characterisation data in both formic acid or ammonium formate (*Figure 71*). The Ascentis Express C18 was selected to represent a standard C18 type stationary phase. The comparison demonstrates the different retentivity of charged peptides on phases with positive or negative character. The Ascentis Express C18 (*Figure 71D*) is a neutral phase with little acidic silanol activity, thus the mode of interaction between the stationary phase and peptide is mainly hydrophobic. The Acclaim WCX possessed a similar elution profile under formic acid conditions to the neutral C18 phase which suggests retention is primarily related to the alkyl proportion of the WCX ligand functionality (*Figure 71A)*. [Tyr26]-Bovine GLP-2 (Peptide Number 24) possessed greater relative retentivity on the Acclaim WCX compared to the Ascentis Express C18 which is possibly indicative of polar interactions (i.e. hydrogen bonding) between the polar carboxylic acid moiety and the tyrosine substituted. The Acquity CSH Fluoro Phenyl

and the Polaris Amide C18 (*Figure 71B* and *C* respectively) possessed similar retentivity for the majority of peptides, where the more positively charged [Gly22]-, [Tyr26]- and [Lys26]-Bovine GLP-2 (16-33) (Peptide Numbers 16, 24 and 26, respectively) were repulsed from the positive character stationary phases in comparison to Bovine GLP-2 (1-15) and [L-Asp11]-Bovine GLP-2 (Peptide Numbers 1 and 9, respectively). The change in relative retention for the peptide [Lys26]- was to a greater degree than the other peptides due to the greater positive net charge (*Table 31*). The more positively charged hydrophobic peptides experience a greater repulsion on the Polaris Amide C18 which has a higher degree of positive charge on the ligand, thus having a narrower elution window. This is also evident from the Extended Tanaka protocol, where the negatively charged benzene sulfonic acid was greatly retained on the Polaris Amide C18 [18].

Under intermediate pH conditions, the Acclaim WCX was negatively charged, which caused the negatively charged hydrophilic peptides to elute on the void. [Lys26]-Bovine GLP-2 (16-33) (Peptide Number 26) possessed significant increases in retentivity on the Acclaim WCX in comparison to the remaining peptides due to the positive net charge of the peptide and the fully charged WCX ligand or accessibility into the stationary phase, and selectivity was notably different to other stationary phases evaluated. The Polaris Amide C18 and the Acquity CSH Fluoro Phenyl, whilst chromatographically similar at low pH, demonstrated significant selectivity differences under intermediate pH conditions. The positive character on the Polaris Amide C18 was still present, as demonstrated by the low relative retention of [Lys26]-Bovine GLP-2 (16-33), whilst the negative charged Bovine GLP-2 (1-15) and [L-Asp11]-Bovine GLP-2 (1-15) (Peptide Number 1 and 9) had greater retentivity in comparison to the other phases under the same conditions. The selectivity on the Acquity CSH Fluoro Phenyl, on the other hand, seemed to resemble the Acclaim WCX which suggests a greater degree of negative character on the phase. This could be due to the non end capped silica which result in a higher number of negatively charged silanol groups at intermediate pH causing repulsion of the negatively

charged peptides, and greater retention of the positive net charge of [Lys26]-Bovine GLP-2 (16-33) (Peptide Number 26).

The peptide [Lys26]-Bovine GLP-2 was compared in both formic acid and ammonium formate on the four phases in *Figure 71*. The peak shape on the C18 phase under ammonium formate conditions was significantly improved to the low pH conditions, (peak width decreased from 0.107 to 0.052), as expected with the low ionic strength of the formic acid and the multiply charged peptide. The amide phase gave good peak shape under both mobile phase conditions with peak widths of 0.054 and 0.074, which demonstrates the usefulness of the phase with positive character with low ionic strength additives like formic acid. The fluoro phenyl phase also produced similar peak widths under both mobile phase conditions (0.100 and 0.093), but exhibited broader peaks compared to the amide. The WCX phase, which was assessed using a greater load during the development of the protocol, produced peak widths of 0.154 and 0.161, under low and intermediate pH, respectively.

These results suggest that a form of mixed mode moiety could be a potential direction for future phases for peptide analysis. The score plot in *Figure 65* suggests an empty design space in the 4th quadrant which could be occupied by a mixed mode phase with differing degrees of positive character to both give selectivity which is completely different to a standard C18 column and to give excellent peak shape (See *Section 3.6.7* for the definition of peak capacity and *Section 3.8.1* for the results from the database). The mixed mode moiety has had a few resurgences throughout stationary phase development history, however, there have been a few limiting factors which have contributed to their lack of success. Anecdotally, many tradition SCX, WCX and mixed alkyl / SCX or WCX mixed mode phases have often been perceived to have low batch to batch reproducibility, which has inhibited their successful implementation for various methods. This alleged reproducibility issue often prevents new methods being developed on modern mixed mode phases, although it is not known whether the same issue might persist on new phases. Newer mixed mode phases would need to be evaluated for batch to batch

reproducibility, but they could offer an interesting alternative for stationary phase development.

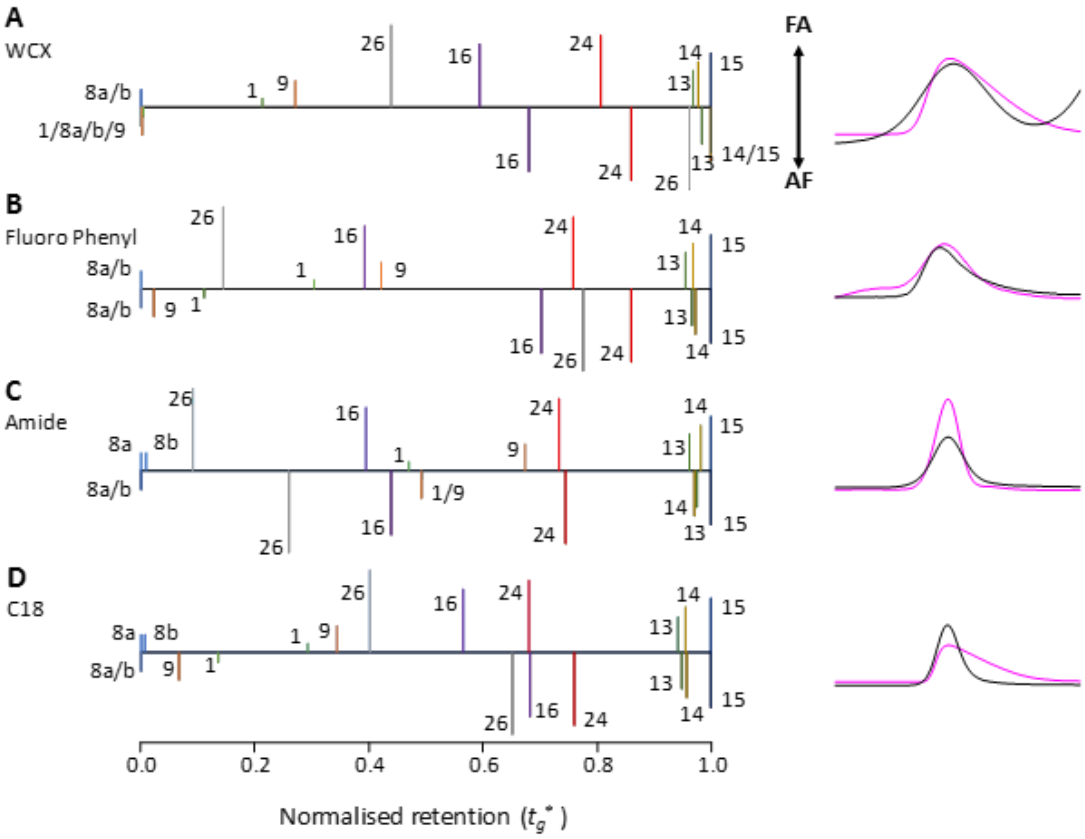

Figure 71 Comparison of normalised retention of the three test mixtures used to characterise the stationary phase in formic acid and ammonium formate on the (A) Acclaim WCX 3 µm TPP, (B) Acquity CSH Fluoro Phenyl 1.7 µm TPP, (C) Polaris Amide C18 3 µm TPP, and (D) Ascentis Express C18 2.7 µm SPP. Peak 1: Bovine GLP-2 (1-15), 8a/b: [Met(O)10]-diastereoisomers, 9: [L-Asp11]-Bovine GLP-2 (1-15), 13: Bovine GLP-2 (16-33), 14: [D-Ser14]-, 15: [Ile26,Leu27]-, 16: [Gly22]-, 24: [Tyr26]-, 26: [Lys26]-Bovine GLP-2 (16-33)

3.9 Mobile Phase Study

3.9.1 Rationale for Mobile Phase Selection

Mobile phases are one of the key operating parameters which can affect selectivity, in addition to the stationary phase. An evaluation of the chromatographic system would not be complete without a study into the effect of different salts, ionic strength, pH and organics. However, with a myriad of combinations of variables including salt type, pH range, type of organic modifier, and additives, the

parameters must be carefully considered to create a feasible package of work. This can be further expanded in the future where this study can provide a fundamental basis from which to work from.

The study was rationally designed to systematically assess a range of pH values using standardised buffers with the addition of different ion pairs or interesting salts. This can allow for a methodical comparison of the different conditions. Additionally, interesting or commonly used additives were evaluated which could potentially identify attractive mobile phase combinations for method development screenings. The results could potentially lead to a greater understanding of retention mechanisms of peptides.

The impact of these variables will only be assessed in the aqueous mobile phase component. Ideally, methods should be created with equal ionic strength in both the aqueous and organic mobile phase reservoirs to avoid changes throughout the gradient. However, as a significant number of variables will be changed through this study, it would not be practical to produce the requisite organic compositions to match the aqueous. In an extension of this work, a smaller study could be performed to produce matching compositions in both the aqueous and organic mobile phase, to determine the data is complementary to the results obtained in this study.

The study was initially performed on a single batch of Ascentis Express C18 material to remove any variation caused by the stationary phase. Stationary phases were dedicated to specific ion pairs to avoid any potential memory effects affecting the validity of the results. An accompanying stationary phase study is described in *Section 3.9.4.4.* The peptide probes used to characterise the mobile phases were those selected to characterise the stationary phases.

The initial study which compared all mobile phases on one stationary phase utilised a premixed solvent of acetonitrile / water (80:20 v/v) for the Mobile Phase B solvent. The gradient was the same as in the original Peptide RPC Column Characterisation Protocol with respect to the MeCN change (i.e. the %B/min change

was consistent). Acetonitrile is the primary organic solvent used for peptide separations due to various physicochemical properties such as low UV cut off (ideal for peptides monitored using 215 nm), low viscosity and pressure drop.

A summary of the mobile phases appraised can be located in *Table 64.* The table contains the buffers, the pH, total ionic strength, the concentration of the additive (i.e. the ion pair), the buffering capacity and its MS compatibility. The buffering capacity measures the resistance of a buffer to changes in pH when acids or bases are added to the solution. Ideally, the buffering capacity should be greater than 5 mM/pH to have sufficient capacity to resist significant changes to the pH. The values in *Table 64* were calculated using BufferMaker software (described in *Section 2.13*). The rationales for each component can be found in *Sections 3.9.1.1* to *3.9.1.6*.

Table 64 Summary of buffers produced to evaluate the effect of salt, pH, ionic strength, chaotropic and kosmotropic salt, and ion pairing reagent. Key: H_3PO_4 = phosphoric acid, $NH_4H_2PO_4$ = ammonium dihydrogen phosphate, FA = formic acid, NH_4FA = ammonium formate, AA = acetic acid, NH_4AA = ammonium acetate, $(NH_4)_2HPO_4$ = ammonium monohydrogen phosphate, NaCl = sodium chloride, Na_2SO_4 = sodium sulfate, $(NH_4)_2SO_4$ = ammonium sulfate, $NaClO_4$ = sodium perchlorate, TEA = triethylamine, TFA = trifluoroacetic acid, HFBA = heptafluorobutyric acid, $BuSO_3$ = sodium butane-1-sulfonic acid, DFA = difluoroacetic acid, MSA = methanesulfonic acid, NH_4OH = ammonium hydroxide, NH_4HCO_3 = ammonium bicarbonate

	Mobile Phase	Mobile Phase Number	pH	Total Ionic Strength (mM)	Additive Concentration (mM)	Approx. Buffering Capacity (mM/pH)	MS Compatible
Base Buffers	$H_3PO_4/NH_4H_2PO_4$	4	2.3	20	-	33	
	FA/NH_4FA	22	3.6	20	-	27	✓
	AA/NH_4AA	28	5.1	20	-	13	✓
	$(NH_4)_2HPO_4/NH_4H_2PO_4$	43	7.5	20	-	4	
	$H_3PO_4/NH_4H_2PO_4$	6	2.3	100	-	97	
	$H_3PO_4/(NH_4)_2HPO_4$	24	3.1	100	-	20	
	$(NH_4)_2HPO_4/NH_4H_2PO_4$	39	7.5	100	-	15	
Salt (NaCl additive)	$NaCl/H_3PO_4/NH_4H_2PO_4$	10	2.3	100	20	33	
	$NaCl/FA/NH_4FA$	23	3.6	100	20	27	
	$NaCl/AA/NH_4AA$	34	5.1	100	20	13	
	$NaCl/(NH_4)_2HPO_4/NH_4H_2PO_4$	38	7.5	100	20	4	
Kosmotropic Salt (Na_2SO_4 or $(NH_4)_2SO_4$ additive)	$Na_2SO_4/H_3PO_4/NH_4H_2PO_4$	9	2.3	100	20	33	
	$(NH_4)_2SO_4/H_3PO_4/NH_4H_2PO_4$	8	2.3	100	20	33	
	$(NH_4)_2SO_4/FA/NH_4FA$	18	3.6	100	20	27	
	$(NH_4)_2SO_4/AA/NH_4AA$	29	5.1	100	20	13	
	$(NH_4)_2SO_4/(NH_4)_2HPO_4/NH_4H_2PO_4$	42	7.5	100	20	4	
Chaotropic Salt ($NaClO_4$ additive)	$NaClO_4/H_3PO_4/NH_4H_2PO_4$	16	2.3	100	20	33	
	$NaClO_4/FA/NH_4FA$	26	3.6	100	20	27	
	$NaClO_4/AA/NH_4AA$	33	5.1	100	20	13	
	$NaClO_4/(NH_4)_2HPO_4/NH_4H_2PO_4$	46	7.5	100	20	4	

TEA (Ion Pair)	TEA/FA/NH_4FA	20	3.6	20	5	27	✓
	TEA/AA/NH_4AA	27	5.1	20	5	13	✓
	TEA/$(NH_4)_2HPO_4$/$NH_4H_2PO_4$	37	7.8	20	5	4	
	TEA/FA/NH_4HCO_3	36	7.9	20	5	3	✓
TFA (Ion Pair)	TFA/H_3PO_4/$NH_4H_2PO_4$	5	2.3	20	5	26	
	TFA/FA/NH_4FA	21	3.6	20	5	20	✓
	TFA/AA/NH_4AA	30	5.1	20	5	13	✓
	TFA/$(NH_4)_2HPO_4$/$NH_4H_2PO_4$	40	7.5	20	5	4	
HFBA (Ion Pair)	HFBA	14	1.8	20	20	48	✓
	HFBA/H_3PO_4/$NH_4H_2PO_4$	13	2.3	20	5	26	
	HFBA/FA/NH_4FA	25	3.6	20	5	20	✓
	HFBA/AA/NH_4AA	32	5.1	20	5	13	✓
	HFBA/$(NH_4)_2HPO_4$/$NH_4H_2PO_4$	49	7.5	20	5	4	
$BuSO_3$ (Ion Pair)	$BuSO_3$/H_3PO_4/$NH_4H_2PO_4$	2	2.3	20	5	27	
	$BuSO_3$/FA/NH_4FA	19	3.6	20	5	20	
	$BuSO_3$/AA/NH_4AA	31	5.1	20	5	10	
	$BuSO_3$/$(NH_4)_2HPO_4$/$NH_4H_2PO_4$	44	7.5	20	5	3	
Miscellaneous	0.1% v/v H_3PO_4 (85% w/w)	3	2.2	8	-	28	
	0.1% v/v FA	1	2.5	2	-	10	✓
	0.1% v/v TFA	11	1.9	13	-	35	✓
	TFA	12	1.8	20	-	69	✓
	0.1% v/v DFA	7	1.9	16	-	-	✓
	0.05% v/v FA / 0.05% v/v TFA	15	2.2	7	-	-	✓
	0.1% v/v MSA	17	1.9	15	-	35	✓
	0.1% v/v NH_4OH (25%)	47	10.8	1	-	0.6	✓
	NH_4FA	41	6.5	20	-	0.1	✓
	NH_4AA	35	7.0	20	-	0.5	✓
	NH_4HCO_3	45	7.9	20	-	3	✓

3.9.1.1 pH Range

The pH measured in the aqueous solution will have a profound effect on ionisable species, such as peptides. The pH can affect the ionisation of functionalities which can be protonated or deprotonated as well as affecting the stationary phase via the

ionisable silanols or functional groups on the ligand moiety. This can impact on the type of interactions the molecule can undergo with the stationary phase, and analyte polarity which can then impact on its retentivity as well as chromatographic performance (i.e. peak shape).

The ionisable amino acids are aspartic acid, glutamine, tyrosine, histidine, lysine and arginine, in addition to the C- and N-terminals, which must be taken into consideration. The pK_a of the amino acids and silanols can be located in *Figure 1* and Reference [139, 140], respectively. The absolute charge *versus* pH for the ionisable amino acids were plotted in *Figure 72*, as well as the absolute charge for silanols and acidic silanols against pH. The pH selection should be primarily based on the charge of the amino acids, to promote either protonation or deprotonation. As such, the pH values selected were pH 2.3, 5.1 and 7.5. This provided a compromise where >90% of the amino acid side chains and the silanols were either ionised or unionised.

At pH 2.3, the C-terminal would be approximately 50% protonated, however, this will be only one amino acid and unavoidable as most peptide separations are performed at low pH. The pH should not be reduced further than pH 2.3 in order to achieve 90% deprotonation, as the vast majority of commercial stationary phases used for peptide separations lack stability under such conditions thus suffer loss of bonded phase by hydrolysis from the silica backbone thereby reducing column lifetime. There are however exceptions to this where it is important to assess common or interesting additives such as 0.1% v/v TFA or methanesulfonic acid (MSA) [154] which both have a pH of 1.9.

In addition to the three pH values stated above, it is suggested pH 3.6 is also used to evaluate the effect of pH. This is despite the greater degree of partial protonation of amino acid side chains, as formate salts are regularly used to analyse peptide separations.

The pH 2.3 and 7.5 can be produced using phosphate buffers, pH 3.6 formed using formate buffers and pH 5.1 created with acetate salts.

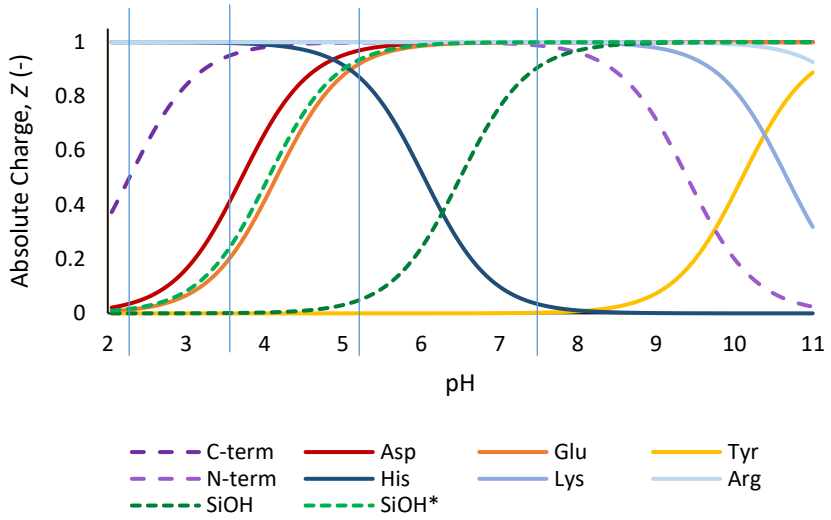

Figure 72 Absolute charge versus pH for amino acids with ionisable side chains, silanols and the C and N terminals. Vertical blue lines indicate the pH values selected for the mobile phase comparison. SiOH denotes the typical pK_a of the silanols whilst SiOH denotes the acidic silanol pK_a*

It is advisable to avoid pH values greater than 7.5 as high pH is an area where amino acids with high pK_a values are partially protonated thus robustness can become a potential problem. It is also possible to undergo on-column deamidation as a result of using high pH conditions [65, 70, 72]. Many buffers suitable for high pH are not robust enough for routine analysis, where the volatility and UV performance at 215 nm are questionable. There can also be reactions with ambient CO_2, which can impact on the reproducibility of the mobile phase. This is in addition to poor stability for many stationary phases which can reduce the column lifetime. There are phases available on the market, such as the Waters BEH range, which can be used at high pH however to produce a manageable experimental design and have a greater representation of what is available on the market, high pH was excluded in the main design. Although carbonate and 0.1% ammonia would produce pH ranges greater than pH 7.5, a column was sacrificed to assess the chromatographic selectivity.

The total net charge for the peptide probes were all calculated using software described in *Section 2.13* for the pH values which will be evaluated through this

study (*Table 65*) based on the information from *Table 64.* The mobile phases assessed covered a range of peptide net charges between -5.0 to +3.7. This should provide a greater understanding of the effect on multiply charged species.

Table 65 Net charge for the peptide probes under different pH conditions.

		Total Net Charge								
Peptide	**Peptide Number**	**pH 1.8**	**pH 2.3**	**pH 2.5**	**pH 3.6**	**pH 5.1**	**pH 6.5**	**pH 7.5**	**pH 7.9**	**pH 10.8**
Bovine GLP-2 (1-15)	1	1.7	1.3	1.2	-0.3	-2.8	-3.7	-4.0	-4.0	-5.0
[Met(O10]-Bovine GLP-2 (1-15)	8	1.7	1.3	1.2	-0.3	-2.8	-4.7	-4.0	-4.0	-5.0
[L-Asp11]-Bovine GLP-2 (1-15)	9	1.7	1.3	1.1	-0.6	-3.8	-3.7	-5.0	-5.0	-6.0
Bovine GLP-2 (16-33)	13	2.7	2.4	2.2	1.3	0.1	0.0	0.0	0.0	-1.6
[D-Ser16]-Bovine GLP-2 (16-33)	14	2.7	2.4	2.2	1.3	0.1	0.0	0.0	0.0	-1.6
[Ile26,Leu27]-Bovine GLP-2 (16-33)	15	2.7	2.4	2.2	1.3	0.1	0.0	0.0	0.0	-1.6
[Gly22]-Bovine GLP-2 (16-33)	16	2.7	2.4	2.2	1.3	0.1	0.0	0.0	0.0	-1.6
[Tyr26]-Bovine GLP-2 (16-33)	24	2.7	2.4	2.2	1.3	0.1	0.0	0.0	0.0	-2.5
[Lys26]-Bovine GLP-2 (16-33)	26	3.7	3.4	3.2	2.3	1.1	1.0	1.0	1.0	-1.3

3.9.1.2 Cation Counter Ion

The cation counter ion should be consistent throughout the different pH values in *Table 64*, to determine the observable differences in selectivity due to the buffer and pH. Common counter ions include ammonium, sodium, potassium and triethyl ammonium ions. These ions provide different properties to the mobile phase which should be considered.

Snyder suggested the silanol activity can be reduced by adding ions that can strongly bind to the silanols [155]. This is in the order $Na^+ < K^+ < NH_4^+ <$ triethyl ammonium$^+$ therefore utilising an ion such as the ammonium ion could reduce the effect of silanol groups or other negatively charged species (i.e. carboxylic acids on the amino acids). Snyder stated that 25 mM potassium ions usually was sufficient to improve the peak shape of most basic small analytes [155].

Another critical parameter includes the solubility of the salt. The general trend suggests that the ammonium ion possesses greater solubility in water than either the sodium or potassium ion [156].

The hygroscopicity of the salt can also impact on the selection of the salt, where sodium or potassium-based salts are less hygroscopic than ammonium salts. However, as previously shown in the hygroscopicity study collated in *Section 3.5.1.1* and 3.7.2.2, the ammonium based mobile phases provided consistent results in regards to pH and chromatographic profiles provided the container was carefully handled (i.e. stored in a desiccator). Failure to handle the ammonium-based salts could result in a loss of ammonia which would alter the pH and potentially the selectivity and reproducibility of the data. An additional measure would be to avoid anhydrous salts since they absorb more water. It is also perceived that solubility is of greater priority than hygroscopicity, thus provided the container is monitored for aggregation this should not prevent the ammonium ion from being selected as the cation.

Based on the properties described above and the inclusion of MS compatible mobile phases which require volatile additives for ionisation, the ammonium ion was selected as the cation counter ion for the different buffers.

3.9.1.3 Ionic Strength

Ionic strength is a measure of the ion concentration in a solution, where it is calculated using Equation 30, which takes into account the charge of the ions present.

$$I = \frac{1}{2}\sum_{i=1}^{n} c_i z_i^2 \qquad \textit{Equation 30}$$

Where c is the concentration and z is the charge of each ion.

As demonstrated through previous chapters, the ionic strength can provide a critical role in the efficiency of the separation. It has previously been observed that the better peak capacities were observed under intermediate pH conditions using 20 mM ionic strength ammonium formate buffer compared to low pH with 0.1% formic acid with an ionic strength of 2 mM. This has also been demonstrated using 20 mM formate buffer adjusted to pH 3.6, which is within close proximity to the pH of formic acid (~pH 2.7), thus demonstrating the improvement is related to ionic strength, and not pH (*Figure 73*). This has also been published in literature by various authors [114, 147, 157]. McCalley showed that high ionic strength is essential in achieving good peak shape for peptides. The ionic strength was increased on a series of formic acid containing mobile phases with vast improvements made to the asymmetry of peptides. By increasing the concentration to 20 mM formic acid plus 20 mM KCl (ionic strength 22 mM) from 20 mM formic acid (ionic strength 1.9 mM), the peak capacity increased by 34% on average for the four peptide peaks assessed and asymmetry decreased on average by 56% [147].

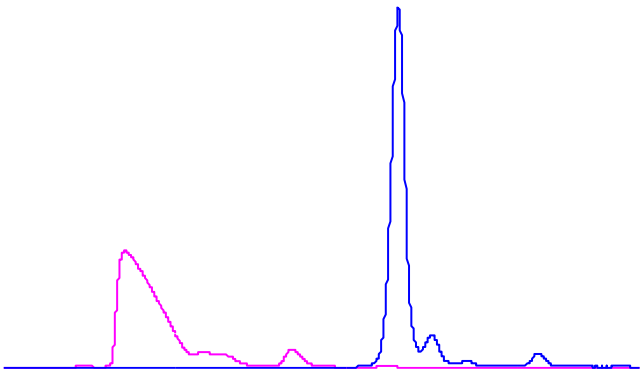

Figure 73 Chromatographic comparison of the effect of ionic strength using Bovine GLP-2 (1-15) where the lower strength 2 mM 0.1% formic acid pH 2.7 (pink trace) produced a stereotypical sharks fin compared against the symmetrical peak 20 mM ammonium formate pH 3.6 (blue trace). Analyses were performed on the Nexera X2 coupled to the 2020 single quadrupole system on the Ascentis Express C18. The formic acid conditions utilised a mobile phase of 0.1% formic acid in water whilst ammonium formate conditions utilised a mobile phase of 20 mM ammonium formate pH 3.6 in water. The organic was acetonitrile / water (80:20 v/v) with a gradient of 5.6-62.5%B over 40 minutes. Flow rate was 0.3 mL/min, column oven temperature was 40 °C, and detection used a combination of UV at 215 nm and MS.

To demonstrate the importance of ionic strength the asymmetry of Bovine GLP-2 (1-15) was measured using different ionic strength and a variety of salts (*Figure 74)*. Scouting experiments suggest that the asymmetry improves substantially above 50 mM and is constant beyond 100 mM for this peptide. Hodges *et al.* also demonstrated the improved peak shapes with 50 mM NaCl or $NaClO_4$ salts [105]. Based on the results in *Figure 74* it would seem to suggest the type of additive (i.e. $(NH_4)_2SO_4$, Na_2SO_4, NaCl, $NaClO_4$) did not cause a significant difference in asymmetry. It is possible that at greater ionic strength, the number of interactions is reduced which could improve peak shape.

As the intention is to be able to discriminate between different buffers and salts, it is important to select an ionic strength which can facilitate this, thus 20 mM should be appropriate for the main comparison of mobile phases. This is quite regularly used within the industry and literature has shown good peak shapes can be obtained from these conditions [47, 157]. Boyes looked at the effect of 20 mM ammonium formate adjusted to pH 3.7 with formic acid [114]. This mobile phase

appeared to yield excellent peak shapes for most basic drugs and peptides on modern columns, and appeared to help retention, particularly as sample load increased [158]. An ionic strength of 100 mM can also be compared to observe the effect of increasing ionic strength on peak shape. This can aid method development where peak shape is critical. Higher concentrations can be used effectively to increase retention in reversed-phase LC by the "salting out" effect or the Le Chatelier's principle to drive solutes into the hydrophobic stationary phase.

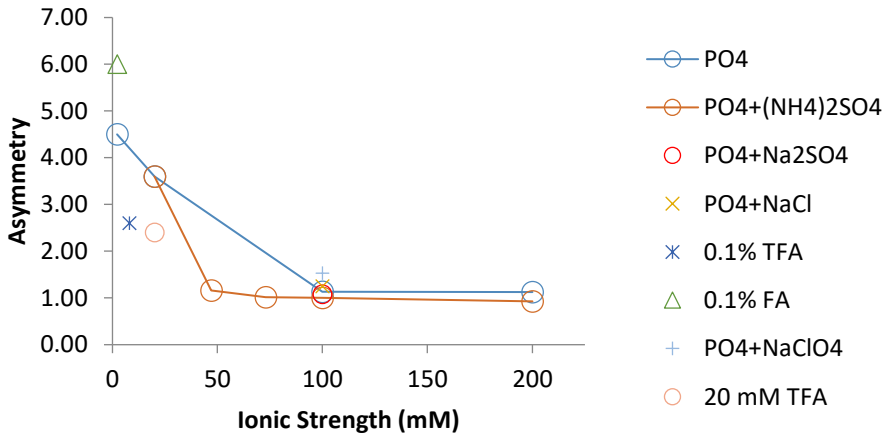

Figure 74 Effect of asymmetry with increasing ionic strength on Bovine GLP-2 (1-15) using different salts. Analyses were performed on the Nexera X2 coupled to the 2020 single quadrupole system on the Ascentis Express C18. The mobile phases are as described in Section 2.12.1.3. The gradient was 5.6-62.5%B over 40 minutes. Flow rate was 0.3 mL/min, column oven temperature was 40 °C, and detection used UV at 215 nm.

3.9.1.4 Ion Pair Reagents

Ion-pairing reagents are detergent-like molecules added to the mobile phase to provide retention to acidic or basic analytes [45]. There are different theories as to how the ion pairing reagent affects selectivity. The possible retention processes include partition model and adsorption model [97, 159, 160]. The partition model suggests that the analyte interacts with the ion pairing agent in the mobile phase initially. The new ion paired species would possess different physicochemical properties to the ionisable analyte, which affects its chromatographic retentivity. The new species can then partition into the stationary phase where it is retained.

The second theory suggests that the ion pair reagent is adsorbed into the stationary phase, where the hydrophobic alkyl tail is attracted to the non-polar stationary phase. The exposed ionic moiety on the ion pair is then available to undergo electrostatic interactions with the analyte which then increases the retention of the species. The analyte properties differ depending on the type of ion pairing reagent used, thus it is advantageous to observe the effect of different types of common ion pairs on the effect of selectivity.

TFA is the most common ion pair used for the analysis of peptides, where good chromatographic performance can be achieved and is MS compatible [161]. It can reduce silanol activity and improve overloading effects, thus is regularly used for peptide applications. Typical levels used within peptide applications are 0.1% v/v TFA, which has an ionic strength of 13 mM. This should be compared against a 20 mM solution of TFA in terms of chromatographic performance and selectivity. A 20 mM solution can also be assessed against the 20 mM salt-based systems.

Literature suggests there are some signal suppression effects whilst using TFA, due to various ion pairing effects during ionisation in the MS source [47, 114, 162]. Difluoroacetic acid (DFA) is a potential alternative to TFA, as it is a weaker ion pair, thus doesn't experience as much ion suppression [163]. Boyes *et al*. suggested DFA is significantly easier to remove from the LC system than TFA and demonstrated no prolonged deleterious effects in the instrument. However, the impact on ESI signal intensities are much greater for peptides and small proteins than larger proteins [162]. They also demonstrated the improved MS response compared to TFA and peak performance in contrast to formic acid [162]. It is typical to also use 0.1% v/v DFA on peptide applications, thus this can be comparable to 0.1% v/v TFA, particularly in regard to the MS signal. The purity and quality of the DFA can be a significant issue for its regular use in peptide separations however, there are a few vendors supplying high quality reagents specifically for MS use (Waters and Supelco).

Another alternative to using TFA could be to use a combination of formic acid and TFA, to obtain the chromatographic performance of TFA and the MS response from formic acid [157].

Other homologous fluorinated carboxylic acid additives are frequently used as hydrophobic anionic ion pairs (i.e. pentafluoropropionic acid (PFPA) and heptafluorobutyric acid (HFBA)). Flieger applied different perfluorinated acids to basic β-blockers to alter the retention behaviour by using different concentrations of ion pair as well as different volumes of methanol [164]. The longer chain on the anionic ion pair increased the retention, efficiency and peak shape of the analytes. It is also possible to influence the retention of analytes by either hydrophobic or electrostatic interactions, by altering the concentration of the ion pair. The adsorption of excess ion pair onto the column changed the polarity of the phase, which in turn altered the retention. HFBA has been used in various applications, including peptide separations, with some good chromatographic performance [74, 164-167].

Triethylamine (TEA) is another common ion pair regularly used for the analysis of peptides, which acts as a cationic reagent. However, the pH 2.3 value standardised for H_3PO_4 / $NH_4H_2PO_4$ could not be obtained with the addition of TEA based on Buffer Maker calculations, therefore this combination was not evaluated. In addition, TEA may not be able to act as an ion pair at this pH as the peptides would be positive charged. A combination of TEA / FA / NH_4HCO_3 pH 7.9 was evaluated instead.

A different range of ion pairs includes the alkylsulfonic acids, which are quite possibly one of the most well-known type of ion pair. These types of ion pair are available in a series of alkyl chains, which affects the properties of the additive, thus the final ion pair with the analyte. However, as alkylsulfonic acids are not MS compatible only $BuSO_3$ was selected to observe the chromatographic effect.

Some chaotropic salts are also known to be ion pairs, however, this shall be evaluated against kosmotropic salts, which shall be discussed in greater detail in

Section 3.9.1.5. The *logD* for each ion pair used at the four pH values was summarised in *Table 66*. Values were determined using Percepta software (ACD/inc) (*Section 2.13*). The value for sodium perchlorate could not be determined for an inorganic molecule therefore was not included within the table.

Table 66 logD values at pH 2.3, 3.6, 5.1 and 7.5 for the ion pair reagents used in the mobile phase study. Sodium perchlorate was not included as the logD could not be determined for inorganic compounds

Ion Pair	pK_a	logD pH 2.3	logD pH 3.6	logD pH 5.1	logD pH 7.5
TFA	0.0 ±0.1	-1.58	-2.62	-3.07	-3.09
DFA	1.3 ±0.1	-0.9	-2.05	-3.34	-3.63
HFBA	0.4 ±0.1	0.69	-0.42	-1.09	-1.13
$BuSO_3$	1.9 ±0.5	-1.35	-2.4	-3.83	-4.32
TEA	10.6 ±0.3	-1.42	-1.42	-1.42	-1.13

3.9.1.5 Kosmotropes and Chaotropes

The meaning of kosmotrope (order-making) and chaotropes (disorder-making) have been applied to several instances, which has created some debate as to the appropriateness of each definition [168, 169]. This merging of definitions makes them a complex phenomenon to understand [168]. The original context for kosmotropes and chaotropes was applied to understand the effect a solute had on proteins (i.e. whether a solute stabilises or destabilises a protein structure, which in turn affects its solubility and folding).

Certain salts affect the solvation shell of peptides and proteins and thus how they interact between the mobile phase and stationary phase. These can be classified based on their ability to structure water (kosmotropic) or break water structures (chaotropic). Both non-ionic and ionic kosmotropic and chaotropic salts exist, however, for the purpose of this study, only ionic salts were considered. The behaviour of ionic kosmotropes and chaotropes follows the Hofmeister series (*Figure 75*), which describes the ability to salt out proteins, where the CO_3^{2-} salt has the greatest propensity to salt out proteins. The order in the Hofmeister series is based on the minimum concentration necessary to cause protein precipitation

[170]. The degree of change made to the solvation shell is dependent on the type of counterion used and concentration [171-173].

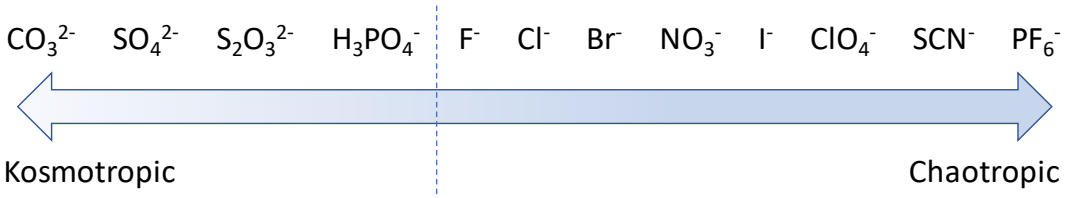

Figure 75 Hofmeister series. Adapted from [171]

There are various assumptions as to how these interesting additives impact chromatography [171]. Chaotropic salts have the potential to form ion pairs with a cation to form a neutral species with different properties which alters the retention in reversed-phase separation systems. The salt could also form interactions with the stationary phase to alter the surface of the silica. There could potentially be a charge deposited on the surface of the silica, which then permits electrostatic interactions between the cation and the chaotrope. Another suggested mechanism is based on the structure of the agent. The chaotropic agent can possess a delocalised charge which affects the degree of solvation. This can impact on the way in which water is ordered, where water is preferentially structured and capable of forming hydrogen bonds. In the presence of a positively charged basic species, such as a peptide, the chaotrope can also disrupt the solvent shell surrounding the analyte. This change in the shell altered the hydrophobicity of the compound, thus altering the retention [174]. It is highly probable that there is a culmination of several mechanisms operating at once.

The kosmotropic salt works in the opposite manner, where the solvent shell is enhanced around the analyte, which based on the Hofmeister series, dictates the ease of which a peptide can precipitate by salting out. The altered solvent shell could alter the effective hydrophobicity of the compound, which can then change the retention profile.

A strong chaotropic salt is difficult to select as there are a number of issues with most chaotropes, namely that they are toxic, have a high UV absorbance and can be quite reactive [171, 172]. Potential candidates include SCN^-, ClO_4^-, NO_3^-, I^-, PF_6^- and BF_4^- ions, which form neutral ion pairs under acidic conditions in reversed-phase chromatography [174]. LoBrutto *et al.* first applied chaotropic salts as an additive in reversed-phase chromatography for amines [172]. They established that the perchlorate ion offered vast improvements in tailing, efficiency, and selectivity, thus demonstrating the advantages of utilising such an additive. Hearn *et al.* further demonstrated the diverse chromatographic responses for proteins which can be achieved using this category of salts [167], which suggests there is merit in evaluating chaotropic salts in an initial study. Hodges *et al.* also utilised perchlorate based mobile phases, where they noted that positive charged peptides exhibited much longer retention with the addition of the chaotropic salt [105, 175]. This was rationalised by the ion pairing properties of the perchlorate ion which increased the hydrophobicity of the peptides to increase retention. The collaboration between Guillarme and Regalado *et al.* demonstrated the use of $NaClO_4$ and KPF_6 as regular mobile phase additives in a generic method development platform for new small molecule drug substances [176, 177]. PF_6^- was showed to possess improved resolution, peak shape and efficiency in addition to vast selectivity differences on a range of small molecule drugs and dimeric catalysts with impurities. They also illustrated the effect of increasing chaotropic concentration to alter retentivity.

Both $(NH_4)_2SO_4$ and Na_2SO_4 shall be evaluated as kosmotropic salts under low pH conditions (100 mM pH 2.3 H_3PO_4 / $NH_4H_2PO_4$) to establish if there is any discernible difference between the ammonium and sodium ion. The counterion is thought to be less influential than the anion. Only $NaClO_4$ was selected as the chaotropic salt as it has been the most commonly used, historically. It was used establish the extent of the selectivity differences to ascertain if it is advantageous to utilise these types of additives.

3.9.1.6 Miscellaneous Mobile Phase Additives

0.1% v/v phosphoric acid (85% w/w) can be appraised against 0.1% v/v formic acid, 0.1% v/v TFA, 0.1% v/v DFA, 0.1% v/v NH_4OH (of a 35% w/w NH_4OH solution), 0.05% v/v TFA / 0.05% v/v FA and 0.1% v/v methane sulfonic acid (MSA). This series of mobile phases can assess chromatographic differences at low pH (except 0.1% NH_4OH) for common acidic modifiers.

3.9.2 Evaluation of Mobile Phase Additives on the Chromatographic Response on the Ascentis Express C18

The retention time (t_g), normalised retention (t_g^*), peak width at 50% ($w_{50\%}$), peak capacities (*PC* and *PC***), tailing and peak area were all recorded for the peptide test mixtures (data not shown), as well as an overloaded degraded sample of Bovine GLP-2 (1-15). The overloaded, degraded sample was analysed to compare impurity profiles between the different mobile phases and to better assess the effect of ionic strength on peak shape for typically overloaded samples. Where applicable, the MS response was also recorded for the test mixtures (response reported in this study was for the Bovine GLP-2 (1-15) (Peptide Number 1) (see *Section 3.9.3* for a discussion of the results).

The delta value responses were recorded in *Table 67* for the different mobile phase combinations, as well as the retention window and average peak width. The delta value information was then analysed using chemometric analysis (PCA). The biplot in *Figure 76* condensed all the variables to two principal components and described approximately 86% of the variability. The position of the delta values within the biplot suggest that the first principal component is dominated by electrostatic interactions (62% of the variability described using PC1), where the probes which measure increases in negative or positive character are at opposite ends of the x-axis (comparison of Δ(9,1) and Δ(26,13) increase in negative charge and increases in positive charge, respectively). The probes Δ(8a,1), Δ(16,13) and Δ(24,13), which measure oxidation, changes in aromatic character and phenolic interactions,

respectively, are all closely located to Δ(26,13). Their position within the biplot needs greater clarity to understand their location. The second principal component appears to be mostly related to steric interactions (comparison of Δ(14,13) and Δ(15,13) which measure racemisation and switch in amino acid sequence (24% of the variability described using PC2).

The pH 10.8 0.1% v/v NH_4OH condition was not recorded in the score plot as the most hydrophilic peptides could not be identified in the chromatogram. This is possibly due to the net charge of the three hydrophilic peptides which have a net charge of either -5.0 or -6.0 at pH 10.8. The silanols would be deprotonated and thus mutual repulsion could cause the peptides to elute on the void. It was initially thought the peptides could exhibit such poor peak shape, each probe could not be distinguished from the baseline. However, an overloaded Bovine GLP-2 (1-15) sample which had a net charge of -5.0 could not be located thus concluded the peptides eluted on the void.

The biplot was interrogated in more detail in *Sections 0-3.9.2.4* based on the rationales previously described.

Table 67 Delta values for the peptide probes determined on the different mobile phase combinations

pH 2.3 20 mM H_3PO_4/$NH_4H_2PO_4$	4	11.480	25.030	13.542	0.104	-0.29	0.05	0.00	0.05	0.05	-0.35	-0.25	-0.49
pH 3.6 20 mM FA/NH_4FA	22	11.670	26.750	15.080	0.099	-0.28	0.03	0.02	0.05	0.05	-0.35	-0.25	-0.47
pH 5.1 20 mM AA/NH_4AA	28	8.636	27.410	18.778	0.096	-0.20	-0.03	0.02	0.06	0.06	-0.30	-0.22	-0.37
pH 7.5 20 mM $(NH_4)_2HPO_4$/$NH_4H_2PO_4$	43	5.295	27.700	22.408	0.113	-0.12	-0.07	0.01	0.05	0.05	-0.26	-0.18	-0.28
pH 2.3 100 mM H_3PO_4 / $NH_4H_2PO_4$	6	13.570	26.140	12.574	0.095	-0.28	0.05	0.00	0.05	0.05	-0.35	-0.25	-0.48
pH 3.1 100 mM H_3PO_4 / $(NH_4)_2HPO_4$	24	13.427	26.470	13.043	0.095	-0.27	0.04	0.01	0.05	0.05	-0.35	-0.25	-0.47
pH 7.5 100 mM $(NH_4)_2HPO_4$ / $NH_4H_2PO_4$	39	8.298	27.690	19.394	0.098	-0.12	-0.06	0.01	0.05	0.05	-0.28	-0.20	-0.33
pH 2.3 100 mM NaCl / H_3PO_4 / $NH_4H_2PO_4$	10	12.606	26.686	14.080	0.096	-0.28	0.05	0.00	0.04	0.04	-0.33	-0.23	-0.46
pH 3.6 100 mM NaCl / FA / NH_4FA	23	13.150	27.440	14.287	0.095	-0.26	0.03	0.02	0.05	0.05	-0.35	-0.24	-0.45
pH 5.1 100 mM NaCl / AA / NH_4AA	34	15.410	38.880	23.469	0.195	-0.15	-0.05	0.01	0.05	0.05	-0.26	-0.18	-0.31
pH 7.5 100 mM NaCl / $(NH_4)_2HPO_4$ / $NH_4H_2PO_4$	38	7.020	26.455	19.435	0.224	-0.15	-0.06	0.01	0.05	0.04	-0.29	-0.20	-0.32
pH 2.3 100 mM Na_2SO_4 / H_3PO_4 / $NH_4H_2PO_4$	9	12.070	26.470	14.395	0.129	-0.28	0.04	0.00	0.04	0.04	-0.34	-0.24	-0.45
pH 2.3 100 mM $(NH_4)_2SO_4$ / H_3PO_4/$NH_4H_2PO_4$	8	11.930	26.280	14.352	0.130	-0.28	0.04	0.00	0.04	0.04	-0.34	-0.24	-0.45
pH 3.6 100 mM $(NH_4)_2SO_4$ / FA / NH_4FA	18	9.614	17.26	7.651	0.099	-0.25	0.03	0.02	0.06	0.06	-0.37	-0.26	-0.48
pH 5.1 100 mM $(NH_4)_2SO_4$ / AA / AH_4AA	29	8.561	26.760	18.197	0.094	-0.20	-0.03	0.02	0.05	0.05	-0.30	-0.22	-0.37
pH 7.5 100 mM $(NH_4)_2SO_4$ / $(NH_4)_2HPO_4$ / $NH_4H_2PO_4$	42	6.563	27.550	20.985	0.106	-0.16	-0.02	0.01	0.05	0.05	-0.27	-0.19	-0.31
Mobile phase number		t_g min	t_g max	t_g range	w_{avg}	Δ(8a,1)	Δ(9,1)	Δ(14,13)	Δ(15,13)	Δ(16,13)	Δ(24,13)	Δ(26,13)	

Table 67 Ctd. Delta values for the peptide probes determined on the different mobile phase combinations

pH 2.3 100 mM $NaHClO_4$ / H_3PO_4 / $NH_4H_2PO_4$	16	15.110	32.050	16.946	0.110	-0.25	0.04	-0.01	0.03	-0.30	-0.21	-0.37
pH 3.6 100 mM $NaClO_4$ / FA / NH_4FA	26	12.820	30.790	17.963	0.114	-0.25	0.02	0.01	0.04	-0.30	-0.20	-0.35
pH 5.1 100 mM $NaClO_4$ / AA / NH_4AA	33	7.918	28.800	20.886	0.101	-0.19	-0.04	0.02	0.05	-0.28	-0.19	-0.31
pH 7.5 100 mM $NaClO_4$ / $(NH_4)_2HPO_4$ / $NH_4H_2PO_4$	46	4.569	28.540	23.969	0.114	-0.11	-0.06	0.01	0.04	-0.25	-0.18	-0.26
pH 3.6 20 mM TEA / FA / NH_4FA	20	11.520	27.360	15.844	0.108	-0.29	0.03	0.02	0.06	-0.35	-0.25	-0.47
pH 5.1 20 mM TEA / AA / NH_4AA	27	9.161	28.400	19.240	0.108	-0.21	-0.02	0.02	0.06	-0.31	-0.22	-0.39
pH 7.8 20 mM TEA / $(NH_4)_2HPO_4$ / $NH_4H_2PO_4$	37	8.905	28.200	19.295	0.098	-0.10	-0.05	0.01	0.05	-0.28	-0.20	-0.32
pH 7.9 20 mM TEA / FA / NH_4HCO_3	36	8.419	27.830	19.410	0.125	-0.10	-0.05	0.01	0.05	-0.28	-0.20	-0.32
pH 2.3 20 mM TFA / H_3PO_4 / $NH_4H_2PO_4$	5	13.790	26.390	12.595	0.097	-0.27	0.05	0.00	0.05	-0.35	-0.25	-0.50
pH 3.6 20 mM TFA / FA / NH_4FA	21	11.800	27.890	16.095	0.107	-0.28	0.03	0.02	0.05	-0.35	-0.25	-0.47
pH 5.1 20 mM TFA / AA / NH_4AA	30	8.225	28.500	20.272	0.111	-0.20	-0.03	0.02	0.06	-0.29	-0.21	-0.35
pH 6.8 20 mM TFA / $(NH_4)_2HPO_4$ / $NH_4H_2PO_4$	40	5.022	26.620	21.596	0.244	-0.15	-0.09	0.01	0.05	-0.27	-0.20	-0.29
pH 1.8 20 mM HFBA	14	22.510	36.820	14.304	0.107	-0.23	0.04	0.00	0.04	-0.32	-0.22	-0.38
pH 2.3 20 mM HFBA / H_3PO_4 / $NH_4H_2PO_4$	13	16.400	28.590	12.188	0.089	-0.24	0.04	0.00	0.04	-0.33	-0.23	-0.41
pH 3.6 20 mM HFBA / FA / NH_4FA	25	14.260	28.520	14.257	0.087	-0.24	0.02	0.02	0.05	-0.32	-0.22	-0.38
pH 5.1 20 mM HFBA / AA / NH_4AA	32	8.742	28.000	19.259	0.091	-0.17	-0.04	0.02	0.05	-0.28	-0.19	-0.29
Mobile phase number		t_g min	t_g max	t_g range	w_{avg}	Δ(8a,1)	Δ(9,1)	Δ(14,13)	Δ(15,13)	Δ(16,13)	Δ(24,13)	Δ(26,13)

Table 67 Ctd. Delta values for the peptide probes determined on the different mobile phase combinations

Mobile phase number	45	35	41	17	15	7	12	11	1	3	44	31	19	2
	pH 7.8 20 mM NH_4HCO_3	**pH 7.0 20 mM NH_4AA**	**pH 6.5 20 mM NH_4FA**	**pH 1.9 0.1% MSA**	**pH 2.2 0.05%TFA / 0.05%FA**	**pH 1.9 0.1% DFA**	**pH 1.8 20 mM TFA**	**pH 1.9 0.1% TFA**	**pH 2.5 0.1% FA**	**pH 2.2 0.1% H_3PO_4**	**pH 7.5 20 mM $BuSO_3$ / $(NH_4)_2HPO_4$ / $NH_4H_2PO_4$**	**pH 5.1 20 mM $BuSO_3$ / AA / NH_4AA**	**pH 3.6 20 mM $BuSO_3$ / FA / NH_4FA**	**pH 2.3 20 mM $BuSO_3$ / H_3PO_4 / $NH_4H_2PO_4$**
t_g min	5.601	7.094	5.329	20.200	21.060	11.900	13.900	13.690	10.640	12.600	5.610	9.429	13.230	14.070
t_g max	27.690	27.490	26.860	33.040	36.900	25.610	28.230	27.870	23.390	24.580	27.740	27.870	27.440	27.120
$_{tg}$ range	22.090	20.395	21.528	12.839	15.838	13.709	14.328	14.180	12.751	11.975	22.130	18.441	14.218	13.044
w_{avg}	0.148	0.147	0.099	0.114	0.164	0.117	0.104	0.107	0.154	0.125	0.100	0.092	0.095	0.057
Δ(8a,1)	-0.11	-0.08	-0.14	-0.39	-0.30	-0.28	-0.27	-0.27	-0.29	-0.27	-0.13	-0.13	-0.25	-0.27
Δ(9,1)	-0.07	-0.10	-0.07	0.06	0.05	0.05	0.05	0.05	0.05	0.05	-0.08	-0.03	0.03	0.04
Δ(14,13)	0.01	0.01	0.01	0.00	0.00	0.00	-0.01	-0.01	0.01	0.00	0.01	0.02	0.02	0.01
Δ(15,13)	0.05	0.05	0.05	0.03	0.03	0.04	0.04	0.04	0.06	0.05	0.05	0.06	0.06	0.05
Δ(16,13)	-0.26	-0.27	-0.27	-0.27	-0.32	-0.34	-0.34	-0.34	-0.38	-0.37	-0.25	-0.30	-0.35	-0.36
Δ(24,13)	-0.18	-0.20	-0.19	-0.18	-0.20	-0.24	-0.23	-0.23	-0.26	-0.26	-0.18	-0.22	-0.25	-0.25
Δ(26,13)	-0.28	-0.29	-0.30	-0.40	-0.47	-0.49	-0.45	-0.46	-0.54	-0.54	-0.27	-0.35	-0.46	-0.48

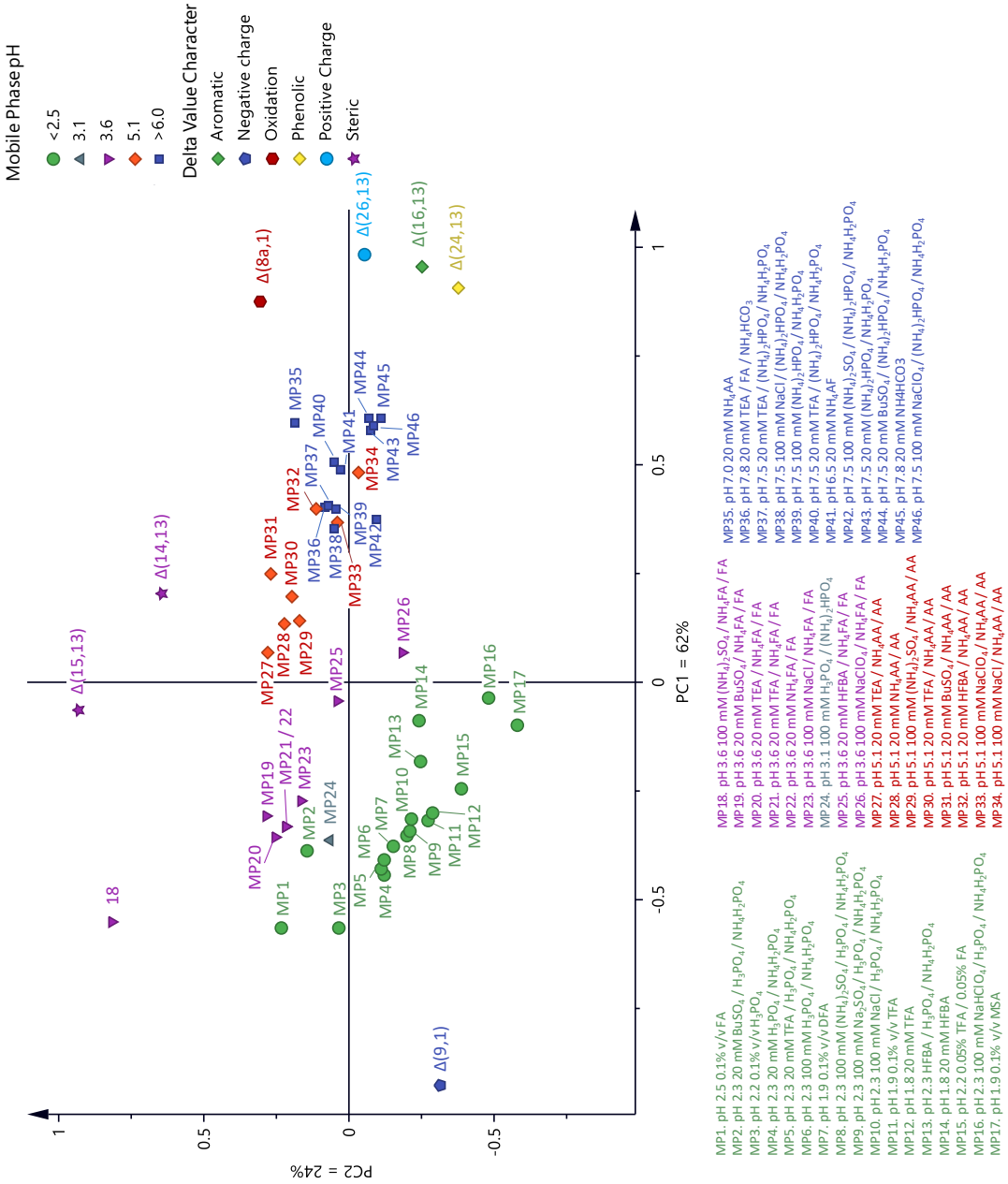

Figure 76 Biplot of the 48 mobile phases described in Table 64 assessed on the Ascentis Express C18

The variables in the biplot aid the understanding for the position of the observation. This is also demonstrated in *Figure 77,* where the chromatograms demonstrated the typical responses observed under various chromatographic conditions for a particular selectivity measure. The direction of each delta value in the PCA is present to illustrate the vector of each parameter. The chromatograms were

aligned for the base sequence peptide which is used to calculate the respective delta value. The pink traces were from mobile phase conditions predominantly in the 3rd and 4th quadrants (i.e. pH values <3.6), whilst the black traces used for comparison were from the 1st or 2nd quadrants (i.e. pH >5.1).

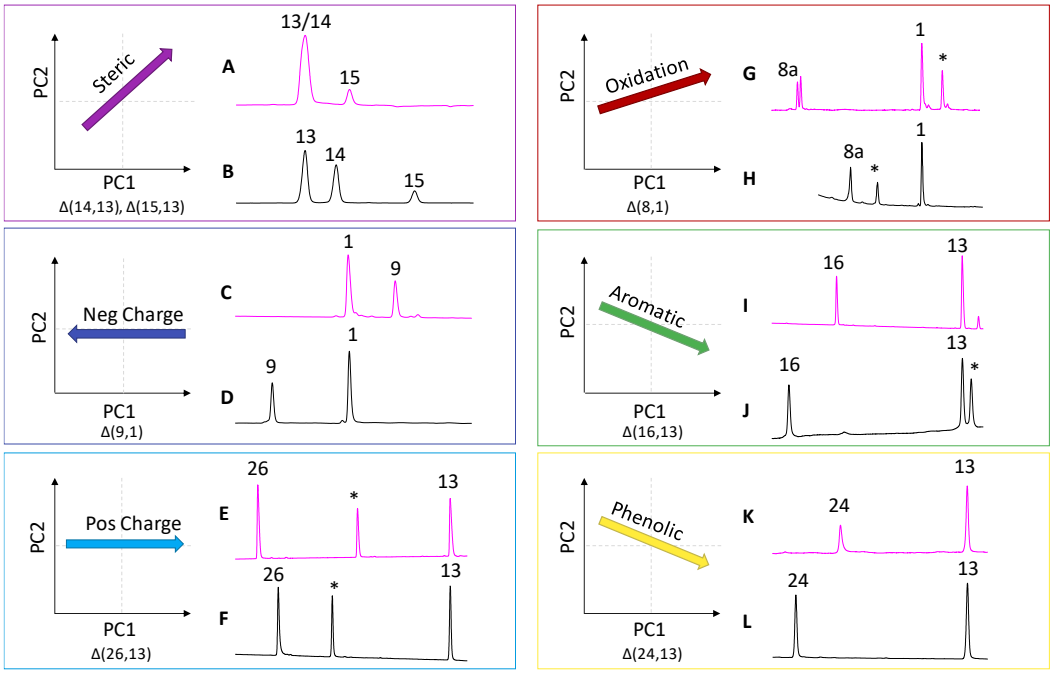

Figure 77 Chromatograms demonstrating selectivity differences determined by the delta values Δ(8a,1), Δ(9,1), Δ(14,13), Δ(15,13), Δ(16,13), Δ(24,13) and Δ(26,13) using the chromatographic conditions (A) pH 1.9 0.1% v/v MSA, (B) pH 5.1 20 mM $BuSO_3$ / AA / NH_4AA, (C) pH 2.2 0.1% v/v H_3PO_4, (D) pH 7.8 20 mM TEA / FA / NH_4HCO_3, (E) pH 2.2 0.1% v/v H_3PO_4, (F) 20 mM pH 7.0 NH_4AA, (G) pH 2.5 0.1% v/v FA, (H) pH 7.9 20 mM $NH4HCO_3$, (I) pH 2.3 20 mM TFA / H_3PO_4 / $NH_4H_2PO_4$, (J) pH 5.1 100 mM NaCl / AA / NH_4AA, (K) pH 3.6 100 mM $(NH_4)_2SO_4$ / FA / NH_4FA, (L) pH 7.5 20 mM $BuSO_3$ / $(NH_4)_2HPO_4$ / $NH_4H_2PO_4$. Analyses were performed on the Nexera X2 coupled to the 2020 single quadrupole system (where applicable) on the Ascentis Express C18. The aqueous portion can be located in Section 2.12.1.3. The organic was acetonitrile / water (80:20 v/v) with a gradient of 5.6-62.5%B over 40 minutes. Flow rate was 0.3 mL/min, column oven temperature was 40 °C, and detection used a combination of UV at 215 nm and MS for peak confirmation. denotes a peptide probe not used to calculate the specific delta value*

The *PC* and *PC*** values were recorded in *Figure 78* where they generally demonstrated complementary information regarding the peptide probes. The *PC*** measurements appeared to suggest there is a slight trend where the chromatographic performance increased with pH. However, this is not supported by

the *PC* measurements, where there is a lack of trend. The results also do not demonstrate the improved chromatographic performance expected with increased ionic strength. This, however, is perhaps unsurprising as the peptide probes are not overloaded, therefore there is less to discriminate between the higher and lower ionic strengths.

The peak capacity was greater in AA / NH_4AA compared to FA / NH_4FA in all circumstances which could be due to the pH of the mobile phases. At pH 3.6, some ionisable amino acids will be partially protonated compared to pH 5.1 which could possibly lead to more tailing and greater peak widths, which would then impact on the measurement of peak capacity.

The greater ionic strength mobile phases did not demonstrate significant improvements in peak capacity which was rationalised based on the sample load. The peaks were not overloaded thus there was little advantage in increasing the ionic strength. In the case of an overloaded sample, it would be expected that the 100 mM ionic strength mobile phases would have more advantages over 20 mM. The peak asymmetry was a better representation for demonstrating the improved chromatographic performance using higher ionic strength (*Figure 79*). pH 2.5 0.1% v/v FA had considerable tailing of the overloaded Bovine GLP-2 (1-15) peptide, where a characteristic shark fin shape was exhibited. This is expected due to the low ionic strength. However, it is also important to note that pH 1.9 0.1% v/v TFA also presented tailing of the peak, which demonstrates that although it is commonly used for peptide applications, TFA may not be the most appropriate additive for a method.

In general, the mobile phases with 100 mM total ionic strength produced quite symmetrical peaks. The peak is usually considered symmetrical with an asymmetry value between 0.8-1.2. The mobile phases which fell within this region were highlighted in *Figure 79* with green bars. The perchlorate mobile phases typically generated excellent peak shape and good peak capacities, however, perchlorate would not be a first choice for a mobile phase additive in a screening strategy due

to the issues previously described. NaCl or $(NH_4)_2SO_4$ could be viable alternatives to increase the ionic strength to 100 mM to generate superior peak shapes.

Figure 78 Peak capacity measurements for the 45 mobile phases evaluated

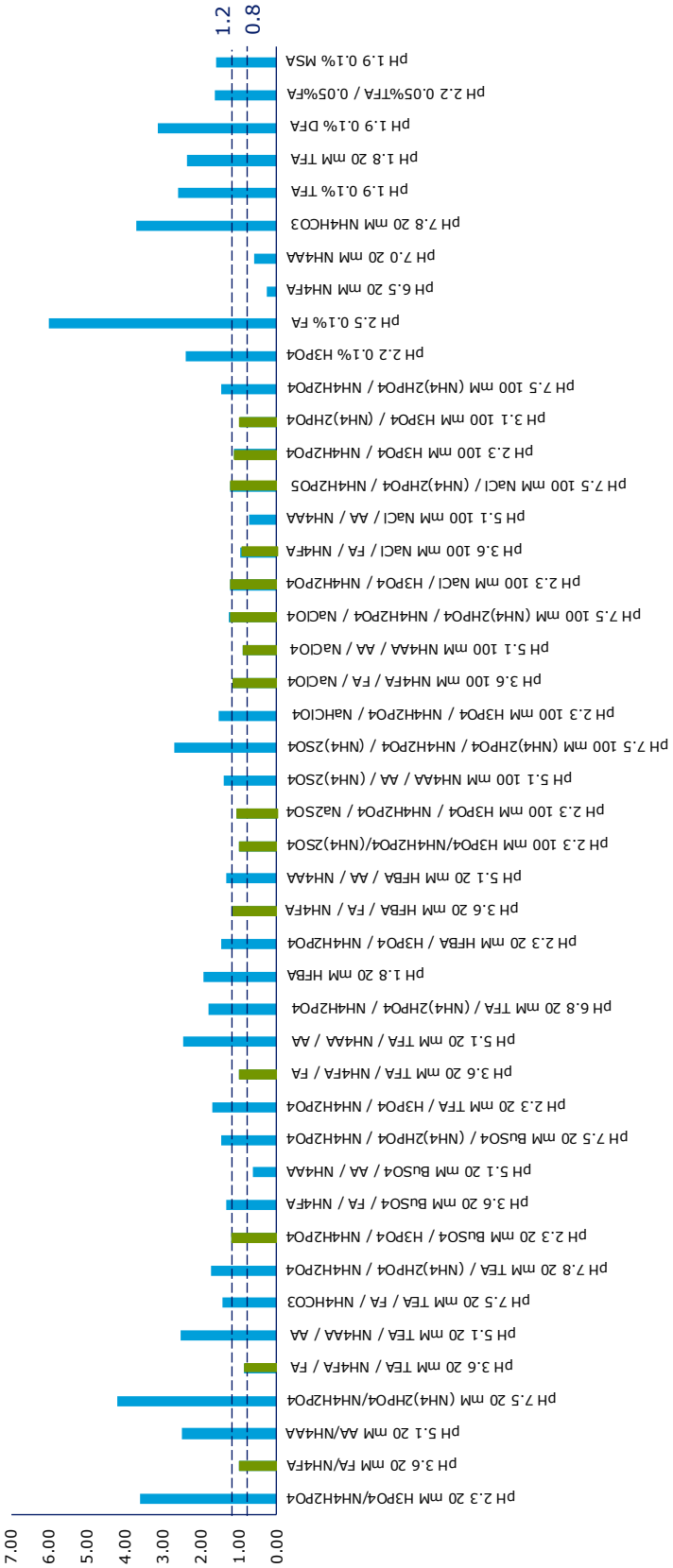

Figure 79 Peak asymmetry measured using overloaded Bovine GLP-2 (1-15) on the different mobile phases. Green bars highlight asymmetry between 0.8-1.2.

3.9.2.1 Effect of pH

The observations from the biplot would suggest the first principal component was dominated by the change in pH, where the pH increases from pH <2.5 in the 3rd and 4th quadrants to pH >6.0 in the 1st and 2nd quadrants. The positions of the pH <2.5 mobile phases are quite widespread in the 3rd and 4th quadrants of the plot, suggesting significant selectivity differences can be observed under low pH conditions. As the pH is increased, the degree of scatter is reduced, until the intermediate pH classification, where the mobile phases are in a cluster. This would suggest that as the pH increases there are fewer observable differences in selectivity. This could possibly be attributed to the overwhelming electrostatic interactions at intermediate pH, which could mask more subtle interactions which can contribute to selectivity differences. This could also perhaps help to rationalise why most methods are developed using lower pH conditions.

The 20 mM ammonium-based buffers at pH 2.3, 3.6, 5.1 and 7.5 were compared in *Figure 80* using an aged sample of Bovine GLP-2 (1-15) with impurities to demonstrate selectivity differences. The chromatograms clearly show selectivity differences with several peaks present in the solution but not all were detected in each of the mobile phase conditions. The identity of the impurities was not established, and peaks were not tracked as the purpose of the sample was to illustrate selectivity differences. It may be advantageous to establish the identity of the impurities in a future study to develop a greater understanding of the elution of peptides.

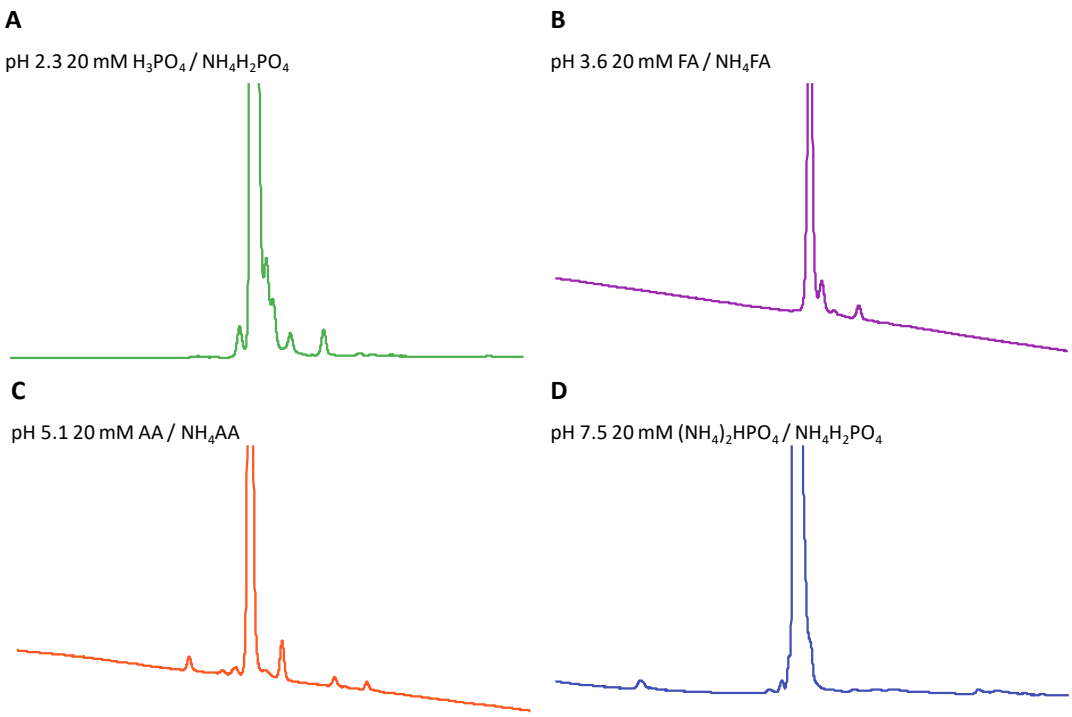

Figure 80 Comparison of the UV chromatographic profile of aged Bovine GLP-2 (1-15) sample using the 20 mM base buffers on the Ascentis Express C18. (A) pH 2.3 20 mM H_3PO_4 / $NH_4H_2PO_4$, (B) pH 3.6 20 mM FA / NH_4FA, (C) pH 5.1 20 mM AA / NH_4AA and (D) pH 7.5 20 mM $(NH_4)_2HPO_4$ / $NH_4H_2PO_4$. Analyses were performed on the Nexera X2 coupled to the 2020 single quadrupole system (where applicable) on the Ascentis Express C18. The aqueous portion can be located in Section 2.12.1.3. The organic was acetonitrile / water (80:20 v/v) with a gradient of 5.6-62.5%B over 40 minutes. Flow rate was 0.3 mL/min, column oven temperature was 40 °C, and detection used a combination of UV at 215 nm and MS.

3.9.2.2 Effect of Ion Pair

The ion pair reagents TEA, TFA, HFBA and $BuSO_3$ were compared against no ion pair with total ion strength of 20 mM as a function of pH. Although $NaClO_4$ is an ion pair, as well as acting as a chaotropic agent, it is not possible to deduce the true impact of the perchlorate ion pair as the ionic strength is 100 mM compared to 20 mM for the other ion pairs. Hodges *et al.* demonstrated the impact of changing the concentration of the perchlorate ion on a series of multiply charged peptides, where the retention of the peptides increased with increased concentration [178]. Hodges *et al*. suggested the trifluoroacetate ion is historically seen to be the most commonly used and effective ion pair reagent. However, their research implied that

despite being less hydrophobic than TFA, the perchlorate ion was the most effective ion pair [178]. However, the response was still included albeit without many conclusions.

The coordinates for each of the ion pair reagent observations were taken from the biplot in *Figure 76* via Simca to produce the plot in *Figure 81*. The plot highlights the disparate response under low pH conditions, and the convergence as the pH increases. All the mobile phases seemed to produce a curved response.

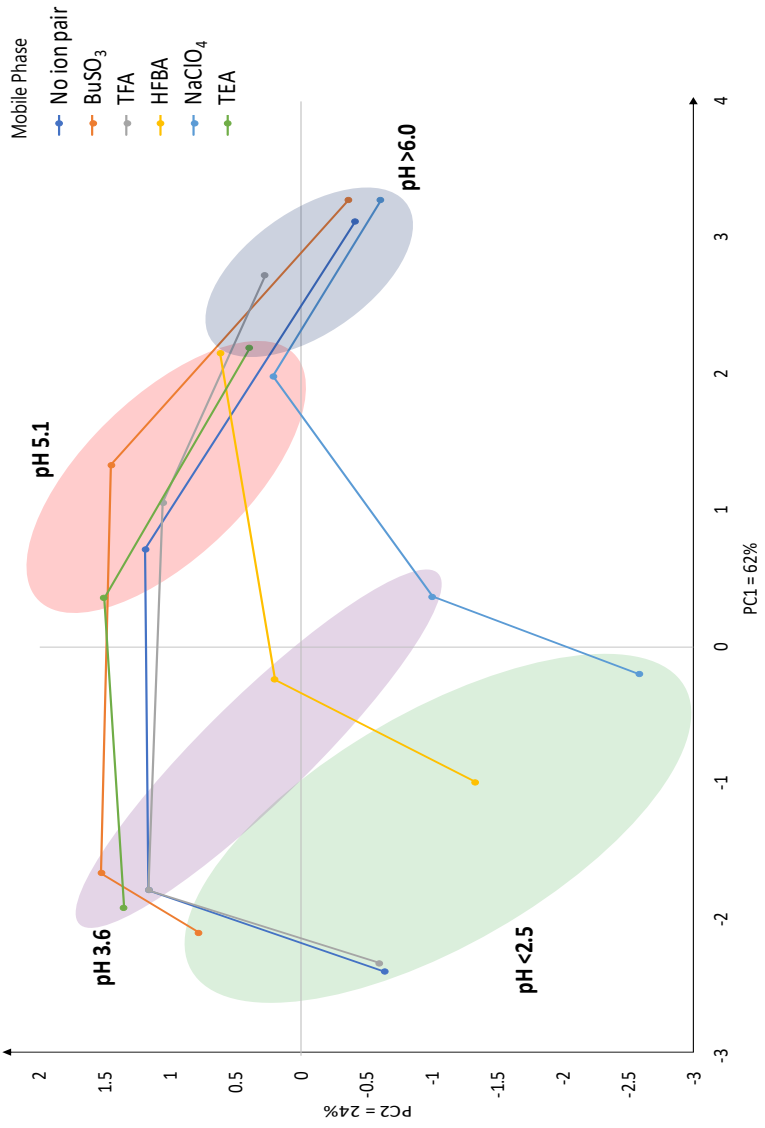

Figure 81 Comparison of ion pair effect at different pH values using the score plot coordinates in Figure 76. The other mobile phases were not included in the plot for ease of viewing the data. The green region denotes the pH <2.5 region, purple denotes pH 3.6, orange denotes pH 5.1 and blue denotes pH >6.0

The largest difference in this section of the plot was between $BuSO_4$ and $NaClO_4$ along the second principal component, which could be attributed to the different retention mechanisms, ionic strength or hydrophobicity of the ion pair. The difference along the y-axis is ascribed to the steric delta values, which can be demonstrated by *Figure 82* by the change in elution order between [L-Ser16]- and [D-Ser16]-Bovine GLP-2 (16-33) (Peptide Numbers 13 and 14, respectively). There is also a greater degree of separation between [Leu26,Ile27]- and [Ile26,Leu27]-Bovine GLP-2 (16-33) (Peptide Numbers 13 and 15, respectively), which is also measured along the y-axis. The difference along the x-axis can be seen to be due to the differences in selectivity between [Lys26]-, [Gly22]- and [Tyr26]-Bovine GLP-2 (16-33) (Peptide Numbers 26, 16 and 24, respectively) in relation to the base sequence (Peptide Number 13). The difference in [Asn11]- and [L-Asp11]-Bovine GLP-2 (1-15) (Peptide Numbers 1 and 9) are also related along the x-axis due to the electrostatic interactions. Based on the position of the observations in the score plot (*Figure 81)*, it might be expected that there would be greater differences between these two peptides, but this is not the case in *Figure 82.* Although in the below example the differences for Δ(9,1) were small, this was not the case for the other pH values.

All the ion pairs possessed greater retention for the peptide probe test mixtures than the non-ion pair condition. The differences were reduced between ion paired mobile phases and no ion pair with pH greater than 5.1, which might suggest that the ion pair is less influential at greater pH values, which corroborates the convergence of the mobile phase results in *Figure 81*.

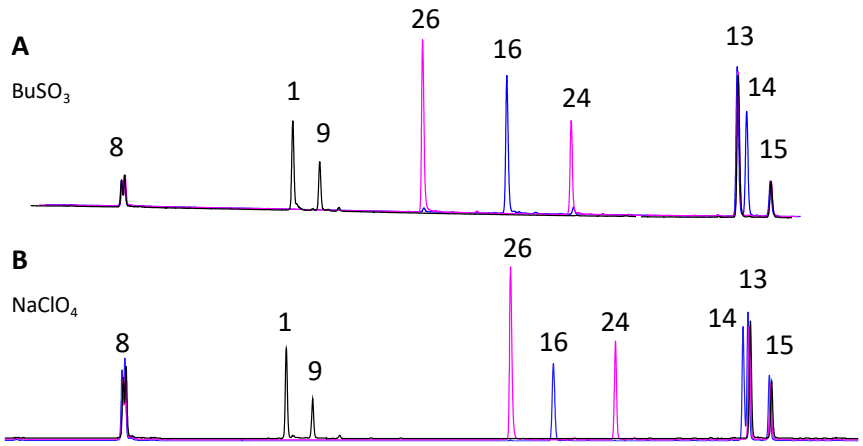

Figure 82 Comparison of the peptide probe test mixtures on the Ascentis Express C18 using (A) pH 2.3 20 mM $BuSO_3$ / H_3PO_4 / $NH_4H_2PO_4$ and (B) pH 2.3 100 mM $NaClO_4$ / H_3PO_4 / $NH_4H_2PO_4$. Analyses were performed on the Nexera X2. The aqueous portion can be located in Section 2.12.1.3. The organic was acetonitrile / water (80:20 v/v) with a gradient of 5.6-62.5%B over 40 minutes. Flow rate was 0.3 mL/min, column oven temperature was 40 °C, and detection used a combination of UV at 215 nm.

The score plot suggested the non-ion paired and TFA ion pair conditions at pH 3.6 were quite close chromatographically as they are superimposed on the score plot (*Figure 76*). This was confirmed with very similar profiles in *Figure 83B,* which compared the conditions using the aged Bovine GLP-2 (1-15) sample. The results between the non-ion pair and TFA at the other pH values were within proximity in the score plot, however, as demonstrated in *Figure 83*, the difference is still significant enough to generate selectivity variances in the profiles of aged Bovine GLP-2 (1-15) sample.

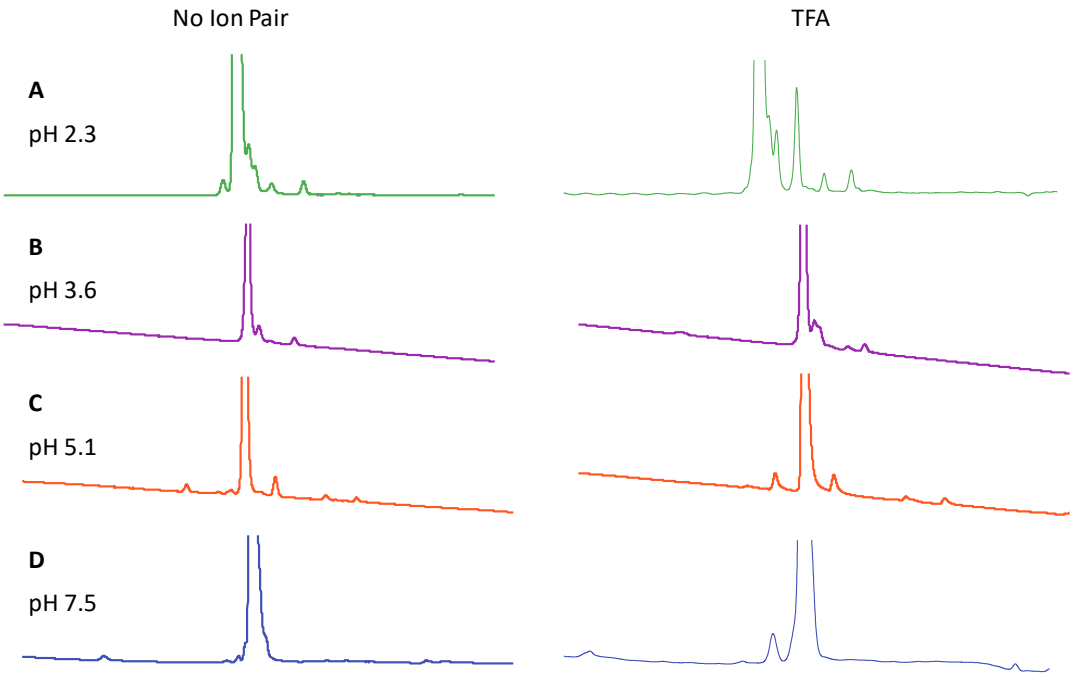

Figure 83 Comparison of no ion pair against TFA mobile phases under different pH conditions on the Ascentis Express C18. (A) pH 2.3 20 mM H_3PO_4 / $NH_4H_2PO_4$, (B) pH 3.6 20 mM FA / NH_4FA, (C) pH 5.1 20 mM AA / NH_4AA and (D) pH 7.5 20 mM $(NH_4)_2HPO_4$ / $NH_4H_2PO_4$. Analyses were performed on the Nexera X2 coupled to the 2020 single quadrupole system (where applicable) on the Ascentis Express C18. The aqueous portion can be located in Section 2.12.1.3. The organic was acetonitrile / water (80:20 v/v) with a gradient of 5.6-62.5%B over 40 minutes. Flow rate was 0.3 mL/min, column oven temperature was 40 °C, and detection used a combination of UV at 215 nm.

The aged Bovine GLP-2 (1-15) sample in *Figure 84* illustrated the differences obtained from the five ion pairs compared against no ion pair at pH 5.1. There are some similarities between the chromatograms produced in TFA and TEA (*Figure 84C* and *F)*. However, the other conditions demonstrate different profiles can be generated using the different ion pairs. It is difficult to correlate these differences with the score plot in *Figure 81.*

There are several applications which have utilised HFBA as an ion pair for peptide separations [112, 154, 166, 179, 180]. However, it was noted in this study that the baseline was quite poor with 180 µL mixer, suggesting insufficient mixing not witness with any of the other ion pairs assessed (*Figure 84E*). It is possible that a larger mixer could improve the mixing capabilities which should improve the

baseline. However, the additive showed little indication of selectivity differences, therefore the additive was not considered further. There are also concerns regarding perfluorinated additives contaminating the instrumentation. Perfluorinated solvents are not compatible with vacuums containing Teflon AF, which in turn affects the degassing capabilities. This in combination with MS source contamination, which was confirmed in this study (see *Section 3.9.3*), highlighted potential drawbacks in using HFBA as an additive.

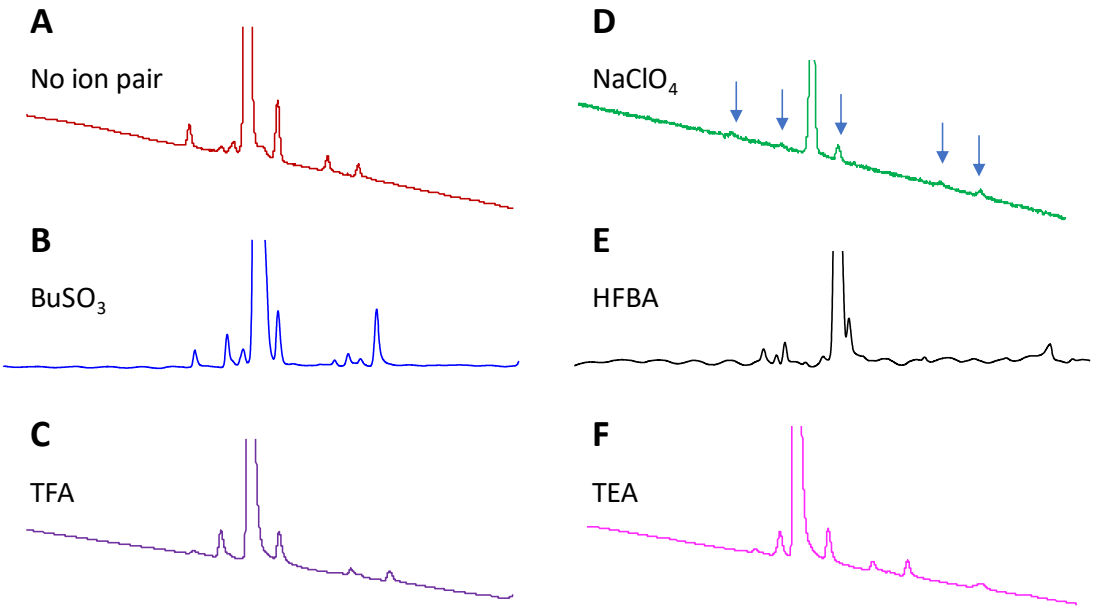

Figure 84 Comparison of aged Bovine GLP-2 (1-15) using pH 5.1 20 mM AA / NH_4AA with 5 mM (A) no ion pair, (B) $BuSO_3$, (C) TFA (D) $NaClO_4$ (E) HFBA and (F) TEA on the Ascentis Express C18. Analyses were performed on the Nexera X2 coupled to the 2020 single quadrupole system (where applicable). The aqueous portion can be located in Section 2.12.1.3. The organic was acetonitrile / water (80:20 v/v) with a gradient of 5.6-62.5%B over 40 minutes. Flow rate was 0.3 mL/min, column oven temperature was 40 °C, and detection used a combination of UV at 215 nm and MS for peak confirmation.

3.9.2.3 Effect of 100 mM Salt Additives

The 100 mM ionic strength mobile phases contained 20 mM salt additives between pH 2.3 and 7.5. It was also decided to investigate the effect of common additives between all four pH ranges using NaCl, $(NH4)_2SO_4$ and $NaClO_4$. There was also the addition of Na_2SO_4 at pH 2.3 evaluated, and 100 mM pH 2.3 and 7.5 without the

presence of any additional salt. Based on the positions within the score plot in *Figure 85*, which was created to help visualise the positions of the observations, the 3rd quadrant contained the pH 2.3 100 mM based mobile phases. The Na_2SO_4 and $(NH_4)_2SO_4$ at pH 2.3 possessed quite similar selectivity, which was confirmed using the profiles of aged Bovine GLP-2 (1-15) (chromatograms not shown). This implies there is little merit in evaluating two similar types of kosmotropic salts at pH <2.3. However, above pH 2.3 demonstrate there are some differences between the two salts. Those two mobile phases also created a cluster with NaCl, and within close proximity to the 100 mM buffer without salts, alluding to similar selectivity. The pH 2.3 100 mM $NaClO_4$ / H_3PO_4 / $NH_4H_2PO_4$ was located furthest from the main cluster of results, which could be a result of the ion pairing effect. The results at pH 3.6 are quite vast, which was quite unusual, considering the relative proximity of the salts at both pH 5.1 and >6.0. It is not understood what has caused the difference, although the position of $NaClO_4$ was not unexpected. The results for pH 5.1 and >6.0 have followed the previous trend of converging with increase in pH. In general, the increase in ionic strength improved the peak shape and peak capacities.

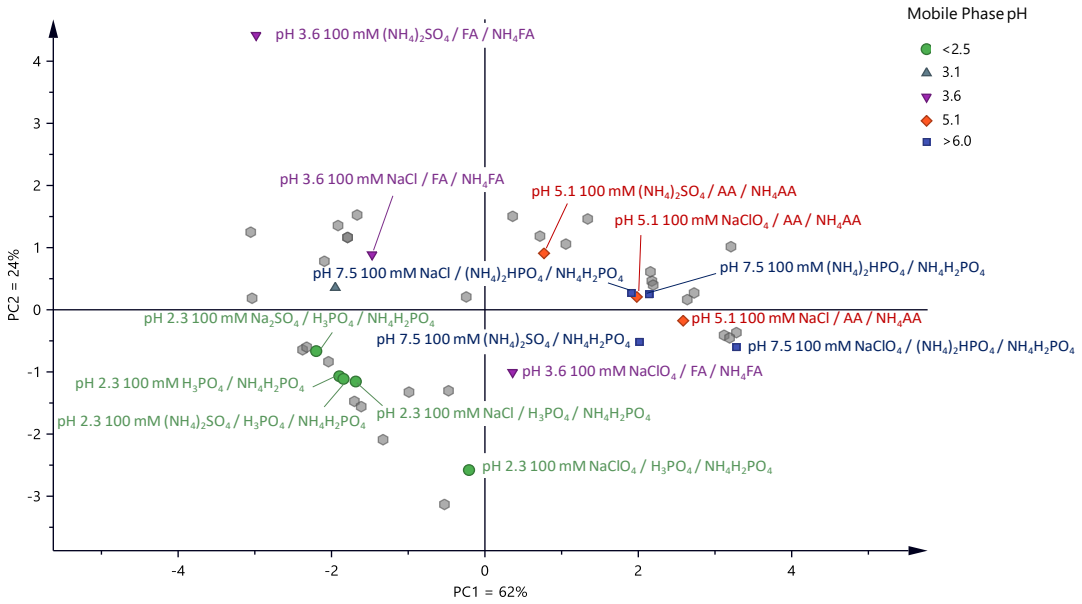

Figure 85 Highlight of the position within the score plot of the 100 mM mobile phases. Grey hexagons correspond to the position of the other mobile phases assessed on the Ascentis Express C18 described in Table 64

Sodium perchlorate often generated interesting chromatographic results with good peak shapes. The positions in the score plot were often on the extremities of the mobile phases assessed, suggested greater differences than some other combinations. Some selectivity differences were displayed in *Figure 86*Figure 87, using an aged Bovine GLP-2 (1-15) sample chromatographed at the four different pH values plus $NaClO_4$. The results highlight the excellent peak shape that can be achieved with perchlorate and a 100 mM ionic strength and the effect that pH has on selectivity.

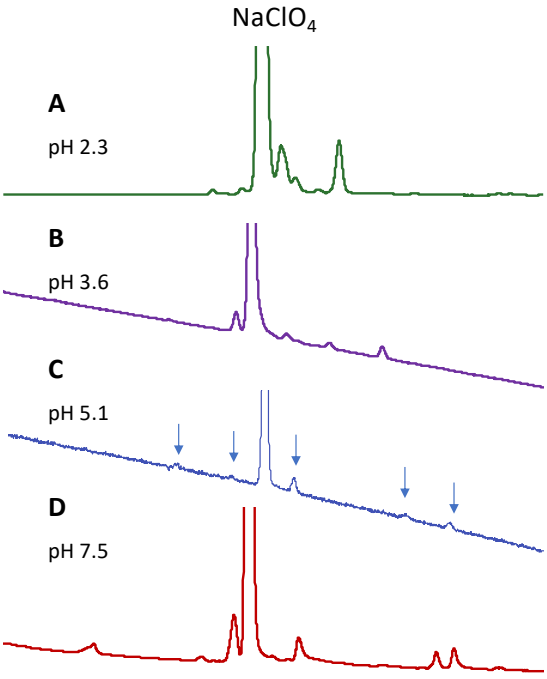

Figure 86 Comparison of the aged Bovine GLP-2 (1-15) on the Ascentis Express C18 using (A) pH 2.3 100 mM $NaClO_4$ / H_3PO_4 / $NH_4H_2PO_4$, (B) pH 3.6 100 mM $NaClO_4$ / FA / NH_4FA (C) pH 5.1 100 mM $NaClO_4$ / AA / NH_4AA and (D) pH 7.5 100 mM $NaClO_4$ / $(NH_4)_2HPO_4$ / $NH_4H_2PO_4$. Analyses were performed on the Nexera X2. The aqueous portion can be located in Section 2.12.1.3. The organic was acetonitrile / water (80:20 v/v) with a gradient of 5.6-62.5%B over 40 minutes. Flow rate was 0.3 mL/min, column oven temperature was 40 °C, and detection used a combination of UV at 215 nm.

Figure 87 demonstrated that it is also possible to have poor peak shape, where the overlaid peptide test mixtures were compared between pH 2.3 100 mM H_3PO_4 / $NH_4H_2PO_4$ without an additive, plus NaCl or plus Na_2SO_4. The conditions without an

additive or with NaCl displayed symmetrical peaks credited to the increased ionic strength, however, despite having the same ionic strength, the Na_2SO_4 condition exhibited tailed peaks for three of the nine peptide probes. The affected peptides were [Lys26]-, [Gly22]- and [Tyr26]-Bovine GLP-2 (16-33) (Peptide Numbers 26, 16 and 24, respectively). It was proposed that these peptides were affected by salting out effects caused by the mobile phase which is feasible based on the Hofmeister series, however, the reason it affected those particular peptides was not confirmed. It cannot be based on net charge as [Lys26]-Bovine GLP-2 (16-33) had a different net charge to the other affected peptides. Additionally, peptides Bovine GLP-2 (16-33), [D-Ser16]- and [Ile26,Leu27]-Bovine GLP-2 (16-33) (Peptide Numbers 13, 14 and 15) were not affected, yet possessed the same net charge as [Gly22]- and [Tyr26]-Bovine GLP-2 (16-33) (Peptide Number 16 and 24). It is possible that it is based on the secondary structure which can promote precipitation by salting out and would be analyte dependent. The salting out effect was also observed when the additive was replaced with $(NH_4)_2SO_4$. The more hydrophilic peptides analysed in pH 7.5 100 mM $(NH_4)_2SO_4$ / $(NH_4)_2HPO_4$ / $NH_4H_2PO_4$ also demonstrated some salting out effects similar to those in *Figure 87*, which supports the suggestion it is analyte dependent.

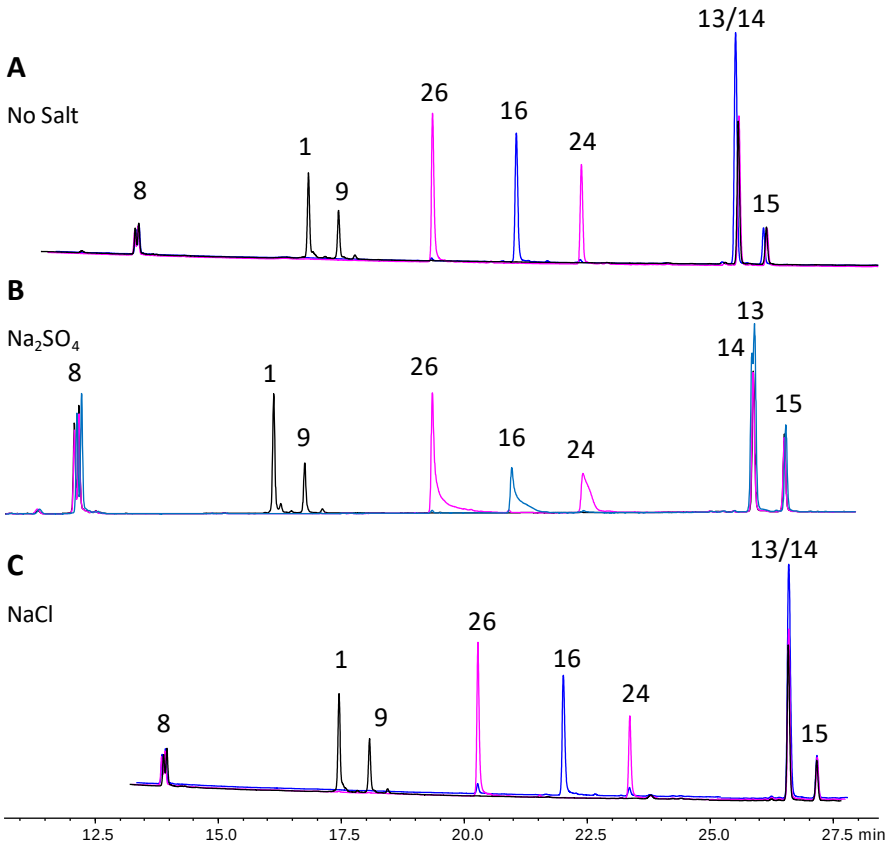

Figure 87 Comparison of the peptide test mixtures on the Ascentis Express C18 using (A) pH 2.3 100 mM H_3PO_4 / $NH_4H_2PO_4$, (B) pH 2.3 100 mM Na_2SO_4 / H_3PO_4 / $NH_4H_2PO_4$ and (C) pH 2.3 100 mM NaCl / H_3PO_4 / $NH_4H_2PO_4$ Analyses were performed on the Nexera X2. The aqueous portion can be located in Section 2.12.1.3. The organic was acetonitrile / water (80:20 v/v) with a gradient of 5.6-62.5%B over 40 minutes. Flow rate was 0.3 mL/min, column oven temperature was 40 °C, and detection used a combination of UV at 215 nm.

3.9.2.4 Comparison of 0.1% v/v acidic modifiers

The acidic modifiers with 0.1% v/v concentrations were compared to ascertain the differences in selectivity. These include H_3PO_4, TFA, FA / TFA, DFA, FA and MSA. The acidic additives typically generated lower peak capacities than the buffered mobile phases, due to the comparatively lower ionic strength. The lack of ionic strength also impacted on the asymmetry of the overloaded Bovine GLP-2 (1-15) sample, where there was quite frequently significant tailing observed. The information provided evidence that although, typically these mobile phases are good for MS responses (excluding the phosphate), it should be used in combination with a salt to

increase the ionic strength which can provide greater chromatographic performance (i.e. peak capacity and peak shape).

In general, these additives were located in the 3rd and 4th quarter, dominated by the Δ(9,1) probe in the first principal component (*Figure 88*). This was due to the switch in elution between low and intermediate pH, where the ionisation of the aspartate variant changed from protonated to deprotonated, thus possessed greater retention with increasingly acidic pH conditions.

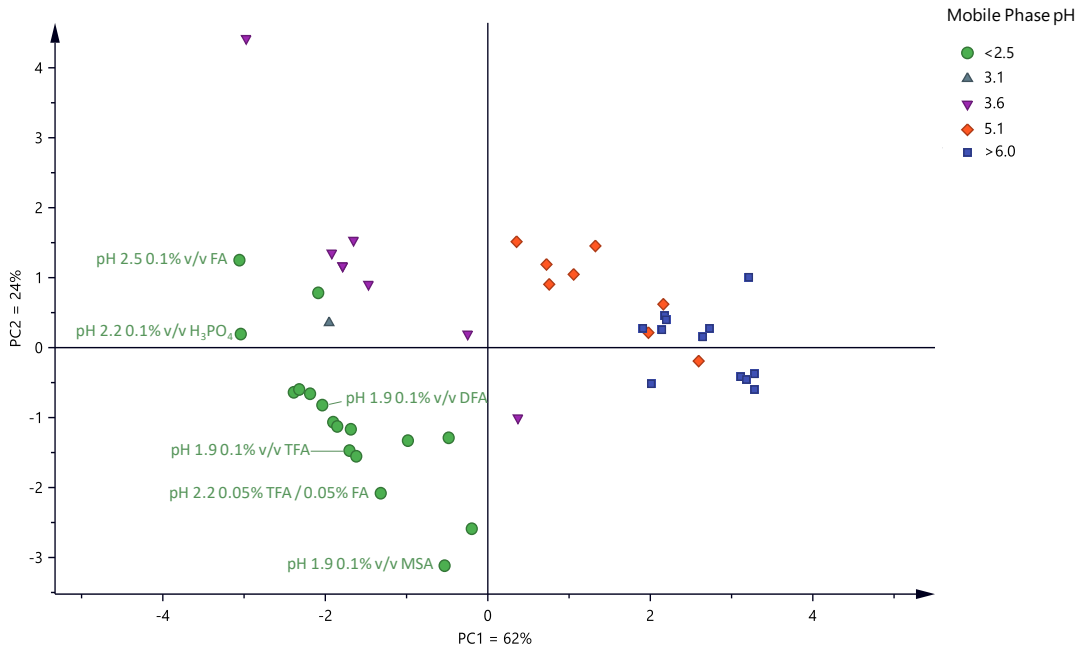

Figure 88 Highlight of the position within the score plot of the 0.1% v/v acidic modifier mobile phases

The largest difference between the acidic modifiers was generated between 0.1% v/v FA and 0.1% v/v MSA along the second principal component. A contribution plot which compared the score contributions of both acids suggested the difference was mainly attributed to Δ(15,13) and Δ(14,13), which coincided with the position of the delta values within the biplot along the y-axis (*Figure 76*). These delta values are both a measure of steric differences. The formic acid gradient created reasonable separation between [L-Ser16]- and [D-Ser16]-Bovine GLP-2 (16-33) (Peptide Numbers 13 and 14, respectively), whilst the 0.1% v/v MSA additive failed to show

any resolution. There was also a greater degree of separation between the [Leu26,Ile27]- and [Ile26,Leu27]-Bovine GLP-2 (16-33) (Peptide Numbers 13 and 15) under the formic acid conditions (*Figure 89*). Formic acid was the only additive assessed in this series to achieve some degree of separation between the racemate species. Although there is near baseline resolution between the racemates using pH 2.5 0.1% v/v FA, there is tailing which contributed to the lack of full resolution. The benefits of using a combination of FA / NH_4FA at pH 3.6 are evidenced in *Figure 90*, where there is ample resolution between the racemates and vast improvements in peak shape comparative to the FA conditions.

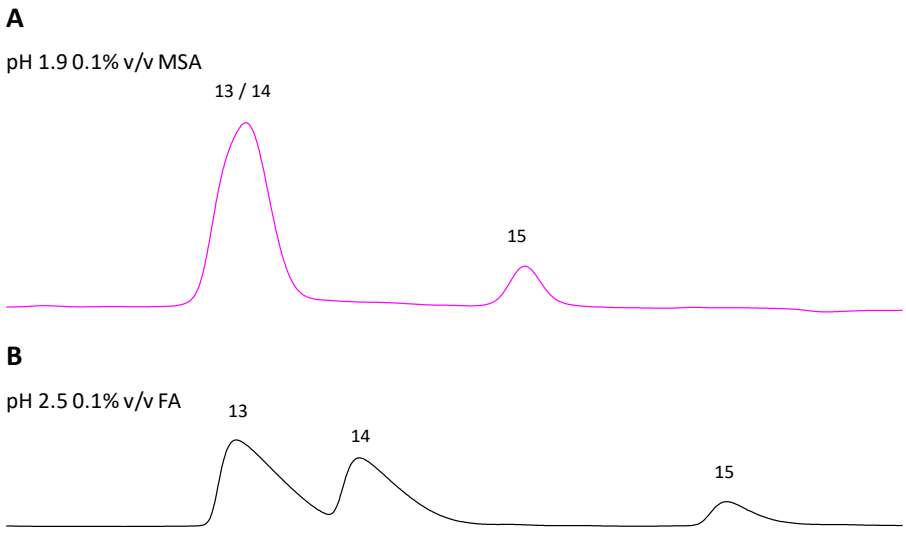

Figure 89 Comparison of (A) 0.1% v/v MSA versus (B) 0.1% v/v FA gradient conditions demonstrating the selectivity differences for Peptide Number 13: Bovine GLP-2 (16-33), Peptide Number 14: [D-Ser16]-Bovine GLP-2 (16-33) and Peptide Number 15: [Ile26,Leu27]-Bovine GLP-2 (16-33). Peaks aligned for Peptide Number 13. Analyses were performed on the Nexera X2 coupled to the 2020 single quadrupole system on the Ascentis Express C18. The aqueous portion can be located in Section 2.12.1.3. The organic was acetonitrile / water (80:20 v/v) with a gradient of 5.6-62.5%B over 40 minutes. Flow rate was 0.3 mL/min, column oven temperature was 40 °C, and detection used a combination of UV at 215 nm and MS for peak confirmation.

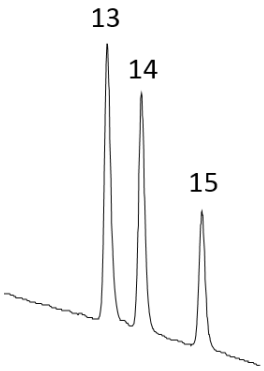

Figure 90 Evidence of the improved resolution which can be achieved using pH 3.6 20 mM FA / NH_4FA in comparison to pH 2.5 0.1% v/v FA alone. Peptide Number 13: Bovine GLP-2 (16-33), Peptide Number 14: [D-Ser16]-Bovine GLP-2 (16-33) and Peptide Number 15: [Ile26,Leu27]-Bovine GLP-2 (16-33). Analyses were performed on the Nexera X2 coupled to the 2020 single quadrupole system on the Ascentis Express C18. The aqueous portion can be located in Section 2.12.1.3. The organic was acetonitrile / water (80:20 v/v) with a gradient of 5.6-62.5%B over 40 minutes. Flow rate was 0.3 mL/min, column oven temperature was 40 °C, and detection used a combination of UV at 215 nm and MS for peak confirmation.

There is some significant distance between the observation positions within the score plot for pH 1.9 0.1% v/v TFA, pH 1.9 0.1% v/v DFA and pH 2.2 0.05% v/v FA / 0.05% v/v TFA (*Figure 88*). These results indicate that there are some differences which can be exhibited from the additives. However, a comparison of the three mobile phases using aged Bovine GLP-2 (1-15) intimated very similar chromatographic profiles, although there was greater tailing exhibited on the 0.05% v/v TFA / 0.05% v/v FA mobile phase. This is suggestive that there may be applications where there are selectivity differences which can be extracted using these mobile phase additives, but they are analyte dependent. Therefore, for greater opportunities to maximise selectivity, mobile phases which are not based on the same additive should be first assessed in a mobile phase screen.

3.9.3 Evaluation of the MS Response

The intensity of TIC and MS signals for Bovine GLP-2 (1-15) were recorded for 18 MS compatible mobile phases, in addition to the average charge and adducts (*Table*

68). The responses were normalised based on the performance of the formic acid conditions in order to compare the TIC and MS signals collected on different occasions. The sample was injected onto an Acquity CSH C18, 1.7 µm, 150 x 1.0 mm column format using a translated gradient to correspond to the 150 x 2.1 mm standardised format. The point of elution was different for the various mobile phases assessed, thus there was varying amounts of acetonitrile which could impact on the desolvation of the droplets, which could affect the signal intensity marginally. However, the elution window of the peak of interest on the mobile phases assessed varied by approximately 20% acetonitrile (14-34% acetonitrile), which was not believed to be of great significance to affect the desolvation. An alternative experimental design could be to employ a tee piece prior to the MS to perform a reverse gradient using acetonitrile via a third pump, however, the protocol employed by this study was designed to explore the signal intensity in the most practically relevant manner to produce more informative results.

The signal intensity ranged from 2E+05 down to 6E+02 highlighting the disparate performance of the MS mobile phase additives (*Table 68*). In order to be of appropriate intensity for identifying impurities at 0.1% levels, the EIC signal needs to be approximately greater than 5E+03 based on prior experience. This would eliminate six of the 18 mobile phases from screening as they fall below this requirement. As expected, the response for formic acid was superior in comparison to all the mobile phases assessed, where formic acid produced a MS signal approximately 2x greater than 0.1% DFA and 33x greater than 20 mM NH_4HCO_3/FA/TEA. This agrees with literature where it is regularly found that the most intense signals are achieved using formic acid conditions [161].

The MS signal is known to be somewhat suppressed by TFA due to a combination of ion pairing effects and surface tension properties. This problem can be addressed in a few different ways to varying degrees of success [179, 180]. Apffel *et al.* described a method called “TFA Fixing” which utilised a make-up pump prior to the mass spectrometer, to tee in an organic solvent with a weak acid such as propionic acid [179]. It is more favourable to deprotonate the weak acid, which drives the

reaction. Therefore, in the presence of the weak acid, a weak ion pair can form with the analyte which favours protonating the analyte which can form a suitable droplet to be analysed by the MS. The research suggested propionic acid was the most appropriate additive assessed, as it had optimal volatility and good performance. The type of organic solvent used can also impact on the sensitivity of the method where the conductivity and the surface tension are reduced. 2-Propanol was found to be optimal with good results also obtained by acetonitrile. This approach was applied to peptides and proteins, with the best results obtained for peptides. The impact on larger proteins is less pronounced, potentially due to the greater number of protonation sites available on the protein to interact with the TFA anions. However, the intensity for TFA was not adversely affected, and in fact provided the fourth greatest signal of the 18 mobile phases assessed.

A high-purity difluoroacetic acid (DFA) can provide an alternative to TFA, with good sensitivity, good chromatographic performance and lower ion-pairing strength. The position within the biplot in *Figure 76* also suggests that the chromatographic selectivity is quite similar. The signal intensity was approximately 2x greater using DFA against TFA, as also observed in Reference [163]. Historically, DFA was not used particularly for LC-MS applications due to poor purity and significant metal content which contaminated the mass spectrometer [163]. However, there are a few vendors on the market who have improved the distillation process to improve the quality of the additive, which makes DFA a viable substitute.

The mobile phases containing TEA had poor MS signals, which could be in part due to the multiply charged ions produced, as well as ion pairing effects. The average charge for the TEA containing mobile phases were between 1.5-1.6, whilst the other mobile phases typically were in the +2 charge (*Table 68* and *Figure 91C)*. The multiple ions reduce the amount of signal for the main peak, thus reducing the total of MS signal.

The HFBA containing mobile phases also produced poor MS signals, which would prohibit their use, particularly for observing low abundant impurities. The ion

pairing and surface tension effects could be quite significant for this particular additive which could impact on the intensity of the signal. The mass spectrometer also exhibited memory effects and required significant cleaning protocols to remove the effects of the additive, thereby rendering the additive undesirable for MS methods.

Table 68 Normalised signal intensity, average charge and adduct for the MS compatible mobile phases with ionic strength using Bovine GLP-2 (1-15). Series ordered based on increasing MS signal.

Mobile Phase	MS Signal	Average Charge	Adducts (minor)*
pH 7.8 20 mM NH_4HCO_3/FA/TEA	6E+02	1.5	Fe
pH 1.8 20 mM HFBA	9E+02	1.9	Na
pH 5.1 20 mM NH_4AA/AA/HFBA	1E+03	2	Na
pH 3.6 20 mM NH_4FA/FA/HFBA	2E+03	2	Na
pH 5.1 20 mM NH_4AA/AA/TEA	2E+03	1.6	
pH 3.6 20 mM NH_4FA/FA/TEA	2E+03	1.6	
pH 6.5 20 mM NH_4FA	6E+03	2	Na
pH 5.1 20 mM NH_4AA/AA/TFA	9E+03	2	Na
pH 5.1 20 mM NH_4AA/AA	1E+04	2	
pH 7.0 20 mM NH_4AA	1E+04	2	Na
pH 7.8 20 mM NH_4HCO_3	1E+04	2	Na
pH 3.6 20 mM NH_4FA/FA/TFA	2E+04	2	Na
pH 10.8 1 mM NH_4OH	3E+04	2	Na
pH 1.9 15 mM 0.1% MSA	3E+04	2	
pH 3.6 20 mM NH_4FA / FA	4E+04	2	Na
pH 1.9 13 mM 0.1% TFA	4E+04	2	
pH 2.2 7 mM 0.05% FA / TFA	5E+04	2	
pH 1.9 16 mM 0.1% DFA	1E+05	2	
pH 2.7 2 mM 0.1% FA	2E+05	2	

** These adducts were extremely low level and the contribution from glassware can be significant.*

Alkali metal ion adduct formation is a common occurrence within mass spectrometry; the most common of which are sodium and potassium adducts with

the characteristic M+23 and M+39 *m/z* values observed ($[M+Na]^+$ and $[M+K]^+$, respectively) [181, 182]. Glassware, solvents or sample preparation are known sources for ion contamination, whilst biological matrix can quite typically contain various salts and metal ions. The presence of Fe^{2+} ions can be attributed to the silica transfer lines, MS capillary and other metal components within the system, but the adduct formation varies depending on the age of the system. Other common adducts include the ammonium ion and adducts with either acetonitrile or methanol from the solvents, however, these were not observed in this study. The impact of metal ions can vary significantly for each analyte of interest, as some compounds are more susceptible to ion adduct formation [181, 183]. In itself, the presence of adducts is not an issue, however, problems can arise if an unstable adduct is used for quantitation which can affect the reproducibility of analysis. Additionally, if several adducts are present, it can reduce the sensitivity of the separation [181, 183]. One approach often used to assist analysis is to include an abundance of ions to promote a particular adduct which should assist with producing stable adducts (i.e. addition of formic acid to promote $[M+H]^+$ or ammonium buffers to promote $[M+NH_4]^+$). The presence of adducts in this study were not that significant and few conclusions can be made from the data as it is quite possible that the metal adducts have originated from the glassware and not the mobile phases.

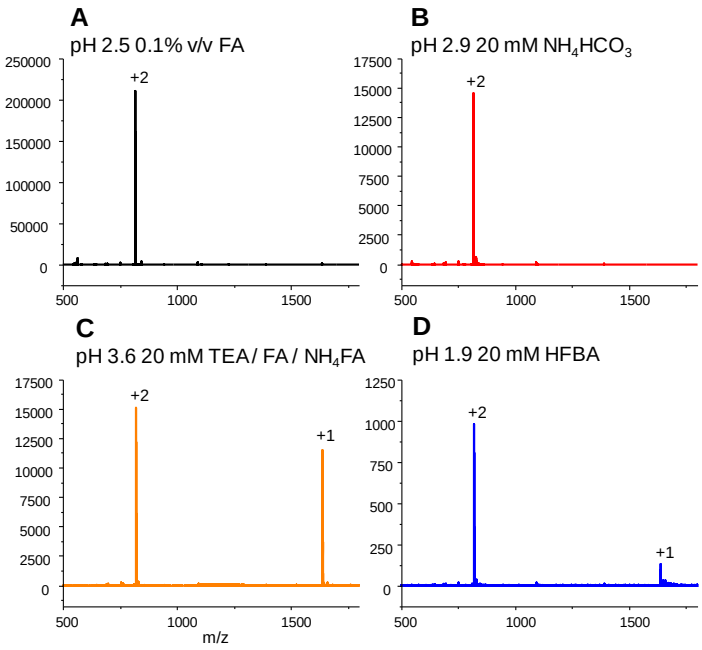

Figure 91 MS signal for A: pH 2.5 0.1% v/v FA, B: pH 7.9 20 mM NH_4HCO_3, C: pH 3.6 20 mM TEA/FA/NH_4FA, D: pH 1.9 20 mM HFBA. Analyses were performed on the Waters Acquity I-Class coupled to Waters Synapt G2-Si with an Acquity CSH C18 (150 x 1 mm, 1.7 µm). The aqueous portion can be located in Section 2.12.1.3. The organic was acetonitrile / water (80:20 v/v) with a translated gradient appropriate to the protocol conditions.

3.9.4 Rationale for the Extended Mobile Phase Study

The initial results on the Ascentis Express C18 demonstrate the extensive differences which can be generated by using different mobile phases (*Figure 76* and *Section 3.9.2*). It is a promising initial study which highlights the power of different additives for method development.

The next stage of the study was extended to evaluate the effect of different organic modifiers and temperature, which are both known to have a large impact on the chromatographic system. The rationale for the different organics and temperature are in *Sections 3.9.4.2* and *3.9.4.3*, respectively.

It is also important to understand how the results generated in the initial study can be applied across a greater range of stationary phases. Therefore, another aspect of the extended study would be to evaluate a subset of mobile phases on a reduced

number of extreme stationary phases to determine the applicability of the initial results. A greater discussion of the rationale is in *Section 3.9.4.4*.

3.9.4.1 Subset of the Most Interesting Mobile Phase Combinations

The results from the biplot in *Figure 76* were evaluated for peak capacity and chromatographic diversity to select mobile phases which could be assessed in the extended studies.

Each quadrant within the score plot was assessed to determine which mobile phases would be the most appropriate for evaluation. The 1st quadrant was dominated by pH 5.1 mobile phases, whilst the 2nd quadrant contain mobile phases with pH values greater than 6. The 3rd quadrant contain mostly mobile phases with pH less than 2.5 and the final, 4th quadrant contain a combination of mobile phases with pH <2.5 and ~3.6. It would therefore be rational to select mobile phases which also cover a range of pH values.

A pH value <2.5 must contain pH 1.9 0.1% v/v TFA (Mobile Phase 11, 3rd quadrant) as it is one of the most widely used mobile phases used for peptides. Another commonly used combination is pH 2.3 100 mM $(NH_4)_2SO_4$/ H_3PO_4/$NH_4H_2PO_4$ (Mobile Phase 8, 3rd quadrant), which can offer vast improvements in peak shape for overloaded species. Although these conditions are located in close proximity, thus implying they could possess similar selectivity, it would be advantageous to compare mobile phases which provide similar selectivity, in order to ascertain if the effect is the same on different stationary phases.

pH 2.5 0.1% v/v FA (Mobile Phase 1, 4th quadrant) is another commonly used additive, particularly for its MS compatibility. Therefore, it is advisable to utilise this mobile phase combination. It is also one of the most extreme additives along the y-axis (second principal component) and is known to show some advantages for separation of isomers.

pH 5.1 20 mM $BuSO_3$ / AA / NH_4AA (Mobile Phase 31, 1st quadrant) has demonstrated some good selectivity differences and peak capacities on the Ascentis Express C18. $BuSO_3$ is also a commonly used ion pair thus should be compared between different organics, temperatures and stationary phases.

pH 6.5 20 mM NH_4FA (Mobile Phase 41, 1st quadrant) is another commonly used additive, particularly for MS applications, and there is already a significant amount of data gathered on this mobile phase, therefore there is a greater appreciation of the interactions of this additive. It is also known from the initial study that there were greater differences experienced at lower pH compared to the intermediate pH conditions on the Ascentis Express C18. It would also be interesting to see if the same tendency is exhibited on different stationary phases. Therefore, the final mobile phase combination to assess is pH 7.5 20 mM $(NH_4)_2HPO_4$ / $NH_4H_2PO_4$ (Mobile Phase 43, 4th quadrant) which is located within close proximity to the pH 6.5 20 mM NH_4FA. It also does not experience salting out effects experienced when using greater ionic strengths of pH 7.5 mobile phases.

Although the perchlorate mobile phases often demonstrated different selectivity, it was not assessed in the extended studies due to the issues with toxicity and reactivity.

The final selected mobile phases are displayed in *Figure 92*.

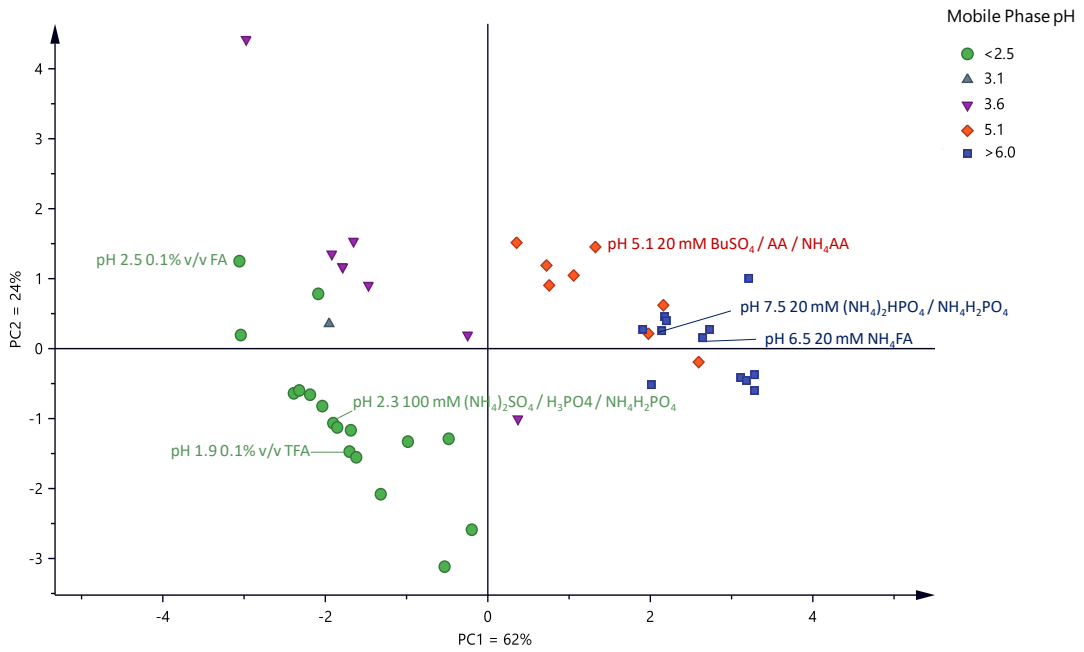

Figure 92 Highlight of the position within the score plot of the mobile phases selected for the extended mobile phase study

3.9.4.2 Organic

Whilst characterising mobile phases, it is advantageous to take the opportunity to observe the effect of different organic solvents. The most common reversed-phase organic modifiers are acetonitrile and methanol, however, there are a plethora of available solvents which could be potentially evaluated for interesting selectivity differences. Snyder *et al*. developed the solvent selectivity triangle which categorised organic solvents based on different properties (*Figure 93*) [184-186]. Each corner of the triangle represents a different characteristic, which are H-B basic, H-B acidic and dipolar, which were deemed the most critical parameters by Snyder based on Rohrschneider's work [187]. The black dots (*Figure 93*) represent common clusters of solvents which were determined by Snyder *et al*. The solvent selectivity triangle can highlight the most appropriate organic modifiers to assess. Solvents which are closely located will not provide significant selectivity differences required for method development, which can be beneficial for reducing the number of permutations for screening. The three most applied organic solvents are methanol

(acidic character), acetonitrile (dipolar character) and tetrahydrofuran (THF, basic character), presumably due to their miscibility, viscosity, UV cut-off, reactivity and cost. The methanol can act as a proton donor with a solute to form hydrogen bonds. The acetonitrile, on the other hand, can form dipole-dipole interactions via the triple bond nitrile group with a solute to form electrostatic interactions. THF possesses basic character where it is a proton acceptor and can thereby form hydrogen bonds with acidic solutes. These mobile phases can be used purely or in combination to provide different elution profiles and can provide complementary selectivity. Pure THF is not often used as it has a UV cut-off of 230 nm which is not inducive for peptide analysis by UV. It also has a few other issues included stability and reactivity with PEEK tubing. Due to the necessity of using UV detection at low wavelengths to analyse non-MS compatible solvents, THF was discounted from this study. Although there are organic modifiers which possess greater acidic, basic or dipolar character, they typically are not the first choice of solvent, potentially due to poor miscibility, toxicity, or high UV cut-off.

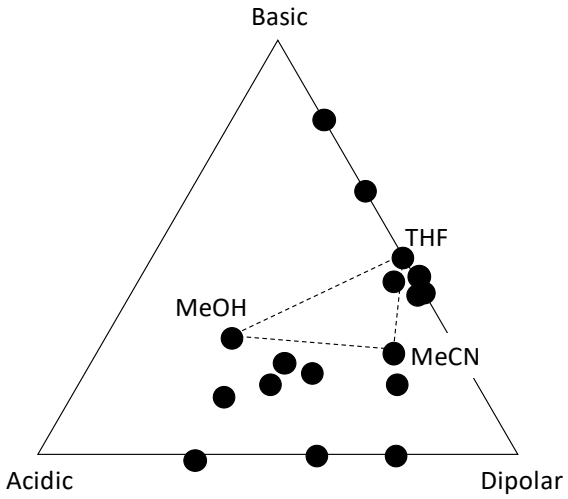

Figure 93 Solvent selectivity triangle adapted from references [188, 189]

Other infrequently used solvents could offer selectivity differences, such as acetone. Although it is not suitable for UV analysis of peptides due to the cut off at 330 nm, it was therefore discounted for this study. However, it could potentially be

useful for MS applications. Fritz *et al*. compared the effect of acetone against acetonitrile or methanol on tryptic digests of proteins using MS detection [190]. They observed shortened retention times and sharp peaks with acetone due to the stronger elution strength in comparison to the other mobile phases assessed, which could be advantageous for reducing run times and solvent costs. They also noted that similar numbers of peptide fragments could be identified as in acetonitrile using the acetone conditions, whilst methanol identified fewer fragments. Ethanol and halogenated alcohols could also offer different properties which could impact on the selectivity of the peptides [191]. However, in the first instance this should be reduced to just two types of typical organic modifier. This will create a manageable comparison.

Simply changing the organic from acetonitrile to methanol has profound effects on selectivity for small molecules [109]. This has also been observed for peptides, where Mant *et al*. conducted a comparison of methanol and acetonitrile on the selectivity of a series of peptides, and identified good retentivity differences [20]. Methanol also can promote π-π interactions between aromatic moieties in the stationary phase and aromatic functionalities in the peptide, whilst acetonitrile is known to quench such interactions [109-111]. It is uncertain as to the reason methanol is not frequently used as a solvent for peptide separations considering such selectivity differences were observed. It could perhaps be due to the higher P_{max} which could limit flow rates for peptide separations. It could also be hypothesised that methanol is not historically used with peptides due to using TFA as an additive. TFA is one of the most commonly used additives for peptides but with the addition of methanol there could potentially be methyl ester formations as the mobile phase ages. Furthermore, artefacts can then be observed in the baseline which can impact on limits of detection.

Another option which could be investigated includes the use of ternary gradients [192-197]. Snyder explained two different types of gradient systems, which were designated as elution strength and selectivity gradients [193]. The selectivity gradient is composed of a changing B solvent composition to affect selectivity. The

elution strength gradient utilises a constant organic composition of two organic modifiers, which then impacts on the separation. It was successfully demonstrated on a 14-compound test mixture reversed phase separation where the organic composition was kept constant using an acetonitrile / THF ternary solvent system. The test mixture failed to be fully resolved when a binary solvent system was applied of either water – acetonitrile, or water – THF [193]. This approach was applied by Euerby *et al*. using a combination of methanol – acetonitrile modifiers to generate a retention model to successfully describe the relationship for ternary solvents [194]. Jandera *et al*. also applied such an approach under normal phase conditions [195]. Coym researched the effect of ternary reversed-phase mobile phases on retention mechanisms using an LSER approach [192].

The addition of 2-PrOH to acetonitrile offers different properties to the eluent which could be inducive for selectivity differences. 2-PrOH is regularly used with proteins as the solvent interacts with the protein to produce a more hydrophobic surface which impacts on the retentivity of the protein. 2-PrOH also has surface and analyte solvation properties which are very different from lower alcohols and acetonitrile. In addition, it has a different heat capacity which can affect the van't Hoff relationship *lnk versus 1/T*. The limitations for 2-PrOH include the increased viscosity which in turn increases the pressure of the system. Thus, the mobile phase reservoir B was standardised as acetonitrile / 2-PrOH / water (60:20:20 v/v/v). However, it is important to evaluate the effect of 2-PrOH therefore different concentrations in 5% intervals between 5-20% were analysed on two of the five most interesting mobile phases.

To summarise, the five most interesting mobile phase combinations (*Section 3.9.4.1*) were evaluated on the Ascentis Express C18 on two additional organic modifiers: methanol / water (80:20 v/v) in direct replacement to acetonitrile / water and the ternary composition of acetonitrile / 2-PrOH / water (various combinations).

The responses from the different mobile phase combinations with the various organic compositions were analysed using PCA to visually identify the degree of scatter. The results can be used to identify the merit of evaluating different organic modifiers during a method development strategy.

3.9.4.3 Temperature

Temperature can have a profound effect on the retentivity of peptides. There are various publications available studying the impact of temperature both on small molecules and peptides, up to large biomolecules [113, 129, 131, 132, 198-201]. Horváth *et al*. used it to increase the efficiency and speed of analyses [202, 203], whilst Rosés *et al*. conducted extensive studies on the effect of temperature under different chromatographic conditions, particularly for ionisable species [199, 204, 205]. The van't Hoff relationship can describe the retention of analytes and temperature, assuming there are no changes in adsorption kinetics (*Equation 31*).

$$ln\,k = \left(\frac{-\Delta H^{\circ}}{RT}\right) + \left(\frac{\Delta S^{\circ}}{R}\right) + ln\,\emptyset \qquad \textit{Equation 31}$$

Where *ΔH* denotes enthalpy, *ΔS* is entropy, *R* is the gas constant, *T* the constant temperature and *ø* is the phase ratio.

This relationship is most appropriate for small molecules, as it is known that peptides can behave differently with temperature, as demonstrated in *lnk versus 1/T* plots. Small molecules generate a characteristic linear response with changes in temperature where typically an increase in temperature results in a decrease in retention (although this is analyte dependent and there are exceptions). Peptides and proteins, however, often have a curvature in the plot with changing [198]. There is now commercially available software which can aptly describe the relationship between peptides and proteins against temperature thus predict retention times, which utilises the relationships described in literature [198, 206, 207].

One of the most notable effects on peptides due to a change of temperature is the impact on any secondary structure which is present. Chen *et al.* synthesised peptides with and without a secondary structure to observe the effect of temperature on conformational differences [200]. Their results imply that there were significantly different responses exhibited by the α-helical peptides compared to the random coil peptides, due to the unfolding of the peptide. They also observed general trends of reduced retention with increased temperature for both the random coil and α-helix, and the degree of retention change was entirely analyte dependent (i.e. there were changes in elution order with changing temperature because the analytes each responded differently to the change in conditions). The change in temperature can also result in changes to analyte solubility in the mobile phase as well as affecting the ionisation state and pK_a.

A change in temperature will also impact on the mobile phase. The viscosity of the solvents changes as a function of temperature (Table 71), whilst also increasing the mass transfer between the mobile phase and the stationary phase. This in turn affects the retention of the analyte of interest. The change in viscosity also changes the pressure of the system which can also impact on pressure sensitive analytes, as well as altering the shape of the van Deemter for the column. In addition to affect the mass transfer of the stationary phase, the increase in temperature can impact on the efficiency of the separation. This can be rationalised using an extended van Deemter equation (*Equation 32*) [208, 209]. Gritti *et al.* performed an extensive review on the van Deemter equation including its limitations and expanding it to be appropriate for modern liquid chromatography [209].

$$H = 2\lambda d_p + \frac{2\gamma D_m}{u} + \frac{(1+6k+11k^2)d_p^2 u}{24(1+k)^2 D_m} + \frac{2kd_f^2 u}{3(1+k)^2 D_s} \qquad \textit{Equation 32}$$

Where λ is the packing factor, d_p is the particle size, γ is the obstruction factor, D_m is the diffusion coefficient, k is the retention factor, d_f is the film thickness and D_s is the diffusion coefficient into stationary phase.

This expanded equation stresses the importance of diffusion coefficients to describe the effect of efficiency. The diffusion coefficient can be discussed in terms of the Wilke-Cheng equation (*Equation 33*) [210].

$$D_m = \frac{7.4x10^{-8}\sqrt{\varphi M}\,T}{V_s^{0.6}\eta} \qquad \textit{Equation 33}$$

Where φ is the solvent association constant, M is the solvent molecular weight, T is temperature, V_s is the analyte molar volume and η is the solvent viscosity.

Table 69 Viscosity of %MeCN versus Temperature (Adapted from [45])

T	%MeCN										
(°C)	0	10	20	30	40	50	60	70	80	90	100
15	1.10	1.18	1.23	1.30	1.09	0.98	0.89	0.81	0.70	0.54	0.40
20	1.00	1.14	1.10	1.13	0.99	0.90	0.81	0.69	0.56	0.50	0.37
25	0.89	1.01	0.98	0.97	0.89	0.82	0.72	0.59	0.52	0.46	0.35
30	0.79	0.90	0.87	0.86	0.80	0.74	0.65	0.52	0.45	0.43	0.32
35	0.70	0.73	0.78	0.76	0.72	0.68	0.59	0.47	0.43	0.39	0.30
40	0.64	0.72	0.70	0.68	0.65	0.62	0.54	0.44	0.41	0.36	0.27
45	0.58	0.61	0.64	0.61	0.59	0.58	0.50	0.43	0.38	0.33	0.25
50	0.54	0.60	0.60	0.57	0.55	0.53	0.46	0.41	0.36	0.31	0.24
55	0.51	0.53	0.56	0.53	0.51	0.49	0.43	0.38	0.34	0.29	0.23
60	0.47	0.52	0.53	0.50	0.49	0.46	0.41	0.35	0.37	0.27	0.22

The LC instrument specification can limit the temperature region in what is practically feasible to work in. Most manufacturers produce a column oven which is capable of achieving temperatures 10 °C below ambient, but there are some which cannot reproducibly work in this region. The upper limit it typically around 80 °C with some specialised ovens achieving much greater temperatures of around 200 °C. These require specialised columns to be able to cope with the extreme temperatures. Most commercial phases should not be used at temperatures greater

than 60 °C for extended periods of time in order to avoid deterioration of the silica support, which can lead to shortened column lifetimes.

The five most chromatographically diverse mobile phases (*Section 3.9.4.1*) were evaluated at 20, 40 and 60 °C on the Ascentis Express C18 in order to ascertain the trends for the ten peaks of interest, including the diastereoisomer of [Met(O)10]-Bovine GLP-2 (1-15) (Peptide Number 8). This region would account for the vast majority of peptide separations. A more comprehensive study could be performed to extend this work which could look at the effect of temperature in 5 °C intervals over a wider range depending on the equipment available, to establish the retention model for peptides of a certain length.

The temperature results were also analysed using PCA to demonstrate the chromatographic differences which can be achieved when temperature is altered. The degraded Bovine GLP-2 (1-15) sample was used to highlight the selectivity differences to emphasises the need to investigate temperature as an operating parameter in the method development strategy.

3.9.4.4 Selection of Stationary Phases to Assess Applicability of Results

The Ascentis Express C18 was selected as a typical neutral stationary phase, based on its location with the score plot in *Figure 65*. The mobile phases described in *Table 64* were all assessed on the Ascentis Express C18 from the same batch of material to purely investigate the effect of the mobile phase without interference from any column batch to batch variations.

However, it is important to assess the applicability of this work on other stationary phases. Therefore, the five most interesting mobile phases which cover the pH range 2.3 – 7.5 were analysed on the Polaris Amide C18, Acquity CSH Fluoro Phenyl and Ascentis Express Biphenyl and compared to the results obtained on the Ascentis Express C18. These phases were selected based on their position within the score plot (*Figure 65*) and good chromatographic performance.

3.9.5 Evaluation of the Effect of Organic Solvents

The subset of six mobile phases was assessed using two different organic modifiers; a direct replacement of acetonitrile with methanol and a ternary solvent system of MeCN / 2-PrOH / H_2O (*Table 70*). The gradient which utilised the MeOH / H_2O B solvent was extended to 100%B with the same %B/min change as the original gradient. Methanol generated greater retention of the peptide probes, thus to accommodate the enhanced retentivity of the peptide probes due to the lower eluting strength of methanol, the gradient was extended. The results were analysed using PCA to produce the score plot in *Figure 94*. The figure was produced for greater ease of understanding the patterns. The additional mobile phases assessed on the Ascentis Express C18, described in *Table 64*, were represented as grey hexagons to reduce the complexity of the figure but still provide an awareness of the disparity in the results. The peak capacities of the different organic mobile phases were comparable to the values achieved in MeCN / H_2O (80:20 v/v) (results not shown).

It was a general trend that the organic solvents differed primarily along the second principal component, where the most positive coordinates in the score plot were obtained from MeCN / 2-PrOH / H_2O, MeCN / H_2O, then finally MeOH / H_2O. The direction of the MeOH / H_2O based mobile phases had a tendency to point towards the 2nd quadrant (i.e. Δ(24,13) and Δ(16,13) which measure phenolic and aromatic interactions). Methanol is a protic solvent which is capable of forming hydrogen bonds with suitable species. It is also possible that the secondary structure of the peptide could differ in the protic solvent, which could expose or conceal functional groups which alters the retention.

pH 5.1 20 mM $BuSO_3$ / AA / NH4AA was the exception to this trend, where the results obtained from MeOH / H_2O (Mobile Phase 31d) affected the pattern. The ion pair could be affected by the different organic solvent, where the properties of the ion pair, thus the retention mechanism, are altered. Thus, the retention profile was

not as expected. However, the result warrants further investigation into the impact of methanol on $BuSO_3$ to ascertain if this is a valid result.

The mobile phases pH 1.9 0.1% v/v TFA and pH 2.3 100 mM $(NH_4)_2SO_4$ / H_3PO_4 / $NH_4H_2PO_4$ were assessed on different combinations of the ternary solvents MeCN / 2-PrOH / H_2O (3rd quadrant, Mobile Phases 11e-h and 8e-h, respectively). The composition of 2-PrOH was assessed in 5% intervals between 5-20%. The results in the score plot denote very little selectivity differences between the different compositions (*Figure 94*), which was also confirmed using the aged Bovine GLP-2 (1-15) sample, where the same profile and number of peaks were detected. There were some subtle differences between the racemate species [L-Ser16]- and [D-Ser16]-Bovine GLP-2 (16-33) (Peptide Numbers 13 and 14), but the overall impression from the results suggest there is little advantage in comparing different compositions during a method development screen. However, it is plausible that a method could be optimised by adjusting the composition of the ternary solvents. A t_g *versus* %2-PrOH plot indicated the retention of the hydrophilic species decreased with an increase in 2-PrOH, whilst the hydrophobic peptides tended to increase in retention with increase in 2-PrOH. The properties of the two organics could imbue different properties to the peptides by potentially altering the solvation shell around the peptides which could alter the ability to interact with the stationary phase, thus impacting on the retention profiles.

The results indicated that selectivity differences can be generated by altering the organic solvent, where the largest difference was obtained by switching between acetonitrile and methanol. 2-PrOH also offered some good selectivity differences which could be advantageous during a scouting screen. This should be recommended as a part of any method development process to investigate the impact of organic solvent.

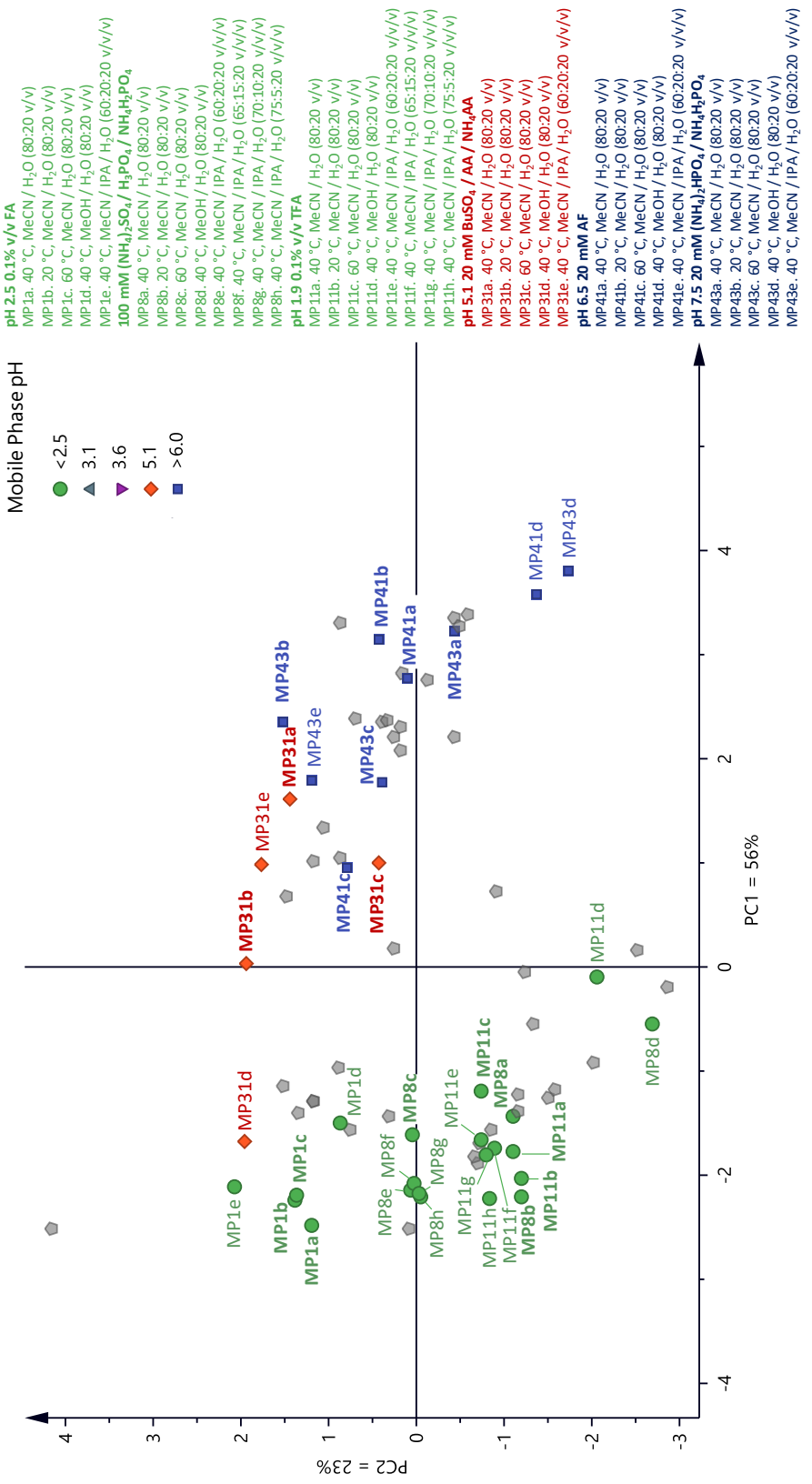

Figure 94 Score plot highlighting the effect of organic modifiers and temperature on a subset of mobile phase combinations. Grey hexagons correspond to the position of the other mobile phases assessed on the Ascentis Express C18 described in Table 64

Table 70 Delta values for the peptide probes determined on the subset of mobile phases with different organic modifier combinations

Mobile phase number	31e	31d	1e	1d	8h	8g	8f	8e	8d	11h	11g	11f	11e	11d
	pH 5.1 $BuSO_3$/AA/NH_4AA MeOH/H_2O (80:20 v/v)		**pH 2.5 0.1% v/v FA MeOH/H_2O (80:20 v/v)**		**pH 2.3 100 mM $(NH_4)_2SO_4/H_3PO_4/NH_4H_2PO_4$ MeCN/2-PrOH/H_2O (75:5:20 v/v)**	**pH 2.3 100 mM $(NH_4)_2SO_4/H_3PO_4/NH_4H_2PO_4$ MeCN/2-PrOH/H_2O (70:10:20 v/v)**	**pH 2.3 100 mM $(NH_4)_2SO_4/H_3PO_4/NH_4H_2PO_4$ MeCN/2-PrOH/H_2O (65:15:20 v/v)**	**pH 2.3 100 mM $(NH_4)_2SO_4/H_3PO_4/NH_4H_2PO_4$ MeCN/2-PrOH/H_2O (60:20:20 v/v)**	**pH 2.3 100 mM $(NH_4)_2SO_4/H_3PO_4/NH_4H_2PO_4$ MeOH/H_2O (80:20 v/v)**	**pH 1.9 0.1% v/v TFA MeCN/2-PrOH/H_2O (75:5:20 v/v)**	**pH 1.9 0.1% v/v TFA MeCN/2-PrOH/H_2O (70:10:20 v/v)**	**pH 1.9 0.1% v/v TFA MeCN/2-PrOH/H_2O (65:15:20 v/v)**	**pH 1.9 0.1% v/v TFA MeCN/2-PrOH/H_2O (60:20:20 v/v)**	**pH 1.9 0.1% v/v TFA MeOH/H_2O (80:20 v/v)**
t_g min	7.005	30.572	9.464	20.551	11.578	11.500	11.280	10.972	23.838	12.723	12.743	12.572	12.28	25.469
t_g max	29.980	55.542	23.566	44.516	26.071	26.930	27.503	27.892	53.363	26.456	27.344	27.796	28.051	48.736
$_{tg}$ range	22.975	24.970	14.102	23.965	14.493	15.430	16.223	16.920	29.525	13.733	14.601	15.224	15.771	23.267
w_{avg}	0.118	0.205	0.132	0.196	0.108	0.113	0.112	0.120	0.178	0.095	0.100	0.104	0.09	0.131
Δ(8a,1)	-0.14	-0.17	-0.28	-0.35	-0.28	-0.27	-0.27	-0.26	-0.31	-0.28	-0.27	-0.27	-0.27	-0.32
Δ(9,1)	0.03	0.16	0.05	0.05	0.05	0.05	0.05	0.05	0.04	0.05	0.05	0.05	0.05	0.05
Δ(14,13)	0.02	0.01	0.02	0.02	0.00	0.00	0.00	0.00	-0.01	0.00	0.00	0.00	0.00	0.00
Δ(15,13)	0.07	0.06	0.06	0.05	0.05	0.05	0.05	0.05	0.04	0.05	0.05	0.05	0.05	0.03
Δ(16,13)	-0.30	-0.35	-0.37	-0.33	-0.37	-0.37	-0.36	-0.36	-.0.30	-0.36	-0.35	-0.35	-0.34	-0.29
Δ(24,13)	-0.23	-0.26	-0.27	-0.22	-0.27	-0.27	-0.27	-0.27	-0.21	-0.27	-0.25	-0.25	-0.25	-0.20
Δ(26,13)	-0.35	-0.42	-0.48	-0.50	-0.48	-0.49	-0.49	-0.49	-0.42	-0.49	-0.48	-0.47	-0.47	-0.41

Table 70 ctd. Delta values for the peptide probes determined on the subset of mobile phases with different organic modifier combinations

pH 6.5 20 mM NH_4FA MeOH/H_2O (80:20 v/v)	41d	14.114	55.288	41.174	0.279	-0.09	0.05	0.00	0.04	-0.20	-0.15	-0.25
pH 7.5 20 mM $(NH_4)_2HPO_4$/$NH_4H_2PO_4$ MeOH/H_2O (80:20 v/v)	43d	14.015	55.377	41.362	0.314	-0.17	-0.06	0.01	0.04	-0.21	-0.16	-0.26
pH 7.5 20 mM $(NH_4)_2HPO_4$/$NH_4H_2PO_4$ MeCN/2-PrOH/H_2O (60:20:20 v/v)	43e	5.480	30.339	24.859	0.169	-0.15	-0.04	0.01	0.06	-0.29	-0.22	-0.33
	Mobile phase number	t_g min	t_g max	$_{tg}$ range	w_{avg}	Δ(8a,1)	Δ(9,1)	Δ(14,13)	Δ(15,13)	Δ(16,13)	Δ(24,13)	Δ(26,13)

3.9.6 Evaluation of the Effect of Temperature

The temperature chromatographic results were analysed using PCA to produce the score plot in *Figure 94 (*delta values in *Table 71*). The results demonstrated that the selectivity differences are reduced compared to the effect of organic or different additive, but it can be useful for optimising separations. For small molecules, the use of temperature in conjunction with t_G often can generate large differences, however, as may be the case here, when temperature is used as the sole variable there is a reduction in the degree of selectivity differences. However, temperature can be used to optimise a separation.

Table 71 Delta values for the peptide probes determined on the subset of mobile phases with different temperatures

pH 1.9 0.1% v/v TFA 20 °C	11b	14.185	26.706	12.521	0.091	-0.30	0.05	-0.01	0.05	-0.37	-0.23	-0.49
pH 1.9 0.1% v/v TFA 60 °C	11c	12.960	24.433	12.473	0.091	-0.24	0.04	0.00	0.04	-0.33	-0.26	-0.45
pH 2.3 100 mM $(NH_4)_2SO_4/H_3PO_4/NH_4H_2PO_4$ 20 °C	8b	12.763	25.685	12.922	0.123	-0.33	0.05	-0.01	0.05	-0.36	-0.24	-0.48
pH 2.3 100 mM $(NH_4)_2SO_4/H_3PO_4/NH_4H_2PO_4$ 60 °C	8c	10.955	24.062	13.107	0.085	-0.24	0.04	0.00	0.05	-0.35	-0.27	-0.47
pH 2.5 0.1% v/v FA 20 °C	1b	11.441	23.247	11.806	0.147	-0.36	0.06	0.02	0.06	-0.36	-0.24	-0.51
pH 2.5 0.1% v/v FA 60 °C	1c	9.695	20.629	10.934	0.118	-0.26	0.05	0.02	0.06	-0.37	-0.26	-0.56
pH 5.1 $BuSO_3/AA/NH_4AA$ 20 °C	31b	9.021	26.692	17.671	0.128	-0.17	0.18	0.02	0.07	-0.30	-0.20	-0.35
pH 5.1 $BuSO_3/AA/NH_4AA$ 60 °C	31c	7.437	26.144	18.707	0.088	-0.13	0.03	0.01	0.05	-0.30	-0.23	-0.34
pH 6.5 20 mM NH_4FA 20 °C	41b	7.514	26.519	19.005	0.115	-0.13	-0.07	0.01	0.06	-0.28	-0.18	-0.21
pH 6.5 20 mM NH_4FA 60 °C	41c	6.101	26.130	20.029	0.121	-0.13	-0.07	0.01	0.05	-0.27	-0.32	-0.31
pH 7.5 20 mM $(NH_4)_2HPO_4/NH_4H_2PO_4$ 20 °C	43b	7.348	26.668	19.320	0.121	-0.15	-0.06	0.02	0.06	-0.28	-0.19	-0.32
pH 7.5 20 mM $(NH_4)_2HPO_4/NH_4H_2PO_4$ 60 °C	43c	6.547	26.175	19.628	0.164	-0.16	-0.05	0.01	0.05	-0.29	-0.22	-0.33
	Mobile phase number	t_g min	t_g max	$_{tg}$ range	w_{avg}	Δ(8a,1)	Δ(9,1)	Δ(14,13)	Δ(15,13)	Δ(16,13)	Δ(24,13)	Δ(26,13)

There were visible differences between the three temperatures assessed, thus demonstrating that the temperature can be an extremely useful tool in the method development arsenal.

The racemates [L-Ser16]- and [D-Ser16]-Bovine GLP-2 (16-33) (Peptides Number 13 and 14, respectively), where compared at 20 and 60 °C in *Figure 95* using the subset of mobile phases. The results demonstrate some interesting separations. Under pH 2.5 0.1% v/v FA conditions (Mobile Phase 1), the selectivity was consistent between the two temperatures, as demonstrated by the delta values 0.016 and 0.017 for 20 and 60 °C, respectively. The increased temperature did however improve the peak widths and reduced the asymmetry, which could prove advantageous for the low ionic strength mobile phase. However, under pH 1.9 0.1% v/v TFA (Mobile Phase 11) conditions, there was a complete loss of resolution between the two racemates under the 60 °C conditions. There was a switch in elution order between the two temperature conditions using the pH 2.3 100 mM $(NH_4)_2SO_4$ / H_3PO_4 / $NH_4H_2PO_4$ (Mobile Phase 8) conditions. Selectivity was reduced with the increase in temperature for both pH 5.1 20 mM $BuSO_3$ / AA / NH_4AA and pH 7.5 20 mM $(NH_4)_2HPO_4$ / $NH_4H_2PO_4$ (Mobile Phase 31 and 43, respectively). At 20 °C, there was baseline resolution between the peaks of interest of 2.8 and 2.2, respectively. This decreased to 2.0 and 1.7 at the higher temperature, whilst the delta value decreased by 0.011 and 0.007, respectively. The two temperatures under pH 6.5 20 mM NH_4FA (Mobile Phase 41) conditions did not change the selectivity, but it did improve the resolution between the peaks. At 20 °C, the resolution between the racemates was 0.7 whilst at 60 °C, the resolution increased to 1.1. The increase in the diffusion rate at the higher temperature generally reduced the peak widths on all the mobile phases assessed which increased the peak capacities.

These results are highly indicative that it is not possible to identify the “ideal temperature” which is capable of separating racemates or other species of interest.

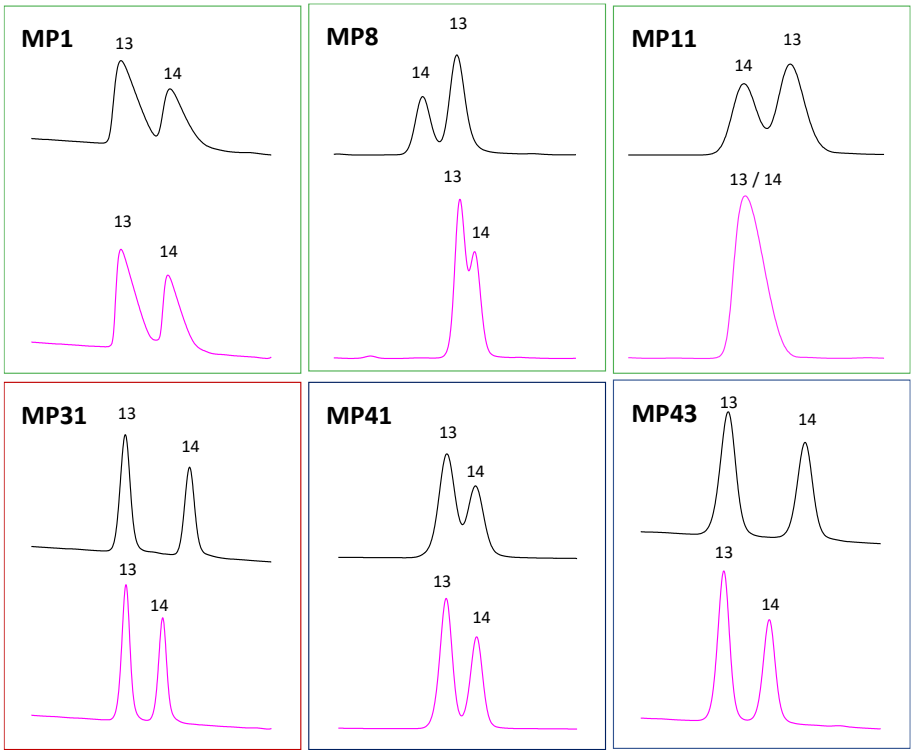

Figure 95 Comparison of the separation achieved between [L-Ser16]- (Peptide Number 13) and [D-Ser16]-Bovine GLP-2 (16-33) (Peptide Number 14) on the subset of mobile phases at 20 and 60 °C (black and pink traces, respectively). The chromatograms were aligned for Peptide Number 13. Mobile Phase 1: pH 2.5 0.1% v/v FA, 8: pH 2.3 100 mM $(NH_4)_2SO_4$ / H_3PO_4 / $NH_4H_2PO_4$, 11: pH 1.9 0.1% v/v TFA, 31: pH 5.1 20 mM $BuSO_3$ / AA / NH_4AA, 41: pH 6.5 20 mM NH_4FA, 43: pH 7.5 20 mM $(NH_4)_2HPO_4$ / $NH_4H_2PO_4$. Analyses were performed on the Nexera X2 coupled to the 2020 single quadrupole system (where applicable) on the Ascentis Express C18. The aqueous portion can be located in Section 2.12.1.3. The organic was acetonitrile / water (80:20 v/v) with a gradient of 5.6-62.5%B over 40 minutes. Flow rate was 0.3 mL/min, and detection used a combination of UV at 215 nm and MS for peak confirmation.

The chromatograms for [Met(O)10]-Bovine GLP-2 (1-15) (Peptide Number 8) diastereoisomers were compared for their discriminating power (*Figure 96*). This subtle separation demonstrated the selectivity differences achieved by the subset of mobile phases at both 20 and 60 °C. The resolution generally increased with the lower temperature, whilst the higher temperature decreased the peak widths. It was generally observed that the diastereoisomers obtained better separation when mobile phases with pH <5.1 were used based on the data from the initial ~40 mobile phase study. This in combination with lower temperature could provide

greater opportunities to separate methionine diastereoisomer species. There were additional peaks observed around the methionine diastereoisomers at 60 °C in the pH 7.5 20 mM $(NH_4)_2HPO_4$ / $NH_4H_2PO_4$ (Mobile Phase 43). The peaks were observed in all three test mixtures under those mobile phase conditions and indicate the artefacts are a true observation. This could possibly be due to impurities drawn out at the higher temperature or potentially on-column degradation.

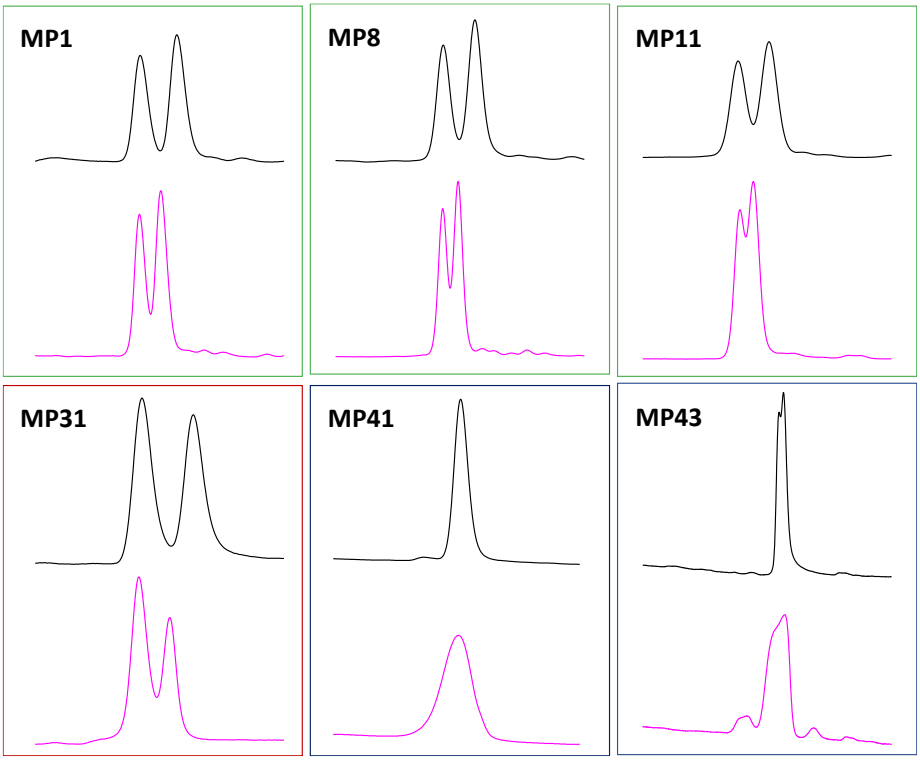

Figure 96 Comparison of the separation achieved between the oxidised [Met(O)10]-Bovine GLP-2 (1-15) diastereoisomers (Peptide Number 8) on the subset of mobile phases at 20 and 60 °C (black and pink traces, respectively). Mobile Phase 1: pH 2.5 0.1% v/v FA, 8: pH 2.3 100 mM $(NH_4)_2SO_4$ / H_3PO_4 / $NH_4H_2PO_4$, 11: pH 1.9 0.1% v/v TFA, 31: pH 5.1 20 mM $BuSO_3$ / AA / NH_4AA, 41: pH 6.5 20 mM NH_4FA, 43: pH 7.5 20 mM $(NH_4)_2HPO_4$ / $NH_4H_2PO_4$. Analyses were performed on the Nexera X2 coupled to the 2020 single quadrupole system (where applicable) on the Ascentis Express C18. The aqueous portion can be located in Section 2.12.1.3. The organic was acetonitrile / water (80:20 v/v) with a gradient of 5.6-62.5%B over 40 minutes. Flow rate was 0.3 mL/min, and detection used a combination of UV at 215 nm and MS for peak confirmation.

The impurity profile for aged Bovine GLP-2 (1-15) was compared at both 20 and 60 °C using the subset of mobile phases on the Ascentis Express C18 (*Figure 97*). The results demonstrated the subtle differences which can be achieved when

temperature is utilised as a parameter to affect selectivity. There were some greater differences attributed to 60 °C using the pH 6.5 20 mM NH_4FA and pH 7.5 20 mM $(NH_4)_2HPO_4$ / $NH_4H_2PO_4$ mobile phase conditions (Mobile Phase 41 and 43) compared to the 20 °C chromatogram. The poor peak shape under these conditions are characteristic of on-column degradation due to the increase in temperature, where there appears to be a zone of interconversion between the main peak and an impurity. This may merit further investigation, with more temperature data points to establish the point of degradation. There were greater differences in the impurity profiles between pH 1.9 0.1% v/v TFA and pH 2.3 100 mM $(NH_4)_2SO_4$ / H_3PO_4 / $NH_4H_2PO_4$ (Mobile Phase 11 and 8, respectively). Based on previous resulted exhibited in preceding discussions, this was expected as there appears to be greater selectivity differences amongst the low pH conditions despite proximity in the score plot in comparison to the intermediate pH conditions.

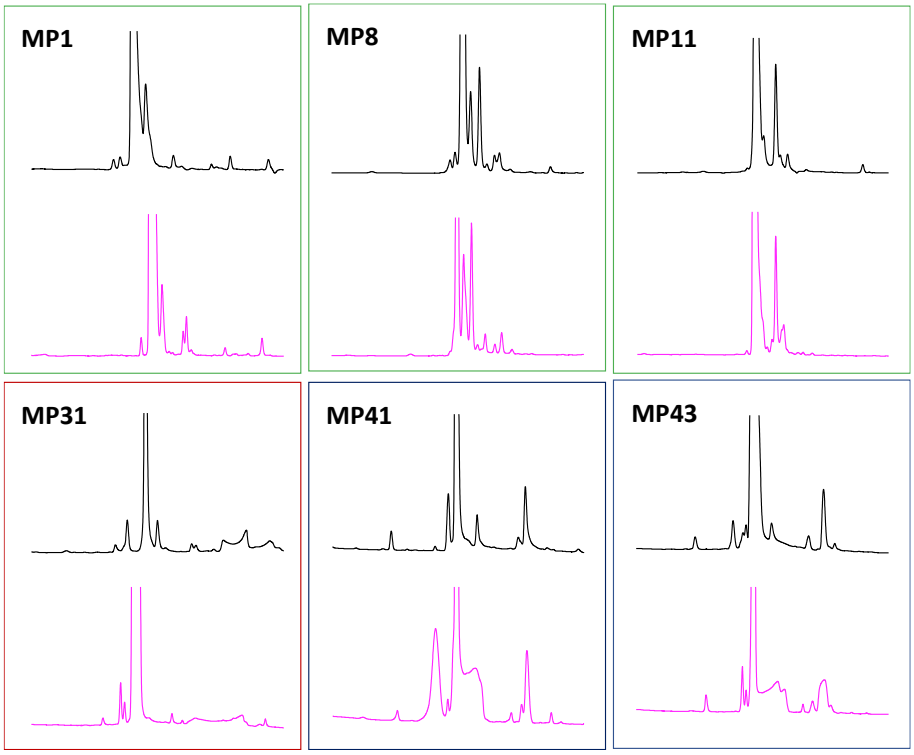

Figure 97 Comparison of the UV profile for aged Bovine GLP-2 (1-15) on the subset of mobile phases at 20 and 60 °C (black and pink traces, respectively). Mobile Phase 1: pH 2.5 0.1% v/v FA, 8: pH 2.3 100 mM $(NH_4)_2SO_4$ / H_3PO_4 / $NH_4H_2PO_4$, 11: pH 1.9 0.1% v/v TFA, 31: pH 5.1 20 mM $BuSO_3$ / AA / NH_4AA, 41: pH 6.5 20 mM NH_4FA, 43: pH 7.5 20 mM $(NH_4)_2HPO_4$ / $NH_4H_2PO_4$ Analyses were performed on the Nexera X2 coupled to the 2020 single quadrupole system (where applicable) on the Ascentis Express C18. The aqueous portion can be located in Section 2.12.1.3. The organic was acetonitrile / water (80:20 v/v) with a gradient of 5.6-62.5%B over 40 minutes. Flow rate was 0.3 mL/min, and detection used a combination of UV at 215 nm and MS.

3.9.7 Evaluation of the Effect of Stationary Phase in Conjunction with Mobile Phase Compositions

Three interesting stationary phases as determined based on their position within the PCA were evaluated using the subset of six interesting mobile phases in order to compare against the Ascentis Express C18. The results were evaluated using PCA to determine the applicability of the initial study on other types of stationary phases (*Figure 98* and *Table 72*).

Polygons were drawn around each of the results for the various stationary phases, in order to establish if there was a common trend between the columns. The

Acquity CSH Fluoro Phenyl could not be evaluated using 20 mM pH 7.5 $NH_4H_2PO_4$ / $(NH_4)_2HPO_4$ (Mobile Phase 43) as three of the hydrophobic peptide probes coeluted with an artefact present in the chromatogram.

The chromatographic response between the Ascentis Express C18 and Ascentis Express Biphenyl were quite similar (purple and blue polygons, respectively). pH increased from left to right for both stationary phases. Both pH 6.5 20 mM NH_4FA and pH 7.5 20 mM $(NH_4)_2HPO_4$ / $NH_4H_2PO_4$ (Mobile Phases 41 and 43, respectively) are in the bottom right of their respective polygons, and both mobile phases are closely located for the corresponding columns suggesting similar selectivity. pH 1.9 0.1% v/v TFA and pH 2.3 100 mM $(NH_4)_2SO_4$ / H_3PO_4 / $NH_4H_2PO_4$ (Mobile Phases 8 and 11) are also closely located on both columns, and also positioned similarly in the bottom left corner of each particular polygon. Finally, pH 2.5 0.1% v/v FA (Mobile Phase 1) is located in the top left corner for both stationary phases. The major difference in response was attributed to the $BuSO_3$ / AA / NH_4AA mobile phase (Mobile Phase 31), which caused the shape of the profiles in *Figure 98* to differ. It is possible that the mode of interaction between the ion pair and the stationary phases are different. It could be feasible that the alkyl chain from the ion pair could be drawn into the stationary phase due to greater accessibility into the phase, thus exposing the SO_3^- moiety of the ion pair. Alternatively, the other stationary phase might not have the ligand architecture to permit the ion pair into the phase, therefore the ion pair would preferentially bind with the peptide probes. This would alter how the analytes would interact with the ion pair and stationary phase, thereby offering different retention profiles. Despite the $BuSO_3$ mobile phase result, it is a positive indication that neutral stationary phases and phases with some negative / polar character react in a similar behaviour which could indicate these results could be transferable to a wider array of commercially available columns of that classification.

The results from the Polaris Amide C18 and Acquity CSH Fluoro Phenyl, however, were extremely diverse to the neutral phase (red and orange polygons, respectively). This is perhaps unsurprising as they demonstrated significant

selectivity differences during the column characterisation, therefore their response to mobile phases could be presumed to be different. The positive character to the stationary phase could play a crucial role in the different selectivity observed between the mobile phases and peptides, where the change in peptide charge using the different mobile phases highlights the differences. There are some similarities between the two positive character phases, which include pH 2.5 0.1% v/v FA (Mobile Phase 1) drawn along the first principal component between the 3rd and 4th quadrant. Both stationary phases also have pH 1.9 0.1% v/v TFA and pH 5.1 20 mM $BuSO_3$ / AA / NH_4AA (Mobile Phase 8 and 31, respectively) closely located within the respectively polygons. This could be due to both TFA and $BuSO_3$ being ion pairs with negative character, and on this type of phase it can cause greater similarities compared to a neutral phase. There are also major differences between the Acquity CSH Fluoro Phenyl and the Polaris Amide C18, which is possibly due to the accessible silanol groups on the Acquity CSH Fluoro Phenyl which are available for electrostatic interactions.

The results indicate that the profiles from the mobile phase study cannot be transferred for phases which possess significant selectivity differences. This would suggest that greater work would need to be done for that class of stationary phase. It would also be interesting to observe any chromatographic differences for phases with greater negative character, or phases which are located within close proximity to the Ascentis Express C18 in the Peptide RPC Column Characterisation score plot. However, due to time constrictions, it was not possible to further evaluate other stationary phases in this study.

Table 72 Delta values for the peptide probes determined on the subset of mobile phases with different stationary phases

pH 1.9 0.1% v/v TFA Polaris Amide C18	11	12.300	24.600	12.300	0.107	-0.28	0.06	-0.01	0.04	-0.37	-0.23	-0.50
pH 1.9 0.1% v/v TFA Acquity CSH Fluoro Phenyl	11	9.214	21.369	12.155	0.082	-0.23	0.04	-0.01	0.02	-0.38	-0.16	-0.51
pH 1.9 0.1% v/v TFA Ascentis Express Biphenyl	11	13.019	25.495	12.476	0.104	-0.27	0.05	-0.01	0.04	-0.35	-0.19	-0.44
pH 2.3 100 mM $(NH_4)_2SO_4/H_3PO_4$/ $NH_4H_2PO_4$ Polaris Amide C18	8	11.940	25.166	13.226	0.128	-0.32	0.06	0.00	0.05	-0.38	-0.24	-0.51
pH 2.3 100 mM $(NH_4)_2SO_4/H_3PO_4$/ $NH_4H_2PO_4$ Acquity CSH Fluoro Phenyl	8	10.606	23.010	12.404	0.107	-0.26	0.06	0.00	0.03	-0.42	-0.18	-0.56
pH 2.3 100 mM $(NH_4)_2SO_4/H_3PO_4$/ $NH_4H_2PO_4$ Ascentis Express Biphenyl	8	11.577	24.062	12.485	0.100	-0.27	0.06	-0.02	0.04	-0.36	-0.21	-0.45
pH 2.5 0.1% v/v FA Polaris Amide C18	1	9.286	18.625	9.339	0.068	-0.47	0.21	0.02	0.04	-0.57	-0.23	-0.87
pH 2.5 0.1% v/v FA Acquity CSH Fluoro Phenyl	1	7.346	16.783	9.437	0.075	-0.30	0.12	0.01	0.04	-0.56	-0.20	-0.81
pH 2.5 0.1% v/v FA Ascentis Express Biphenyl	1	11.167	24.445	13.278	0.135	-0.27	0.05	0.00	0.05	-0.37	-0.20	-0.52
pH 5.1 $BuSO_3$/AA/NH_4AA Polaris Amide C18	31	11.778	23.294	11.516	0.130	-0.30	0.06	0.01	0.05	-0.38	-0.23	-0.53
pH 5.1 $BuSO_3$/AA/NH_4AA Acquity CSH Fluoro Phenyl	31	9.350	20.657	11.307	0.097	-0.25	0.06	0.00	0.03	-0.44	-0.17	-0.61
pH 5.1 $BuSO_3$/AA/NH_4AA Ascentis Express Biphenyl	31	13.076	25.989	12.913	0.140	-0.27	0.05	0.00	0.04	-0.34	-0.20	-0.45
pH 6.5 20 mM NH_4FA Polaris Amide C18	41	16.454	31.739	15.285	0.126	-0.49	0.00	0.00	0.02	-0.53	-0.23	-0.72
pH 6.5 20 mM NH_4FA Acquity CSH Fluoro Phenyl	41	2.374	25.006	22.632	0.095	-0.11	-0.09	0.01	0.03	-0.26	-0.11	-0.19
pH 6.5 20 mM NH_4FA Ascentis Express Biphenyl	41	3.320	24.604	21.284	0.065	-0.14	-0.08	0.01	0.04	-0.24	-0.13	-0.21
pH 7.5 20 mM $(NH_4)_2HPO_4/NH_4H_2PO_4$ Polaris Amide C18	43	8.203	28.710	20.507	0.158	-0.13	-0.05	0.01	0.06	-0.30	-0.20	-0.37
pH 7.5 20 mM $(NH_4)_2HPO_4/NH_4H_2PO_4$ Ascentis Express Biphenyl	43	5.254	24.345	19.091	0.107	-0.15	-0.09	0.01	0.04	-0.25	-0.14	-0.25
Mobile phase number		t_g min	t_g max	$_{tg}$ range	w_{avg}	Δ(8a,1)	Δ(9,1)	Δ(14,13)	Δ(15,13)	Δ(16,13)	Δ(24,13)	Δ(26,13)

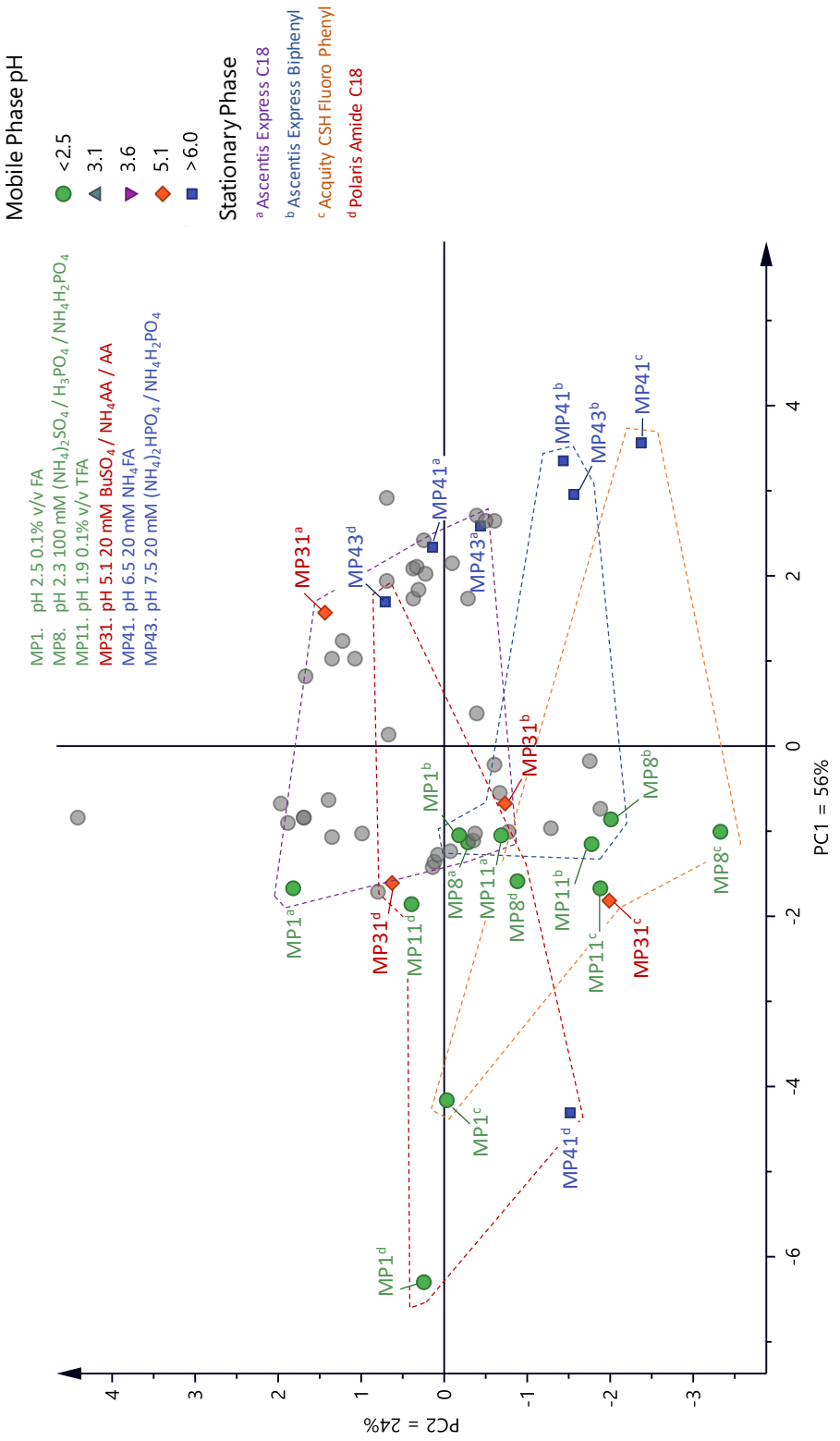

Figure 98 Score plot highlighting the effect of stationary phase on different mobile phase combinations. Grey circles correspond to the position of the other mobile phases assessed on the Ascentis Express C18 described in Table 64

By combining both stationary phases and mobile phases, greater opportunities can be generated to separate all compounds within the mixture, thus develop a method with sufficient selectivity differences. This was demonstrated in *Figure 99*, where the four stationary phases were compared using pH 2.3 100 mM $(NH_4)_2SO_4$ / H_3PO_4 / $NH_4H_2PO_4$ and pH 5.1 20 mM $BuSO_3$ / AA / NH_4AA on an aged sample of Bovine GLP-2 (1-15). Although the peaks were not tracked, it is possible to see the differences in selectivity and more peaks drawn out which could possibly be missed if not screened appropriately. This simple example demonstrates the necessity of performing a method development screen which utilises both important operating parameters to maximise selectivity.

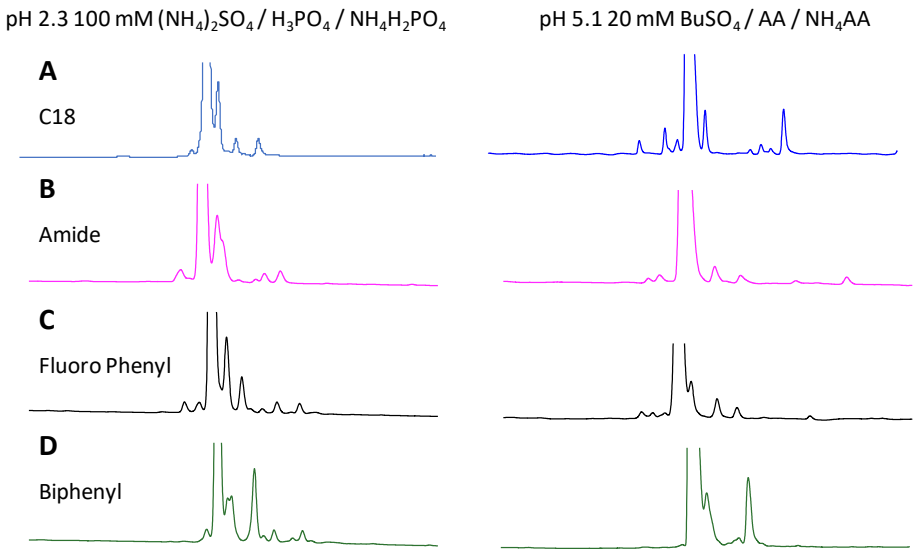

Figure 99 Chromatograms of aged Bovine GLP-2 (1-15) to illustrate selectivity differences generated on two different mobile phases on the (A) Ascentis Express C18, (B) Polaris Amide C18, (C) Acquity CSH Fluoro Phenyl and (D) Ascentis Express Biphenyl. Analyses were performed on the Nexera X2 coupled to the 2020 single quadrupole system (where applicable). The aqueous portion can be located in Section 2.12.1.3. The organic was acetonitrile / water (80:20 v/v) with a gradient of 5.6-62.5%B over 40 minutes. Flow rate was 0.3 mL/min, column oven temperature was 40 °C, and detection used a combination of UV at 215 nm and MS.

4. Future Work

There are many possible further expansions to this research, which could expand the knowledge and understanding of peptide separation systems. The Peptide RPC Column Characterisation Protocol has provided a firm basis for classifying different stationary phases and their potential major interactions which influence selectivity. The database has shown that stationary phases can be selected based on a range of selectivity profiles. This should be further validated in combination with the mobile phase study to demonstrate maximum selectivity differences on peptide tryptic digests.

The Peptide RPC Column Characterisation protocol could be applied to stationary phases with other more interesting and novel chemistries to understand their position within the score plot. This could bring to light deficiencies in the current commercialised stationary phase capabilities. It can also help to drive further development of stationary phase design to fill the dearth of the positive character phases.

The mobile phase study has provided a foundation for further study which could include an expansion in the use of different organic modifiers. This could include evaluating more combinations of ternary mobile phases. The study could also be performed on a greater number of columns from different classifications to understand the extent to which this work can be applied. Temperature studies can also be extended to cover a wider range of temperatures which could offer potential for problematic separations of racemates. A study with more temperature data points could help to rationalise the retention time relationships, which cannot be done on the current dataset.

The mobile phase study could also be further expanded to include other interesting and novel additives. Some of the most interesting and better chromatographic performance (i.e. peak capacity and peak shape) was achieved using perchlorate as a chaotropic agent. However, perchlorate offers potential issues in terms of its toxicity and propensity to explode. An alternative which could be interesting to

investigate is PF_5. Although it is still toxic, it does not have the same issue with reactivity.

Upon the evaluation of stationary and mobile phases, the information could lead to a method development roadmap to aid characterisation of complex peptides and samples within the biopharmaceutical market. This would be the first comprehensive process to aid method development for the characterisation of peptide digests. It will also help to identify and rank the importance of operating parameters for peptide analysis. This would also include matching mobile phase A and B solvents UV absorbance to obtain a flatter baseline.

5. Conclusions

A protocol for the characterisation of stationary phases using peptides as probes was successfully developed. The protocol utilised two gradient mobile phase systems at low and intermediate pH to cover different degrees of ionisation of both peptides and stationary phases.

The peptides were rationally designed in order to systematically change characteristics deemed important for retentivity and selectivity, including hydrophobicity, aromaticity, degree of hydrogen bonding, electrostatic interactions, steric interactions and important degradation pathways. The peptide mixtures were injected onto 14 different stationary phases possessing different chromatographic characteristics, which were grouped into neutral phases (i.e. phases with high ligand density and a large degree of end-capping), negative character phases (i.e. phases with a reduced ligand coverage or no end-capping present) and finally positive character phases (i.e. phases with a positively charged functional group in addition to the RP ligand or a small surface positive charge). Peptides were identified using SIM, or where differentiation by mass was not possible (i.e. isomers) different peak area ratios were used through varying relative concentrations in the mixtures.

A range of normalised retention differences, denoted as delta values, were calculated which covered the interactions of interest to assess selectivity differences. The data was analysed using Principal Component Analysis, which highlighted groupings of stationary phases resembling the three groups described above. The number of delta values and peptides were systematically reduced whilst ensuring that the integrity of the score plot was maintained.

Further evaluation of the data indicated that the most crucial interactions between stationary phases and peptides are hydrophobic in nature, in combination with polar interactions. These results, which are based on biologically relevant peptides, suggest that it is polar interactions and the second order structure of the adsorbed peptide in the stationary phase that to a large extent contributes to the selectivity differences seen between columns. This was highlighted by the large selectivity

differences exhibited for peptides with the same degree of hydrophobicity. Another interesting observation was the large retention differences exhibited for racemic species, which only differ by the orientation of one of the amino acids.

The robustness of the Peptide RPC Column Characterisation protocol was assessed using reduced factorial design and PCA, with various factors being systematically altered to deduce the impact on subtle changes to the protocol. The results indicated that the formic acid gradient can be seen to provide robust results within the given tolerances of this study. The ammonium formate gradient, however, required mitigation to improve robustness by carefully controlling the concentration of acetonitrile in the B solvent. All other parameters assessed did not influence the robustness.

The sample load for the columns was also determined and the potential impact on switching between low and intermediate pH for certain commercially available stationary phases was evaluated. Both studies had ramifications for the protocol and mitigation was put in place to address both phenomena.

In addition, the instrument variability on three different LC configurations and column batch to batch variability was assessed to ascertain the degree of variability which could be expected. Both the LC and column variability were minimal and highlights that the differences between stationary phases observed using the Peptide RPC Column Characterisation protocol are caused by chromatographic selectivity differences, rather than random error.

A novel column characterisation protocol which employed peptides as probes was applied successfully to 38 out of 41 stationary phases. The results were placed in a database and critically assessed using PCA. Each phase was classified into one of three groups; neutral, negative / polar or positive character, where the column classification was justified based on its position within the score plot and prior knowledge of the phase. This approach allows easy identification of phases which could be chromatographically similar or dissimilar, depending on their location relative to another column.

The results of the Peptide RPC Column Characterisation Protocol were compared against two protocols based on small molecules which highlighted a lack of correlation between the two sets of test probes. Consequently, there is a need for a peptide probe-based protocol to select appropriate stationary phases for peptide separations.

Finally, the ability of the database to predict was validated at low and mid pH using two tryptic protein digests. It was successfully demonstrated that selectivity differences can be observed chromatographically and allowed a diverse range of phases to be selected. In addition, stationary phases can be selected which possess similar selectivity, thereby allowing a back-up column to be selected if necessary.

The mobile phase study was conducted initially on a standard C18 ligand stationary phase to evaluate the impact of different pH values, salts, ionic strengths and acidic modifiers. These results emphasised the greater chromatographic selectivity generated under low pH conditions which was then reduced as the pH increased to intermediate conditions. This was rationalised by attributing it to the reduction in the subtle interaction which are available at low pH, but are overwhelmed by electrostatic interactions at intermediate pH.

The study was expanded to evaluate the impact of two different organic modifiers and two additional temperatures on six mobile phases. The change in selectivity difference demonstrated by the methanol containing solvent in comparison with acetonitrile underlined the need to consider different solvents in method development screenings. The four different ternary acetonitrile / 2-PrOH solvents did not show significant selectivity differences therefore it would only be advantageous to assess one concentration. There were smaller differences in the PCA based on temperature, however, it is a parameter which is typically used to optimise separations, therefore it is expected that there are reduced differences in comparison to changing organic modifier or changing salt counterion.

The applicability of the mobile phase data on a greater number of stationary phases was assessed. The Polaris Amide C18, Acquity CSH Fluoro Phenyl and Ascentis

Express Biphenyl were selected for the comparison based on their diverse chromatographic performance in the Peptide RPC Column Characterisation Protocol, and compared against the Ascentis Express C18. These columns were assessed on the same six reduced mobile phases as the extended mobile phase study. The Ascentis Express Biphenyl behaved in a similar pattern to the Ascentis Express C18, except on the $BuSO_3$ based mobile phase. This was rationalised by attributing it to a different ion pairing mechanism operating on the two phases. The Polaris Amide C18 and the Acquity CSH Fluoro Phenyl, however, demonstrated some dramatic differences compared to the Ascentis Express C18. It is possible that these phases possess such different chromatographic behaviour due to a positive charge on the stationary phase, which may limit the overall conclusions on these types of phases compared to those made from the main study on high purity C18 phases (i.e. neutral and negatively charged RPC columns based on high purity silica).

The overall impression from these results confirm the immense difficulty the analyst is faced with in selecting a mobile phase or stationary phase which is ideal for a particular type of separation. There is hope amongst the industry that there is a holy grail for selecting a particular column or chromatographic condition to, for example, successfully separate all racemate but the results from these studies have demonstrated the diverse chromatographic selectivities generated which would suggest this is not possible. These results emphasise the need for a good and rational method development strategy. The findings of this work are evidence that it is important to have a good selectivity screen of stationary phases and mobile phases to maximise selectivity, which will hopefully assist in the development of such strategies. The outcomes from this study provide a good fundamental platform for understanding the factors which influence peptide separation.

vi. References

1. *Radio Compass Blog, Top Drugs by Sales Revenue in 2015: Who Sold the Biggest Blockbuster Drugs?* 2016 08/07/2019]; Available from: http://www.pharmacompass.com/radio-compass-blog/top-drugs-by-sales-revenue-in-2015-who-sold-the-biggest-blockbuster-drugs.
2. A. Philippidis. *The top 15 best selling drugs of 2016*. 08/07/2019]; Available from: https://www.genengnews.com/a-lists/the-top-15-best-selling-drugs-of-2016/.
3. *Top Drugs by Sales Revenue 2016*. 08/07/2019]; Available from: https://www.linkedin.com/pulse/top-drugs-sales-revenue-2016-michael-meegan?articleId=9190660974980732402.
4. A. Philippidis. *The Top 15 Best-Selling Drugs of 2017*. 08/07/2019]; Available from: https://www.genengnews.com/a-lists/the-top-15-best-selling-drugs-of-2017.
5. A. Philippidis. *Top 15 Best-Selling Drugs of 2018*. 08/07/2019]; Available from: https://www.genengnews.com/a-lists/top-15-best-selling-drugs-of-2018.
6. J.J. Zhang, *The global biomanufacturing outsourcing market.* BioPharm International, 2015. **28**(3).
7. L. Moruz and L. Käll, *Peptide retention time predictions.* Mass Spec. Rev., 2017. **36**: p. 615-623.
8. N. Pfeifer, A. Leinenback, C.G. Huber and O. Kohlbacher, *Statistical learning of peptide retention behaviour in chromatographic separations: a new kernel-based approach for computational proteomics.* BMC Bioinformatics, 2007. **8**: p. 468-482.
9. B. Tripet, D. Capeniene, J.M. Kovacs, C.T. Mant, O.V. Krokhin, and R.S. Hodges, *Requirements for prediction of peptide retention time in reversed-phase high performance liquid chromatography: Hydrophilicity / hydrophobicity of side-chains at the N- and C-termini of peptides are dramatically affected by the end groups and location.* J. Chromatogr. A., 2007. **1141**: p. 212-225.
10. O. Krokhin, *Peptide retention prediction in reversed-phase chromatography: Proteomic applications.* Expert. Rev. Proteomics, 2012. **9**: p. 1-4.
11. V. Spicer, A. Yamchuk, J. Cortens, S. Sousa, W. Ens, K.G. Standing, J.A. Wilkins, and O.V. Krokhin, *Sequence specific retention calculator. A family of peptide retention time prediction algorithms in reversed-phase HPLC: Applicability to various chromatographic conditions and columns.* Anal. Chem., 2007. **79**: p. 8762-8768.
12. T. Baczek., P. Wiczling, M. Marszałł, Y.V. Heyden and R. Kaliszan, *Prediction of peptide retention at different HPLC conditions from multiple linear regression models.* J. Proteome. Res., 2005. **4**: p. 555-563.
13. N.S. Wilson, M.D. Nelson, J.W. Dolan, L.R. Snyder, R.G. Wolcott, and P.W. Carr, *Column selectivity in reversed-phase liquid chromatography I. A general quantitative relationship.* J. Chromatogr. A., 2002. **961**: p. 171-193.

14. J.W. Dolan, A. Maule, D. Bingley, L. Wrisley, C.C. Chan, M. Angod, C. Lunte, R. Krisko, J.M. Winston, B.A. Homeier, D.V. McCalley, and L.R. Snyder, *Choosing an equivalent replacement column for a reversed-phase liquid chromatographic assay procedure.* J. Chromatogr. A., 2004. **1057**: p. 59-74.
15. L.R. Snyder, A. Maule, A. Heebsh, R. Cuellar, S. Paulson, J. Carrano, L. Wrisley, C.C. Chan, N. Pearson, J.W. Dolan, and J.J. Gilroy, *A fast, convenient and rugged procedure for characterising the selectivity of alkyl-silica columns.* J. Chromatogr. A., 2004. **1057**: p. 49-57.
16. N.S. Wilson, M.D. Nelson, J.W. Dolan, L.R. Snyder and P.W. Carr, *Column selectivity in reversed-phase liquid chromatography II. Effect of a change in conditions.* J. Chromatogr. A., 2002. **961**: p. 195-215.
17. M.R. Euerby and P. Petersson, *Chromatographic classification and comparison of commercially available reversed-phase liquid chromatographic columns using principal component analysis.* J. Chromatogr. A., 2003. **994**: p. 13-36.
18. M.R. Euerby and P. Petersson, *Chromatographic classification and comparison of commercially available reversed-phase liquid chromatographic columns containing polar embedded groups / amino endcappings using principal component analysis.* J. Chromatogr. A., 2005. **1088**: p. 1-15.
19. M.R. Euerby, P. Petersson, W. Campbell and W. Roe, *Chromatographic classification and comparison of commercially available reversed-phase liquid chromatographic columns containing phenyl moieties using principal component analysis.* J. Chromatogr. A., 2007. **1154**: p. 138-151.
20. C.T. Mant, D. Cepeniene and R.S. Hodges, *Reversed-phase HPLC of peptides: Assessing column and solvent selectivity on standard polar-embedded and polar endcapped columns.* J. Sep. Sci, 2010. **33**: p. 3005-3021.
21. C.T. Mant and R.S. Hodges, *Design of peptide standards with the same composition and minimal sequence variation to monitor performance / selectivity of reversed-phase matrices.* J. Chromatogr. A., 2012. **1230**: p. 30-40.
22. J. Clayden, N. Greeves and S. Warren, *Organic Chemistry*. 2012, UK: Oxford University Press.
23. R.B. Merrifield, *Solid Phase Peptide Synthesis I. The synthesis of a tetrapeptide.* J. Am. Chem. Soc. , 1963. **85**: p. 2149-2154.
24. M. Stawikowski and G.B. Fields, *Introduction to Peptide Synthesis. Current Protocols in Protein Science*. 2012, Chichester, UK: John Wiley & Sons.
25. V.K. Sarin, S.B.H. Kent, A.R. Mitchell and R.B. Merrifield, *A general approach to the quantitation of synthetic efficiency in solid phase peptide synthesis as a function of chain length.* J. Am. Chem. Soc., 1984. **106**: p. 7845-7850.
26. A. Isidro-Llobet, M. Álvarez and F. Albericio, *Amino acid protecting groups.* Chem. Rev., 2009. **109**: p. 2455-2504.
27. R.B. Merrifield, *New approaches to the chemical synthesis of peptides.* Recent Prog. Horm. Res. , 1967. **23**: p. 451-482.

28. N. Srinivasan, A. Yurek-George and A. Ganesan, *Rapid deprotection of N-Boc amines by TFA combined with freebase generation using ion-exchange resins.* Mol. Divers., 2005. **9**: p. 291-293.
29. D.M. Shendage, R. Fröhlich and G. Haufe, *Highly efficient stereoconservative amidation and deamidation of α- amino acids.* Org. Lett., 2004. **6**: p. 3675-3678.
30. H. Bouleghlem, N.E. Aouf and S. Zidane, *A novel method for the deprotection of N-Boc-D-glucosamine-Ac by irradiation via microwave.* Int. J. Chem. Eng. App, 2016. **7**: p. 209-212.
31. M.W. Pennington, *HF cleavage and deprotection procedures for peptides synthesised using a Boc/Bzl strategy.* Meth. Mol. Biol. , 1994. **35**: p. 41-62.
32. L.A. Carpino and G.Y. Han, *The 9-fluorenylmethoxycarbonyl amino protecting group.* J. Org. Chem., 1972. **37**: p. 3404-3409.
33. L.A. Carpino and G.Y. Han, *The 9-fluorenylmethoxycarbonyl function, a new base sensitive amino protecting group.* J. Am. Chem. Soc., 1970. **92**: p. 5748-5749.
34. R. Behrendt, P. White and J. Offer, *Advances in Fmoc solid phase peptide synthesis.* J. Pep. Sci, 2016. **22**: p. 4-27.
35. S.A. Palasek, Z.J. Cox and J.M. Collins, *Limiting racemisation and aspartimide formation in microwave-enhanced Fmoc solid phase peptide synthesis.* J. Pep. Sci, 2007. **13**: p. 143-148.
36. J.P. Tam, F.S. Tjoeng and R.B. Merrifield, *Design and synthesis of multidetachable resin supports for solid phase peptide synthesis.* J. Am. Chem. Soc., 1980. **102**: p. 6117-6127.
37. P. Tofteng Shelton and K.J. Jensen, *Linkers, Resins and General Procedures for Solid-Phase Peptide Synthesis*, in *Peptide Synthesis and Applications*, P.T.S. K.J. Jensen, S. Pedersen, Editor. 2013, Humana Press, : Totowa, NJ.
38. *Recombinant Gene Expression*. 3rd Ed. ed. 2012, New Delhi, India: Humana Press.
39. Y. Li, *Recombinant production of antimicrobial peptides in Escherichia coli: A review.* Protein Expr. Purif., 2011. **80**: p. 260-267.
40. V. Rodríguez, J.A. Asenjo and B.A. Andrews, *Design and implementation of a high yield production system for recombinant expression of peptides.* Microb. Cell Fact., 2014. **13**: p. 65-75.
41. F.C. Stevens, *Calmodulin: An Introduction.* Can. J. Biochem. Cell. Biol, 1983. **61**: p. 906-910.
42. A. Klug, *The Discovery of Zinc Fingers and Their Applications in Gene Regulation and Genome Manipulation.* Annu. Rev. Biochem., 2010. **79**: p. 213-231.
43. S. Feketes, J. Veuthey and D. Guillarme, *New trends in reversed-phase liquid chromatographic separations of therapeutic peptides and proteins: Theory and applications.* J. Pharm. Biomed. Anal., 2012. **69**: p. 9-27.
44. L.N. Bell, *Peptide Stability in Solids and Solutions.* Biotechnol. Prog., 1997. **13**: p. 342-346.

45. L.R. Snyder, J. Kirkland and J.W. Dolan, *Introduction to Modern Liquid Chromatography*. 3rd Ed. ed. 2010, New Jersey: John Wiley & Sons.
46. L.R. Snyder and J.W. Dolan, *Chapter 6.1 Separation of large molecules*, in *High-Performance gradient elution*. 2007, John Wiley & Sons, Inc: Hoboken, NJ. p. 228-248.
47. D.V. McCalley, *Choice of buffer for the analysis of basic peptides in reversed-phase HPLC.* LCGC Asia Pacific, 2005. **8**: p. 40-47.
48. D.V. McCalley, *Study of overloading of basic drugs and peptides in reversed-phase high performance liquid chromatography using pH adjustment of weak acid mobile phases suitable for mass spectrometry.* J. Chromatogr. A., 2005. **1075**: p. 57-64.
49. C. Markopoulou, T. Tweedlie, D. Watson, G.G. Skellern, H. Reda, P. Petersson, H. Bradstock, and M.R. Euerby, *A study of the relative importance of lipophilic, π-π, and dipole-dipole interactions on cyanopropyl, phenyl and alkyl LC phases bonded onto the same base silica.* Chromatographia, 2009. **70**: p. 705-715.
50. M.R. Euerby, M. James and P. Petersson, *Practical implication of the Tanaka stationary phase characterisation methodology using ultra high performance liquid chromatography conditions.* J. Chromatogr. A., 2012. **1228**: p. 165-174.
51. M.R. Euerby, P. Petersson and M. James, *Translations between differing liquid chromatography formats: Advantages, principles and possible pitfalls.* LCGC Europe, 2015: p. 310-320.
52. *Chromatographic Separation Techniques*, in *European Pharmacopoeia 7.0*. p. 70-77.
53. *Personal correspondence with M. Dittman (Agilent)*.
54. R.E. Majors and M. Przybyciel, *Columns for Reversed-Phase LC Separations in Highly Aqueous Mobile Phases.* LCGC North America, 2002. **20**: p. 584-593.
55. C.R. Aurand, H. Cramer, J. McKenzie, D.S. Bell and R.E. Bell, *Avoiding Reversed-Phase Chromatography Problems Through Informed Method Development Practices: Choosing the Stationary Phase Chemistry.* LCGC North America, 2014. **32**: p. 704-717.
56. C.F. Poole and N. Lenca, *Reversed-Phase Liquid Chromatography*, in *Liquid Chromatography, Fundamentals and Instrumentation*, C.F. Poole, Editor. 2017, Elsevier: Amsterdam. p. 111.
57. M. J. Moon, S. Park, D.K. Kim, E.B. Cho, J.I. Hwang, H. Vaudry, and J.Y. Seong, *Structural and molecular conservation of glucagon-like peptide-1 and its receptor confers selective ligand-receptor interactions.* Frontiers in Endocrinology, 2012. **3**: p. 1-9.
58. R.I. Boysen and M.T.W. Hearn, *High-Performance Liquid Chromatography of Peptides and Proteins*, in *Amino Acids, Peptides and Proteins in Organic Chemistry: Analysis and Function of Amino Acids and Peptides*, A.B. Hughes, Editor. 2011, Wiley: Chichester. p. 167-210.
59. Y. Yang, *Peptide Racemisation*, in *Side Reactions in Peptide Synthesis*. 2015, Academic Press: Cambridge, MA. p. 257-292.

60. O. Takahashi, R. Kirikoshi and N. Manabe, *Racemisation of serine residues, catalysed by dihydrogen phosphate ion: A computational study.* Catalysts, 2017. **7**: p. 1-10.
61. G.G. Smith and G.V. Reddy, *Effect of the side chain on the racemisation of amino acids in aqueous solution.* J. Org. Chem., 1989. **54**: p. 4529-4535.
62. *Oxone, Potassium Peroxomonosulfate*. 08/07/2019]; Available from: http://www.organic-chemistry.org/chemicals/oxidations/oxone-potassiumperoxomonosulfate.shtm.
63. J. Holzmann, A. Hausberger, A. Rupprechter and H. Toll, *Top-down MS for rapid methionine oxidation site assignment in filgrastim.* Anal. Bioanal. Chem., 2013. **405**: p. 6667-6674.
64. R.C. Stephenson and S. Clarke, *Succinimide formation from aspartyl and asparaginyl peptides as a model for the spontaneous degradation of proteins.* J. Biol. Chem., 1989. **264**: p. 6164-6170.
65. T. Geiger and S. Clarke, *Deamidation, isomerisation, and racemisation at asparaginyl and aspartyl residues in peptides.* J. Biol. Chem., 1987. **262**: p. 785-794.
66. J.L. Radkieqicz, H. Zipse, S. Clarke and K.N. Houl, *Accelerated racemisation of aspartic acid and asparagine residues via succinimide intermediates: An ab initio theoretical exporation of mechanism.* J. Am. Chem. Soc., 1996. **118**: p. 9148-9155.
67. M.J. Collins, E.R. Waite and A.C.v. Duin, *Predicting protein decomposition: the case of aspartic acid racemisation kinetics.* Philos. Trans. R. Soc. Lond. B. Biol. Sci., 1999. **354**: p. 51-64.
68. K. Aki, N. Fujii and N. Fujii, *Kinetics of isomerisation and inversion of aspartate 58 of αA-crystalline peptide mimics under physiological conditions.* PLoS One, 2013. **8**: p. 1698.
69. O. Takahashi, R. Kirikoshi and N. Manabe, *Racmisation of the succinimide intermediate formed in proteins and peptides: A computational study of the mechanism catalysed by dihydrogen phosphate ion.* Int. J. Mol. Sci, 2016. **17**: p. 1698-1708.
70. R. Tyler-Cross and V. Schirch, *Effects of amino acid sequence, buffers, and ionic strength on the rate and mechanism of deamidation of asparagine residues in small peptides.* J. Biol. Chem., 1991. **266**: p. 22549-22556.
71. X. Li, C. Lin and P.B. O'Connor, *Glutamine deamidation: Differentiation of glutamic acid and γ-glutamic acid inpeptides by electron capture dissociation.* Anal. Chem., 2010. **82**: p. 3606-3615.
72. H. Yang and R.A. Zubarev, *Mass spectrometric analysis of asparagine deamidation and aspartate isomerisation in polypeptides.* Electrophoresis, 2010. **31**: p. 1764-1772.
73. N.E. Robinson, *Protein deamidation.* PNAS, 2002. **99**: p. 5283-5288.
74. C.T. Mant and R.S. Hodges, *Context dependent effects on the hydrophilicity / hydrophobicity of side-chains during reversed-phase high performance liquid chromatography: Implications for prediction of peptide retention behaviour.* J. Chromatogr. A., 2006. **1125**: p. 211-219.

75. J. W.C. Johnson, *Secondary structure of proteins through circular dichroism spectroscopy.* Annu. Rev. Biophys. Biophys. Chem., 1988. **17**: p. 145-166.
76. S.M. Kelly, T.J. Jess and N.C. Price, *How to study proteins by circular dichroism.* Biochem. Biophys. Acta., 2005. **1751**: p. 119-139.
77. N.J. Greenfield, *Using circular dichroism spectra to estimate protein secondary structure* Nat. Protoc., 2006. **1**: p. 2876-2890.
78. U.D. Neue, *Stationary phase characterisation and method development.* J. Sep. Sci, 2007. **30**: p. 1611-1627.
79. K. Kimata, K. Iwaguchi, S. Onichi, K. Jinno, R. Eksteen, K. Hosoya, M. Araki, and N. Tanaka, *Chromatographic characterisation of silica C18 packing materials. Correlation between a preparation method and retention behaviour of stationary phase.* J. Chromatogr. Sci., 1989. **27**: p. 721-728.
80. C. West, E. Lemasson, S. Bertin, P. Hennig and E. Lesellier, *An improved classification of stationary phases for ultra-high performance supercritical fluid chromatography.* J. Chromatogr. A., 2016. **1440**: p. 212-228.
81. E. Lesellier and C. West, *Σpider diagram: A universal and versatile approach for system comparison and classification. Part 2: Stationary phase properties.* J. Chromatogr. A., 2018. **1574**: p. 71-81.
82. *U.S. Pharmacopeial Convention*. 10/07/2019]; Available from: http://apps.usp.org/app/USPNF/columnsIntro.html.
83. P. Žuvela, M. Skoczylas, J.J. Liu, T. Bączek, R. Kaliszan, M. Wah Wong, and B. Buszewski, *Column characterisation and selection systems in reversed-phase high-performance liquid chromatography.* Chem. Rev., 2019. **119**: p. 3674-3729.
84. E. Cruz, M.R. Euerby, C.M. Johnson and C.A. Hackett, *Chromatographic classification of commercially available reversed-phase HPLC columns.* Chromatographia, 1997. **44**: p. 151-161.
85. H. Engelhardt and T. Lobert, *Chromatographic determination of metallic impurities in reversed-phase HPLC columns.* Anal. Chem., 1999. **71**: p. 1885-1892.
86. *ACD/Labs Column Selector*. 10/07/2019]; Available from: http://www.acdlabs.com/resources/freeware/colsel/index.php.
87. E.M. Borges, *Silica, hybrid silica, hydride silica and non-silica stationary phases for liquid chromtography.* J. Chromatogr. Sci., 2015. **53**: p. 580-597.
88. E.M. Borges, *How to select equivalent and complementary reversed-phase liquid chromatography columns from column characterisation databases.* Anal. Chim. Acta, 2014. **807**: p. 143-152.
89. E. Lesellier and C. West, *Description and comparison of chromatographic tests and chemometric methods for packed column classification.* J. Chromatogr. A., 2007. **1158**: p. 329-360.
90. U.D. Neue, K. Van Tran, P.C. Iraneta and B.A. Alden, *Characterisation of HPLC packings.* J. Sep. Sci, 2003. **26**: p. 174-186.
91. E. Lesellier, *A simple and interactive column classification for reversed-phase liquid chromatography: The carotenoid test, Part 1: Studied properties, probes and fundamentals.* LCGC North America, 2016. **34**: p. 766-777.

92. M.R. Euerby, C.M. Johnson, I.D. Rushin and D.A.S.S. Tennekoon, *Investigation into the epimerisation of tipredane ethylsulphoxide diastereoisomers during chromatographic analysis on reversed-phase silica I. Investigation into the reaction mechanism.* J. Chromatogr. A., 1995. **705**: p. 219-227.
93. M.R. Euerby, C.M. Johnson, I.D. Rushin and D.A.S.S. Tennekoon, *Investigations into the epimerisation of tipredane ethylsulphoxide diastereoisomers during chromatographic analysis on reversed-phase silica II. The involvement of metals in commercially available C18 silicas.* J. Chromatogr. A., 1995. **705**: p. 229-245.
94. D. Stoll. *HPLC columns - HPLC column selectivity measurements of more than 600 reversed phase columns from over 30 manufacturers*. 10/07/2019]; Available from: http://www.hplccolumns.org/about/index.php.
95. P. Petersson and M. Euerby, *An evaluation of the robustness of the Tanaka characterisation protocol for reversed-phase liquid chromatography columns.* J. Sep. Sci, 2005. **28**: p. 2120-2129.
96. I.T. Jolliffe, *Principal Component Analysis*. 2011, Berlin: Springer.
97. J.W. Dolan, *Ion pairing - Blessing or curse?* LCGC North America, 2008. **26**: p. 170-174.
98. L. Greenspan, *Humidity fixed points of binary saturated aqueous solutions.* J. Res. 'N.B.S. -Phys. & Chem., 1977. **81**: p. 89-96.
99. *Equilibrium relative humidity, saturated salt solutions*. 10/07/2019]; Available from: http://www.omega.com/temperature/z/pdf/z103.pdf
100. D.V. McCalley, *Hydrophilic Interaction Liquid Chromatography: An Update.* LCGC Europe, 2019. **32**: p. 114-125.
101. P. Petersson, B.O. Boateng, J.K. Field and M.R. Euerby, *A practical approach to modelling of reversed-phase liquid chromatographic separations: Advantages, principles and possible pitfalls.* LCGC Europe, 2018. **31**: p. 120-143.
102. L.R. Snyder and J.W. Dolan, *High performance gradient elution*. 2007, Hoboken, NJ: John Wiley & Sons.
103. P. Jandera and J. Churácék, *Gradient elution in column liquid chromatography*. 1st Ed. ed. 1985, Amsterdam: Elsevier.
104. N. Lundell, *Implementation and use of gradient predictions for optimisation of reversed-phase liquid chromatography of pepties.* J. Chromatogr., 1993. **639**: p. 97-115.
105. J.M. Kovacs, C.T. Mant and R.S. Hodges, *Determination of intrinsic hydrophilicity / hydrophobicity of amino acid side chains in peptides in the absence of nearest-neighbour or conformation effects.* Biopolymers (Pept. Sci.), 2006. **84**: p. 283-297.
106. S.M. Melnikov, A. Höltzel, A. Seidel-Morgenstern and L. Tallarek, *Adsorption of water-acetonitrile mixtures to model silica surfaces.* J. Phys. Chem. C., 2013. **117**: p. 6620-6631.

107. S. Bocian, A. Felinger and B. Buszewski, *Comparison of solvent adsorption on chemically bonded stationary phases in RP-LC.* Chromatographia, 2008. **68**: p. s19-s26.
108. S. Bocian, P. Vajda, A. Felinger and B. Buszewski, *Solvent excess adsorption on the stationary phases for reversed-phase liquid chromatography with polar functional groups.* J. Chromatogr. A., 2008. **1204**: p. 35-41.
109. M.R. Euerby, M. Fever, J. Hulse, M. James, P. Petersson, and C. Pipe, *Maximisation of selectivity in reversed-phase liquid chromatographic method development strategies.* LCGC Europe, 2016. **29**: p. 8-21.
110. M. Yang, S. Fazio, D. Munch and P. Drumm, *Impact of methanol and acetonitrile on separations based on pi-pi interactions with a reversed-phase phenyl column.* J. Chromatogr. A., 2005. **1097**: p. 124-129.
111. K. Croes, A. Steffens, D.H. Marchand and L.R. Snyder, *Relevance of π-π and dipole-dipole interactions for retention on cyano and phenyl columns in reversed-phase liquid chromatography.* J. Chromatogr. A., 2005. **1098**: p. 123-130.
112. C.T. Mant, J.M. Kovacs, H.M. Kim, D.D. Pollock and R.S. Hodges, *Intrinsic amino acid side chain hydrophilicity / hydrophobicity coefficients determined by reversed-phase high performance liquid chromatography of model peptide: Comparison with other hydrophilicity / hydrophobicity scales.* Pept. Sci., 2009. **92**: p. 573-595.
113. J.W. Dolan, L.R. Snyder, N.M. Djordjevi, D.W. Hill and T.J. Waeghe, *Reversed-phase liquid chromatographic separation of complex samples by optimising temperature and gradient time I. Peak capacity limitations.* J. Chromatogr. A., 1999. **857**: p. 1-20.
114. D. Johnson, B. Boyes and R. Orlando, *The use of ammonium formate as a mobile phase modifier for LC-MS/MS analysis of tryptic digests.* J. Biomol. Tech., 2013. **24**: p. 287-297.
115. D.V. McCalley, *Overload for ionised solutes in reversed-phase high performance liquid chromatography.* Anal. Chem., 2006. **78**: p. 2532-2538.
116. S.M.C. Buckenmaier, D.V. McCalley and M.R. Euerby, *Overloading study of bases using polymeric RP-HPLC columns as an aid to rationalisation of overloading on silica-ODS phases.* Anal. Chem., 2002. **74**: p. 4672-4681.
117. P.C. Iraneta, K.F. Wyndham, D.R. McCabe and T.H. Water. *A review of Waters hybrid particle technology. Part 3. Charged Surface Hybrid (CSH) technology and its uses in liquid chromatography*. 2011 11/07/2019]; Available from: http://www.waters.com/webassets/cms/library/docs/720003929en.pdf.
118. M. Gilar, K. Berthelette, K. Kalikova, D. Folprechtova, E. Tesarova, and B. Alden. *Pure mode or mixed mode chromatography?* in *HPLC2019*. 2019. Milan, Italy.
119. D.H. Marchand, L.A. Williams, J.W. Dolan and L.R. Snyder, *Slow equilibration of reversed-phase columns for the separation of ionised solutes.* J. Chromatogr. A., 2003. **1015**: p. 53-64.

120. D.B. Hibbert, *Experimental design in chromatography: a tutorial review.* J. Chromatogr. B. Analyt. Technol. Biomed. Life Sci. , 2012. **910**: p. 2-13.
121. B.J. Stojanovic, *Factorial based designs in liquid chromatography.* Chromatographia, 2013. **76**: p. 227-240.
122. V. Czitrom, *One-factor-at-a-time versus designed experiments.* The American Statistician, 1999. **53**: p. 126-131.
123. C.S. Paim, H. Gonçalves, A. Lange, D. Miron and M. Steppe, *Validation of UV spectrophotmetric method for quantitative determination of entacapone in tablets using experimental design of Plackett-Burman for robustness evaluation and comparison with HPLC.* Anal. Letters, 2008. **41**: p. 571-581.
124. B. Dejaegher and Y.V. Heyden, *Experimental designs and their recent advances in set-up, data interpretation and analytical applications.* J. Pharm. Biomed. Anal., 2007. **1158**: p. 158-167.
125. R.G. Wolcott, J.W. Dolan, L.R. Snyder, S.R. Bakalyar, M.A. Arnold, and J.A. Nichols, *Control of column temperature in reversed-phase liquid chromatography.* J. Chromatogr. A., 2000. **869**: p. 211.
126. M.M. Fallas, M.R. Hadley and D.V. McCalley, *Practical assessment of frictional heating effects and thermostat design on the performance of conventional (3 µm and 5 µm) columns in reversed-phase high performance liquid chromatography.* J. Chromatogr. A., 2009. **1216**: p. 3961-3969.
127. A. de Villiers, H. Lauer, R. Szucs, S. Goodall and P. Sandra, *Influence of frictional heating on temperature gradients in ultra high pressure liquid chromatography on 2.1 mm I.D. columns.* J. Chromatogr. A., 2006. **1113**: p. 84-91.
128. J. P. Grinias, D.S. Keil and J.W. Jorgenson, *Observation of enhanced heat dissipation in columns packed with superficially porous particles.* J. Chromatogr. A., 2014. **1371**: p. 261-264.
129. S. Feketes, K. Horvath and D. Guillarme, *Influence of pressure and temperature on molar volume and retention properties of peptides in ultra high pressure liquid chromatography.* J. Chromatogr. A., 2013. **1311**: p. 65-71.
130. K.J. Fountain, U.D. Neue, E.S. Grumbach and D.M. Diehl, *Effects of extra column band spreading, liquid chromatography system operating pressure, and column temperature on the performance of sub-2 µm porous particles.* J. Chromatogr. A., 2009. **1216**: p. 5979-5988.
131. F. Gritti and G. Guiochon, *Complete temperature profiles in ultra high pressure liquid chromatography columns.* Anal. Chem., 2008. **80**: p. 5009-5020.
132. F. Gritti and G. Guiochon, *Adsorption mechanisms and effect of temperature in reversed-phase liquid chromatography. Meaning of the classical van't Hoff plot in chromatography.* Anal. Chem., 2006. **78**: p. 4642-4653.
133. S. Heinisch, G. Desmet, D. Clicq and J.L. Rocca, *Kinetex plot equations for evaluating the real performance of the combined used of high temperature and ultra high pressure in liquid chromatography. Application to commercial*

instruments and 2.1 and 1 mm I.D. columns. J. Chromatogr. A., 2008. **1203**: p. 124-136.
134. *Personal correspondance with M. Euerby (Shimadzu and Uni. Strathclyde) and P. Petersson (Novo Nordisk and Uni. Uppsala).*
135. J.C. Miller and J.N. Miller, *Statistics for analytical chemistry*. 3rd Ed. ed. 1993, Chichester: Ellis Horwood Ltd.
136. D.C. Montomery, E.A. Peck and G.G. Vining, *Introduction to linear regression analysis*. 5th Ed. ed. 2012, New Jersey: Wiley & Sons, Inc.
137. G.E.P. Box, J.S. Hunter and W. Hunter, *Statistics for experimenters: Design, innovation and discovery*. 2nd Ed. ed. 2005, New Jersey: Wiley.
138. A. Méndez, E. Bosch, M. Rosés and U.D. Neue, *Comparison of the acidity of residual silanol groups in several liquid chromatography columns.* J. Chromatogr. A., 2003. **986**: p. 33-44.
139. U.D. Neue, *HPLC columns: Theory, technology and practice*. 1st Ed. ed. 1997, Canada: Wiley-VCH.
140. U.D. Neue, C.H. Phoebe, K. Van Tran, Y.F. Cheng and Z. Lu, *Dependence of reversed-phase retention of ionisable analytes on pH, concentration of organic solvent and silanol activity.* J. Chromatogr. A., 2001. **925**: p. 49-67.
141. M. Kele and G. Guiochon, *Repeatability and reproducibility of retention data and band profiles on reversed-phase liquid chromtography columns: I. Experimental protocols.* J. Chromatogr. A., 1999. **830**: p. 41-54.
142. M. Kele and G. Guoichon, *Repeatability and reproducibility of retention data and band profiles on reversed-phase liquid chromatography columns: II. Results obtained from Symmetry C18 columns.* J. Chromatogr. A., 1999. **830**: p. 55-79.
143. M. Kele and G. Guoichon, *Repeatability and reproducibility of retention data and band profiles on reversed-phase liquid chromatography columns: III. Results obtained from Kromasil C18 columns.* J. Chromatogr. A., 1999. **855**: p. 423-453.
144. M. Kele and G. Guoichon, *Repeatability and reproducibility of retention data and band profiles on reversed-phase liquid chromatography columns: IV. Results obtained with Luna C18 (2) columns* J. Chromatogr. A., 2000. **869**: p. 181-209.
145. M. Kele and G. Guoichon, *Repeatability and reproducibility of retention data and band profiles on reversed-phase liquid chromatography columns: V. Results obtained with Vydac 218TP C18 columns.* J. Chromatogr. A., 2001. **913**: p. 89-112.
146. M. Kele and G. Guoichon, *Repeatability and reproducibility of retention data and band profiles on six batches of monolithic columns.* J. Chromatogr. A., 2002. **960**: p. 19-49.
147. D.V. McCalley, *Effect of buffer on peak shape of peptides in reversed-phase high performance liquid chromatography.* J. Chromatogr. A., 2004. **1038**: p. 77-84.
148. J.K. Field, M.R. Euerby and P. Petersson, *Investigation into reversed-phase chromatography peptide separation systems Part II: An evaluation of the*

robustness of a protocol for column characterisation. J. Chromatogr. A., 2019. **1603**: p. 102-112.
149. P. Chatterjee, *Microbiological stability / shelf life determination of LC mobile phases and stock buffers*, in *Strathclyde Institute of Pharmacy and Biomedical Sciences*. 2008, University of Strathclyde: Glasgow.
150. Agilent and Technologies, *The Advantages of Polymeric PLRP-S Media.* 2011.
151. M.R. Euerby, D. Hassey, P. Petersson, J.W. Dolan and L.R. Snyder. *An evaluation of different means of measuring reversed-phase column selecitivty*. in *HPLC2002*. 2002. Montreal, Canada.
152. J.K. Field, M.R. Euerby, P. Petersson, J. Lau and H. Thøgersen, *Investigation into reversed-phase chromatography peptide separation systems part I: Development of a protocol for column characterisation.* J. Chromatogr. A., 2019. **1603**: p. 113-129.
153. U.D. Neue, J.E. O'Gara and A. Méndez, *Selectivity in reversed-phase separations. Influence of the stationary phase.* J. Chromatogr. A., 2006. **1127**: p. 161-174.
154. D.V. McCalley, *Effect of mobile phase additives on solute retention at low aqueous pH in hydrophilic interaction liquid chromatography.* J. Chromatogr. A., 2017. **1483**: p. 71-79.
155. L.R. Snyder, J.J. Kirkland and J.L. Glach, *Practical HPLC method development*. 2nd Ed. ed. 1997, New York, NY: Wiley.
156. A.P. Schellinger and P.W. Carr, *Solubility of buffers in aqueous-organic eluents for reversed-phase liquid chromatography.* LCGC North America, 2004. **22**: p. 544-548.
157. B. Bobály, A. Beck, J. Fekete, D. Guillarme and S. Fekete, *Systematic evaluation of mobile phase additives for the LC-MS characterisation of therapeutic proteins.* Talanta, 2015. **136**: p. 60-67.
158. D.V. McCalley, *The challenges of the analysis of basic compounds by high performance liquid chromatography: Some possible approaches for improved separations.* J. Chromatogr. A., 2010. **1217**: p. 858-880.
159. L.R. Snyder, J.J. Kirkland and J.W. Dolan, *Chapter 7.4 Ion-Pair Chromatography (IPC)*, in *Introduction to modern liquid chromatography*. 2010, Wiley & Sons: New Jersey. p. 331-347.
160. A. Vailaya and C. Horvath, *Retention in reversed-phase chromatography: partition or adsorption.* J. Chromatogr. A., 1998. **829**: p. 1-27.
161. H.J Issaq, S.D. Fox, M. Mahadevan, T.P. Conrads and T.D. Veenstra, *Effect of experimental parameters on the HPLC separation of peptides and proteins.* J. Liquid Chromatogr. & Rel. Tech., 2003. **26**: p. 2255-2283.
162. M.W. Dong and B.E. Boyes, *Modern trends and best practices in mobile phase selection in reversed phase chromatography.* LCGC North America, 2018. **36**: p. 752-768.
163. J. Nguyen, J. Smith, O.V. Friese, J.C. Rouse, D.P. Walsh, X. Zhang, N. Ranbaduge, and M.A. Lauber. *A new LC-MS approach for enhancing subunit-level profiling of mABs and ADCs*. in *ASMS*. 2018. San Diego, CA.

164. J. Flieger, *Application of perfluorinated acids as ion-pairing reagents for reversed-phase chromatography and retention hydrophobicity relationships studies of selected β-blockers.* J. Chromatogr. A., 2010. **1217**: p. 540-549.
165. M. Shibue, C.T. Mant and R.S. Hodges, *Effect of anionic ion-pairing reagent hydrophobicity on selectivity of peptide separations by reversed-phase liquid chromatography.* J. Chromatogr. A., 2005. **1080**: p. 68-75.
166. D.V. McCalley, *Study of retention and peak shape in hydrophilic interactions chromatography over a wide pH range.* J. Chromatogr. A., 2015. **1411**: p. 41-49.
167. A.N. Hodder, M.I. Aguilar and M.T. Hearn, *High performance liquid chromatography of amino acids, peptides and proteins. LXXXIX. The influence of different displacer salts on the retention properties of proteins separated by gradient anion-exchange chromatography.* J. Chromatogr., 1989. **476**: p. 391-411.
168. M. Chaplin. *Kosmotropes and Chaotropes*. 2019 18/09/2019]; Available from: http://www1.lsbu.ac.uk/water/kosmotropes_chaotropes.html.
169. P. Ball and J.E. Hallsworth, *Water structure and chaotropicity: their uses, abuses and biological implications.* Phys. Chem. Chen. Phys., 2015. **17**: p. 8297-8305.
170. A.M. Hyde, S.L. Zultanski, J.H. Waldman, Y. Zhong, M. Shevlin, and F. Peng, *General principles and strategies for salting-out informd by the Hofmeister series.* Org. Process Res. Dev., 2017. **21**: p. 1355-1370.
171. A. Makarov, R. LoBrutto and Y. Kazakevich, *Liophilic mobile phase additives in reversed phase HPLC.* J. Liquid Chromatogr. & Rel. Tech., 2008. **31**: p. 1533-1567.
172. R. LoBrutto, A. Jones, Y.V. Kazakevich and H.M. McNair, *Effect of the eluent pH and acidic modifiers in high-performance liquid chromatography retention of basic analytes.* J. Chromatogr. A., 2001. **913**: p. 173-187.
173. J. Flieger, *The effect of chaotropic mobile phase additives on the separation of selected alkaloids in reversed-phase high-performance liquid chromatography.* J. Chromatogr. A., 2006. **1113**: p. 37-44.
174. Y.V. Kazakevich and R. LoBrutto, *Chapter 4 Reversed-Phase HPLC*, in *HPLC for pharmaceutical scientists*, Y.V. Kazakevich and R. LoBrutto, Editors. 2007, Wiley: Hoboken, New Jersey. p. 139-240.
175. C.T. Mant, A. Byars, S. Ankarlo, Z. Jiang and R.S. Hodges, *Separation of highly charged (+5 to +10) amphipathic α-helical peptide standards by cation-exchange and reversed-phase high performance liquid chromatography.* J. Chromatogr. A., 2018. **1574**: p. 60-70.
176. E.L. Regalado, I.A. Haidar Ahmed, R. Bennett, V. D'Atri, A.A. Makarov, G.R.Humphrey, I. Mangion, and D. Guillarme, *The emergence of universal chromatographic methods in the research and development of new drug substances.* Acc. Chem. Res., 2019. **63**: p. 1990-2002.
177. I.A. Haidar Ahmed, W. Chen, H.M. Halsey, A. Klapars, J. Limanto, G.F. Pirrone, T. Nowak, R. Bennett, R. Hartman, A.A. Makarov, I. Mangion, and E.L. Regalado, *Multi-column ultra-high performance liquid chromatography*

screening with chaotropic agents and computer-assisted separation modeling enables process development of new drug substances. Analyst, 2019. **144**: p. 2872-2880.
178. M. Shibue, C.T. Mant and R.S. Hodges, *The perchlorate anion is more effective than the trifluoroacetate anion as an ion-pairing reagent for reversed-phase chromatography for peptides.* J. Chromatogr. A., 2005. **1080**: p. 49-57.
179. A. Apffel, S. Fischer, G. Goldberg, P.C. Goodley and F.E. Kuhlmann, *Enhanced sensitivity for peptide mapping with electrospray liquid chromatography-mass spectrometry in the presence of signal suppression due to trifluoroacetic acid containing mobile phases.* J. Chromatogr. A., 1995. **712**: p. 177-190.
180. M.C. García, *The effect of the mobile phase additives on sensitivity in the analysis of peptides and proteins by high-performance liquid chromatography-electrospray mass spectrometry.* J. Chromatogr. B., 2005. **825**: p. 111-123.
181. A. Kruve and K. Kaupmees, *Adduct formation in ESI-MS by mobile phase additives.* J. Am. Soc. Mass Spectrom. , 2017. **28**: p. 887-894.
182. A.L. Rockwood, M.M. Kushnir and N.J. Clarke, *Chapter 2 - Mass Spectrometry*, in *Principles and applications of clinical mass spectrometry*. 2018, Elsevier: Amsterdam, Netherlands.
183. F. Klink. *Dealing with metal adduct ions in electrospray*. Available from: https://blog.sepscience.com/massspectrometry/ms-solutions-3-dealing-with-metal-adduct-ions-in-electrospray-part-1.
184. L.R. Snyder, P.W. Carr and S.C. Rutan, *Solvatochromically based solvent selectivity triangle.* J. Chromatogr. A., 1993. **656**: p. 537-547.
185. S.C. Rutan, P.W. Carr, W.J. Cheong, J.H. Park and L.R. Snyder, *Re-evaluation of the solvent triangle and comparison to solvatochromic based scales of solvent strength and selectivity.* J. Chromatogr. A., 1989. **463**: p. 21-37.
186. L.R. Snyder, *Classification of the solvent properties of common liquids.* J. Chromatogr. A., 1974. **92**: p. 223-230.
187. L. Rohrschneider, *Eine methode zur chrakterisierung von gaschromatographischen trennflüssigkeiten.* J. Chromatogr. A., 1966. **22**: p. 6-22.
188. J.W. Dolan, *Selectivity in reversed-phase LC separation, Part I: Solvent type selectivity.* LCGC North America, 2010. **28**: p. 1022-1027.
189. L.R. Snyder, J.J. Kirkland and J.W. Dolan, *Chapter 2.3 Retention*, in *Introduction to modern liquid chromatography*. 2010, John Wiley & Sons: Hoboken, New Jersey. p. 34.
190. R. Fritz, W. Ruth and U. Kragl, *Assessment of acetone as an alternative to acetonitrile in peptide analysis by liquid chromatography/mass spectrometry.* Rapid. Commun. Mass Spectrom. , 2009. **23**: p. 2139-2145.
191. B. Basiri, H. Van Hattum, W.D. van Dongen, M.M Murph and M.G. Bartlett, *The role of fluorinated alcohols as mobile phase modifiers for LCMS analysis of oligonucleotides.* J. Am. Soc. Mass Spectrom., 2017. **28**: p. 190-199.

192. J.W. Coym, *Evaluation of ternary mobile phases for reversed-phase liquid chromatography: Effect of composition on retention mechanisms.* J. Chromatogr. A., 2010. **1217**: p. 5957-5964.
193. L.R. Snyder and J.W. Dolan, *Chapter 8.4 Ternary- or quarternary solvent gradients*. 2007, John Wiley & Sons: Hoboken, New Jersey. p. 365-367.
194. M.R. Euerby, F. Scannapieco, H. Rieger and I. Molnár, *Retention modelling in ternary solvent-strength gradient elution reversed-phase chromatography using 30 mm columns.* J. Chromatogr. A., 2006. **1121**: p. 219-227.
195. P. Jandera, L. Petránek and M. Kučerová, *Characterisation and prediction of retention in isocratic and gradient-elution normal-phase high-performance liquid chromatography on polar bonded stationary phases with binary and ternary solvent systems.* J. Chromatogr. A., 1997. **791**: p. 1-19.
196. P.J. Schoenmakers, H.A.H. Billiet and L.D. Galan, *Systematic study of ternary solvent behaviour in reversed-phase liquid chromatography.* J. Chromatogr. A., 1981. **218**: p. 261-284.
197. R. Bennett and S.B. Olesik, *Enhanced fluidity liquid chromatography of inulin fructans using ternary solvent strength and selectivity gradients.* Anal. Chim. Acta, 2018. **999**: p. 161-168.
198. P. Petersson, J. Munch, M.R. Euerby, A. Vazhentsev, M. McBrien, S.K. Bhal, and K. Kassam, *Adaptation of retention models to allow optimisation of peptide and protein separations.* Chromatography Today, 2014: p. 15-18.
199. L.G. Gagliardi, C.B. Castells, C. Ràfols, M. Rosés and E. Bosch, *Effect of temperature on the chromatographic retention of ionisable compounds II. Acetonitrile-water mobile phases.* J. Chromatogr. A., 2005. **1077**: p. 159-169.
200. Y. Chen, C.T. Mant and R.S. Hodges, *Temperature selectivity effects in reversed-phase liquid chromatography due to conformation differences between helical and non-helical peptides.* J. Chromatogr. A., 2003. **1010**: p. 45-61.
201. K. Horváth, S. Horváth and D. Lukács, *Effect of axial temperature gradient on chromatographic efficiency under adiabatic conditions.* J. Chromatogr. A., 2017. **1483**: p. 80-85.
202. M.H. Chen and C. Horváth, *Temperature programming and gradient eltuoin in reversed phase chromatography with packed capillary columns.* J. Chromatogr. A., 1997. **788**: p. 51-61.
203. F.D. Antia and C. Horváth, *High performance liquid chromatography at elevated temperatures: examination of conditions for the rapid separation of large molecules.* J. Chromatogr. A., 1988. **435**: p. 1-15.
204. M. Rosés, X. Subirats and E. Bosch, *Retention models for ionisable comopunds in reversed phase liquid chromatography: Effect of variation of mobile phase composition and temperature.* J. Chromatogr. A., 2009. **1216**: p. 1756-1775.
205. P. Agrafiotou, C. Rafols, C. Castells, E. Bosch and M. Rosés, *Simulateous effect of pH, temperature and mobile phase composition in the chromatographic retention of ionisable compounds.* J. Chromatogr. A., 2011. **1218**: p. 4995-5009.

206. A.W. Purcell, G.L. Zhao, M.I. Aguilar and M.T.W. Hearn, *Comparison between the isocratic and gradient retention behaviour of polypeptides in reversed-phase liquid chromatographic environments.* J. Chromatogr. A., 1999. **852**: p. 43-57.
207. R.I. Boysen, A.J.O. Jong and M.T.W. Hearn, *Binding behaviour and conformational properties of globular proteins in the presence of immobilised non-polar ligands used in reversed-phase liquid chromatography.* J. Chromatogr. A., 2005. **1079**: p. 173-186.
208. T. Alvarez-Segura, E. Cabo-Calvet, J.J. Baeza-Baeza and M.C. Garcia-Alvarez-Coque, *Study of the column efficiency using gradient elution based on van Deemter plots.* J. Chromatogr. A., 2019. **1584**: p. 126-134.
209. F. Gritti and G. Guiochon, *The van Deemter equation: Assumptions, limits and adjustment to modern high performance liquid chromatography.* J. Chromatogr. A., 2013. **1302**: p. 1-13.
210. K. Miyabe and R. Isogai, *Estimation of molecular diffusivity in liquid phase systems by the Wilke-Chang equation.* J. Chromatogr. A., 2011. **1218**: p. 6639-6645.
211. M.A. Stadalius, H.S. Gold and L.R. Snyder, *Optimisation model for the gradient elution separation of peptide mixtures by reversed-phase high performance liquid chromatography: Verification of band width relationships for acetonitrile-water mobile phases.* J. Chromatogr. A., 1985. **327**: p. 27-45.

vii. Appendix I

Figure 100 Example of an injector programme for TM1 designed to reduce the waste of peptides.

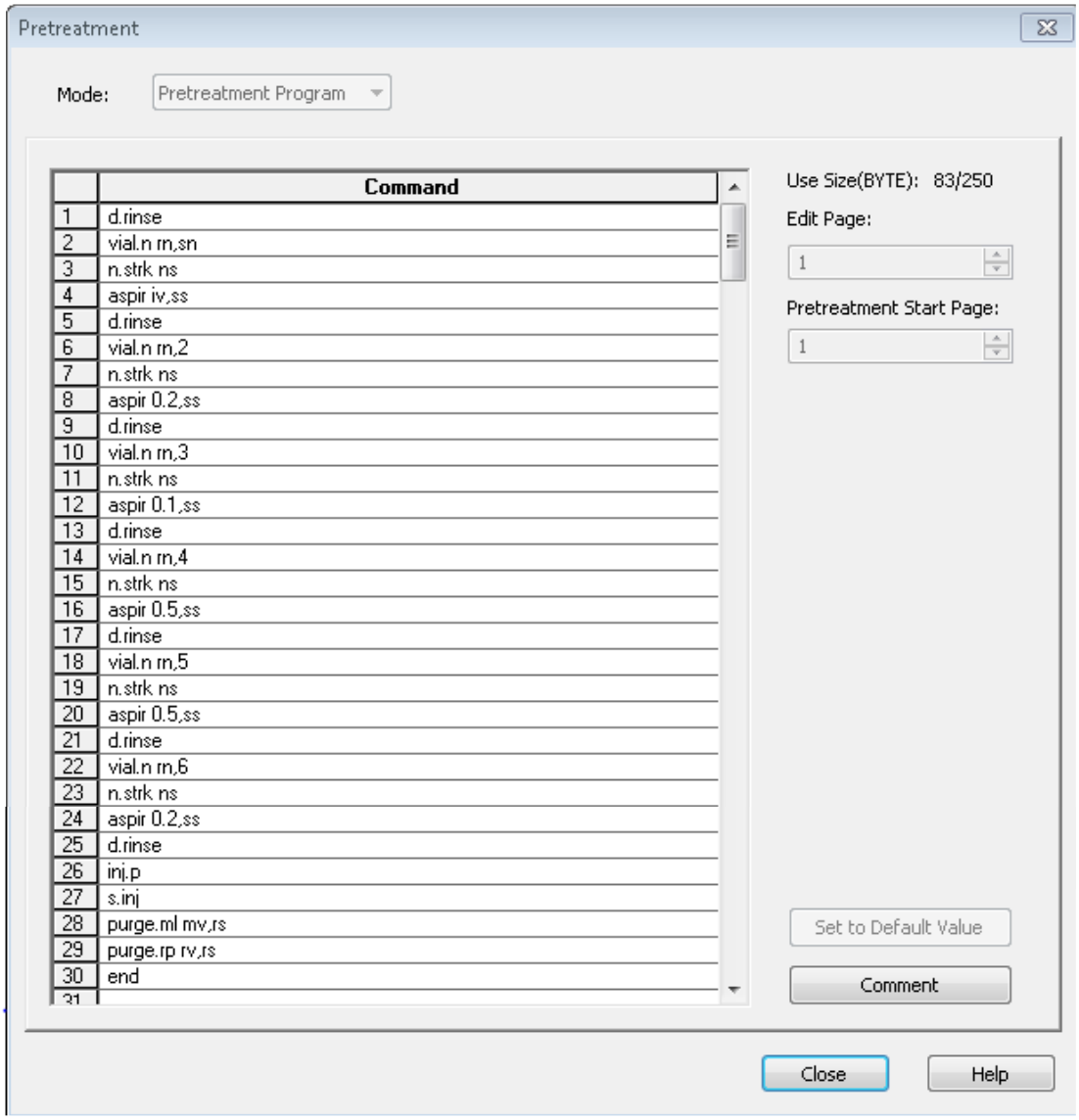

viii. Appendix II

Table 73 A robustness comparison of four different alpha value calculations using seven peptides / proteins with known constants [211], with varying operating conditions.

Condition #1																				Gradient selectivity, α*			
Substance	MW [Da]	logkw=a	S=m	F	Φ0	Φmax	tG	Vm	Vd	VG	k0(5)	B(3)	Vmg(7)	k*(17)	Vg(6)	Vg2/Vg1	Vg2/Vd1	k*2/k*1	1+dV'g0'V'g1
																(1)	(2)	(3)	(4)
	Da	-		mL/min	-	-	min	mL	mL	mL	-	1/mL	mL	-	mL	-	-	-	-
Bradykinin	630	3.36	12.8	0.3	0.05	0.8	40	0.3	0.5	12	524.81	0.0625	0.299	3.60	3.88	N/A	N/A	N/A	N/A
Leucine enkephalin	600	3.18	11.3	0.3	0.05	0.8	40	0.3	0.5	12	412.1	0.0625	0.299	4.06	4.06	1.05	1.06	1.13	1.06
Ribonuclease A	12500	12.3	41.3	0.3	0.05	0.8	40	0.3	0.5	12	2E+10	0.0625	0.300	1.12	4.86	1.20	1.25	0.28	1.25
Angiotensin	1300	4.74	15.2	0.3	0.05	0.8	40	0.3	0.5	12	9549.9	0.0625	0.300	3.05	4.80	0.99	0.98	2.72	0.98
Insulin	6000	7.89	22.7	0.3	0.05	0.8	40	0.3	0.5	12	6E+06	0.0625	0.300	2.04	5.55	1.16	1.19	0.67	1.19
Glucagon	3500	8.1	22.3	0.3	0.05	0.8	40	0.3	0.5	12	1E+07	0.0625	0.300	2.08	5.80	1.04	1.05	1.02	1.05
Lysozyme	14000	15.4	39.2	0.3	0.05	0.8	40	0.3	0.5	12	3E+13	0.0625	0.300	1.18	6.38	1.10	1.12	0.57	1.12

Condition #2																				Gradient selectivity, α*			
Substance	MW [Da]	logkw=a	S=m	F	Φ0	Φmax	tG	Vm	Vd	VG	k0	B	Vmg	k*	Vg	Vg2/Vg1	Vg2/Vd1	k*2/k*1	1+dV'g0'V'g1
	Da	-		mL/min	-	-	min	mL	mL	mL	-	1/mL	mL	-	mL	-	-	-	-
Bradykinin	630	3.36	12.8	0.2	0.05	0.8	40	0.3	0.5	8	524.81	0.0938	0.299	2.40	3.00	N/A	N/A	N/A	N/A
Leucine enkephalin	600	3.18	11.3	0.2	0.05	0.8	40	0.3	0.5	8	412.1	0.0938	0.299	2.72	3.14	1.05	1.06	1.13	1.06
Ribonuclease A	12500	12.3	41.3	0.2	0.05	0.8	40	0.3	0.5	8	2E+10	0.0938	0.300	0.75	3.55	1.13	1.18	0.28	1.18
Angiotensin	1300	4.74	15.2	0.2	0.05	0.8	40	0.3	0.5	8	9549.9	0.0938	0.300	2.03	3.59	1.01	1.01	2.72	1.01
Insulin	6000	7.89	22.7	0.2	0.05	0.8	40	0.3	0.5	8	6E+06	0.0938	0.300	1.36	4.05	1.13	1.17	0.67	1.17
Glucagon	3500	8.1	22.3	0.2	0.05	0.8	40	0.3	0.5	8	1E+07	0.0938	0.300	1.39	4.22	1.04	1.05	1.02	1.05
Lysozyme	14000	15.4	39.2	0.2	0.05	0.8	40	0.3	0.5	8	3E+13	0.0938	0.300	0.79	4.57	1.08	1.10	0.57	1.10

Average ratio for selectivity meassure cond#2/cond#1 substance 1-7

Ratio for selectivity meassure cond. #2/cond.#1	
1.00	1.00
0.95	0.94
1.02	1.03
0.98	1.00
1.00	1.00
0.98	0.99
0.988	**0.991**

Changing Vm from 0.3 to 0.2
Changing F from 0.3 to 0.28
Changing Φ 0 from 0.05 to 0.0485
Changing Φ 0 from 0.8 to 0.776
Changing Vd from 0.5 to 0.1

Average ratio for selectivity meassure cond#2/cond#1 substance

Gradient selectivity, α*			
Vg2/Vg1	Vg2/Vd1	k*2/k*1	1+dV'g0'V'g1
1.000	1.011	1.001	1.011
0.998	0.998	1.000	0.998
1.000	0.999	1.000	0.999
1.001	1.001	1.000	1.001
1.007	1.000	1.000	1.000

Changing Vm from 0.3 to 0.2
Changing F from 0.3 to 0.28
Changing Φ 0 from 0.05 to 0.0485
Changing Φ 0 from 0.8 to 0.776
Changing Vd from 0.5 to 0.1

Difference from 1		
0.010	0.011	0.011
-0.002	-0.002	-0.002
0.000	0.000	-0.001
0.001	0.001	0.000
0.007	**0.000**	**0.000**

probability
very unlil
very likel
very likel
very likel
likely

ix. Appendix III

Table 74 Raw t_g data for TM1 in formic acid conditions

Ascentis Express C18 468	10.706	10.789	14.423	15.009	22.826	23.581
Ascentis Express RP-Amide	9.169	9.239	12.444	13.124	20.350	20.789
Ascentis Express C8	9.715	9.792	13.342	13.990	21.214	22.393
Ascentis Express Phenyl Hexyl	10.187	10.256	13.486	14.124	20.891	21.529
Ascentis Express Biphenyl	11.167	11.201	14.707	15.425	23.746	24.445
Bioshell Peptide CN	8.594	8.651	12.146	12.813	22.907	23.600
Luna Omega C18	12.171	12.252	15.991	15.991	24.369	25.063
Luna Omega PS C18	10.052	10.131	13.591	14.292	20.732	21.316
Luna Omega Polar C18	12.586	12.670	16.396	17.090	24.897	25.552
Kinetex C18	11.020	11.074	14.379	15.043	23.296	23.841
Kinetex Evo C18	9.582	9.663	13.053	13.720	21.912	21.912
Kinetex C8	10.433	10.504	14.170	14.844	23.128	23.920
Kinetex Biphenyl	13.529	13.561	17.316	18.076	26.232	27.080
Kinetex F5	10.162	10.231	13.762	14.438	23.281	23.831
Fortis Diphenyl	12.181	12.238	15.885	16.607	24.306	25.068
Polaris Amide C18	9.286	9.360	13.673	15.588	18.278	18.625
Poroshell Bonus-RP	8.736	8.814	12.234	13.114	18.963	19.397
Poroshell PFP	7.709	7.791	10.970	11.697	17.982	18.529
Poroshell Phenyl Hexyl	11.527	11.603	15.243	15.936	23.713	24.413
Poroshell SB-AQ	10.370	10.452	13.843	14.496	23.932	23.932
Poroshell HPH-C8	9.584	9.670	13.260	13.912	21.112	21.860
Poroshell HPH-C18	10.819	10.907	14.568	15.229	22.943	23.643
PLRP-S	11.558	11.558	14.693	15.368	23.456	23.802
Zorbax SB-C18	11.576	11.663	15.407	16.064	24.240	24.982
Zorbax SB-C8	11.915	11.985	15.617	16.293	24.713	25.456
Zorbax 300 SB-C18	11.606	11.704	15.643	16.290	25.605	26.327
Chromolith RP-18e	8.641	8.725	11.886	12.431	19.371	19.969
Acquity BEH C4	9.123	9.215	12.819	13.484	22.094	22.875
Acquity BEH C8	11.897	11.981	16.111	16.800	25.214	26.086
Acquity BEH C18	12.103	12.188	16.166	16.846	25.183	25.929
Acquity BEH C18 300	11.590	11.678	15.681	16.341	24.925	25.692
Acquity BEH Shield RP18	10.216	10.286	13.871	14.573	21.457	21.993
Acquity CSH C18	10.452	10.546	14.420	15.155	21.985	22.674
Acquity CSH Fluoro phenyl	7.346	7.346	10.216	11.314	16.367	16.783
Acquity CSH Phenyl Hexyl	9.241	9.330	12.823	13.694	18.979	19.606
Acquity HSS C18	11.640	11.721	15.581	16.240	23.775	24.477
Acquity HSS C18-SB	12.790	12.877	16.696	17.369	28.494	28.901
Acquity HSS T3	12.904	12.990	16.884	17.576	26.146	26.978
Cortecs T3	11.868	11.952	15.824	16.503	25.299	26.198
Peptide	[Met(O)10]-Bovine GLP-2 (1-15)	[Met(O)10]-Bovine GLP-2 (1-15)	Bovine GLP-2 (1-15)	[L-Asp11]-Bovine GLP-2 (1-15)	Bovine GLP-2 (16-33)	[Ile26,Leu27]-Bovine GLP-2 (16-33)
Peptide Number	8a	8b	1	9	13	15

Table 75 Raw t_g data for TM2 in formic acid conditions

Ascentis Express C18	10.602	10.686	19.290	15.724	22.612	23.359
Ascentis Express RP-Amide	9.174	9.245	18.214	13.555	20.374	20.812
Ascentis Express C8	9.714	9.790	17.785	14.400	21.159	22.059
Ascentis Express Phenyl Hexyl	10.145	10.214	18.151	14.613	20.817	21.446
Ascentis Express Biphenyl	11.103	11.137	21.090	16.796	23.744	24.457
Bioshell Peptide CN	8.601	8.660	20.186	16.283	22.820	23.495
Luna Omega C18	12.161	12.241	20.961	17.065	24.351	25.044
Luna Omega PS C18	10.003	10.083	17.691	13.787	20.718	21.299
Luna Omega Polar C18	12.581	12.664	21.511	17.412	24.858	25.518
Kinetex C18	11.048	11.103	20.479	16.510	23.303	23.846
Kinetex Evo C18	9.528	9.609	18.511	14.711	21.559	21.559
Kinetex C8	10.433	10.504	19.374	15.583	22.689	23.546
Kinetex Biphenyl	13.441	13.476	23.455	18.938	26.024	26.850
Kinetex F5	10.356	10.414	20.166	16.096	23.157	23.703
Fortis Diphenyl	12.133	12.190	21.460	17.037	24.165	24.911
Polaris Amide C18	9.292	9.365	16.159	10.136	18.303	18.647
Poroshell Bonus-RP	8.748	8.824	16.882	11.993	18.950	19.380
Poroshell PFP	7.715	7.795	15.366	11.021	17.986	18.533
Poroshell Phenyl Hexyl	11.505	11.582	20.784	16.930	23.652	24.346
Poroshell SB-AQ	10.340	10.422	20.834	16.454	23.897	23.897
Poroshell HPH-C8	9.579	9.665	17.782	14.340	21.074	21.819
Poroshell HPH-C18	10.789	10.877	19.561	16.032	22.882	23.582
PLRP-S	11.538	11.538	21.201	16.715	23.385	23.728
Zorbax SB-C18	11.579	11.666	20.766	16.807	24.189	24.921
Zorbax SB-C8	11.877	11.947	21.317	17.079	24.636	25.387
Zorbax 300 SB-C18	11.606	11.703	21.968	18.194	25.555	26.276
Chromolith RP-18e	8.633	8.716	16.348	13.244	19.323	19.919
Acquity BEH C4	9.133	9.223	18.951	15.155	22.082	22.863
Acquity BEH C8	11.868	11.952	21.226	17.510	25.150	26.019
Acquity BEH C18	12.080	12.166	21.493	17.715	25.113	25.855
Acquity BEH C18 300	11.602	11.689	21.241	17.658	24.900	25.664
Acquity BEH Shield RP18	10.214	10.285	18.914	14.712	21.432	21.968
Acquity CSH C18	10.408	10.501	18.549	14.448	21.942	22.637
Acquity CSH Fluoro phenyl	7.304	7.304	14.486	8.651	16.354	16.768
Acquity CSH Phenyl Hexyl	9.246	9.334	16.087	11.767	18.950	19.576
Acquity HSS C18	11.640	11.723	20.300	16.541	23.802	24.504
Acquity HSS C18-SB	12.788	12.875	24.818	19.379	28.445	28.855
Acquity HSS T3	12.871	12.957	22.474	18.326	26.061	26.854
Cortecs T3	11.851	11.938	21.642	17.675	25.213	26.056
Peptide	[Met(O)10]-Bovine GLP-2 (1-15)	[Met(O)10]-Bovine GLP-2 (1-15)	[Tyr26]-Bovine GLP-2 (16-33)	[Lys26]-Bovine GLP-2 (16-33)	Bovine GLP-2 (16-33)	[Ile26,Leu27]-Bovine GLP-2 (16-33)
Peptide Number	8a	8b	24	26	13	15

Table 76 Raw t_g data for TM3 in formic acid conditions

Ascentis Express C18	10.567	10.651	17.712	22.456	22.645	23.223
Ascentis Express RP-Amide	9.161	9.232	15.672	20.360	20.438	20.818
Ascentis Express C8	9.699	9.775	16.431	21.075	21.253	21.955
Ascentis Express Phenyl Hexyl	10.115	10.184	16.459	20.756	20.842	21.406
Ascentis Express Biphenyl	11.168	11.202	18.778	23.635	23.635	24.432
Bioshell Peptide CN	8.567	8.631	17.798	22.630	22.630	23.348
Luna Omega C18	12.136	12.215	19.417	24.316	24.478	25.030
Luna Omega PS C18	10.005	10.086	15.942	20.697	20.868	21.280
Luna Omega Polar C18	12.564	12.648	19.839	24.834	24.984	25.511
Kinetex C18	11.022	11.076	18.416	23.266	23.266	23.847
Kinetex Evo C18	9.515	9.594	16.408	21.235	21.235	21.235
Kinetex C8	10.433	10.504	17.721	22.647	22.811	23.536
Kinetex Biphenyl	13.305	13.331	20.899	25.750	25.750	26.653
Kinetex F5	10.345	10.403	18.006	23.045	23.045	23.647
Fortis Diphenyl	12.106	12.163	19.135	24.051	24.051	24.816
Polaris Amide C18	9.298	9.372	12.971	18.262	18.445	18.600
Poroshell Bonus-RP	8.760	8.837	14.314	18.988	19.179	19.429
Poroshell PFP	7.718	7.800	13.078	17.975	18.081	18.524
Poroshell Phenyl Hexyl	11.495	11.571	18.916	23.585	23.641	24.314
Poroshell SB-AQ	10.332	10.414	18.431	23.798	23.798	23.798
Poroshell HPH-C8	9.556	9.643	16.358	21.029	21.198	21.782
Poroshell HPH-C18	10.764	10.853	18.029	22.799	22.969	23.516
PLRP-S	11.511	11.511	18.402	23.259	23.259	23.661
Zorbax SB-C18	11.565	11.652	19.088	24.161	24.321	24.910
Zorbax SB-C8	11.838	11.908	19.529	24.595	24.707	25.358
Zorbax 300 SB-C18	11.591	11.689	20.272	25.484	25.592	26.229
Chromolith RP-18e	8.609	8.693	15.024	19.242	19.373	19.854
Acquity BEH C4	9.136	9.225	17.072	22.068	22.193	22.863
Acquity BEH C8	11.847	11.930	19.938	25.082	25.229	25.967
Acquity BEH C18	12.063	12.149	20.104	25.103	25.232	25.862
Acquity BEH C18 300	11.581	11.669	19.872	24.866	24.988	25.645
Acquity BEH Shield RP18	10.212	10.281	16.765	21.406	21.538	21.945
Acquity CSH C18	10.397	10.487	16.802	21.907	22.097	22.598
Acquity CSH Fluoro phenyl	7.282	7.282	10.987	16.330	16.445	16.743
Acquity CSH Phenyl Hexyl	9.246	9.334	14.178	18.961	19.139	19.592
Acquity HSS C18	11.612	11.694	18.867	23.764	23.912	24.478
Acquity HSS C18-SB	12.794	12.881	22.198	28.366	28.366	28.871
Acquity HSS T3	12.874	12.961	20.817	26.019	26.139	26.819
Cortecs T3	11.834	11.921	19.887	25.126	25.204	25.943
Peptide	[Met(O)10]-Bovine GLP-2 (1-15)	[Met(O)10]-Bovine GLP-2 (1-15)	[Gly22]-Bovine GLP-2 (16-33)	Bovine GLP-2 (16-33)	[D-Ser16]-Bovine GLP-2 (16-33)	[Ile26,Leu27]-Bovine GLP-2 (16-33)
Peptide Number	8a	8b	16	13	14	15

Table 77 t_g^* for TM1 in formic acid conditions

Ascentis Express C18	0.000	0.006	0.289	0.334	0.941	1.000
Ascentis Express RP-Amide	0.000	0.006	0.282	0.340	0.962	1.000
Ascentis Express C8	0.000	0.006	0.286	0.337	0.907	1.000
Ascentis Express Phenyl Hexyl	0.000	0.006	0.291	0.347	0.944	1.000
Ascentis Express Biphenyl	0.000	0.003	0.267	0.321	0.947	1.000
Bioshell Peptide CN	0.000	0.004	0.237	0.281	0.954	1.000
Luna Omega C18	0.000	0.006	0.296	0.296	0.946	1.000
Luna Omega PS C18	0.000	0.007	0.314	0.376	0.948	1.000
Luna Omega Polar C18	0.000	0.006	0.294	0.347	0.949	1.000
Kinetex C18	0.000	0.004	0.262	0.314	0.957	1.000
Kinetex Evo C18	0.000	0.007	0.282	0.336	1.000	1.000
Kinetex C8	0.000	0.005	0.277	0.327	0.941	1.000
Kinetex Biphenyl	0.000	0.002	0.279	0.336	0.937	1.000
Kinetex F5	0.000	0.005	0.263	0.313	0.960	1.000
Fortis Diphenyl	0.000	0.004	0.287	0.343	0.941	1.000
Polaris Amide C18	0.000	0.008	0.470	0.675	0.963	1.000
Poroshell Bonus-RP	0.000	0.007	0.328	0.411	0.959	1.000
Poroshell PFP	0.000	0.008	0.301	0.369	0.949	1.000
Poroshell Phenyl Hexyl	0.000	0.006	0.288	0.342	0.946	1.000
Poroshell SB-AQ	0.000	0.006	0.256	0.304	1.000	1.000
Poroshell HPH-C8	0.000	0.007	0.299	0.353	0.939	1.000
Poroshell HPH-C18	0.000	0.007	0.292	0.344	0.945	1.000
PLRP-S	0.000	0.000	0.256	0.311	0.972	1.000
Zorbax SB-C18	0.000	0.006	0.286	0.335	0.945	1.000
Zorbax SB-C8	0.000	0.005	0.273	0.323	0.945	1.000
Zorbax 300 SB-C18	0.000	0.007	0.274	0.318	0.951	1.000
Chromolith RP-18e	0.000	0.007	0.286	0.335	0.947	1.000
Acquity BEH C4	0.000	0.007	0.269	0.317	0.943	1.000
Acquity BEH C8	0.000	0.006	0.297	0.346	0.939	1.000
Acquity BEH C18	0.000	0.006	0.294	0.343	0.946	1.000
Acquity BEH C18 300	0.000	0.006	0.290	0.337	0.946	1.000
Acquity BEH Shield RP18	0.000	0.006	0.310	0.370	0.954	1.000
Acquity CSH C18	0.000	0.008	0.325	0.385	0.944	1.000
Acquity CSH Fluoro phenyl	0.000	0.000	0.304	0.420	0.956	1.000
Acquity CSH Phenyl Hexyl	0.000	0.009	0.346	0.430	0.940	1.000
Acquity HSS C18	0.000	0.006	0.307	0.358	0.945	1.000
Acquity HSS C18-SB	0.000	0.005	0.242	0.284	0.975	1.000
Acquity HSS T3	0.000	0.006	0.283	0.332	0.941	1.000
Cortecs T3	0.000	0.006	0.276	0.323	0.937	1.000
Peptide	[Met(O)10]-Bovine GLP-2 (1-15)	[Met(O)10]-Bovine GLP-2 (1-15)	Bovine GLP-2 (1-15)	[L-Asp11]-Bovine GLP-2 (1-15)	Bovine GLP-2 (16-33)	[Ile26,Leu27]-Bovine GLP-2 (16-33)
Peptide Number	8a	8b	1	9	13	15

Table 78 t_g^* for TM2 in formic acid conditions

Ascentis Express C18	0.000	0.007	0.681	0.402	0.941	1.000
Ascentis Express RP-Amide	0.000	0.006	0.777	0.376	0.962	1.000
Ascentis Express C8	0.000	0.006	0.654	0.380	0.927	1.000
Ascentis Express Phenyl Hexyl	0.000	0.006	0.708	0.395	0.944	1.000
Ascentis Express Biphenyl	0.000	0.003	0.748	0.426	0.947	1.000
Bioshell Peptide CN	0.000	0.004	0.778	0.516	0.955	1.000
Luna Omega C18	0.000	0.006	0.683	0.381	0.946	1.000
Luna Omega PS C18	0.000	0.007	0.681	0.335	0.949	1.000
Luna Omega Polar C18	0.000	0.006	0.690	0.373	0.949	1.000
Kinetex C18	0.000	0.004	0.737	0.427	0.958	1.000
Kinetex Evo C18	0.000	0.007	0.747	0.431	1.000	1.000
Kinetex C8	0.000	0.005	0.682	0.393	0.935	1.000
Kinetex Biphenyl	0.000	0.003	0.747	0.410	0.938	1.000
Kinetex F5	0.000	0.004	0.735	0.430	0.959	1.000
Fortis Diphenyl	0.000	0.004	0.730	0.384	0.942	1.000
Polaris Amide C18	0.000	0.008	0.734	0.090	0.963	1.000
Poroshell Bonus-RP	0.000	0.007	0.765	0.305	0.960	1.000
Poroshell PFP	0.000	0.007	0.707	0.306	0.949	1.000
Poroshell Phenyl Hexyl	0.000	0.006	0.723	0.422	0.946	1.000
Poroshell SB-AQ	0.000	0.006	0.774	0.451	1.000	1.000
Poroshell HPH-C8	0.000	0.007	0.670	0.389	0.939	1.000
Poroshell HPH-C18	0.000	0.007	0.686	0.410	0.945	1.000
PLRP-S	0.000	0.000	0.793	0.425	0.972	1.000
Zorbax SB-C18	0.000	0.007	0.689	0.392	0.945	1.000
Zorbax SB-C8	0.000	0.005	0.699	0.385	0.944	1.000
Zorbax 300 SB-C18	0.000	0.007	0.706	0.449	0.951	1.000
Chromolith RP-18e	0.000	0.007	0.684	0.409	0.947	1.000
Acquity BEH C4	0.000	0.007	0.715	0.439	0.943	1.000
Acquity BEH C8	0.000	0.006	0.661	0.399	0.939	1.000
Acquity BEH C18	0.000	0.006	0.683	0.409	0.946	1.000
Acquity BEH C18 300	0.000	0.006	0.685	0.431	0.946	1.000
Acquity BEH Shield RP18	0.000	0.006	0.740	0.383	0.954	1.000
Acquity CSH C18	0.000	0.008	0.666	0.330	0.943	1.000
Acquity CSH Fluoro phenyl	0.000	0.000	0.759	0.142	0.956	1.000
Acquity CSH Phenyl Hexyl	0.000	0.009	0.662	0.244	0.939	1.000
Acquity HSS C18	0.000	0.006	0.673	0.381	0.945	1.000
Acquity HSS C18-SB	0.000	0.005	0.749	0.410	0.974	1.000
Acquity HSS T3	0.000	0.006	0.687	0.390	0.943	1.000
Cortecs T3	0.000	0.006	0.689	0.410	0.941	1.000
Peptide	[Met(O)10]-Bovine GLP-2 (1-15)	[Met(O)10]-Bovine GLP-2 (1-15)	[Tyr26]-Bovine GLP-2 (16-33)	[Lys26]-Bovine GLP-2 (16-33)	Bovine GLP-2 (16-33)	[Ile26,Leu27]-Bovine GLP-2 (16-33)
Peptide Number	8a	8b	24	26	13	15

Table 79 t_g^* for TM3 in formic acid conditions

Ascentis Express C18	0.000	0.007	0.565	0.939	0.954	1.000
Ascentis Express RP-Amide	0.000	0.006	0.559	0.961	0.967	1.000
Ascentis Express C8	0.000	0.006	0.549	0.928	0.943	1.000
Ascentis Express Phenyl Hexyl	0.000	0.006	0.562	0.942	0.950	1.000
Ascentis Express Biphenyl	0.000	0.003	0.574	0.940	0.940	1.000
Bioshell Peptide CN	0.000	0.004	0.625	0.951	0.951	1.000
Luna Omega C18	0.000	0.006	0.565	0.945	0.957	1.000
Luna Omega PS C18	0.000	0.007	0.527	0.948	0.963	1.000
Luna Omega Polar C18	0.000	0.006	0.562	0.948	0.959	1.000
Kinetex C18	0.000	0.004	0.577	0.955	0.955	1.000
Kinetex Evo C18	0.000	0.007	0.588	1.000	1.000	1.000
Kinetex C8	0.000	0.005	0.556	0.932	0.945	1.000
Kinetex Biphenyl	0.000	0.002	0.569	0.932	0.932	1.000
Kinetex F5	0.000	0.004	0.576	0.955	0.955	1.000
Fortis Diphenyl	0.000	0.004	0.553	0.940	0.940	1.000
Polaris Amide C18	0.000	0.008	0.395	0.964	0.983	1.000
Poroshell Bonus-RP	0.000	0.007	0.521	0.959	0.977	1.000
Poroshell PFP	0.000	0.008	0.496	0.949	0.959	1.000
Poroshell Phenyl Hexyl	0.000	0.006	0.579	0.943	0.947	1.000
Poroshell SB-AQ	0.000	0.006	0.601	1.000	1.000	1.000
Poroshell HPH-C8	0.000	0.007	0.556	0.938	0.952	1.000
Poroshell HPH-C18	0.000	0.007	0.570	0.944	0.957	1.000
PLRP-S	0.000	0.000	0.567	0.967	0.967	1.000
Zorbax SB-C18	0.000	0.007	0.564	0.944	0.956	1.000
Zorbax SB-C8	0.000	0.005	0.569	0.944	0.952	1.000
Zorbax 300 SB-C18	0.000	0.007	0.593	0.949	0.956	1.000
Chromolith RP-18e	0.000	0.007	0.570	0.946	0.957	1.000
Acquity BEH C4	0.000	0.006	0.578	0.942	0.951	1.000
Acquity BEH C8	0.000	0.006	0.573	0.937	0.948	1.000
Acquity BEH C18	0.000	0.006	0.583	0.945	0.954	1.000
Acquity BEH C18 300	0.000	0.006	0.590	0.945	0.953	1.000
Acquity BEH Shield RP18	0.000	0.006	0.559	0.954	0.965	1.000
Acquity CSH C18	0.000	0.007	0.525	0.943	0.959	1.000
Acquity CSH Fluoro phenyl	0.000	0.000	0.392	0.956	0.969	1.000
Acquity CSH Phenyl Hexyl	0.000	0.009	0.477	0.939	0.956	1.000
Acquity HSS C18	0.000	0.006	0.564	0.945	0.956	1.000
Acquity HSS C18-SB	0.000	0.005	0.585	0.969	0.969	1.000
Acquity HSS T3	0.000	0.006	0.570	0.943	0.951	1.000
Cortecs T3	0.000	0.006	0.571	0.942	0.948	1.000

Peptide Number	Peptide
8a	[Met(O)10]-Bovine GLP-2 (1-15)
8b	[Met(O)10]-Bovine GLP-2 (1-15)
16	[Gly22]-Bovine GLP-2 (16-33)
13	Bovine GLP-2 (16-33)
14	[D-Ser16]-Bovine GLP-2 (16-33)
15	[Ile26,Leu27]-Bovine GLP-2 (16-33)

Table 80 Raw t_g data for TM1 in ammonium formate conditions

Ascentis Express C18 468	5.396	5.396	8.362	6.958	25.575	26.663
Ascentis Express RP-Amide	3.449	3.449	6.649	5.080	25.251	26.138
Ascentis Express C8	5.304	5.304	8.227	6.824	25.615	26.702
Ascentis Express Phenyl Hexyl	4.460	4.460	7.383	5.970	24.012	24.939
Ascentis Express Biphenyl	3.320	3.320	6.207	4.446	23.745	24.604
Bioshel Peptide C18	4.561	4.561	7.378	5.885	26.649	27.613
Luna Omega C18	6.674	6.674	9.620	8.021	27.978	29.147
Luna Omega PS C18	7.260	7.260	9.052	7.395	27.870	28.920
Luna Omega Polar C18	6.693	6.693	9.632	8.042	28.494	29.663
Kinetex C18 (repeat)	5.772	5.772	8.989	7.894	24.699	25.588
Kinetex Evo C18	5.064	5.064	8.052	6.555	25.754	26.810
Kinetex C8	4.605	4.605	7.733	7.733	25.821	27.059
Kinetex Biphenyl	5.127	5.127	7.818	6.186	25.585	26.472
Kinetex F5	3.384	3.384	6.389	4.806	24.198	25.055
Fortis Diphenyl	4.817	4.817	8.524	8.524	27.336	28.477
Polaris Amide C18	16.454	16.454	23.961	23.961	31.371	31.739
Poroshell Bonus-RP	6.071	6.071	9.350	8.001	27.532	28.486
Poroshell PFP	4.056	4.056	6.932	5.401	24.475	25.370
Poroshell Phenyl Hexyl	4.684	4.684	7.899	6.026	25.429	26.418
Poroshell SB-AQ	3.995	3.995	7.446	5.748	26.815	27.976
Poroshell HPH-C8	5.386	5.386	8.645	7.265	26.131	27.312
Poroshell HPH-C18	5.924	5.924	9.049	7.675	26.393	27.510
PLRP-S	5.180	5.180	7.863	6.301	26.350	26.988
Zorbax SB-C18	5.924	5.924	9.049	7.675	26.393	27.510
Zorbax SB-C8	4.223	4.223	7.543	5.573	26.252	27.254
Zorbax 300 SB-C18	5.233	5.233	8.282	6.656	26.975	28.013
AdvancedBio Peptide Map	6.413	6.413	9.464	8.004	27.529	28.694
Chromolith RP-18e	4.335	4.335	6.933	5.711	22.699	23.638
Acquity BEH C4	3.069	3.069	6.462	4.345	25.819	27.152
Acquity BEH C8	6.101	6.101	9.393	7.782	28.530	29.960
Acquity BEH C18	6.356	6.356	9.456	7.927	27.894	29.128
Acquity BEH C18 300	5.899	5.899	9.123	7.639	27.159	28.390
Acquity BEH Shield RP18	6.386	6.386	9.286	7.601	27.411	28.541
Acquity CSH C18	6.696	6.696	9.768	8.333	28.302	29.496
Acquity CSH Fluoro phenyl	2.374	2.374	4.878	2.846	24.271	25.006
Acquity CSH Phenyl Hexyl	5.122	5.122	8.291	6.532	26.557	27.587
Acquity HSS C18	6.788	6.788	9.904	8.551	28.071	29.307
Acquity HSS C18-SB	4.150	4.150	6.831	4.979	32.965	33.687
Acquity HSS T3	7.090	7.090	10.068	8.642	28.918	30.104
Cortecs T3	6.067	6.067	9.312	7.620	27.721	28.880
Peptide	[Met(O)10]-Bovine GLP-2 (1-15)	[Met(O)10]-Bovine GLP-2 (1-15)	Bovine GLP-2 (1-15)	[L-Asp11]-Bovine GLP-2 (1-15)	Bovine GLP-2 (16-33)	[Ile26,Leu27]-Bovine GLP-2 (16-33)
Peptide Number	8a	8b	1	9	13	15

Table 81 Raw t_g data for TM2 in ammonium formate conditions

Ascentis Express C18 468	5.381	5.381	21.476	19.141	25.567	26.655
Ascentis Express RP-Amide	3.807	3.807	22.228	19.322	25.267	26.149
Ascentis Express C8	5.270	5.270	21.580	19.243	25.657	26.737
Ascentis Express Phenyl Hexyl	4.633	4.633	20.790	18.680	24.016	24.934
Ascentis Express Biphenyl	3.196	3.196	20.972	19.235	23.753	24.601
Bioshel Peptide C18	4.499	4.499	22.702	20.662	26.590	27.564
Luna Omega C18	6.369	6.369	23.797	21.200	28.002	29.167
Luna Omega PS C18	7.254	7.254	23.930	21.012	27.840	28.887
Luna Omega Polar C18	6.522	6.676	24.334	21.838	28.483	29.645
Kinetex C18 (repeat)	5.735	5.735	21.634	19.134	24.853	25.731
Kinetex Evo C18	5.019	5.019	21.894	19.342	25.764	26.817
Kinetex C8	4.465	4.465	21.748	19.239	25.803	27.035
Kinetex Biphenyl	4.994	4.994	22.613	22.613	25.540	26.428
Kinetex F5	3.301	3.301	20.992	18.904	24.206	25.064
Fortis Diphenyl	4.937	4.937	24.125	22.067	27.317	28.456
Polaris Amide C18	16.121	16.121	27.761	20.156	31.372	31.744
Poroshell Bonus-RP	6.069	6.069	24.570	20.562	27.515	28.468
Poroshell PFP	4.056	4.056	21.334	19.222	24.472	25.363
Poroshell Phenyl Hexyl	4.690	4.690	21.954	19.785	25.436	26.429
Poroshell SB-AQ	3.856	3.856	23.078	20.457	26.834	28.000
Poroshell HPH-C8	5.270	5.270	21.796	19.319	26.155	27.328
Poroshell HPH-C18	5.859	5.859	22.226	19.679	26.393	27.508
PLRP-S	5.067	5.067	23.826	21.027	26.366	26.970
Zorbax SB-C18	5.709	5.709	22.696	20.792	26.733	27.779
Zorbax SB-C8	4.224	4.224	22.323	20.818	26.223	27.226
Zorbax 300 SB-C18	5.282	5.282	22.835	20.822	26.988	28.021
AdvancedBio Peptide Map	6.381	6.381	23.207	20.620	27.527	28.692
Chromolith RP-18e	4.308	4.308	18.989	16.902	22.693	23.624
Acquity BEH C4	2.969	2.969	21.902	19.159	25.835	27.169
Acquity BEH C8	6.116	6.116	23.600	21.317	28.542	29.970
Acquity BEH C18	6.363	6.363	23.396	20.994	27.899	29.134
Acquity BEH C18 300	5.939	5.939	22.695	20.345	27.156	28.382
Acquity BEH Shield RP18	5.299	5.299	23.871	20.623	27.422	28.551
Acquity CSH C18	6.644	6.644	24.164	21.526	28.298	29.485
Acquity CSH Fluoro phenyl	2.374	2.374	21.821	19.925	24.267	25.001
Acquity CSH Phenyl Hexyl	5.087	5.087	23.090	20.615	26.557	27.591
Acquity HSS C18	6.800	6.800	23.587	21.014	28.021	29.261
Acquity HSS C18-SB	4.150	4.150	27.260	28.208	33.005	33.729
Acquity HSS T3	7.097	7.097	24.504	21.864	28.907	30.099
Cortecs T3	6.049	6.049	23.483	20.997	27.719	28.872
Peptide	[Met(O)10]-Bovine GLP-2 (1-15)	[Met(O)10]-Bovine GLP-2 (1-15)	[Tyr26]-Bovine GLP-2 (16-33)	[Lys26]-Bovine GLP-2 (16-33)	Bovine GLP-2 (16-33)	[Ile26,Leu27]-Bovine GLP-2 (16-33)
Peptide Number	8a	8b	24	26	13	15

Table 82 Raw t_g data for TM3 in ammonium formate conditions

Ascentis Express C18 468	5.389	5.389	19.838	25.575	25.766	26.663
Ascentis Express RP-Amide	3.377	3.377	19.452	25.269	25.421	26.151
Ascentis Express C8	5.253	5.253	19.941	25.656	25.831	26.737
Ascentis Express Phenyl Hexyl	4.626	4.626	18.800	24.059	24.258	24.976
Ascentis Express Biphenyl	3.075	3.075	18.549	23.743	23.920	24.588
Bioshell Peptide C18	4.499	4.499	20.376	26.572	26.789	27.537
Luna Omega C18	6.640	6.640	22.027	28.023	28.231	29.189
Luna Omega PS C18	7.270	7.270	21.832	27.853	28.006	28.901
Luna Omega Polar C18	6.506	6.661	22.331	28.446	28.636	29.610
Kinetex C18 (repeat)	5.703	5.703	19.280	24.798	25.022	25.685
Kinetex Evo C18	5.060	5.060	19.902	25.734	25.895	26.786
Kinetex C8	4.448	4.448	19.905	25.853	25.991	27.074
Kinetex Biphenyl	4.933	4.933	20.142	25.421	25.581	26.301
Kinetex F5	3.312	3.312	18.617	24.240	24.428	25.091
Fortis Diphenyl	5.196	5.196	21.531	27.291	27.528	28.427
Polaris Amide C18	16.503	16.503	23.197	31.320	31.320	31.750
Poroshell Bonus-RP	6.061	6.061	21.492	27.509	27.680	28.461
Poroshell PFP	4.056	4.056	18.836	24.474	24.660	25.362
Poroshell Phenyl Hexyl	4.684	4.684	19.944	25.430	25.557	26.421
Poroshell SB-AQ	3.810	3.810	20.317	26.779	26.936	27.940
Poroshell HPH-C8	5.247	5.247	20.250	26.162	26.340	27.339
Poroshell HPH-C18	5.853	5.853	20.513	26.380	26.580	27.500
PLRP-S	5.066	5.066	20.267	26.545	26.545	26.867
Zorbax SB-C18	5.682	5.682	20.856	26.721	26.999	27.763
Zorbax SB-C8	4.208	4.208	20.293	26.248	26.411	27.251
Zorbax 300 SB-C18	5.123	5.123	20.812	26.976	27.134	28.005
AdvancedBio Peptide Map	6.384	6.384	21.509	27.519	27.707	28.682
Chromolith RP-18e	4.302	4.302	17.372	22.685	22.840	23.619
Acquity BEH C4	2.929	2.929	19.546	25.865	25.915	27.165
Acquity BEH C8	6.129	6.129	22.293	28.533	28.698	29.964
Acquity BEH C18	6.387	6.387	21.855	27.885	28.054	29.122
Acquity BEH C18 300	5.973	5.973	21.171	27.163	27.332	28.388
Acquity BEH Shield RP18	5.425	5.425	21.571	27.447	27.637	28.573
Acquity CSH C18	6.656	6.656	22.229	28.306	28.507	29.492
Acquity CSH Fluoro phenyl	2.374	2.374	18.287	24.273	24.403	25.002
Acquity CSH Phenyl Hexyl	5.071	5.071	20.882	26.549	26.712	27.580
Acquity HSS C18	6.802	6.802	21.982	28.031	28.238	29.261
Acquity HSS C18-SB	4.150	4.150	24.055	33.081	33.177	33.793
Acquity HSS T3	7.059	7.059	22.663	28.889	29.081	30.083
Cortecs T3	6.084	6.084	21.659	27.708	27.861	28.860
Peptide	[Met(O)10]-Bovine GLP-2 (1-15)	[Met(O)10]-Bovine GLP-2 (1-15)	[Gly22]-Bovine GLP-2 (16-33)	Bovine GLP-2 (16-33)	[D-Ser16]-Bovine GLP-2 (16-33)	[Ile26,Leu27]-Bovine GLP-2 (16-33)
Peptide Number	8a	8b	16	13	14	15

Table 83 t_g^* for TM1 in ammonium formate conditions

Ascentis Express C18 468	0.000	0.000	0.139	0.073	0.949	1.000
Ascentis Express RP-Amide	0.000	0.000	0.141	0.072	0.961	1.000
Ascentis Express C8	0.000	0.000	0.137	0.071	0.949	1.000
Ascentis Express Phenyl Hexyl	0.000	0.000	0.143	0.074	0.955	1.000
Ascentis Express Biphenyl	0.000	0.000	0.136	0.053	0.960	1.000
Bioshel Peptide C18	0.000	0.000	0.122	0.057	0.958	1.000
Luna Omega C18	0.000	0.000	0.131	0.060	0.948	1.000
Luna Omega PS C18	0.000	0.000	0.083	0.006	0.952	1.000
Luna Omega Polar C18	0.000	0.000	0.128	0.059	0.949	1.000
Kinetex C18 (repeat)	0.000	0.000	0.162	0.107	0.955	1.000
Kinetex Evo C18	0.000	0.000	0.137	0.069	0.951	1.000
Kinetex C8	0.000	0.000	0.139	0.139	0.945	1.000
Kinetex Biphenyl	0.000	0.000	0.126	0.050	0.958	1.000
Kinetex F5	0.000	0.000	0.139	0.066	0.960	1.000
Fortis Diphenyl	0.000	0.000	0.157	0.157	0.952	1.000
Polaris Amide C18	0.000	0.000	0.491	0.491	0.976	1.000
Poroshell Bonus-RP	0.000	0.000	0.146	0.086	0.957	1.000
Poroshell PFP	0.000	0.000	0.135	0.063	0.958	1.000
Poroshell Phenyl Hexyl	0.000	0.000	0.148	0.062	0.954	1.000
Poroshell SB-AQ	0.000	0.000	0.144	0.073	0.952	1.000
Poroshell HPH-C8	0.000	0.000	0.149	0.086	0.946	1.000
Poroshell HPH-C18	0.000	0.000	0.145	0.081	0.948	1.000
PLRP-S	0.000	0.000	0.123	0.051	0.971	1.000
Zorbax SB-C18	0.000	0.000	0.145	0.081	0.948	1.000
Zorbax SB-C8	0.000	0.000	0.144	0.059	0.956	1.000
Zorbax 300 SB-C18	0.000	0.000	0.134	0.062	0.954	1.000
AdvancedBio Peptide Map	0.000	0.000	0.137	0.071	0.948	1.000
Chromolith RP-18e	0.000	0.000	0.135	0.071	0.951	1.000
Acquity BEH C4	0.000	0.000	0.141	0.053	0.945	1.000
Acquity BEH C8	0.000	0.000	0.138	0.070	0.940	1.000
Acquity BEH C18	0.000	0.000	0.136	0.069	0.946	1.000
Acquity BEH C18 300	0.000	0.000	0.143	0.077	0.945	1.000
Acquity BEH Shield RP18	0.000	0.000	0.131	0.055	0.949	1.000
Acquity CSH C18	0.000	0.000	0.135	0.072	0.948	1.000
Acquity CSH Fluoro phenyl	0.000	0.000	0.111	0.021	0.968	1.000
Acquity CSH Phenyl Hexyl	0.000	0.000	0.141	0.063	0.954	1.000
Acquity HSS C18	0.000	0.000	0.138	0.078	0.945	1.000
Acquity HSS C18-SB	0.000	0.000	0.091	0.028	0.976	1.000
Acquity HSS T3	0.000	0.000	0.129	0.067	0.948	1.000
Cortecs T3	0.000	0.000	0.142	0.068	0.949	1.000

Peptide Number	Peptide
8a	[Met(O)10]-Bovine GLP-2 (1-15)
8b	[Met(O)10]-Bovine GLP-2 (1-15)
1	Bovine GLP-2 (1-15)
9	[L-Asp11]-Bovine GLP-2 (1-15)
13	Bovine GLP-2 (16-33)
15	[Ile26,Leu27]-Bovine GLP-2 (16-33)

Table 84 t_g^* for TM2 in ammonium formate conditions

Ascentis Express C18 468	0.000	0.000	0.757	0.647	0.949	1.000
Ascentis Express RP-Amide	0.000	0.000	0.825	0.694	0.961	1.000
Ascentis Express C8	0.000	0.000	0.760	0.651	0.950	1.000
Ascentis Express Phenyl Hexyl	0.000	0.000	0.796	0.692	0.955	1.000
Ascentis Express Biphenyl	0.000	0.000	0.830	0.749	0.960	1.000
Bioshel Peptide C18	0.000	0.000	0.789	0.701	0.958	1.000
Luna Omega C18	0.000	0.000	0.764	0.651	0.949	1.000
Luna Omega PS C18	0.000	0.000	0.771	0.636	0.952	1.000
Luna Omega Polar C18	0.000	0.007	0.770	0.662	0.950	1.000
Kinetex C18 (repeat)	0.000	0.000	0.795	0.670	0.956	1.000
Kinetex Evo C18	0.000	0.000	0.774	0.657	0.952	1.000
Kinetex C8	0.000	0.000	0.766	0.655	0.945	1.000
Kinetex Biphenyl	0.000	0.000	0.822	0.822	0.959	1.000
Kinetex F5	0.000	0.000	0.813	0.717	0.961	1.000
Fortis Diphenyl	0.000	0.000	0.816	0.728	0.952	1.000
Polaris Amide C18	0.000	0.000	0.745	0.258	0.976	1.000
Poroshell Bonus-RP	0.000	0.000	0.826	0.647	0.957	1.000
Poroshell PFP	0.000	0.000	0.811	0.712	0.958	1.000
Poroshell Phenyl Hexyl	0.000	0.000	0.794	0.694	0.954	1.000
Poroshell SB-AQ	0.000	0.000	0.796	0.688	0.952	1.000
Poroshell HPH-C8	0.000	0.000	0.749	0.637	0.947	1.000
Poroshell HPH-C18	0.000	0.000	0.756	0.638	0.948	1.000
PLRP-S	0.000	0.000	0.856	0.729	0.972	1.000
Zorbax SB-C18	0.000	0.000	0.770	0.683	0.953	1.000
Zorbax SB-C8	0.000	0.000	0.787	0.721	0.956	1.000
Zorbax 300 SB-C18	0.000	0.000	0.772	0.683	0.955	1.000
AdvancedBio Peptide Map	0.000	0.000	0.754	0.638	0.948	1.000
Chromolith RP-18e	0.000	0.000	0.760	0.652	0.952	1.000
Acquity BEH C4	0.000	0.000	0.782	0.669	0.945	1.000
Acquity BEH C8	0.000	0.000	0.733	0.637	0.940	1.000
Acquity BEH C18	0.000	0.000	0.748	0.643	0.946	1.000
Acquity BEH C18 300	0.000	0.000	0.747	0.642	0.945	1.000
Acquity BEH Shield RP18	0.000	0.000	0.799	0.659	0.951	1.000
Acquity CSH C18	0.000	0.000	0.767	0.652	0.948	1.000
Acquity CSH Fluoro phenyl	0.000	0.000	0.859	0.776	0.968	1.000
Acquity CSH Phenyl Hexyl	0.000	0.000	0.800	0.690	0.954	1.000
Acquity HSS C18	0.000	0.000	0.747	0.633	0.945	1.000
Acquity HSS C18-SB	0.000	0.000	0.781	0.813	0.976	1.000
Acquity HSS T3	0.000	0.000	0.757	0.642	0.948	1.000
Cortecs T3	0.000	0.000	0.764	0.655	0.949	1.000
Peptide	[Met(O)10]-Bovine GLP-2 (1-15)	[Met(O)10]-Bovine GLP-2 (1-15)	[Tyr26]-Bovine GLP-2 (16-33)	[Lys26]-Bovine GLP-2 (16-33)	Bovine GLP-2 (16-33)	[Ile26,Leu27]-Bovine GLP-2 (16-33)
Peptide Number	8a	8b	24	26	13	15

Table 85 t_g^* for TM3 in ammonium formate conditions

Ascentis Express C18 468	0.000	0.000	0.679	0.949	0.958	1.000
Ascentis Express RP-Amide	0.000	0.000	0.706	0.961	0.968	1.000
Ascentis Express C8	0.000	0.000	0.684	0.950	0.958	1.000
Ascentis Express Phenyl Hexyl	0.000	0.000	0.697	0.955	0.965	1.000
Ascentis Express Biphenyl	0.000	0.000	0.719	0.961	0.969	1.000
Bioshell Peptide C18	0.000	0.000	0.689	0.958	0.968	1.000
Luna Omega C18	0.000	0.000	0.682	0.948	0.958	1.000
Luna Omega PS C18	0.000	0.000	0.673	0.952	0.959	1.000
Luna Omega Polar C18	0.000	0.007	0.685	0.950	0.958	1.000
Kinetex C18 (repeat)	0.000	0.000	0.679	0.956	0.967	1.000
Kinetex Evo C18	0.000	0.000	0.683	0.952	0.959	1.000
Kinetex C8	0.000	0.000	0.683	0.946	0.952	1.000
Kinetex Biphenyl	0.000	0.000	0.712	0.959	0.966	1.000
Kinetex F5	0.000	0.000	0.703	0.961	0.970	1.000
Fortis Diphenyl	0.000	0.000	0.703	0.951	0.961	1.000
Polaris Amide C18	0.000	0.000	0.439	0.972	0.972	1.000
Poroshell Bonus-RP	0.000	0.000	0.689	0.958	0.965	1.000
Poroshell PFP	0.000	0.000	0.694	0.958	0.967	1.000
Poroshell Phenyl Hexyl	0.000	0.000	0.702	0.954	0.960	1.000
Poroshell SB-AQ	0.000	0.000	0.684	0.952	0.958	1.000
Poroshell HPH-C8	0.000	0.000	0.679	0.947	0.955	1.000
Poroshell HPH-C18	0.000	0.000	0.677	0.948	0.957	1.000
PLRP-S	0.000	0.000	0.697	0.985	0.985	1.000
Zorbax SB-C18	0.000	0.000	0.687	0.953	0.965	1.000
Zorbax SB-C8	0.000	0.000	0.698	0.956	0.964	1.000
Zorbax 300 SB-C18	0.000	0.000	0.686	0.955	0.962	1.000
AdvancedBio Peptide Map	0.000	0.000	0.678	0.948	0.956	1.000
Chromolith RP-18e	0.000	0.000	0.677	0.952	0.960	1.000
Acquity BEH C4	0.000	0.000	0.686	0.946	0.948	1.000
Acquity BEH C8	0.000	0.000	0.678	0.940	0.947	1.000
Acquity BEH C18	0.000	0.000	0.680	0.946	0.953	1.000
Acquity BEH C18 300	0.000	0.000	0.678	0.945	0.953	1.000
Acquity BEH Shield RP18	0.000	0.000	0.698	0.951	0.960	1.000
Acquity CSH C18	0.000	0.000	0.682	0.948	0.957	1.000
Acquity CSH Fluoro phenyl	0.000	0.000	0.703	0.968	0.974	1.000
Acquity CSH Phenyl Hexyl	0.000	0.000	0.702	0.954	0.961	1.000
Acquity HSS C18	0.000	0.000	0.676	0.945	0.954	1.000
Acquity HSS C18-SB	0.000	0.000	0.671	0.976	0.979	1.000
Acquity HSS T3	0.000	0.000	0.678	0.948	0.956	1.000
Cortecs T3	0.000	0.000	0.684	0.949	0.956	1.000

Peptide Number	Peptide
8a	[Met(O)10]-Bovine GLP-2 (1-15)
8b	[Met(O)10]-Bovine GLP-2 (1-15)
16	[Gly22]-Bovine GLP-2 (16-33)
13	Bovine GLP-2 (16-33)
14	[D-Ser16]-Bovine GLP-2 (16-33)
5	[Ile26,Leu27]-Bovine GLP-2 (16-33)